THE

STABILISATION OF

HIGH OXIDATION STATES

IN

TRANSITION AND MAIN GROUP

ELEMENTS

by
Mary Manikas B.Sc.(Hons.) (Adelaide)

This thesis is presented for the degree of
Doctor of Philosophy

Department of Chemistry
University of Adelaide
December, 1993

Awarded 1994

Contents

Chapter 3   AMIDE COMPLEXES

ERRATA SHEET

page 1/line 18	delete '**from**'
page 8/line 9	Ti(β-dik)$_2$X$_2$
page 19/third structure	The carbon atom with the methyl group attached should not be protonated.
page 28/line 1	**These** infrared data **are** ...
page 69/line 13	hydroxyl
page 144/line 23	hydration
page 145/line 1	positive

Abstract

Schiff bases and azo dyes with the potential to behave as dinegative tridentate ligands were used to investigate the formation of stable chelate complexes with post-transition metals. These ligands which are capable of forming five- and six-membered chelate rings using ONO donor atoms formed SnL_2 and/or GeL_2 complexes, containing the metal in the high oxidation state (IV). However, attempts to form SiL_2, PbL_2, $[SbL_2]^-$, $[SbL_2]^+$, SeL_2 and TeL_2 complexes with these ligands were unsuccessful. For comparison purposes, N-salicylidene-o-hydroxybenzylamine, a variant of the Schiff base salicylideneamino-o-hydroxy-benzene capable of forming two six-membered chelate rings, was also used. Products were characterised by elemental and spectral analyses. As well as using synthetic techniques, electrochemical methods were employed to explore the stability of oxidation state (IV) in the SnL_2 and GeL_2 complexes. M(IV)/M(III) and M(III)/M(II) couples were observed and their reduction potentials were found to be dependant on the electronic properties of the ligand.

The complexing ability of the ligands mentioned above was also investigated with diphenylgermanium(IV), -tin(IV) and -lead(IV) and triphenylantimony(V). The stability of the maximum oxidation state for the group (IV) metals and for antimony, was studied electrochemically. M(IV)/M(III) and Sb(V)/Sb(IV) couples were observed, respectively, and were found to be dependant on the type of ligand. For each dinegative tridentate ligand, a series of dimethyltin(IV) and n-dibutyltin(IV) complexes was also prepared and the stability of oxidation state (IV) investigated. Crystal structures of the Schiff base salicylideneamino-o-hydroxybenzene complexed to diphenylgermanium(IV), diphenyltin(IV), diphenyllead(IV) and triphenylantimony(V) were determined and the coordination geometry compared with that in analogous complexes. A trigonal bipyramidal arrangement was observed for the five donor atoms in the tin and germanium coordination sphere. In the case of lead, there was a distorted octahedral arrangement as a result of dimerisation. A distorted octahedral arrangement was observed for the six donor atoms in the antimony complex.

Using amides containing ONO donor atoms and the potential to function as trinegative tridentate ligands, a series of transition metal amide compounds of the type $K_2[ML_2]$ were prepared. Similar ligands of varying electron donating ability were used as well as some naphthol homologues.

Complexation to manganese, titanium, vanadium and iron was investigated. The attainment of oxidation state (IV) was investigated in the solid state by spectroscopic and elemental analysis, and in solution by electrochemistry, electronic spectroscopy, conductance and magnetic moment measurements.

Finally, attempts were made to develop new dinegative tridentate ligands and investigate their ability to complex transition metals in a high oxidation state. The Schiff base salicylideneamino-*o*-hydroxybenzene was chosen as a general formula for the type of compounds we aimed to prepare, modifying it by replacing the azomethine (-CH=N-) group with $-CH_2O-$, $-CO_2-$ and -CH=CH- in order to obtain an ether, ester and alkene, respectively.

Statement

This work contains no material which has been accepted for the award of any other degree or diploma in any university or other tertiary institution and, to the best of my knowledge and belief, contains no material previously published or written by another person, except where due reference has been made in the text.

I give consent to this copy of my thesis, when deposited in the University Library, being available for loan and photocopying.

SIGNED: DATE: 10/12/93

Mary Manikas

Acknowledgements

I would like to thank my supervisor Dr. A.A. Diamantis for his guidance and encouragement during the course of this work. I wish to extend my thanks to Dr. E.R.T. Tiekink for the crystal structure determinations and for supplying some of the diorganotin starting materials. My sincere thanks to my fellow students for their support, advice and friendship, epecially to my fiancee Theo Rodopoulos (who also proof read this thesis) and Rob Jones (who also supplied the Schiff base ligand N-salicylidene-*o*-hydroxybenzylamine). The support from the technical workshops, laboratory staff and spectral services in the deparment is much appreciated.

The financial support of an Australian Postgraduate Research Award for the period of my candidature is gratefully acknowledged.

Special thanks are due to my family for their continued love, understanding and support.

Abbreviations

The following abbreviations were used in this work:

acac	acetylacetonate
diars	o-phenylenebis(dimethylarsine)
DmitH$_2$	4,5-dimercapto-1,3-dithiole-2-thione
py	pyridine
dtbc	3,5-di-*tert*-butylcatecholate
phen	phenanthroline
β-dik	β-diketonate
bpy	2,2'-bipyridine
SatH	2-(o-hydroxyphenyl)benzothiazoline
dpm	2,2,6,6-tetramethylheptane-3,5-dionate
pac	2,2-dimethylhexane-3,5-dionate
tart	tartrate tetraanion
NBS	N-bromosuccinimide
BzacH	benzoylacetone
SalH	salicylaldehyde
HapH	hydroxyacetophenone
BhH	benzoylhydrazine
ApH	o-aminophenol
SalhH	salicylic hydrazide
HbaH	o-hydroxybenzylamine
ApH	aminophenol
β-NapH	β-naphthol
p^{Cl}-PhenolH	p^{Cl}-phenol
p^{Me}-ApH	2-amino-p-cresol
18-crown-6	1,4,7,10,13,16-hexacyclooctadecane
15-crown-5	1,4,7,10,13-pentaoxacyclopentadecane
Me	methyl
Et	ethyl
Pr	propyl
n-Bu	n-butyl
n-OBu	n-butoxide
i-OPr	*iso*-propoxide
Ph	phenyl

Ar	aromatic
OAc	acetyl
Et$_4$NClO$_4$	tetraethylammonium perchlorate
Bu$_4$NBF$_4$	tetrabutylammonium tetrafluoroborate
DMSO	dimethylsulphoxide
CDCl$_3$	deuterated chloroform
(CD$_3$)$_2$SO	deuterated dimethylsulphoxide
MeOH	methanol
CD$_3$OD	deuterated methanol
5,6-chelating	ligand forming five-and six-membered chelate rings upon complexation
6,6-chelating	ligand forming two six-membered chelate rings upon complexation
PVC	polyvinyl chloride
TLC	thin layer chromatography
HPLC	high performance liquid chromatography
PPE	polyphosphate ester
EI	electron impact
FAB	fast atom bombardment
LUMO	lowest unoccupied molecular orbital
HOMO	highest occupied molecular orbital
CV	cyclic voltammetry
NPV	normal pulse voltammetry
OSWV	Osteryoung square wave voltammetry
DPV	differential pulse voltammetry
SCE	saturated calomel electrode
GC	glassy-carbon electrode
V	volts
mV	millivolts (10^{-3} V)
Å	angstroms (10^{-10} m)
μm	micrometres (10^{-6} m)
Λ_m	molar conductance
tga	thermogravimetric analysis
b.p.	boiling point
m.p.	melting point
dec.	decomposes
atm	atmosphere
pH	$-\log_{10}[H_3O^+]$

For infrared data:

s	strong
m	medium
w	weak
sh	shoulder
ms	medium to strong
mw	medium to weak
msh	medium shoulder
mbr	medium and broad
cm^{-1}	wavenumber
v	frequency (cm^{-1})

For NMR data:

ppm	parts per million
δ	chemical shift (ppm)
X	optical electronegativity
t	triplet
s	singlet
m	multiplet
br	broad
NMR	nuclear magnetic resonance
TMS	trimethylsilane
Hz	hertz (s^{-1})
MHz	megahertz ($10^6\ s^{-1}$)
nm	nanometre ($10^{-9}\ m$)

For UV-VIS data:

UV-VIS	ultraviolet-visible
ILT	intraligand transition
CT	charge transfer
LMCT	ligand-to-metal charge transfer
ε	molar extinction coefficient
Δ_o	crystal field splitting

Dinegative tridentate ligands

Abbreviations for the Schiff base ligands are derived from the component carbonyl and amine starting materials. For example, the Schiff base 4-phenyl-butane-2,4-dionebenzoylhydrazone, formed by the condensation of benzoylacetone(BzacH) and benzoylhydrazine (BhH) is abbreviated $BzacBhH_2$, with H_2 indicating the protonated form of the ligand. The azo dyes are abbreviated according to the diazonium salts and hydroxy aromatic compounds involved in their formation.

$BzacBhH_2$	4-phenylbutane-2,4-dionebenzoylhydrazone
$BzacSalhH_2$	4-phenylbutane-2,4-dionesalicyloylhydrazone
$HapBhH_2$	2-hydroxyacetophenonebenzoylhydrazone
$SalApH_2$	salicylideneamino-*o*-hydroxybenzene
$SalBhH_2$	salicylaldehydebenzoylhydrazone
$SalHbaH_2$	N-Salicylidene-*o*-hydroxybenzylamine
$SalSalhH_2$	salicylaldehydesalicyloylhydrazone
$Ap\text{-}\beta\text{-}NapH_2$	*o*-hydroxybenzeneazo-β-naphthol
$p^{Me}\text{-}Ap\text{-}\beta\text{-}NapH_2$	*p*-methyl-*o*-hydroxybenzeneazo-β-naphthol
$Ap\text{-}p^{Cl}\text{-}PhenolH_2$	*o*-hydroxybenzeneazo-*p*-chloro-phenol

Trinegative tridentate ligands:

H_3L^1	N-(2-hydroxyphenyl)salicylamide
H_3L^2	N-(2-hydroxyphenyl)-5-chlorosalicylamide
H_3L^3	N-(5-chloro-2-hydroxyphenyl)salicylamide
H_3L^4	N-(5-chloro-2-hydroxyphenyl)-5-chlorosalicylamide
H_3L^5	N-(2-hydroxyphenyl)-3-methylsalicylamide
H_3L^6	N-(5-chloro-2-hydroxyphenyl)-3-methylsalicylamide
H_3L^7	N-(2-naphthol)salicylamide
H_3L^8	N-(2-naphthol)-5-chlorosalicylamide
H_3L^9	N-(2-naphthol)-3-methylsalicylamide

Chapter 1

INTRODUCTION

1.1 General Introduction

The pronounced biological activity of metal complexes has resulted in a significant interest in coordination chemistry. The vital roles which many metalloproteins and metalloenzymes perform in natural systems are associated with catalytic activity.[1-5] Metal ions in unusual high oxidation states possess electron transfer properties and provide the major source of metallooxidants.

Highly electronegative ligands such as oxide, fluoride or chloride are most effective in giving rise to a high oxidation state in the metal,[6a-f] as shown in Table 1.1 which includes metals used in this study. The stabilisation of high oxidation states in transition metal ions is depicted in Figure 1.1 for transition metals.[6g] The ligands possess filled π orbitals which are lower in energy than the transition metal t_{2g} bonding orbitals. By interacting with ligand orbitals of the same symmetry the t_{2g} orbitals become destabilised relative to the metal antibonding (e_g^*) orbitals. Hence, it becomes easier to lose an electron from from this raised level, or harder to add an electron to this level, known as the highest occupied molecular orbital (HOMO). Thus, reduction of the complex becomes more difficult.

The range of metal complexes arising from these monodentate inorganic ligands, however, is very restricted. This challenged chemists to develop new chemical enviroments, or ligand complements, compatible with oxidising metal centres. Of the highly electronegative ligands mentioned above, only oxygen is able to coordinate from within a chelating system. Consequently, the idea of incorporating such centres into polydentate ligands originated. Resultant compounds of such electron rich polyanion chelates would possess even greater inertness and thermodynamic stability, and at the same time stabilise the high oxidation states in accordance with the scheme shown in Figure 1.1. Knowledge of the chemical behaviour of such molecules can serve to increase the understanding of the function and design of catalysts and electron transfer reagents.

Table 1.1: Ligands Stabilising High Oxidation State Metal Centres.

Oxidation State	Example[a]
Ti(IV)	$Ti(acac)_2Cl_2$, TiF_6^{2-}, $K_2Ti_2O_5$
V(V)	$VOCl_3$, VF_5, V_2O_5, VF_6^-
V(IV)	VCl_4, VO_2
Cr(V)	CrO_4^{3-}, CrF_5, $CrOCl_4^-$
Cr(VI)	CrO_4^{2-}
Mn(V)	MnO_4^{3-}
Mn(IV)	MnO_2, $MnCl_6^{2-}$
Fe(III)	$FeCl_4^-$, Fe_2O_3
Fe(VI)	FeO_4^{2-}
Ge(IV)	GeO_2, $GeCl_4(py)_2$
Sn(IV)	SnF_4, SnO_2, $SnCl_6^{2-}$
Pb(IV)	$PbCl_6^{2-}$, Pb_3O_4

[a] Reference 6a-f.
acac = acetylacetonate anion; py = pyridine.

The amount of research on synthetic models which can mimic biological compounds is enormous.[3,7-11] Ligand structural features can enhance the knowledge on the way in which the metal functions.[1] Modifications of the ligand structure have an effect on the redox potential of the metal ion. The introduction of substituents on the ligands and the effect of ring size in a chelate ring have been thoroughly investigated.[1] Through suitable ligand design it is possible to discover factors which alter the coordination sphere and electronic properties of the central metal atom. These features can then be compared with the activity of natural products.
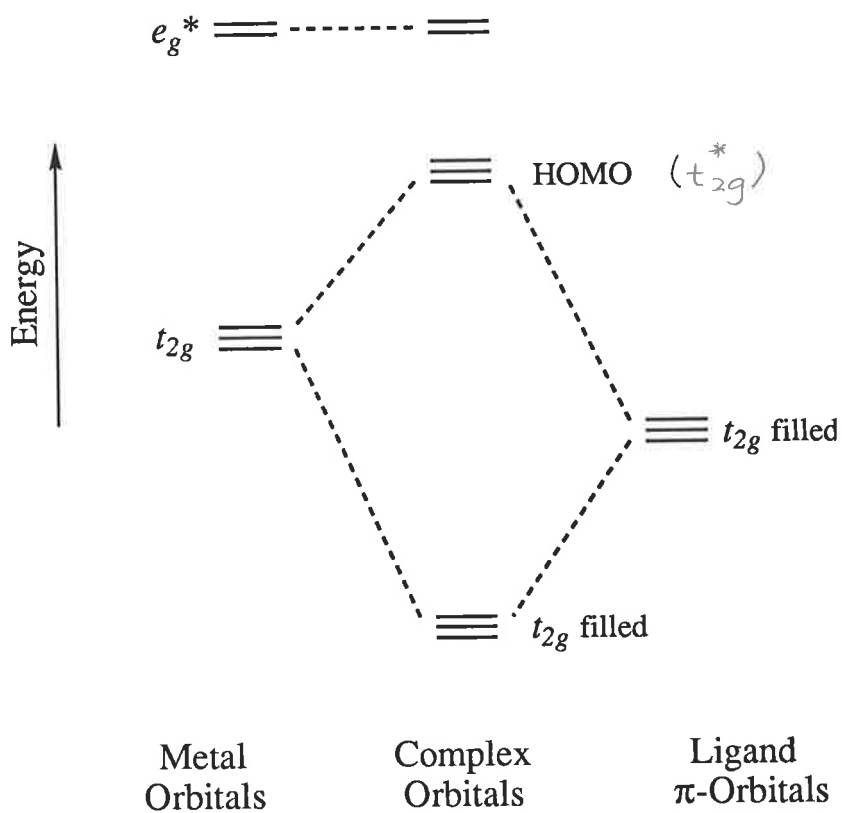
Figure 1.1: *Energy level diagram showing the interaction between the ligand π orbitals and the metal t_{2g} orbitals.*

1.2 Biometals

1.2.1 Manganese

Present in trace amounts, manganese seems to be vital to nearly all forms of life. Associated with the redox function of manganese in biological systems is the metal's ability to adopt a wide range of oxidation states. The very stable Mn(II) cation ($3d^5$) dominates the coordination chemistry of this element. Less is known about the metal in higher oxidation states Mn(IV) - Mn(VII). Manganese(VII) is shown only in compounds containing oxide ligands such as Mn_2O_7, MnO_3X (X = F, Cl) and $KMnO_4$.[12] These compounds are strongly oxidising and unstable.[12] Manganese(VI) and -(V) compounds are stable only in basic solution (e.g. MnO_2Cl_2 and $MnOCl_3$), with disproportionation a common reaction in neutral or acidic media.[12] Reduction potential data reveals that in basic conditions the oxidation potential of the lower oxidation states is strengthened.[13] Except for MnO_2, because of its insolubility, manganese(IV) compounds are not particularly stable. Many are known to be readily hydrolysed and reduced.[12]

Manganese plays an important role in the photosynthetic evolution of molecular oxygen.[7,14-16] Here, in higher oxidation state, manganese acts as a catalyst in the oxidation of water. Manganese is also known to be an active catalytic centre in mitochondrial and various bacterial superoxide dismutases.[16] These discoveries and the recognition of manganese as a vital component in numerous other biological systems, has resulted in much work committed to the preparation and study of the redox behaviour and reactivity of new manganese complexes. Stable complexes of manganese(III) and (IV) can be considered as effective mimics for the function of manganese in biological processes. Thus, an increasing interest has developed in coordination compounds with manganese in oxidation states (III) and (IV).

1.2.2 Vanadium

Vanadium is an important biometal which is able to participate in biological processes in both anionic and cationic forms.[17] Its biological importance was discovered around 1904 where significant concentrations of the metal were found in certain marine animals. Initially, the function of vanadium was

thought to involve oxygen transport, but no agreement on the actual role of the element in these animals exists even today. However, since then, many other possible biochemical roles for vanadium have unfolded, including its requirement in chlorophyll synthesis.[17] A lot of interest has generated from the discovery of the element's presence at the active site of many enzymes, including the nitrogenases in the *Azotobacter* nitrogen-fixing bacterium and the haloperoxidases in sea algae.[17] The diagonal relationship between molybdenum and vanadium in the periodic table, resulting in a strong resemblance between them, has seen the development of model compounds for vanadium nitrogenase.[17,18]

Vanadium can exist in several oxidation states, but only the higher oxidation states are involved in physiological systems, with V(IV) and V(V) the most common, associated with VO^{2+} and VO_2^+, respectively. Oxidation states below (III) are reducing and commonly do not survive in aqueous media.[11] The biological activity of vanadium has challenged many chemists to prepare model compounds, as the coordination chemistry can elucidate the role played by vanadium in biological systems. A vast range of polydentate ligands have been used in different studies.[11,17,19-28] Numerous complexes of vanadium have been proven active in therapeutic applications.[17] For example, a hydrazine complex has shown high activity against tuberculosis mycobacteria, and peroxovanadate(V) complexes have shown insulin-like action in diabetic rats as well as antitumor activity in particular forms of leukemia. The coordination of the histidine (imidazolylalanine) constituent of proteins to biometals such as Fe(II)/(III) and Mn(II)/(III)/(IV) has prompted an interest in similar interactions with vanadium.[17]

1.2.3 Iron

Iron participates in a vast range of biological processes, too many to be reviewed here. However, some references to higher oxidation states are highlighted. Iron occurs at the active centre of molecules which are involved in oxygen and electron transport, as well as being present in metalloenzymes.[6h] Common oxidation states for iron are (II) and (III) and the coordination chemistry of higher oxidation states is limited. The complexes in high oxidation states are important reactive intermediates in enzymatic oxidations.[4,5,29] Indication that porphyriniron(IV) is contained in oxidised forms of horseradish peroxidase and catalase has led to an interest in the

biological chemistry of iron(IV).[5,30] Fe(V) has also been reported in biological systems, but much less frequently.[31]

Iron(IV) complexes are rare. Stable compounds do exist in this oxidation state, such as *trans*-dichlorobis(*o*-phenylenebis(dimethylarsine))iron(IV) tetrafluoroborate, [Fe(diars)$_2$Cl$_2$](BF$_4$)$_2$.[5] Fe(IV) is also contained in some bis(dithiolene) chelates but the oxidation state remains ambiguous because the redox reaction could be centred on the ligand (Section 1.3.1).[32] An iron(IV) porphyrin has also been prepared, as have dithiocarbamate complexes.[33] Studies on the latter as model compounds for iron-sulphur complexes, like the ferredoxins, have also been carried out.[5] In another report, a seven-coordinate Fe(IV) complex is suggested in an oxidative addition model for the binding of dioxygen to haemoglobin.[31] Interest in the physicochemical properties of high valent iron is increasing.[34,35]

1.3 Chemical Enviroments

Atoms in biological molecules that can act as donors are sulphur (sulphide, thiolate), nitrogen (amide, amine) and oxygen (oxide, hydroxide, water, carboxylate, alcoholate and phenolate). Numerous examples of ligands containing such donor atoms, complexed to transition metals, exist. Many have been found to have the same effect as oxo or halide ligands in stabilising the high oxidation states of transition metals.

1.3.1 Ligands that Stabilise High Oxidation States

As depicted in Figure 1.1, the higher oxidation states of transition metals are attained with ligands containing π-donor atoms. The majority of this class of compounds contain oxygen donor atoms, such as enolates (including dihydroxy phenols[36]), β-diketonates and carboxylates.

Polyhydroxy complexes have been found to be able to stabilise high oxidation states in transition metals. Catechol (1,2-dihydroxybenzene) and its substituted derivatives are effective bidentate chelates. Examples include the non-vanadyl complexes bis(triethylammonium)tris(catecholato)vanadium(IV),[37] bis(catecholato)vanadium(IV)[38] and the disodium salt of dichlorobis(3,5-di-*tert*-butyl-catecholato)vanadium(IV).[38] Similar compounds of titanium are also known ($[Et_3NH]_2[Ti(O_2C_6H_4)_3]$).[39] The catecholates have also been used to prepare tris(bidentate) complexes of the form $Tl_2[V(RC_6H_3O_2)_3]$ (R=H, 3-CH$_3$, 4-CH$_3$ and 3-OCH$_3$),[40] mixed ligand complexes such as (catecholato)bis(β-diketonato)vanadium(IV),[41] $V(bpy)(C_6Cl_4O_2)_2$ (bpy = 2,2'-bipyridine)[21] and [V(dtbc)$_2$(phen)].CH$_2$Cl$_2$ (dtbc = 3,5-di-*tert*-butylcatecholate; phen = phenanthroline),[42] as well as bis(catecholato)iron(III).[43] Stable manganese catechol complexes have been prepared to mimic the manganese cofactor of photosystem II and manganese superoxide dismutases.[16] The high affinity for catecholate oxygen donor atoms has also been demonstrated by main group elements, as illustrated by the tellurium(IV) complex $Te(C_6H_4O_2)_2$,[44,45] the five coordinate bis(catecholato) complexes of silicon(IV) of the type [RSiL$_2$]$^-$ (R = Ph, Me, Et or *n*-Pr; L = dianion of catechol or its derivatives),[46] the arsenic complex $K[As(O_2C_6H_4)_2]^{6i}$ and the phosphorus compound $CH_3P(O_2C_6H_4)_2$.[6j]

Although metal β-diketones were discovered around 1887, it was not until 1945 that aromaticity within the β-diketonate ring was put forward.[47] As well as coordinating to a metal as a bidentate chelate, β-diketones can be monodentate and bridge metal atoms. Complex formation with these ligands has been thoroughly studied with transition metals. Hexachloroantimonate(V) salts of tris(acetylacetonato)vanadium(IV) and tris(1-phenyl-1,3-butane-dionato)vanadium(IV),[48] as well as tris(β-diketonato)Ru(III)[49] complexes with acetylacetonate and 4,4,4-trifluoro-1-phenyl-1,3-butanedionate,[49] and the dihalobis-β-diketonates, $Ti(\beta\text{-dik})X_2$ (X = Cl, F, Br; β-dik = anion of acetylacetone, dibenzoylmethane and benzoylacetone)[50] are some examples. Numerous examples also exist with non-transition elements such as diorganotellurium(IV) bis(β-diketonato) with acetylacetonate,[51] 2,2,6,6-tetra-methylheptane-3,5-dionate[51] and benzoylacetonate,[52] as well as complexes with the group(IV) elements[53,54] such as $[Si(acac)_3]Cl$.[55,56]

Oxygen-containing functional groups found in proteins, such as the carboxylate of glutamic and aspartic acids and the alkoxo group of serine, has led to the preparation of model compounds containing these types of coordination.[11] Numerous vanadium-oxygen coordination complexes of ligands containing carboxylates have been developed which may have some significance to biological processes.[11] Carboxylate bridged complexes of V(III) and V(IV) as well as mononuclear carboxylato complexes of V(V) are known. The latter are believed to be models for the binding of vanadium to bromoperoxidases. Peroxo complexes of vanadium have become important models for haloperoxidase enzymes, vanadium transferrin complexes have been prepared, and vanadium-alkoxo complexation has recently been investigated.[11] These electron rich oxygen donor ligands are also capable of attaining high oxidation states with main group elements. This area of work has received much attention since such compounds have important technological applications. Organotin(IV) carboxylate compounds[57-59] have industrial (catalysts and PVC stabilisers),[60,61] agricultural (biocides)[60,62] and biological (anti-tumor activity)[60] applications. Dicarboxylic acids,[61,63] nicotinic acid and nicotinic acid N-oxide,[64] picolinic acid and picolinic acid N-oxide,[65] pyridine-2-carboxylic acid,[62] pyrazine carboxylic acids[62] and maleanic acids[58] are examples of some of the compounds studied. Diorganotin benzoates have shown antitumor activity, with doses for prevention of tumor growth considerably lower than that required for *cis*-platin compounds.[66] In addition to these studies, Gielen *et al.* synthesised diethyl- and dibutyltin(IV) complexes of methylthio-*o*-substituted aza

derivatives of the benzoates, which were also found to inhibit tumor growth.[66] Much interest exists in amino acid and peptide systems.[59] Other main group elements[67,68] and transition metals[69,70] have also been investigated with such ligands.

Sulphur atoms are also very good π-donors. Because thiolates occur extensively in metalloproteins and their is evidence for vanadium-sulphur coordination in vanadium-nitrogenase, much interest now lies in the preparation of vanadium-sulphur complexes.[11] 1,2-Dithiolene complexes such as $V[S_2C_2(C_6H_5)_2]_3$ and $[V(S_2C_2\{CN\}_2)_3][(CH_3)_4N]_2$ have been reported.[71] It should be mentioned that 1,2-dithiolenes are among the category of ligands which produce a range of compounds with the metal, apparently, in many different oxidation states. There is ambiguity in the assignment of the metal oxidation states because the extended ligand π systems allow delocalisation of electrons onto the ligands, resulting in oxidation-reduction processes between essentially similar structures which differ only in their electron populations.[6k] This is represented below in Equation 1.1.

$$[Ni(S_2C_2Ph_2)_2] \underset{-e^-}{\overset{+e^-}{\rightleftharpoons}} [Ni(S_2C_2Ph_2)_2]^- \underset{-e^-}{\overset{+e^-}{\rightleftharpoons}} [Ni(S_2C_2Ph_2)_2]^{2-} \qquad \textbf{(1.1)}$$
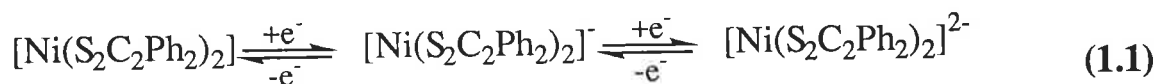
The neutral complex can be considered as a Ni(0) complex of two dithioketones, a Ni(II) complex of one dithioketone and one dithiolate anion, or as a Ni(IV) complex of two dithiolate anions. The ambiguity here is over the extent to which electrons are in the metal d orbitals or delocalised over the ligand.

1.3.2 Schiff Base Ligands

An abundance of information exists on metal complexes of Schiff base ligands. The great flexibility in their formation has produced many ligands of diverse structural type. Condensation of β-diketones or o-hydroxy carbonyls with monodentate amines and condensation of aldehydes or ketones with semicarbazide hydrochloride both yield bidentate ON donor Schiff bases,

with N-substituted salicylideneimines (*o*-HOArCR=NR') and semicarbazones (RR'C=NNHCONH$_2$) among well known examples of these types of compounds widely used for coordination to transition metals[72-75] and main group elements.[76-80] Alternatively, the condensation of β-diketones or *o*-hydroxy carbonyls with chelating amines can yield tridentate ONO donor Schiff base ligands.

Sulphur containing compounds have also attracted interest because of their biological importance and, as a result, a great number of Schiff base compounds comprising sulphur have been similarly developed. Bidentate SN donor compounds can be derived from the condensation of thiol carbonyls with monodentate amines, or carbonyls with a chelating amine (e.g. thiosemicarbazide). The latter group of ligands are known as the thiosemicarbazones. Examples include thiosemicarbazones of furfuraldehyde, *o*-hydroxyacetophenone, 2-methoxybenzaldehyde, salicylaldehyde, benzil, benzylmethylketone and *o*-hydroxynaphthaldehyde, all studied by Nath *et al.*,[78,81] and Schiff bases derived from S-benzyldithiocarbazate[82] and 2-hydroxy-3-methoxybenzaldehyde,[82] 2-hydroxy-1-naphthaldehyde[82] or pyridine-2-carboxaldehyde.[83] Tridentate SNO Schiff bases are derived from the condensation of hydroxy carbonyls with a chelating amine (e.g. dithiosemicarbazates). With many of these sulphur drugs, increased biological activity is observed when they are supplied as metal complexes.[78,84,85] This area has been thoroughly investigated and interest still exists in this work due to the increasing potential of these complexes.[86-88]

Many vanadium(IV) complexes contain, in their coordination sphere, oxo, thiolato or halide ions to achieve this high oxidation state, such as VO(acac)$_2$, VO(acac)$_2$py, V(S$_2$CMe)$_4$, V(acac)$_2$Cl$_2$ and VCl$_4$(diars)$_2$ (diars = *o*-phenylenebis(dimethylarsine)).[6b] Dinegative tridentate ligands have been able to replace these electron rich functions to form stable vanadium(IV) products, suggesting that the π-donor ability of these dinegative tridentate ligands is comparable to that of the replaced ligands. In 1976, Diamantis prepared the bis(tridentate) non-vanadyl complex, bis(pentane-2,4-dionebenzoylhydrazonato)vanadium(IV) complex, abbreviated V(AcacBh)$_2$.[89] The ligand is a dinegative, tridentate Schiff base of ONO donor type, as shown below, and forms five- and six-membered chelate rings with the metal atom.

$$^-\text{O} \qquad \text{N} \qquad \text{O}^-$$

V(BcacBh)$_2$[90] and V(SalBh)$_2$[91] were later prepared in the same laboratory. A wide range of Schiff bases have since been prepared from the appropriate bidentate carbonyl and amine components, which has resulted in the formation of many VL$_2$ complexes.[92] Vanadium complexes of dinegative tridentate ONO donor azo dye ligands then followed. Analogous ML$_2$ complexes with other transition metals have also been investigated with dinegative tridentate Schiff base ligands. For example, the ruthenium(IV) complexes Ru(BzacBh)$_2$ and Ru(BzacSalh)$_2$ from RuCl$_3$.3H$_2$O, prepared by Moritz,[93] and numerous titanium(IV) complexes.[92] Currently, similar studies are being carried out with the metals manganese, chromium and iron to achieve oxidation state (IV) with the same ligands developed by Salam.[94]

Much attention over the last two decades has been the use of amino acids in providing the amino group for Schiff base formation. Nath *et al.* have prepared transition metal complexes of pyridoxal (vitamin B$_6$ aldehyde)-amino acid Schiff bases.[10] It is thought that these Schiff bases are intermediates in biologically important amination processes.

Thiosemicarbazones, which have been formed by condensation of the aldehyde -CHO and thiosemicarbazide -NH$_2$ functions, have shown antifungal and antibacterial activity.[95] These include thiosemicarbazones derived from the condensation of 2-pyridine-carboxaldehyde with thiosemicarbazide or 4-phenyl-thiosemicarbazide, and *p*-anisaldehyde with thiosemicarbazide. Increased biological activity was produced when these Schiff bases were complexed to organotin(IV).[95] Anti-cancer activity has been observed with NS and ONS donor dithiocarbazates. In particular, S-methyl and S-benzyldithiocarbazate Schiff bases complexed to non-transition metals have been the topic of many studies over the past decade because of evident biological activity. This has resulted in numerous Sn(IV),[82] Pb(IV),[82] Si(IV)[87] and organosilicon(IV)[87] complexes.

1.4 Research Aims

The aims in our research were (i) to extend the studies fruitfully explored by Salam[92] by expanding the range of metals to include main group metals for which dinegative ONO donor type ligands (Schiff base and azo dye) can attain a high oxidation state, (ii) to develop ONO donor type ligands which are potentially trinegative, in the hope of attaining oxidation state (IV) with titanium, vanadium, manganese and iron, and (iii) to develop new tridentate ligands and investigate their ability to complex transition and main group elements. The work is divided into four sections.

1.4.1 Bis(Tridentate) Complexes

Using dinegative tridentate Schiff base and azo dye ligands of varying electron donating ability we sought to investigate the formation of ML_2 type compounds with elements of main groups (IV), (V) and (VI). The stability of the high oxidation state was explored using synthetic and electrochemical techniques. Products of reactions were characterised by elemental and spectral analysis. For one of the Schiff base ligands (5,6-chelating), complexation of its 6,6-chelating derivative was also carried out in order to make comparisons in stability.

5,6-chelating Schiff base   *6,6-chelating Schiff base*

1.4.2 Organometal Complexes

From extensive studies carried out on biometals, considerable interest has been with the transition metals. Since nowhere near as many accounts on non-transition and organometal complexes with such important ligands exist, it was of great interest to also investigate this area.

As some of the main group elements studied did not show the coordination of two tridentate ligands, diorgano (for elements germanium, tin and lead) and triorgano (for antimony) derivatives, in which one dinegative tridentate ligand was complexed, were synthesised using the same variety of ligands employed in Section 1.4.1. The stability of oxidation state (IV) was studied electrochemically. Furthermore, for each dinegative tridentate ligand, a series of diorganotin(IV) compounds in which the organo substituent was varied were prepared and the stability of their oxidation state (IV) was investigated. The geometry of the coordination in these complexes was also of interest. Crystal structures were determined for Schiff base salicylideneamino-*o*-hydroxybenzene complexed to diphenylgermanium(IV), diphenyltin(IV), diphenyllead(IV) and triphenylantimony(V).

1.4.3 Amide Complexes

The aim in this section was to further studies made by Koikawa *et al.*[96] with trinegative ONO donor amide ligands used to prepare $K_2[ML_2]$ type compounds. Similar ligands of varying electron donating ability, as well as naphthol homologues were prepared and used. Complexation to manganese, titanium, vanadium and iron was investigated. Formation of the aimed oxidation state (IV) was investigated in the solid state, by spectroscopic and elemental analysis, as well as in solution, by electrochemistry, electronic spectroscopy, conductance and magnetic moment measurements.

1.4.4 Other Ligands

Attempts were made to synthesise tridentate ligands, analogous to the Schiff base salicylideneamino-*o*-hydroxybenzene, in which the two aromatic hydroxy functions were bridged by an ether (-CH$_2$O-), ester (-CO$_2$-) or alkene (-CH=CH-) function instead of an azomethine (-CH=N-) group. Studies would then be carried out to determine if such compounds are also able to form complexes containing the metal in a high oxidation state.

Chapter 2

SCHIFF BASE AND AZO DYE COMPLEXES

2.1 Introduction

Chelating ligands which have the same effect as highly electronegative halide or oxide ions in stabilising the high oxidation state of various transition metals have been developed in this laboratory. Dinegative tridentate ONO donor Schiff base and azo dye ligands have proved most successful in producing a wide range of VL_2 complexes.[92] Since then, their use has been extended to include the formation of ML_2 complexes, where M = titanium,[92] ruthenium,[93] group (IV) elements,[97] and more recently, manganese, chromium and iron.[94]

ML_2 complexes of the group (IV) elements germanium and tin with Schiff base and azo dye ligands were investigated in 1987.[97] Their formation was not surprising, as oxygen donor chelates are known to achieve high oxidation states with many main group (IV) elements and the heavier elements in groups (V) and (VI). The catecholates are a prime example among others included in Table 2.1. Although with the non-metals phosphorus and arsenic it is customary to describe the oxygen bonded compounds as esters, it is noteworthy that the analogous catecholates have been reported.[6i,j]

It was considered worthwhile to extend the work on germanium and tin with azo dye ligands and to also prepare ML_2 type complexes of silicon and lead, as well as antimony from group (V) and selenium and tellurium from group (VI). Heavier post-transition metals have group number oxidation states corresponding to d^{10} configurations, such as Sn(IV), Pb(IV), In(III) and Sb(V). However, these metals have a tendency to use only their p electrons and as a result exhibit oxidation states two less than their group number.[98a] This is termed the "inert s^2 pair effect" (the energy of the s orbital is lowered due to relativistic effects[99]). It is worth mentioning that in previous work attempts to prepare $M^{II}L$ or $(Bu_4N)_2[M^{II}L_2]$ complexes of germanium and tin always resulted in the formation of the $M^{IV}L_2$ complex.[97] Common oxidation states for group (IV) elements are (II) and (IV), with the stability of

Table 2.1: Examples of Compounds in which Chelating Ligands have been used to Achieve High Metal Oxidation States.

Element	Example
Silicon	$Si(O_2C_6H_4)_2{}^a$, $[Si(acac)_3]^{+a}$
Germanium	$Ge(acac)_2Cl_2{}^b$, $[Ge(O_2C_6H_4)_3]^{2-c}$, $[Ge(O_4C_2)_3]^{2-d}$
Tin	$Sn(acac)_2Br_2{}^b$, $Sn(BzacBh)_2{}^e$
Antimony	$K_2[Sb_2(tart)_2].3H_2O^f$, $(acac)SbCl_4{}^g$
Tellurium	$Te(O_2C_6H_4)_2{}^h$
Phosphorus	$CH_3P(O_2C_6H_4)_2{}^i$
Arsenic	$K[As(O_2C_6H_4)_2]^j$

a Reference 6f; *b* Reference 53; *c* Reference 100; *d* Reference 101 ; *e* Reference 97; *f* Reference 61; *g* Reference 54; *h* Reference 44; *i* Reference6j; *j* Reference 6i. acac = acetylacetonate anion; tart = tartrate tetraanion.

M(II) relative to M(IV) increasing down the group. This is attributed to the inert pair effect. A notable exception is the organometallic chemistry of tin and lead which is almost confined to oxidation state (IV). In contrast, the majority of inorganic lead compounds are halides and oxides containing Pb(II). Inorganic Pb(IV) compounds are either very reactive, unstable short-lived materials, or have not been reported. For example, lead tetraacetate is a powerful oxidising agent. Organolead compounds, R_4Pb (R = alkyl or aryl), are stable compared with the divalent R_2Pb compounds. The contrast between the two types of compounds is best seen in the mixed ligand compounds R_nPbX_{4-n} (X = electronegative donor) in which stability decreases as n increases.[102] Kaupp and Schleyer accounted for this by population analysis of molecular wave functions.[103] They concluded that the metal charge is enhanced by the electronegative donor, increasing the difference in size of the $6s$ and $6p$ orbitals. As a result, the participation of the $6p$ orbitals to covalently bond to Pb(IV) is lessened as the number of electronegative groups increases. While these effects weaken the bonds, the increasing *s*-character essentially produces shorter bond lengths. The inert-pair effect suggests that the metal *s* orbitals do not take part in bonding because they are too low in energy, whereas the explanation above by Kaupp and Schleyer suggests sp^n hybridisation becomes less favourable as the difference in radial

extensions of the s and p orbitals increases, resulting in weaker covalent bonds.

In group (IV), although GeL$_2$ and SnL$_2$ could be obtained readily, PbL$_2$ could not be achieved inspite of the various forcing conditions used. These are described in the sections to follow. Similarly with groups (V) and (VI), we were unable to prepare six coordinate complexes of the type [ML$_2$]$^{+/-}$ or ML$_2$, respectively. Thus, it seemed that our tridentate ligands behaved more like the halide/oxide ligands with the metals germanium and tin. Inspite the extra advantage of a six coordinate complex, the tridentate ligands employed were unable to stabilise lead, group (V) and (VI) elements in their highest oxidation states. We were able, however, to prepare organo derivatives of these elements with the dinegative tridentate ligands, achieving high valent compounds (Ph$_2$PbL and Ph$_3$SbL complexes were attempted only). Similar R$_2$ML type (R = Me, n-Bu or Ph) compounds of germanium and tin were also prepared.

The research on organometal complexes of non-transition elements with ligands capable of attaining the elements in high oxidation states has become increasingly popular. Most work is committed to the development of tin compounds, however interest has also spread to germanium,[104] lead[105-112] and antimony.[113-127] Research in this area has been stimulated by the recognition of the pharmacological potential of tin compounds.

Initial studies investigating antitumor activity of organotin compounds were carried out in 1929.[128] By 1982 around 1500 organotin compounds had been examined for antitumor properties.[129] Although only a small percentage of the compounds were active in certain types of leukaemia, pronounced activity was found to occur with the diorganotin compounds. Their great potential as antitumor agents is strengthened because of their low toxicity. Over the last decade much interest has been in this area, with most work limited to P388 Lymphocyte leukaemia in mice.[9,85,128,129,130]

Currently, organotin compounds have an industrial economic importance.[131] Industrially they are used as wood preservatives, active elements for antifouling paints, biocides in agriculture and as stabilisers for PVC polymers affording protection against degradation by exposure to air, light or heat.[132]

Seven Schiff bases (six 5,6-chelating and one 6,6-chelating) and three azo dyes (5,6-chelating) of varying electron donating ability were used as ligands

to produce complexes. Two of the azo dyes and all Schiff bases were chosen to investigate the formation of ML_2 complexes of group (IV), group (V) and group (VI) elements. Four of these Schiff bases and two azo dyes, all 5,6-chelating, were chosen to prepare diorganometal(chelate) complexes with group (IV) elements and triorganometal(chelate) complexes with antimony. All complexes successfully prepared were characterised by spectroscopic and elemental analyses and the stability of the high oxidation state investigated by electrochemical techniques.

Of special interest was the coordination geometry of the organometal compounds, in particular any differences in stereochemistry down group (IV). In discussing the structural types of organometal compounds of groups (IV) and (V) it is customary to differentiate between the number of organic substituents by the prefix tetra-, tri-, and di- and the total coordination number which can be increased by the attachment of anionic ligands. The crystal structure for each metal complex of deprotonated salicylideneamino-*o*-hydroxybenzene was determined.

2.2 Ligands

2.2.1 Schiff Bases

The Schiff bases were formed by the condensation of benzoylacetone (BzacH), salicylaldehyde (SalH) or *o*-hydroxyacetophenone (HapH) with benzoylhydrazine (BhH), *o*-aminophenol (ApH), salicylic hydrazide (SalhH) or *o*-hydroxybenzylamine (HbaH). Nucleophilic addition to the carbonyl, in which the nucleophile carries an acidic proton, followed by elimination of water, yields the Schiff base. In this study seven Schiff base ligands were used, all dinegative tridentate ONO donors forming five- and six-membered rings, and in one case two six-membered rings, on coordination to a metal. Their names, structures, and abbreviations derived from the component carbonyl and amine starting materials, are presented in Table 2.2.

Crystallographic studies have revealed that Schiff base ligands retain their planar form upon coordination, and in ML_2 type complexes of these ligands, geometries range from trigonal prismatic to *meridional* octahedral.[133]

2.2.2 Azo Dyes

These compounds were formed by the coupling of the diazonium salt of the aminophenol (p^{Me}-ApH or ApH) to β-naphthol (β-NapH) or p^{Cl}-phenol (p^{Cl}-PhenolH). For the preparation of Ap-p^{Cl}-PhenolH$_2$, direct coupling of the diazonium salt of *o*-aminophenol with p^{Cl}-phenol was not possible[92]. The hydroxyl group in p^{Cl}-phenol had to be protected by methylation before coupling to *o*-aminophenol could take place. Aluminium chloride was then used to remove the protecting group. The names, structures and abbreviations for these ligands are also shown in Table 2.2. The diazo -N=N- group in these compounds is isosteric with the azomethine >C=N group in Schiff bases.[92]

During an attempt to purify the SnL_2 complex of the azo dye Ap-β-Nap, crystals of the protonated ligand suitable for X-ray analysis were obtained instead. The structure is depicted in Figure 2.1. Intra- and intermolecular hydrogen bonding was observed.[134] A surprising feature of the structure was that the azo dye was found to exist in the hydrazone form as represented in Figure 2.2. Similar observations have previously been made.[135,136]

Table 2.2: Names, Abbreviations and Structures of the Protonated Schiff Base and Azo Dye Ligands used in this Study.
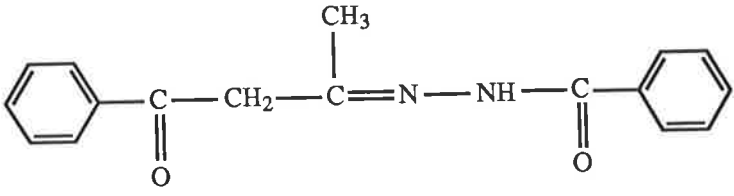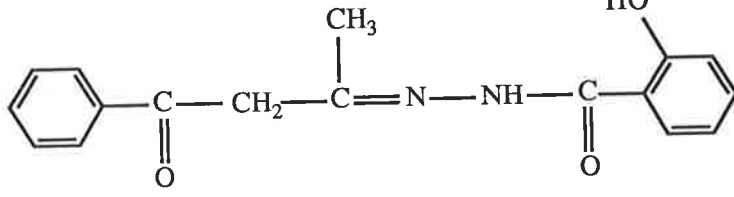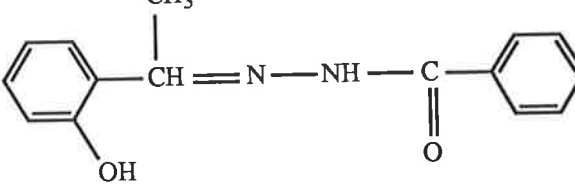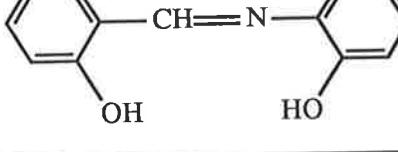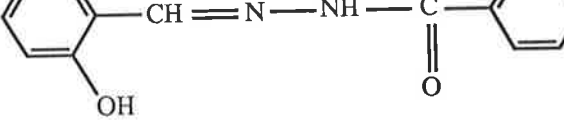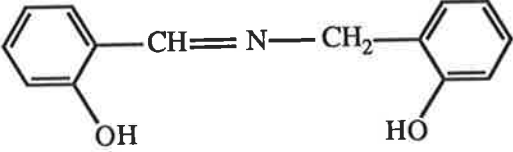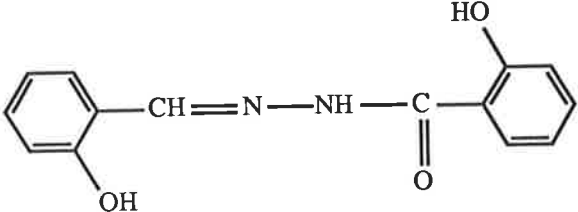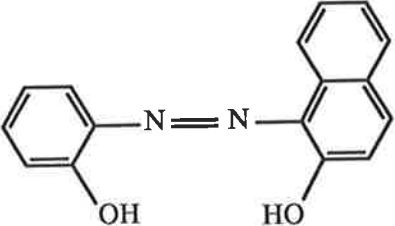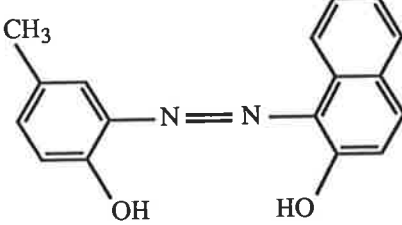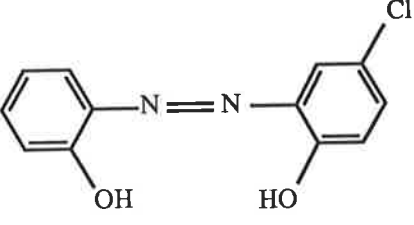
Name (Abbreviation)	Structure
Schiff Bases: 4-phenylbutane-2,4-dione-benzoylhydrazone (BzacBhH$_2$)	
4-phenylbutane-2,4-dione-salicyloylhydrazone (BzacSalhH$_2$)	
2-hydroxyacetophenone-benzoylhydrazone (HapBhH$_2$)	
salicylideneamino-*o*-hydroxybenzene (SalApH$_2$)	
salicylaldehydebenzoylhydrazone (SalBhH$_2$)	

Table 2.2: continued...

N-Salicylidene-*o*-hydroxybenzylamine (SalHbaH₂)	
salicylaldehydesalicyloylhydrazone (SalSalhH₂)	
Azo Dyes: *o*-hydroxybenzeneazo-β-naphthol (Ap-β-NapH₂)	
p-methyl-*o*-hydroxybenzeneazo-β-naphthol (*p*Me-Ap-β-NapH₂)	
o-hydroxybenzeneazo-*p*-chlorophenol (Ap-*p*Cl-PhenolH₂)	

molecule b
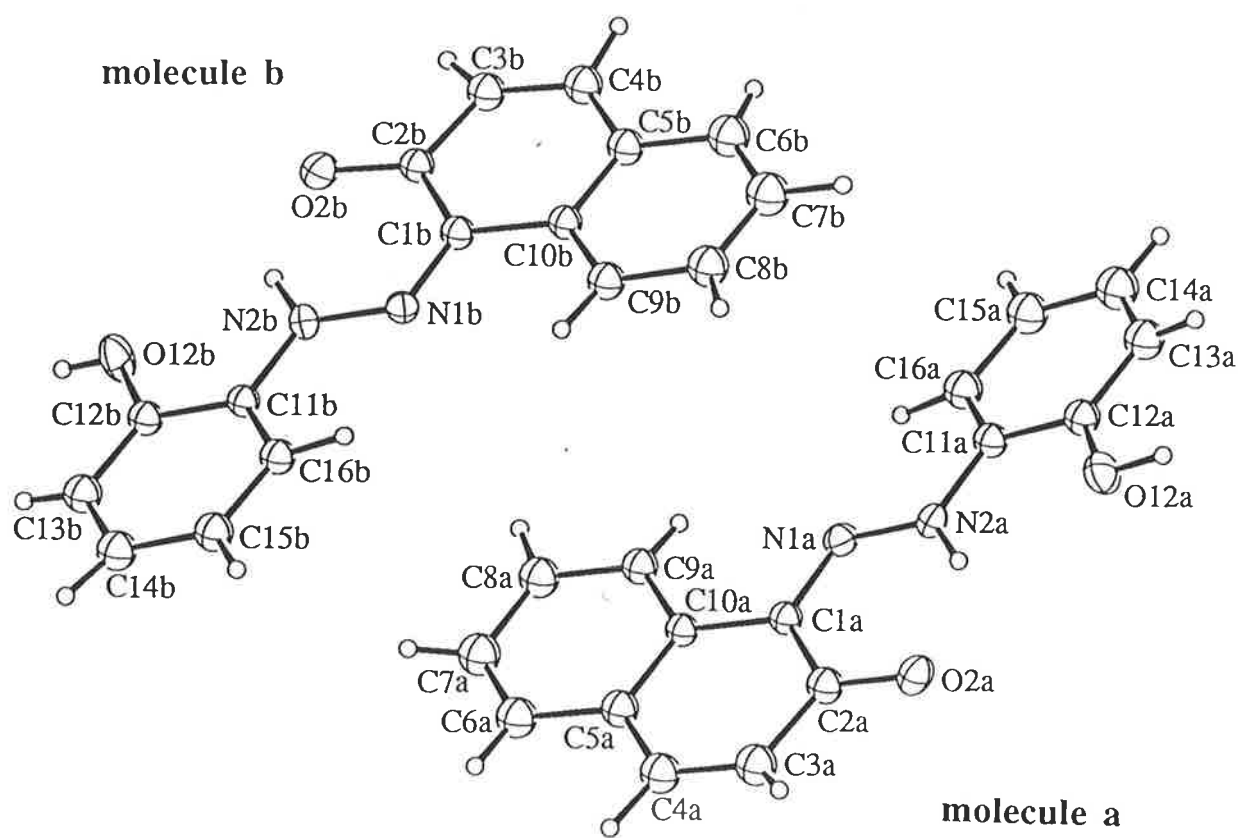
molecule a

Figure 2.1: *The molecular structure of the azo dye Ap-β-NapH2.*

Azo form   **Hydrazo form**
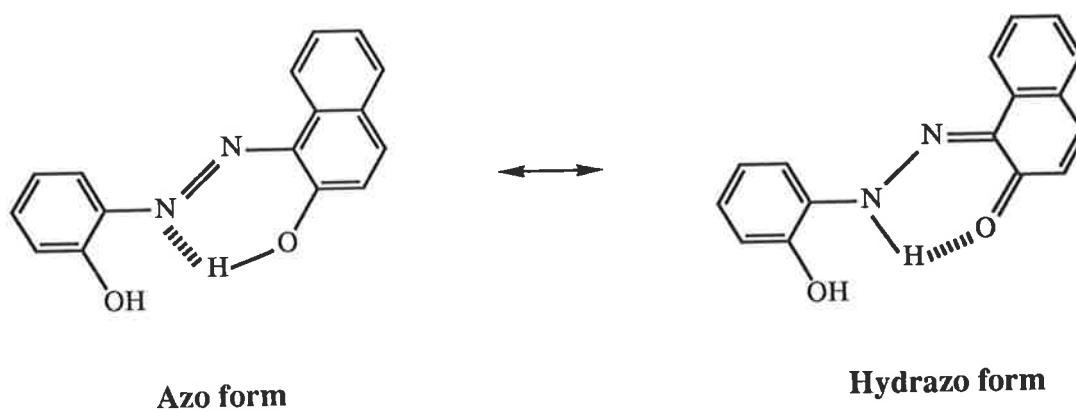
Figure 2.2: *Azo-hydrazo tautomerism for the azo dye Ap-β-NapH₂*

2.3 Preparation of Complexes

2.3.1 Bis(Dinegative Tridentate) Complexes

Attempts were made to synthesise ML_2 complexes with elements of group (IV) (silicon, germanium, tin and lead) and group (VI) (selenium and tellurium), as well as $[ML_2]A$ complexes of antimony from group (V), where A = alkali metal or halide. The general procedure for the preparation of these complexes was the same as that employed for GeL_2 and SnL_2 complexes in previous work.[97] The metal-containing starting material was added to an ethanolic solution of two mole equivalent ligand and at least four mole equivalent base.

2.3.1.1 Silicon Complexes

Attempts were made to prepare SiL_2 complexes, where L = BzacBh, SalAp and Ap-β-Nap, using silicon tetrachloride as the source of metal. Experiments involving the $BzacBhH_2$ ligand, carried out at room temperature or under refluxing conditions and using lithium acetate or sodium ethoxide as the base, yielded identical products. The products obtained were either white or pale yellow in colour and examined by infrared (Section 2.5) and mass spectroscopy (Section 2.4). In addition, one product was also examined by ^{1}H-NMR spectroscopy. It was obvious from the spectral analyses that the products were not the expected SiL_2 compounds, and it was clear that the acidic protons of $BzacBhH_2$ had not been replaced under the conditions used. In an attempt to minimise the solvolysis of silicon tetrachloride, the reaction with $BzacBhH_2$ was also carried out in dichloromethane at low temperatures. Although a different product was formed, and elimination of the acidic protons was suggested by spectral analysis, the product again was not the expected SiL_2 complex.

Varying the metal to ligand ratio from 2:1 to 1:1 yielded identical products with the Schiff base $SalApH_2$. Whereas, recrystallisation of the product obtained with the azo dye $Ap-β-NapH_2$ resulted in decomposition.

No further attempts were made to synthesise complexes of the type SiL_2 because clearly, the reaction did not proceed in the anticipated way. This may

be due to the strong reactivity of the silicon tetrachloride or steric hinderance which may result from the small size of silicon.

2.3.1.2 *Germanium and Tin Complexes*

GeL_2 complexes, where L = the azo dye ligands Ap-β−Nap and Ap-p^{Cl}-Phenol, and SnL_2 complexes, where L = the azo dye Ap-β−Nap and Schiff base SalHba, were successfully prepared. The $SalHbaH_2$ Schiff base was of interest because it is the 6,6-chelating homologue of SalAp, i.e. a methylene group is situated between the aromatic ring and NH group in the aminophenol moiety. The starting materials for the synthesis of the GeL_2 and SnL_2 complexes were germanium tetrachloride and tin dichloride, respectively, and lithium acetate as the base. As germanium tetrachloride is susceptible to hydrolysis, reactions were carried out under an atmosphere of dinitrogen. Tin dichloride, instead of tin tetrachloride, was used as the starting material for convenience. The tin reactions were protected from moisture, due to the starting material's susceptibility to hydrolysis, with a silica-gel drying tube. It has been shown that this tin starting material also produces $Sn^{IV}L_2$ complexes even under an atmosphere of dinitrogen.[97]

The complexes of the azo dyes were equally strongly coloured as the protonated ligand, while that of the Schiff base SalHba was pale yellow. All compounds were high melting, and ML_2 formation was supported by spectroscopic and elemental analyses.

2.3.1.3 *Lead Complexes*

Two moles of the protonated ligands $BzacBhH_2$, $BzacSalhH_2$, $HapBhH_2$, $SalApH_2$, $SalBhH_2$, $SalSalhH_2$ and p^{Cl}-Ap-β-NapH_2$ were each reacted with one mole of lead nitrate using lithium acetate as the base (four mole equivalent). Reactions were performed open to the atmosphere to facilitate the oxidation of Pb(II). Except for the orange or brown product obtained with $SalApH_2$, all other ligands produced yellow compounds which decomposed or melted at high temperatures. Complexation of each ligand was confirmed by infrared spectroscopy, however mass spectroscopy and elemental analysis revealed only a 1:1 metal to ligand complex was formed in all cases. This stoichiometric ratio was further supported by the fact that $BzacBhH_2$ and

SalApH$_2$ produced identical products to those described above when the reactions were carried out with a 1:1 lead nitrate to ligand mole ratio.

Several variations to the experimental procedure described above were made in order to try and synthesise the PbL$_2$ complexes. Replacing lithium acetate with a stronger base, such as sodium ethoxide, in the reaction of lead nitrate with SalSalhH$_2$ yielded the 1:1 product again. Attempts were also made to synthesise the PbL$_2$ complex of SalAp by using lead tetraacetate as the starting material instead of lead nitrate. The reaction was carried out at room temperature (i) in dichloromethane using sodium ethoxide as the base, (ii) in dichloromethane using triethylamine as the base, and (iii) in dimethylsulphoxide using sodium ethoxide as the base. The lead tetraacetate was usually added dropwise to ensure that the ligand was always in excess.[137] Based on infrared spectroscopy and elemental analysis identical products to those obtained with lead nitrate were produced.

As the products from the reactions with SalApH$_2$ and SalSalH$_2$ were the divalent Pb^{II}L compounds, an attempt in each case was made to obtain the Pb^{IV}L$_2$ compound using the PbL compound as the starting material. Pb(SalAp) and Pb(SalSalh) were each reacted with one mole equivalent of the appropriate ligand and two mole equivalent of sodium ethoxide, in dimethylsulphoxide. Oxidising conditions were enhanced by bubbling oxygen through the solution. The reaction with Pb(SalAp) seemed to produce a decomposition product, whereas elemental analysis on the product from Pb(SalSalh) supported the PbL formulation.

2.3.1.4 *Antimony Compounds*

Attempts to prepare the bis(dinegative tridentate) antimony(V) complexes of the type [Sb^{V}L$_2$]X, where X = Br$^-$ or Cl$^-$ depending on the reaction mixture, were made with the Schiff bases BzacBhH$_2$ and SalApH$_2$. With the former, antimony tribromide was used as the source of metal and sodium ethoxide as the base. The reaction was performed in ethanol under atmospheric conditions using varying refluxing times (4 hrs and 24 hrs). Products obtained were yellow or orange in colour. The infrared spectra of some products indicated the presence of unsubstituted acidic protons suggesting that the BzacBhH$_2$ ligand did not coordinate as a dinegative anion. Inorganic materials were among the products isolated from this series of reactions. One

reaction with SalApH$_2$ was carried out using antimony pentachloride as the metal source and sodium ethoxide as the base, under an atmosphere of dinitrogen and refluxing. Although the mass spectrum showed a weak peak at approximately the formula weight of [Sb(SalAp)$_2$]Cl, more intense peaks at higher m/e were also observed. Elemental analysis of this product did not support the [Sb(SalAp)$_2$]Cl formulation.

The existence of anionic complexes of antimony(III) such as potassium pyroantimonate and potassium antimonyl tartrate led to attempts to replace these ligands with the dinegative tridentate Schiff base ligands. We endeavoured to prepare the K[Sb^{III}(BzacBh)$_2$] complex and the Na[Sb^{III}L$_2$] complex of SalAp and BzacBh. Since potassium pyroantimonate is insoluble in ethanol, an aqueous solution of this material was added to a cloudy ethanolic solution of BzacBhH$_2$ and the solution heated under reflux. No base would be required if the desired reaction shown by Equation 2.1 took place.

$$KSb(OH)_6 0 \cdot 5H_2O + 2BzacBhH_2 \longrightarrow K[Sb(BzacBh)_2] + 4 \cdot 5H_2O + 2OH^- \quad \text{(2.1)}$$

Attempts to prepare K[Sb^{III}(BzacBh)$_2$] were also carried out using potassium antimonyl tartrate hydrate as the source of metal. This also was dissolved in water before it was added to an ethanolic solution of two mole equivalent BzacBhH$_2$ and four mole equivalent base. A range of temperatures, reflux times, bases and solvents were employed. In one case, no base was added in case deprotonation of the Schiff base by the tartrate tetraanion occurred. No product, using either antimony starting material, from this series of reactions produced an infrared spectrum supportive of the desired coordination. The spectra indicated the presence of unsubstituted acidic protons suggesting that the BzacBhH$_2$ ligand did not coordinate as a dinegative anion. The products obtained were either white, off-white, or yellow in colour. Inorganic materials and unreacted ligand were among these products.

In the series of reactions which attempt to form the antimony(III) complexes of the type Na[Sb^{III}L$_2$], antimony(III) trihalide starting materials were used and reactions were performed under an atmosphere of dinitrogen to avoid any oxidation to antimony(V). An orange solid was obtained when antimony tribromide was reacted with two mole equivalent BzacBhH$_2$ and four mole

equivalent sodium ethoxide in ethanol. The infrared spectrum of this material did not support the desired coordination. Antimony trichloride was then used as the starting material for two reactions with SalApH$_2$. Reactions in ethanol, using sodium ethoxide as the base, were carried out (i) at room temperature under an atmosphere of dinitrogen (dry box), and (ii) under an atmosphere of dinitrogen with refluxing. Orange solids were yielded in both cases. Coordination of SalAp was supported by infrared spectroscopy but not by mass spectroscopy or elemental analysis. For both ligands, although mass spectra gave peaks with m/e values well below that of the desired complex, there was evidence from the fragmentation pattern that the products may have contained the SbL fragment .

2.3.1.5   *Selenium and Tellurium Compounds*

Preliminary work was also carried out in an effort to obtain SeL$_2$ and TeL$_2$ complexes with Schiff base ligands. Apart from the unreacted ligands which were detected in the products obtained from this series of experiments, the selenium and tellurium containing products obtained here remain uncharacterised.

Selenium tetrachloride was reacted with two mole equivalent of BzacBhH$_2$ and excess base (triethylamine). Perfoming the experiment in dichloromethane or ethanol produced a material which could not be uncomplexed BzacBhH$_2$ or complexed BzacBh since it contained no peaks in the v(C=N) region of the infrared spectrum. A control experiment revealed this product to be identical to that produced from the reaction between only the tetrahalide and triethylamine.

Attempts were made to prepare ML$_2$ complexes of tellurium with BzacBhH$_2$, SalApH$_2$ and Ap-p^{Cl}-PhenolH$_2$ from the starting materials tellurium tetrachloride or tellurium oxide. Reactions of tellurium tetrachloride with BzacBhH$_2$ produced a material showing strong carbonyl stretching in its infrared spectrum, and in another case, the infrared spectrum of the product suggested that an inorganic material was obtained. Tellurium oxide was then used for reactions with SalApH$_2$ and Ap-p^{Cl}-PhenolH$_2$. Products here were unreacted ligand, and in the case of SalApH$_2$, a product showing a C=N stretch at a frequency higher than that observed in the protonated Schiff base

was obtained. This infrared data is unsupportive of the expected coordination from the azomethine nitrogen atom.

It should be mentioned that organometal(IV) complexes with these two elements have been successfully prepared.[51,52,67,138-140] Studies have also been carried out to test whether these types of compounds exhibit any biological activity.[141]

2.3.2 Di- and Triorganometal(Dinegative Tridentate) Complexes

The Schiff base ligands BzacBhH$_2$, BzacSalhH$_2$, SalApH$_2$ and SalBhH$_2$, and the azo dye ligands Ap-β-NapH$_2$ and pMe-Ap-β-NapH$_2$ were used to prepare complexes of the type R$_2$ML, where M = Ge, Sn and Pb, and R$_3$SbL. Phenyl derivatives (R = Ph) of all these elements were prepared with each dinegative tridentate ligand. In the case of tin, the methyl and n-butyl derivatives were also prepared.

A general procedure was followed for the preparation of all complexes. The di/tri-organometal dichloride starting material was added to one mole equivalent disodium salt of the Schiff base or azo dye, in benzene. The mixture was heated under reflux in an atmosphere of dinitrogen to protect the moisture-sensitive di/tri-organometal dichloride. The product was recovered after the sodium chloride, formed during the reaction, was filtered off. The Schiff bases produced yellow to orange coloured compounds and the azo dyes produced brown, purple-brown or burgundy coloured compounds.

Some methyl and phenyl derivatives were purified by recrystallisation from dichloromethane/hexane. However, for the remaining derivatives, the dichloromethane (or chloroform or benzene) solutions of the complexes remained cloudy even after heating. These cloudy solutions were therefore filtered through cotton wool, evaporated to dryness, and the product washed thoroughly with hexane. The R$_2$ML or R$_3$ML formulation for all the complexes was supported by spectroscopic and elemental analyses except for some azo dye complexes.

The n-butyltin(IV) complexes of the Schiff bases BzacBh, BzacSalh and SalBh were all yellow viscous oils. The SalAp ligand and all the azo dye ligands produced orange-brown and purple low melting solids, respectively.

The infrared and mass spectra supported the R_2ML formulation. Due to the nature of these complexes, electronic spectra were not recorded.

During the course of this work we became aware that the preparation of some of these complexes had been reported by other workers. More specifically, these were, $Ph_2Pb(SalAp)$,[105] $Me_2Sn(SalAp)$,[142-145] $Ph_2Sn(SalAp)$,[142,143] and $Ph_3Sb(SalAp)$.[123] However, our interest included a comprehensive structural and electrochemical study of a range of complexes, and for these reasons these compounds were prepared and included in our study.

2.4 Mass Spectra

2.4.1 Introduction

Mass spectroscopy is a convenient and quick method for establishing the presence of a desired product amongst isolated materials. It is useful for establishing the reproducibility of a preparative method, stability of compounds on purifying, and the presence of product in various fractions. The spectral peaks of charged fragments resulting from the breakdown of the initial material can be related to the structure of the complete molecule. Ionisation techniques used were the standard electron impact (EI) process and, in particular for high melting compounds, fast atom bombardment (FAB). In almost all cases, the expected molecular ion peak was observed protonated.

2.4.2 Bis(Dinegative Tridentate) Complexes

Products from all reactions performed were studied by mass spectroscopy and the data is summarised in Table 2.3. In the case of some unsuccessful syntheses, the Table includes results from various methods of preparation. An intense molecular ion peak characteristic of ML_2 was observed for the azo dye and Schiff base complexes of germanium and tin. Germanium has five isotopes with relative abundances: 76 (7·8%), 74 (36·5%), 73 (7·8%), 72 (27·4%) and 70 (20·5%). Tin has ten isotopes, with the three highest relative abundances: 120 (32·4%), 118 (24·3%) and 116 (14·7%). The presence of the isotopic pattern for these elements in almost all compounds further supported the formulation. In these cases, only the highest isotopic peak is reported. In a few cases where the spectra were recorded over a wider m/e range, peaks corresponding to ML fragments were also observed for these elements.

No spectral peak due to PbL_2 was observed in the mass spectra of the products obtained from the attempted syntheses of PbL_2 complexes. However, there was in each case an intense peak characteristic of PbL. Lead has four isotopes with relative abundances: 208 (52·4%), 207 (22·1%), 206 (24·1%) and 204 (1·4%). The isotopic pattern for lead was observed in the mass spectrum of all the products. Often there were few much weaker peaks in the region between the observed PbL peak and the expected PbL_2 peak, which were not included in Table 2.3. Since the microanalytical data

supported the PbL formulation, and since the same product was obtained from $PbCl_2$ in the absence of oxidising conditions, these lead compounds are undoubtedly lead(II) complexes. A large number of different Schiff base ligands produced the same 1:1 lead to ligand composition. From microanalysis, there was no indication that solvent or any other ligands were present to give a stable coordination number of six. Since all the ligands are flat planar molecules, one possibility is that a polymerisation involving the primary coordination sphere, such as stacking the planar units, may be taking place.[137] Their insolubility in common organic solvents, which also lends support to these lead complexes being polymeric, prevented us from obtaining crystals suitable for crystal structure determination.

Mass spectroscopy showed attempts to prepare SiL_2 complexes to be unsuccessful. No product showed a characteristic formula weight peak or SiL fragment in its mass spectrum. The same lack of success was met in the attempted preparations of SeL_2 and TeL_2 complexes. Excluding unreacted ligand, products from these reactions remain uncharacterised. Since the infrared spectra of the products obtained from the attempted SeL_2 and TeL_2 preparations indicated that the desired ML_2 complex was not obtained, only two samples were examined by mass spectroscopy. Results for these can be found in the Experimental Chapter of this study. From the attempts to prepare $[Sb^{III}L_2]^-$, some of the products obtained showed a peak characteristic of the SbL fragment. In the attempted synthesis of $[Sb(SalAp)_2]Cl$, a peak which may correspond to $[SbL_2]Cl$ (m/e = 582) was observed in the mass spectrum of the product obtained. However, more intense peaks at higher m/e values were also observed. Except for the products obtained from trying to prepare $K[Sb(BzacBh)_2]$ and the product obtained from one of the attempted syntheses of $Na[Sb(SalAp)_2]$ (method *(i)*), all other samples examined by mass spectroscopy showed, approximately, the isotopic pattern of antimony [^{121}Sb (57·3%) and ^{123}Sb (42·7%)]. Only a few chosen examples of the antimony compounds are included in Table 2.3, with the results obtained from other attempts listed in the Experimental Chapter.

Table 2.3: Mass Spectral Data for the Attempted Syntheses of ML_2 and $[ML_2]^{+/-}$ Type Complexes.

Complex	F.W. Calc. ML_2	F.W. Calc. ML	$\frac{m}{e}$ Found
SiL₂ attempts:			
Si(BzacBh)₂ *methods (i)-(iii)**	584	306	495, 481, 469, 423, 333
Si(SalAp)₂	450	239	342, 264, 250
Si(Ap-β-Nap)₂ *crude*	552	290	541, 507, 483, 471, 449, 391
GeL₂ complexes:			
Ge(Ap-β-Nap)₂	597	334	598†
Ge(Ap-pCl-Phenol)₂	565	319	566†
SnL₂ complexes:			
Sn(SalHba)₂	569	343	569†, 345
Sn(Ap-β-Nap)₂	643	380	644†, 381
PbL Complexes:			
Pb(BzacBh)	763	485	486†
Pb(BzacSalh)	795	501	503†
Pb(HapBh)	711	459	461†
Pb(SalAp) *method (ii)**	629	418	420†
Pb(SalBh)	683	445	447†
Pb(SalSalh) *method (i)**	715	461	462†
Sb(III) attempts:	A[ML₂]	ML	
K[Sb(BzacBh)₂] *method (iii)**	717	400	567, 287, 280 (LH₂), 262
Na[Sb(BzacBh)₂]	701	400	551†, 460, 446, 399
Na[Sb(SalAp)₂] *method (i)**	567	332	482, 460, 329
*method (ii)**			424†, 412, 332
Sb(V) attempts:			
[Sb(SalAp)₂]Cl	579	332	630†, 615, 582

* Details of the methods used are found in the Experimental Chapter.

† The expected isotopic pattern for the element was observed, only the highest peaks are reported.

A = alkali metal or halide ion, where appropriate.

L = Schiff base or azo dye ligand.

2.4.3 Organometal(Dinegative Tridentate) Complexes

All products obtained from the syntheses of organometallic compounds containing one dinegative tridentate ligand gave good mass spectra confirming their proposed structures, except Me_2SnL and Ph_2PbL, where L = Ap-β-Nap. Furthermore, in cases where the expected molecular ion was observed, the isotopic patterns for Ge, Sn, Pb and Sb, as discussed above in Section 2.4.2, were also observed in the appropriate complex spectra. Most of the compounds prepared were diorgano compounds of the type R_2ML, where M = Ge, Sn or Pb, and R = Me, n-Bu or Ph. In these compounds, the progressive loss of an R group gave rise to peaks characteristic of the fragments RML and ML. In the case of Sb, where compounds of the type R_3SbL were prepared, peaks characteristic of the fragment R_2SbL were also observed. Spectral data for all these complexes is given in Table 2.4. In some cases, where the spectra were recorded over a sufficiently large m/e range, a formula weight peak characteristic for R_2M (for the group (IV) metals) and R_3M (for antimony) was also observed. However, these peaks were less intense than the R_2ML, RML and ML fragments.

Table 2.4: Mass Spectral Data for the Organometal Complexes.

Complex	F.W. Calc.		$\frac{m}{e}$ Found		
	R_2ML	ML	$R_2ML^\dagger$	$RML^\dagger$	$ML^\dagger$
R_2GeL complexes:					
$Ph_2Ge(BzacBh)$	505	350	506	429	
$Ph_2Ge(BzacSalh)$	521	366	522	444	
$Ph_2Ge(SalAp)$	438	283	439	362	285
$Ph_2Ge(SalBh)$	465	310	466	389	307
$Ph_2Ge(Ap-\beta-Nap)$	489	334	492		
$Ph_2Ge(p^{Me}-Ap-\beta-Nap)$	503	348	505	428	350
R_2SnL complexes:					
$Me_2Sn(BzacBh)$	427	397	428	413	397
$Me_2Sn(BzacSalh)$	443	413	444	429	414
$Me_2Sn(SalAp)$	359	329	360	345	330
$Me_2Sn(SalBh)$	387	356	388	373	358
$Me_2Sn(Ap-\beta-Nap)$	411	380			329
$Me_2Sn(p^{Me}-Ap-\beta-Nap)$	425	394	426	410	397
$Bu_2Sn(BzacBh)$	511	397	512	455	398
$Bu_2Sn(BzacSalh)$	527	413	528	471	414
$Bu_2Sn(SalAp)$	444	329	445	387	329
$Bu_2Sn(SalBh)$	471	356	472	414	357
$Bu_2Sn(Ap-\beta-Nap)$	495	380	496	439	382
$Bu_2Sn(p^{Me}-Ap-\beta-Nap)$	509	394	510	453	396
$Ph_2Sn(BzacBh)$	551	397	552	474	397
$Ph_2Sn(BzacSalh)$	567	413	568	491	415
$Ph_2Sn(SalAp)$	484	329	485	408	330
$Ph_2Sn(SalBh)$	511	356	512	434	
$Ph_2Sn(Ap-\beta-Nap)$	535	380	536	460	381
$Ph_2Sn(p^{Me}-Ap-\beta-Nap)$	549	394	550	473	396

R₂PbL complexes:						
Ph₂Pb(BzacBh)	639	485	640	563	486	
Ph₂Pb(BzacSalh)	655	501	657	583	503	
Ph₂Pb(SalAp)	572	418	573	496	419	
Ph₂Pb(SalBh)	599	445	601	523	447	
Ph₂Pb(Ap-β-Nap)	623	469				617, 613 528, 516
Ph₂Pb(p^{Me}-Ap-β-Nap)	637	483	643, 638	561	484	
	R₃ML	**ML**	**R₃ML†**	**R₂ML†**	**RML†**	**ML†**
R₃SbL Complexes:						
Ph₃Sb(BzacBh)	631	400	631	553	476	399
Ph₃Sb(BzacSalh)	647	416	647	569	491	415
Ph₃Sb(SalAp)	564	332	564	486	409	332
Ph₃Sb(SalBh)	591	359	593	512	436	359
Ph₃Sb(Ap-β-Nap)	615	384	608	533	460	387
Ph₃Sb(p^{Me}-Ap-β-Nap)	629	398	628	551	475	399

† Isotopic pattern was observed for the metal, but only the most intense peak is reported.
R = Organo substituent Me, *n*-Bu or Ph.
L = Schiff base or azo dye ligands.

2.5 Infrared Spectra

2.5.1 Introduction

The products of all attempted preparations were examined by infrared spectroscopy. Indication of the desired reaction having taken place was provided by comparing the spectra of the products with the spectra of the appropriate protonated ligands. The possibility of keto-enol tautomerism exists in some of the protonated ligands. Evidence of complexation were (i) the conversion of ketonic >C=O to enolic >C-O on complexation of Schiff base ligands derived from a β-diketone and/or aroyl hydrazine, (ii) the elimination of the acidic proton from the >N-H function in complexes of the hydrazone Schiff base ligands, (iii) the elimination of the acidic hydroxyl proton in ligands containing -O-H functional groups, and (iv) changes in the vibrational frequencies, upon complexation, of the bonds containing a donor atom (e.g. >C=N-, -N=N- and >C-O).

In the protonated ligands, the stretching frequency of a free >N-H group occurs in the range 3460 - 3420 cm^{-1}.[146] Association of this group with a carbonyl group (>N-H·····O=C<) is reported to result in a lower stretching frequency (3320 - 3240 cm^{-1}), whilst association with an adjacent N atom results in an absorption in the range 3300 - 3150 cm^{-1}.[92] This latter association is seen in the benzoylhydrazone and salicyloylhydrazone ligands used in this study. Absorptions due to free O-H groups occur in the range 3650 - 3590 cm^{-1}.[147a] Shifts to a lower frequency (3200 - 2500 cm^{-1})[147a] or broadening of these peaks are due to hydrogen bonding.[92,147a] The lower the frequency the stronger the hydrogen bond.

Changes in the vibrational frequencies of the multiple bonds containing a donor atom are well documented. Pickard and Polly in their studies on ketamines, observed two peaks in the region 1720 - 1590 cm^{-1}.[148] They assigned the higher frequency peak (1720 - 1660 cm^{-1}) to v(C=O) and the lower frequency peak (1680 - 1590 cm^{-1}) to v(C=N). A large number of >C=N containing compounds have been used in the complexation of various metals. Saraswat *et al.* assigned peaks in the range 1616 - 1645 cm^{-1} to v(C=N) in their study of N-substituted salicylideneimines.[76] In their study on Schiff bases derived from S-methyl- and S-benzyldithiocarbazates, Nath *et al.* reported frequency ranges of 1610 - 1600 cm^{-1} and 1620 - 1600 cm^{-1} for

v(C=N).[86,87] In similar studies by Saxena *et al.*, a frequency of 1605 cm^{-1} was reported for v(C=N).[149]

Numerous infrared studies of aromatic Schiff base complexes have shown absorptions due to aromatic v(C=C) to overlap with absorptions due to v(C=N), with the result being a very strong band.[92,142] β-Diketonato complexes of tin(IV) have been studied by Sharma *et al.* and peaks in the region 1535 - 1525 cm^{-1} have been assigned to v(C=C).[150] Teyssie and Charette reported that the aromatic v(C=C) at 1585 cm^{-1} in salicylidene-alkylamine ligands shifts to 1540 cm^{-1} on complexation and remains independent of the nature of the metal.[92] A number of absorptions due to the phenyl groups, in a variety of phenyltin compounds, can be observed over a wide range (1475 -670 cm^{-1}).[151] In a complex of the type Ph$_2$SnL, where L = the dianion of the Schiff base N,N'-(2-hydroxytrimethylene)bis(salicyl-aldimine), a phenyl ring absorption had been assigned at 1497 cm^{-1}.[142]

In his study of VL$_2$ complexes of azo dyes, Salam observed that the N=N stretching frequency between 1630 and 1600 cm^{-1} for the protonated uncomplexed ligand shifted to a lower frequency in the range 1620 - 1597 cm^{-1} on coordination of one of these nitrogen atoms.[92]

Absorptions due to phenolic v(C-O) have been reported to occur in the 1280 - 1270 cm^{-1} region, with shifts to a higher frequency (1300 - 1290 cm^{-1}) occurring upon complexation.[76,152-154]

The stretching frequencies produced by the complexes obtained in this work were tentatively assigned by considering the absorption bands mentioned above.

2.5.2 Ligands

The infrared spectra of products isolated from the preparation of ML$_2$ and organometal complexes were compared with those of the appropriate protonated ligand. A summary of the ligand infrared data is shown in Table 2.5. Ligands BzacBhH$_2$, BzacSalhH$_2$, HapBhH$_2$, SalBhH$_2$ and SalSalhH$_2$ contain the acyl hydrazone group =N-NH-CO-. Peaks observed in the 3355 - 3200 cm^{-1} region were assigned to v(N-H). Absence of these absorptions would indicate coordination of the deprotonated >N-H group.

The absence of v(O-H) in the spectra of BzacBhH$_2$, HapBhH$_2$ and SalBhH$_2$ suggests that the keto tautomer predominates in the solid state of these Schiff bases. Ligands BzacSalhH$_2$, SalApH$_2$, SalHbaH$_2$ and SalSalhH$_2$ showed weak absorptions in the region 2715 - 2552 cm^{-1} due to intramolecular hydrogen bonding of the O-H function with the azomethine nitrogen atom.[147a] As a result, the N-H stretching frequency of BzacSalhH$_2$ at 3265 cm^{-1} was quite weak, as was the v(N-H) of SalHbaH$_2$ at 3430 cm^{-1}. Absence of these absorptions in the metal complexes would suggest coordination *via* enolic/phenolic oxygen atoms. Weak absorptions appearing in the 3406 - 3226 cm^{-1} and 2787 - 2697 cm^{-1} regions of the azo dye spectra were attributed to -O$\cdots$H-N- and -O-H$\cdots$N- interactions, respectively. Absence of these absorptions would indicate coordination of the phenolic oxygen atoms to the metal.

Two peaks were observed between 1674 and 1615 cm^{-1} in the infrared spectra of the protonated Schiff base ligands BzacBhH$_2$, HapBhH$_2$, SalBhH$_2$ and SalSalhH$_2$. The higher frequency band was assigned to v(C=O) and the lower frequency band to v(C=N). Ligands BzacSalhH$_2$ and SalApH$_2$ showed only one peak in this region, around 1630 cm^{-1}, which was assigned to v(C=N). The absence of a v(C=O) indicates that BzacSalhH$_2$ favours the enol tautomer. SalHbaH$_2$ has two absorptions in this region, at 1660 and 1611 cm^{-1}. Since no carbonyl group exists in the structure of this Schiff base, both peaks can only be attributed to v(C=N). Absorptions in the range 1618 - 1606 cm^{-1} were assigned to v(C=C) in the Schiff base ligands. These are tentative assignments as some of these absorptions may in fact be due to v(C=N). Shifts in the v(C=N) region and the absence of an v(C=O), where appropriate, would support the coordination of the ligands *via* the azomethine nitrogen and enolic oxygen atoms.

In the azo dye ligands, absorptions between 1630 and 1596 cm^{-1} were assigned to v(N=N) consistent with assignments made by Salam for the conventional structure of this type of ligand.[92] In view of the X-ray structure of Ap-β-NapH$_2$ and other work,[134-136] showing these ligands to exist in the hydrazone form, it would be more correct to assign absorptions in this region to v(C=O) or to coupling between v(C=O) and v(C=N) which is also possible.[137] Evidence of coupling having taken place, giving a more complex pattern in the 1630 - 1596 cm^{-1} region of the infrared spectrum, was seen in some of the spectra.

Table 2.5: Infrared Spectral Data for Schiff Base and Azo Dye Ligands.

Ligand (LH$_2$)	Tentative Assignments (cm^{-1})					
	v(N-H)	v(O-H···N)	v(C=O)	v(C=N)	v(C=C)	v(C-O)
Schiff Bases:						
BzacBhH$_2$	3355 s		1663 s	1625 s	1618 s	1287 s
	3228 s				1581 s	
BzacSalhH$_2$	3265 w	2715 w		1630 s	1607 m	1238 s
HapBhH$_2$	3230 s		1657 s	1615 s	1587 m	1290 s
SalApH$_2$		2700 w		1632 s	1615 s	1277 s
		2575 w			1594 s	
SalBhH$_2$	3270 s		1674 s	1622 s	1606 s	1274 s
					1580 s	
SalHbaH$_2$	3430 w	2683 m		1660 s	1600 s	1282 s
		2598 w		1611 s		
		2552 m				
SalSalhH$_2$	3200 m	2670 m	1662 s	1620 s	1563 s	1229 s
		2570 m				
Azo Dyes:	v(N-H···O)	v(O-H···N)		v(N=N)*	v(C=C)	v(C-O)
Ap-β-NapH$_2$	3406 w	2697 w		1619 m	1549 m	1308 s
				1596 m		
p^{Me}-Ap-β-NapH$_2$		2697 w		1630 m	1549 s	1291 s
				1617 s		
				1602 m		
Ap-p^{Cl}-PhenolH$_2$	3226 w	2787 w		1622 s	1558 s	1268 s

*This may be due to coupling between v(C=O) and v(C=N).

s = strong; m = medium; w = weak.

2.5.3 Bis(Dinegative Tridentate) Complexes

The infrared spectra of all the products obtained from the attempted preparations of complexes that contain two dinegative tridentate ligands per metal were recorded. The results for the germanium, tin and lead compounds are summarised in Table 2.6, and the results for the silicon and antimony compounds are summarised in Table 2.7.

2.5.3.1 Synthetic Studies with Germanium, Tin and Lead

Evidence of successful coordination of the dinegative tridentate ligands to these elements was observed by infrared spectroscopy. In the products obtained from reactions with tin and lead, the Schiff base ligands containing the hydrazide moiety is deprotonated since no v(N-H) and hydrogen bonded v(O-H) are seen. Products in which the ligands were derived from benzoylhydrazine or salicylic hydrazide did not exhibit a v(C=O) but they did exhibit a v(C-O). This indicated that these ligands were coordinated in the enolic form. For the protonated uncomplexed Schiff base ligands the v(C=N) were observed in the 1660 - 1611 cm^{-1} region. A downward shift in the v(C=N) frequency on complexation (1627 - 1570 cm^{-1}) indicated that coordination from the azomethine nitrogen atom had occurred. In all the spectra of these group (IV) metal complexes peaks in the region 1553 - 1530 cm^{-1} were assigned to v(C=C) and peaks in the region 1321 - 1298 cm^{-1} were assigned to v(C-O).

Inspite of the difference in coordination number and oxidation state of the metal, the infrared spectra of the Pb^{II}L complexes are comparable to the analogous Ge^{IV}L$_2$ and Sn^{IV}L$_2$ complexes, where L = BzacBh, BzacSalh, SalAp and SalBh,[97] and VL$_2$ complexes, where L = SalSalh and HapBh.[92] For example, the v(C=N) for the protonated SalApH$_2$ ligand appeared at 1632 cm^{-1}. Upon complexation to germanium and tin, this absorption shifted by 19 cm^{-1} and 22 cm^{-1}, respectively, to a lower frequency. Similarly, complexation to lead produced an absorption 20 cm^{-1} lower in frequency than the protonated SalApH$_2$ ligand.

The spectra of the germanium and tin ML$_2$ complexes with Ap-β-Nap and/or Ap-p^{Cl}-Phenol compare well with the analogous VL$_2$ complexes prepared by Salam.[92] Upon complexation, the downward shift in frequency of the v(N=N) (1615 - 1563 cm^{-1}) in comparison to that of the protonated uncomplexed dye

(1630 - 1596 cm^{-1}) implied that coordination from an azo nitrogen atom had occurred. A noteworthy observation was that the spectrum of Sn(SalHba)$_2$ was very similar to that of Sn(SalAp)$_2$.[97] This was not that surprising since the structure of the two ligands is very similar.

2.5.3.2 *Synthetic Studies with Silicon*

Of the three ligands we tried to complex with silicon, only the product obtained from the attempted synthesis of Si(Ap-β-Nap)$_2$ showed some promise. Peaks in the ν(N=N) region of the infrared spectrum had shifted to lower frequencies indicating coordination of an azo nitrogen and the ν(O-H) had disappeared indicating deprotonation of the ligand. These absorptions and that due to ν(C-O) compare well with the analogous complexes of germanium and tin (see Table 2.6). However, this material was unstable as its infrared spectrum changed upon recrystallisation. An extra peak in the ν(N=N) region appeared.

Spectra of the products obtained from the attempted preparations of Si(BzacBh)$_2$ did not agree with the expected product. Different preparations gave slightly different results (see Experimental Chapter). Some typical results are shown in Table 2.7. Although the ν(C=O) was absent, the products gave strong absorptions in the ν(N-H) region which implied that deprotonation at the hydrazide nitrogen had not occurred. Thus, the BzacBhH$_2$ ligand did not coordinate in the anticipated tridentate way. In one attempt, both the ν(C=N) and ν(C=C) were absent indicating that the ligand was completely altered by the reaction.

The ν(C=N) for the product obtained from the attempted synthesis of Si(SalAp)$_2$ was observed at a slightly higher frequency than that for the free ligand, suggesting that the expected coordination at the azomethine nitrogen atom had not taken place.

2.5.3.3 *Synthetic Studies with Antimony*

Only Schiff bases BzacBhH$_2$ and SalApH$_2$ were used in the attempts to synthesise [Sb^{V}L$_2$]$^+$ and [Sb^{III}L$_2$]$^-$ type complexes. Some typical results are recorded in Table 2.7 and details of individual attempts are given in the Experimental Chapter. Inorganic materials and unreacted ligand were among the products afforded in these syntheses. Reactions with SalApH$_2$ showed

Table 2.6: Infrared Spectral Data for ML$_2$ Complexes of Germanium(IV) and Tin(IV), and ML Complexes of Lead(II).

Complex	Tentative Assignments (cm^{-1})		
	v(C=N)	v(C=C)	v(C-O)
L = BzacBh:			
Ge(BzacBh)$_2$[a]	1611 s	1534 m	1310 s
	1598 s		
	1588 s		
Sn(BzacBh)$_2$[a]	1590 s	1529 s	1303 s
	1576 m		
Pb(BzacBh)	1595 s	1530 s	1305 m
	1570 m		
L = BzacSalH:			
Ge(BzacSalh)$_2$[a]	1623 s	1515 s	1310 s
	1593 s		
	1578 sh		
Sn(BzacSalh)$_2$[a]	1622 s	1503	1301 s
	1589 s		
	1570 m		
Pb(BzacSalh)	1607 s	1552 s	1315 s
	1582 s	1538 s	
L = HapBh:			
Pb(HapBh)$_2$	1600 s	1553 s	1310 m
	1592 s		
	1586 s		
V(HapBh)$_2$[b]	1600 s	1543 s	1320 s
	1590 msh		
	1565 s		
L = SalAp:			
Ge(SalAp)$_2$[a]	1613 s	1544 s	1300 s
	1593 s		
Sn(SalAp)$_2$[a]	1610 s	1543 s	1299 s
	1588 s		

Pb(SalAp)	1612 s 1587 m	1542 s	1305 m
L = SalBh:			
Ge(SalBh)$_2$[a]	1627 s 1603 s 1587 m	1552 s	1305 m
Sn(SalBh)$_2$[a]	1618 s 1595 s	1547 s	1305 m
Pb(SalBh)	1604 s	1550 m	1305 w
L = SalHba:			
Sn(SalHba)$_2$	1627 s 1600 m	1546 s	1298 m
L = SalSalh:			
Pb(SalSalh)	1612 s 1589 s	1542 s	1312 s
V(SalSalh)$_2$[b]	1625 s 1600 s 1587 s	1542 s	1312 m

	v(N=N)	v(C=C)	v(C-O)
L = Ap-β-Nap:			
Ge(Ap-β-Nap)$_2$	1615 m 1594 s 1573 m	1551 s	1318 s
Sn(Ap-β-Nap)$_2$	1612 m 1591 s 1568 s	1547 s	1314 s
V(Ap-β-Nap)$_2$[b]	1617 sh 1597 msh 1584 sh	1550 m	1325 s
L = Ap-p^{Cl}-Phenol:			
Ge(Ap-p^{Cl}-Phenol)$_2$	1602 s 1563 m	1537 m	1321 w
V(Ap-p^{Cl}-Phenol)$_2$[b]	1605 ms 1592 ms	1540 mw	1325 w

[a] Reference 97; [b] Reference 92.
s = strong; m = medium; w = weak; ms = medium strong; mw = medium weak;
msh = medium shoulder.

some evidence of coordination as the v(C=N) in some of the products obtained was observed to be in the 1605 - 1559 cm^{-1} region (lower than that for the free ligand) and the v(O-H) of the phenolic group was absent suggesting deprotonation must have occurred.

Products from the reactions with BzacBhH$_2$ were irreproducible and showed that the ligand was not attached in the expected way. A typical result for the attempted synthesis of Na[Sb(BzacBh)$_2$] recorded in Table 2.7 showed the absence of the carbonyl function. The v(C=N) in this product occurred at a higher frequency (~1637 cm^{-1}) than that in the uncomplexed ligand (1625 cm^{-1}). This does not support the coordination of the azomethine nitrogen. Absorptions were also observed in the v(O-H) and v(N-H) regions suggesting that replacement of the acidic protons on the hydrazide function had not taken place. The product obtained in the attempt to synthesise [Sb(BzacBh)$_2$]Br gave an infrared spectrum containing several peak in the v(O-H) and v(N-H) region. Recrystallisation of this material resulted in decomposition as a strong carbonyl stretching was introduced at 1662 cm^{-1} and most of the v(C=N) stretching frequencies disappeared.

2.5.3.4 *Synthetic Studies with Selenium and Tellurium*

Since no evidence of the desired reaction having taken place was gained from the infrared spectra of the products obtained from the attempts to synthesise SeL$_2$ and TeL$_2$ compounds, the infrared data was not listed in Table 2.7. This data can be found in the Experimental Chapter.

Table 2.7: Infrared Spectral Data for the Attempted Preparations of SiL_2 and $[SbL_2]^{+/-}$ Complexes.

Complex	Tentative Assignments (cm^{-1})			
	v(O-H)/ v(N-H)	v(C=N)	v(C=C)	v(C-O)
L = BzacBh:				
Si(BzacBh)$_2$	3130 m	1615 s	1536 m	1294 s
	3100 m	1596 s		1268 s
	2618 s			
Na[Sb(BzacBh)$_2$]	3549 m	1637 m	1538 s	1303 m
	3455 m	1617 m		
	3411 s	1590 s		
	2727 w			
K[Sb(BzacBh)$_2$]	3584 w	1662 s*	1556 s	1316 s
	3401 mbr	1602 s	1535 s	
	3225 s	1581 s		
	2728 w			
L = SalAp:				
Si(SalAp)$_2$		1645 s	1583 s	1284 s
		1610 s		1231 s
[Sb(SalAp)$_2$]Cl		1605 s	1548 s	1302 m
		1592 msh		
Na[Sb(SalAp)$_2$]		1603 s	1537 s	1315 s
		1579 m		
		1559 m		
	v(O-H)/ v(N-H)	v(N=N)	v(C=C)	v(C-O)
L = Ap-β-Nap:				
Si(Ap-β-Nap)$_2$		1611 m		1322 w
		1590 w		
		1568 m		

* This absorption appeared upon recrystallisation and is probably due to v(C=O).
w = weak; m = medium; s = strong; mbr = medium and broad; mw = medium to weak; msh = medium shoulder.

2.5.4 Organometal(Dinegative Tridentate) Complexes

Before examining the coordination of each ligand individually, some general points should be noted. For the uncomplexed ligands, peaks in the 1618 - 1580 cm^{-1} region were assigned to aromatic v(C=C). However, the peak at the higher frequency end of this range may possibly be associated with v(C=N), since upon complexation it shifted to a lower frequency in the range 1566 - 1500 cm^{-1}. Distinguishing between the aromatic v(C=C) of the ligands and the phenyl substituents directly attached to the metal proved difficult, even when comparing spectra of Ph$_2$SnL with the analogous Me$_2$SnL or n-Bu$_2$SnL. The v(C-O) stretching frequency, observed between 1308 and 1238 cm^{-1} for the protonated ligands, shifted to a higher frequency between 1329 and 1300 cm^{-1} after coordination of the oxygen atom to the metal. This assignment is consistent with assignments made in other infrared studies.[58,76,142,155] The spectral data for the organometal complexes is given in Table 2.8.

2.5.4.1 *Coordination of BzacBhH$_2$*

In the uncomplexed state, this ligand seemed to exist in the keto form since it showed no v(O-H) absorptions and a strong absorption at 1663 cm^{-1} due to v(C=O). Strong peaks at 3355 and 3228 cm^{-1} were assigned to v(N-H). In the complexes of this ligand, the absence of absorptions due to the N-H bond, as well as the absence of carbonyl stretching, indicated coordination of the enol tautomer of this Schiff base had occurred. Coordination of the ligand in the enol form was confirmed by the appearance of a v(C-O) in all the organometal compounds of BzacBhH$_2$ (1327 - 1301 cm^{-1}). The v(C=N) observed at 1625 cm^{-1} for uncomplexed BzacBhH$_2$ showed a downward shift of 17 - 36 cm^{-1} in the complexes. This indicated that coordination at the azomethine nitrogen atom had taken place. Bands around 1600 cm^{-1} are characteristic of the conjugate >C=N-N=C<, and they further supported coordination by enolic oxygens.

2.5.4.2 *Coordination of BzacSalhH$_2$*

This ligand exists in the enol form in the uncomplexed state. When complexed, the disappearance of the absorptions due to intramolecularly hydrogen bonded N-H and O-H groups, v(N-H···O) and v(O-H···N), respectively, appearing at 3265 and 2715 cm^{-1}, respectively, indicated that

coordination of the ligand in the enol form was successful. The two or three absorptions seen in the 1624 - 1565 cm^{-1} region of the complex infrared spectra were assigned to v(C=N). These frequencies were lower than the corresponding absorptions in the uncomplexed ligand spectrum (1630 cm^{-1}) indicating coordination occurred at the nitrogen of the azomethine group.

2.5.4.3   *Coordination of SalApH$_2$*

Absorptions at 2700 and 2575 cm^{-1} in the infrared spectrum of uncomplexed SalApH$_2$, attributed to intramolecularly hydrogen bonded v(O-H), were absent in all the complexes. This is indicative of deprotonation of the phenolic groups. Two peaks, and in one case three peaks, were observed in the 1612 - 1586 cm^{-1} region of the SalApH$_2$ complex infrared spectra. These were assigned to v(C=N). Furthermore, they occurred at lower frequencies than the assigned v(C=N) in the uncomplexed ligand spectrum (1632 and 1615 cm^{-1}). However, the lower frequency absorption may be associated with v(C=C).

2.5.4.4   *Coordination of SalBhH$_2$*

The protonated uncomplexed ligand showed a strong absorption at 3270 cm^{-1} due to the N-H group and a strong carbonyl stretch at 1674 cm^{-1}. Both the v(N-H) and v(C=O) were absent in the spectra of the complexes obtained with this Schiff base, suggesting coordination of the deprotonated enol tautomer. Except for Ph$_2$Ge(SalBh), two peaks were observed in the 1613 - 1568 cm^{-1} region, assigned to v(C=N). As observed with other Schiff base ligands, these absorptions were of lower frequency than the v(C=N) in the uncomplexed ligand (1622 cm^{-1}).

2.5.4.5   *Coordination of Azo Dyes*

The absorptions due to the hydrogen bonded N-H (3406 cm^{-1} in Ap-β-NapH$_2$ only) and O-H (2697 cm^{-1} in both) groups in the spectra of the uncomplexed azo dye ligands Ap-β-NapH$_2$ and p^{Me}-Ap-β-NapH$_2$ were absent in the spectra of the complexes indicating deprotonation of the phenolic groups. Two or three absorptions were seen in the 1618 - 1564 cm^{-1} region of the azo dye complex spectra which were attributed to v(N=N). In addition, two v(N=N) were observed in the uncomplexed Ap-β-NapH$_2$ spectrum and three in the spectrum of uncomplexed p^{Me}-Ap-β-NapH$_2$.

Table 2.8: Infrared Spectral Data for the Organometal Complexes of Germanium(IV), Tin(IV), Lead(IV) and Antimony(V).

Complex	Tentative Assignments (cm^{-1})		
	v(C=N)	v(C=C)	v(C-O)
L = BzacBh:			
Ph$_2$Ge(BzacBh)	1591 s	1537 s	1301 m
Me$_2$Sn(BzacBh)	1592 s	1532 s	1304 s
Bu$_2$Sn(BzacBh)	1591 s	1529 s	1303 s
Ph$_2$Sn(BzacBh)	1593 s	1535 s	1302 m
Ph$_2$Pb(BzacBh)	1589 s	1520 s	1327 w
Ph$_3$Sb(BzacBh)	1608 s	1522	1302 m
L = BzacSalh:			
Ph$_2$Ge(BzacSalh)	1623 s	1541 s	1321 m
	1596 s	1517 s	
	1570 s		
Me$_2$Sn(BzacSalh)	1600 s	1529 s	1308 s
	1587 s		
	1565 s		
Bu$_2$Sn(BzacSalh)	1624 s	1566 s	1305 s
	1598 s		
	1590 s		
Ph$_2$Sn(BzacSalh)	1622 s	1528 s	1302 s
	1592 s		
	1572 s		
Ph$_2$Pb(BzacSalh)	1598 s	1564 s	1302 s
	1587 s		
Ph$_3$Sb(BzacSalh)	1624 s	1513 s	1300 m
	1605 s		
	1589 s		
L = SalAp:			
Ph$_2$Ge(SalAp)	1612 s	1541 s	1323 s
	1595 m		
Me$_2$Sn(SalAp)	1608 s	1532 s	1324 m
	1588 s		

	v(N=N)	v(C=C)	v(C-O)
Bu₂Sn(SalAp)	1607 s	1535 s	1320 s
	1589 s		
Ph₂Sn(SalAp)	1605 s	1540 s	1315 s
	1587 s		
Ph₂Pb(SalAp)	1600 s	1527 s	1329 s
	1586 s		
Ph₃Sb(SalAp)	1610 s	1543 s	1300 s
	1601 s		
	1589 s		
L = SalBh:			
Ph₂Ge(SalBh)	1613 s	1550 s	1309 s
Me₂Sn(SalBh)	1606 s	1544 s	1309 s
	1599 s		
Bu₂Sn(SalBh)	1610 s	1543 s	1308 s
	1600 sh		
Ph₂Sn(SalBh)	1609 s	1545 s	1307 s
	1597 s		
Ph₂Pb(SalBh)	1597 s	1547 s	1302 s
	1568 s		
Ph₃Sb(SalBh)	1612 s	1549 s	1303 m
	1598 s		
	v(N=N)	**v(C=C)**	**v(C-O)**
L = Ap-β-Nap:			
Ph₂Ge(Ap-β-Nap)	1611 s	1548 sh	1321 w
	1591 s		
	1568 s		
Me₂Sn(Ap-β-Nap)	1614 s	1548 s	1327 w
	1595 s		
	1571 m		
Bu₂Sn(Ap-β-Nap)	1615 s	1548 s	1313 s
	1599 s		
	1568 s		
Ph₂Sn(Ap-β-Nap)	1614 m	1546 s	1320 s
	1594 s	1500 s	
	1567 s		

Table 2.8: continued...

Ph$_2$Pb(Ap-β-Nap)	1612 s	1549 s	1314 msh
	1596 s		
Ph$_3$Sb(Ap-β-Nap)	1615 m	1548 s	1317 s
	1594 s		
	1564 s		
L = p^{Me}-Ap-β-Nap:			
Ph$_2$Ge(p^{Me}-Ap-β-Nap)	1618 s	1550 s	1314 m
	1594 s		
Me$_2$Sn(p^{Me}-Ap-β-Nap)	1613 m	1546 s	1321 w
	1603 m	1501 s	
	1595 s		
Bu$_2$Sn(p^{Me}-Ap-β-Nap)	1616 m	1547 s	1322 w
	1597 s	1506 s	
		1500 s	
Ph$_2$Sn(p^{Me}-Ap-β-Nap)	1607 m	1546 s	1314 wsh
	1594 m		
Ph$_2$Pb(p^{Me}-Ap-β-Nap)	1612 s	1566 s	1324 m
	1599 s	1544 s	
		1508 s	
Ph$_3$Sb(p^{Me}-Ap-β-Nap)	1611 s	1546 s	1305 s
	1592 s		

s = strong; m = medium; w = weak; msh = medium shoulder; wsh = weak shoulder.

2.6 Electronic Spectra

2.6.1 Introduction

Interpretation of the electronic spectra can reveal information on the interaction between the electronic levels of the ligand and metal. The ligands used in this study contain π systems and atoms with lone pairs of electrons. The ligand π systems consist of delocalised π molecular orbitals associated with the whole of the conjugated chelate system and a secondary π system due to the aromatic ring components of the ligands. With the Schiff base and azo dye ligands employed in this study the possibility, therefore, of $n \rightarrow \pi^*$ and $\pi \rightarrow \pi^*$ transitions exists. The former is an electronic transition from a non-bonding orbital (lone pair) to an antibonding π orbital, and is of lower energy than the latter transition in which electron transfer occurs from a bonding π orbital to an antibonding π orbital. Furthermore, the intensity of the $n \rightarrow \pi^*$ transitions is usually low beause they are symmetry forbidden and, thus, they are often not seen.[147b]

The possibility of intraligand transitions as well as charge transfer from the ligand to the metal exists in the Schiff base and azo dye complexes prepared in this study.[92] Since the metals in the complexes prepared exist in a high oxidation state and because of the π-donating nature of the Schiff base and azo dye ligands, the likelihood of charge transfer taking place from the ligand orbitals to the metal orbitals exists. This transition, known as ligand-to-metal charge transfer (LMCT), is quite common.[6m,156a] As the metal d orbitals below the valence shells are full, charge transfer is likely to take place from the lower energy, filled bonding molecular orbitals (having mostly ligand character) to a higher energy, empty antibonding molecular orbital (having mostly metal s and p orbital character).

Kutal recently published a review on the spectroscopic and photochemical properties of d^{10} metal complexes.[157] In this review, he used the energy level diagram shown in Figure 2.3 to illustrate some of the electronic transitions possible in an octahedral compound. An intraligand transition is represented by ν_1 and a ligand-to-metal charge transfer transition is represented by ν_2.
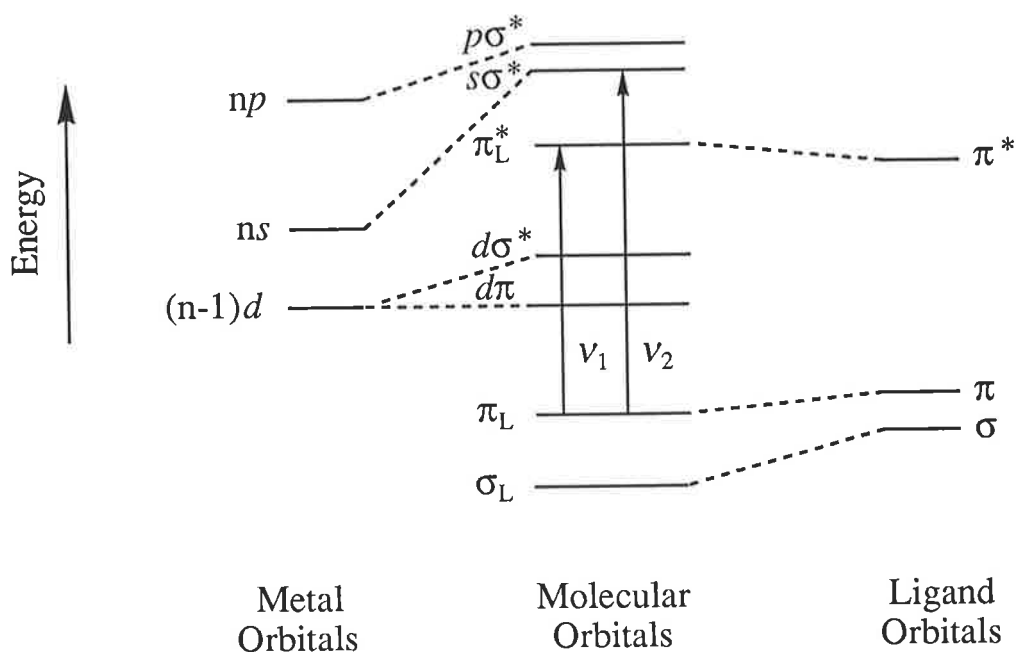
Figure 2.3: *The molecular orbital diagram resulting from the mixing of the valence orbitals of a transition metal with orbitals of the same symmetry of six ligands at the vertices of an octahedron (Reference 157).*

2.6.2 Ligands

The electronic spectra of all the protonated ligands were recorded in dichloromethane, except $SalHbaH_2$ which was recorded in dimethylsulphoxide due to insufficient solubility in dichloromethane. Results for these are summarised with their complexes in Tables 2.9 and 2.10. In each case, the spectra of the protonated Schiff base ligands contained two or three absorption bands in the 248 - 354 nm region. These were attributed to $\pi \rightarrow \pi^*$ transitions and were labelled as superscripts T(1), T(2) and T(3) in order of increasing wavelength. The protonated azo dye ligands showed two or three absorption bands in the 325 - 476 nm region and were labelled as superscripts T(1), T(2) and T(3) in order of increasing wavelength. Lone pair of electrons on the nitrogen atoms can give rise to $n \rightarrow \pi^*$ transitions. As mentioned earlier, these are generally weak because they are symmetry forbidden transitions.[147b] However, it is possible, in conjugated systems, for the

intensity of these transitions to be enhanced through vibrational borrowing from allowed $\pi \rightarrow \pi^*$ transitions.[158] The absorption appearing at the longest wavelength (at the extreme blue end of the visible region) in each azo dye spectrum was assigned to this kind of transition (superscript T(3)).

2.6.3 Complexes

2.6.3.1 *Bis(Dinegative Tridentate) Complexes*

For the bis(dinegative tridentate) complexes, electronic spectra were only recorded for the four successful GeL_2 and SnL_2 preparations. Three of these were azo dye complexes and one was a Schiff base complex. The spectra of all the azo dye complexes of this type were recorded in dichloromethane. Owing to the insolubility of the Schiff base $SalHbaH_2$ in this solvent, the spectrum of this ligand and its tin complex, $Sn(SalHba)_2$, were studied in dimethylsulphoxide. The lead(II) complexes were not sufficiently soluble to be studied in solution.

The complex spectra are shown in Figures 2.4 and 2.5, in some cases with the appropriate ligand spectrum. Two or three absorption bands were observed in the spectra of the ML_2 complexes, where M = Ge and Sn, and assignments for these are listed in Table 2.9. The $\pi \rightarrow \pi^*$ transitions labelled superscripts T(1) and T(2) in the protonated ligand spectra appeared at longer wavelengths upon complexation in agreement with coordination having taken place.[159] In Table 2.9 these are labelled ILT(1) and ILT(2), respectively. An intense absorption appeared in the visible region of each complex spectrum and was assigned to LMCT (labelled CT(2) in Table 2.9). This appeared at 362 nm in the spectrum of the Schiff base complex $Sn(SalHba)_2$, and in the 556 - 576 nm region in the azo dye complex spectra. Molar absorptivities for these absorptions were 5.4×10^3 dm^3 mol^{-1} cm^{-1} for $Sn(SalHba)_2$, and between 2.7×10^4 and 5.21×10^4 dm^3 mol^{-1} cm^{-1} for the azo dye complexes.

In Table 2.9 the electronic spectral data for the azo dye ML_2 complexes of germanium and tin are compared with the analogous vanadium complexes studied by Salam.[92] Charge transfer bands in the germanium and tin complexes occurred at shorter wavelengths in comparison to those of the analogous vanadium complexes. This suggests that the vacant orbitals of germanium and tin are higher in energy than those of vanadium, as expected,

since vanadium contains empty $3d$ orbitals whereas germanium and tin contain the configuration $3d^{10}$ and $4d^{10}$, respectively.

The electronic spectra of the GeL_2 and the SnL_2 complexes of Ap-β-NapH$_2$ and p-methyl-o-hydroxybenzeneazo-β-naphthol (p^{Me}-Ap-β-NapH$_2$)[97] were very similar indicating that the same interactions were occurring between the two ligands and the two metals. On comparing the GeL_2 and SnL_2 complexes of Ap-β-NapH$_2$ and p^{Me}-Ap-β-NapH$_2$, it can be seen that the absorptions in the GeL_2 spectra occur at higher wavelengths than those in the SnL_2 spectra suggesting that the energy of the germanium orbitals are lower than those of tin.

For the SnL_2 complexes, where L = the 6,6-chelate SalHba and the 5,6-chelate SalAp, the $\pi \rightarrow \pi^*$ intraligand transitions appeared at shorter wavelengths in the $Sn(SalHba)_2$ complex.
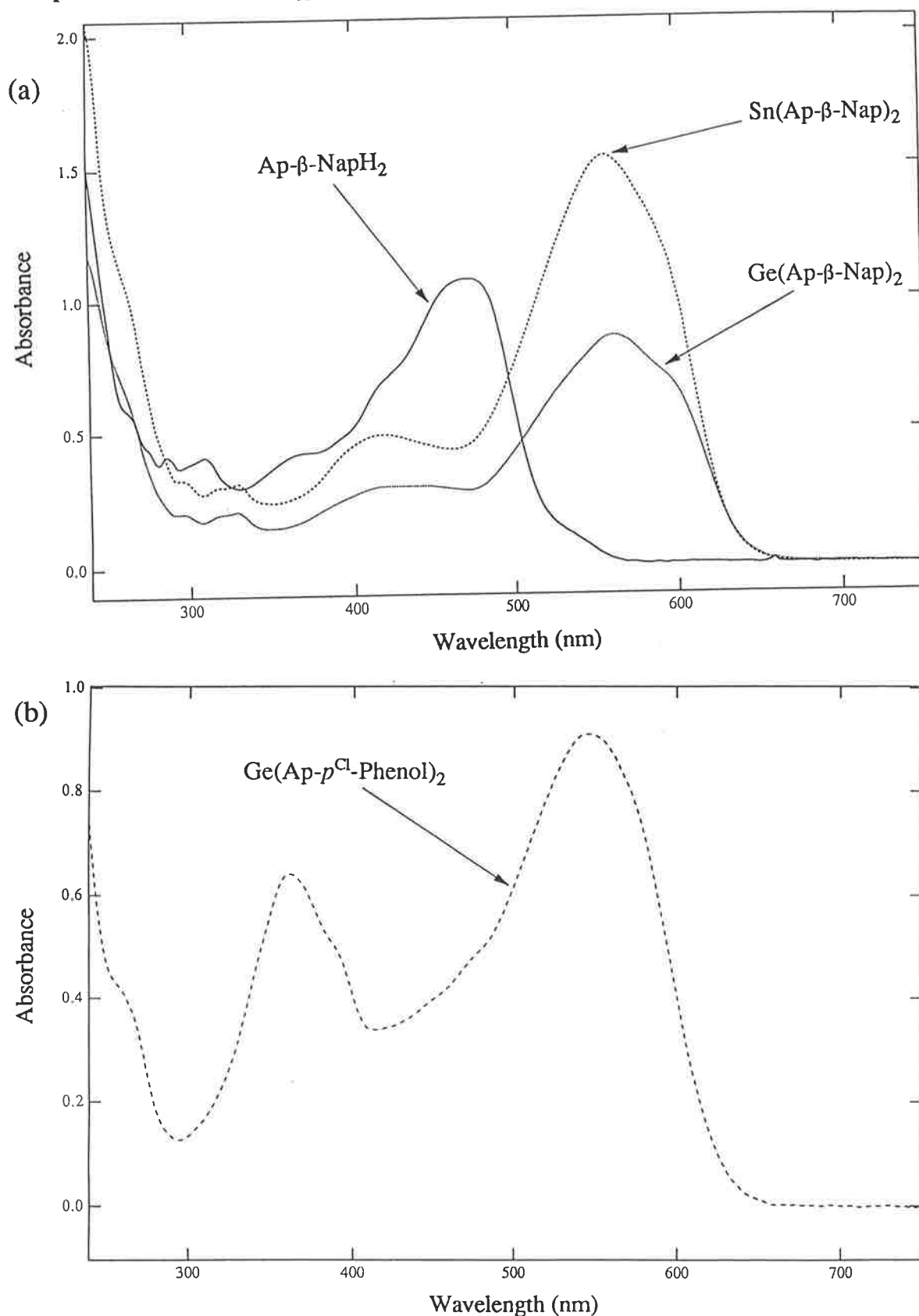
Figure 2.4: *(a) Overlay of the electronic spectra of Ap-β-NapH$_2$, Ge(Ap-β-Nap)$_2$, and Sn(Ap-β-Nap)$_2$ in dichloromethane. (b) Electronic spectrum of Ge(Ap-p^{Cl}-Phenol)$_2$ in dichloromethane.*
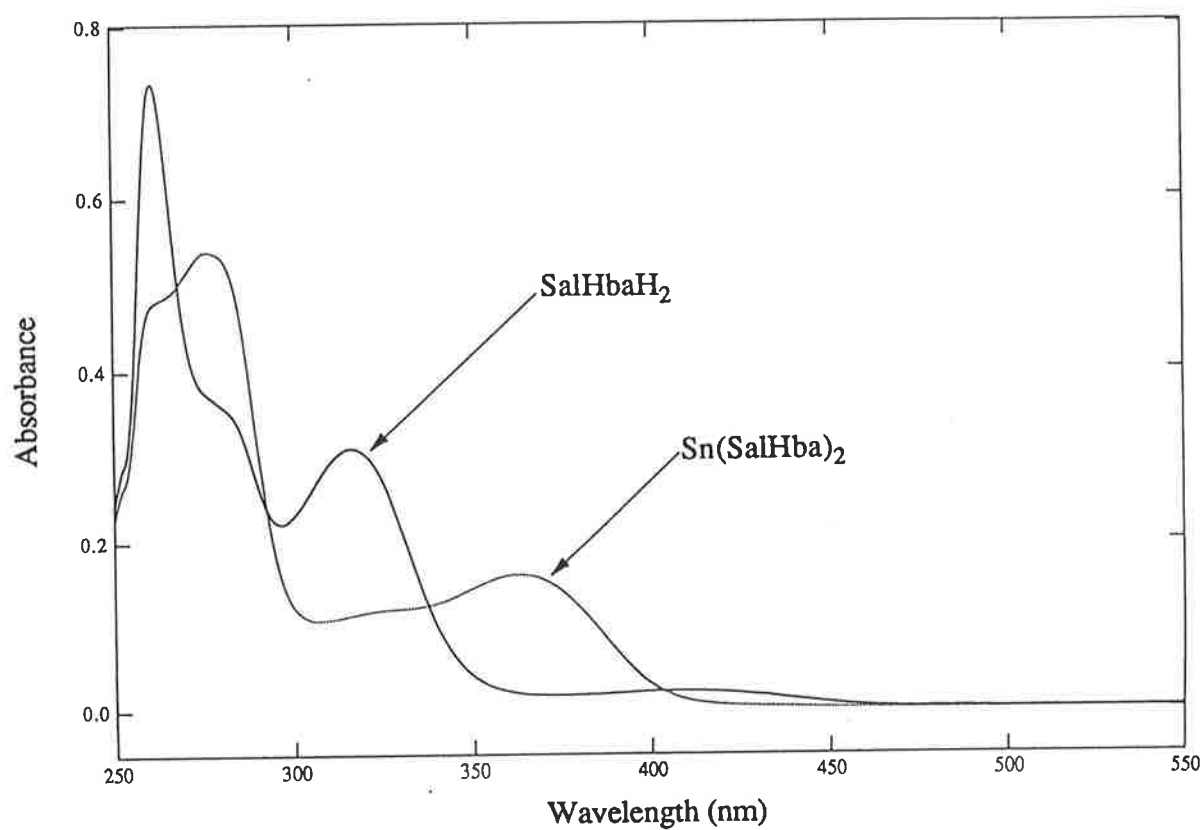
Figure 2.5: *Overlay of the electronic spectra of SalHbaH₂ and Sn(SalHba)₂ in dimethylsulphoxide.*

Table 2.9: Electronic Spectral Data for ML$_2$ Complexes in Dichloromethane or Dimethylsulphoxide.

Ligand/ Complex	Wavelength (nm) [log ε]				
	CT(2)¥	CT(1)¥	ILT(3)¥	ILT(2)¥	ILT(1)¥
LH$_2$ = SalHbaH$_2$*				316 [3·65]T(2)	278 shT(1)
Sn(SalHba)$_2$*	362 [3·73]			334 sh [3·61]	278 [4·25]
Sn(SalAp)$_2$*,†	429 [4·44]			394 sh [4·25]	316 [4·21]
LH$_2$ = Ap-β-NapH$_2$			474 [4·21]T(3)	425 shT(2)	377 shT(1)
Ge(Ap-β-Nap)$_2$	562 [4·43]		hidden by CT		424 [3·97]
Sn(Ap-β-Nap)$_2$	556 [4·72]				418 [4·22]
V(Ap-β-Nap)$_2$‡	622 [4·13]	466 [4·45]			371 [4·66]
LH$_2$ = pMe-Ap-β-NapH$_2$			476 [4·20]T(3)	425 shT(2)	372 shT(1)
Ge(pMe-Ap-β-Nap)$_2$†	576 [4·60]		hidden by CT		417 [4·15]
Sn(pMe-Ap-β-Nap)$_2$†	572 [4·54]				413 [4·08]
V(pMe-Ap-β-Nap)$_2$‡	630 fl sh [4·01]	473 [4·42]			371 [4·36]
LH$_2$ = Ap-pCl-PhenolH$_2$‡			437T(3)‡		325T(1)‡
Ge(Ap-pCl-Phenol)$_2$	548 [448]				362 [4·33]
V(Ap-pCl-Phenol)$_2$‡	595 sh	435 fl sh [4·18]		380 sh	334 [4·27]

¥ Label for this transition is only for the complexes; * Electronic spectra recorded in dimethylsulphoxide; † Reference 97; ‡ Reference 92. T(1), T(2) and T(3) refer to transitions in the protonated ligands; sh = shoulder; fl sh = flat shoulder.

2.6.3.2 *Organometal Complexes*

All organometal complexes were examined by electronic spectroscopy in dichloromethane and assignments of the observed transitions were made by comparison with the spectra of the appropriate ligand. Overlays of spectra for each ligand complexed to germanium, tin, lead and antimony are shown in Figures 2.6 - 2.11. Results for these complexes are summarised in Table 2.10. The spectra of the organometal complexes were little affected by the nature of the organo substituent (Me, *n*-Bu or Ph). Due to the solvent used, there was little information available from the spectra below 250 nm.

The $\pi \rightarrow \pi^*$ transitions labelled superscripts T(1), T(2) and T(3) in the protonated Schiff base ligand spectra and superscripts T(1) and T(2) in the protonated azo dye ligand spectra, generally appeared at lower energies (i.e. longer wavelengths) upon complexation. The corresponding transitions in the spectra of the complexes are labelled ILT(1), ILT(2) and ILT(3). Sutton makes the generalisation that ligand absorption bands become shifted to a longer wavelength on complexation.[159] For some complexes, the longer wavelength ILT overlapped with the charge transfer band of the complex (CT(1)) and resulted in this transition appearing as a shoulder. This is illustrated well in the spectra of the complexes of SalApH$_2$ (Figure 2.8). In the complex spectra, ILT(1) and ILT(2) were assigned to bands detected in the 246 - 400 nm region, approximately, and were attributed to $\pi \rightarrow \pi^*$ transitions in the chelate ring and the aromatic rings in the ligands. The phenyl groups of the organometal moiety, able to give rise to additional $\pi \rightarrow \pi^*$ transitions, appear to make little difference to the organometal complex spectra. For example, the spectrum of Ph$_2$Sn(SalAp) was very similar to that of Me$_2$Sn(SalAp).

The most dominant feature of the organometal complex spectra were the strong absorptions due to LMCT. These appeared at the longer wavelength end of the spectra. Two bands, labelled CT(1) and CT(2), were usually seen. Furthermore, CT(2) commonly appeared as a shoulder in many of the complex spectra. These transitions are consistent with the proposed coordination of the ligands to the post-transition metals germanium, tin, lead and antimony.

As discussed in Section 2.6.2, in the electronic spectra of the azo dye ligands there are present intense $n \rightarrow \pi^*$ transitions as a result of vibrational borrowing from $\pi \rightarrow \pi^*$ transitions (labelled superscript T(3)). For the organometal

complexes, the absorptions labelled CT(1) in the azo dye complexes are either purely ILT(3) or a result of these intraligand transitions which have overlapped with new charge transfer. These bands appeared at around the same wavelength or at a slightly longer wavelength than the T(3) band in the spectra of the protonateded azo dyes. The T(3) band in the protonated azo dye spectra were ususally somewhat less intense in the respective complex spectra (CT(1) < T(3)) because the possibility of vibrational borrowing from the $\pi \rightarrow \pi^*$ transitions may be reduced in these complexes.

With each of the Schiff base ligands used, there seems to be a general trend between the energy of the CT transitions and the central metal. The energy of these transitions decreases in the order: $Ph_3SbL > Ph_2SnL > Ph_2PbL > Ph_2GeL$. No particular trend was observed with the azo dye complexes. In the case of the group(IV) metal complexes of Schiff base ligands, the reason that the charge transfer bands in the diphenyllead complexes usually occurred at lower energy than the corresponding bands in the diphenyltin complexes was attributed to the greater optical electronegativity (X) of lead(IV) ($X = 1.9$) relative to tin(IV) ($X = 1.5$).[157]

In comparing our results with that of other workers, allowances have to be made for the different solvents used. An abundance of organometal complex systems were found in the literature. The main conclusions in those studies are summarised below.

Nath *et al.* prepared and studied some S-benzyldithiocarbazate Schiff bases complexes of dimethyl- and diphenyltin(IV).[87] Absorptions in the 218 - 222 nm, 240 - 300 nm and 323 - 350 nm regions of the protonated ligand spectra were assigned to $\pi \rightarrow \pi^*$ transitions due to the phenyl ring, the >C=N chromophore and the secondary band of the benzene ring, respectively. Upon complexation, these absorptions were observed in the 222 - 230 nm, 300 - 320 nm and 350 - 355 nm regions of the electronic spectra. Hence, the $\pi \rightarrow \pi^*$ transitions in the protonated ligand spectra appeared at longer wavelengths in the spectra of the complexes. Similar observations have been made with dichloro diphenyltin(IV) complexes of neutral bidentate Schiff bases containing NS donor systems,[86] trimethyl- and triphenyltin(IV) complexes of mononegative tridentate Schiff bases containing ONS donor systems,[86] dibutyltin(IV) complexes of Schiff bases derived from amino acids,[10] organotin(IV) complexes of tridentate dithiocarbazate Schiff bases containing ONS donor atoms,[85,149] dimethyl- and dibutyltin(IV) derivatives of

ketamines,[160] organolead(IV) complexes of the type R_2PbL, where R = Me or Ph and L = the dianion of planar tridentate ligands with ONO or ONS donor systems,[105] and di- and triphenyltin(IV) complexes of semi- and thiosemicarbazones.[78,81] Some Schiff bases containing ONN donor systems have shown intense absorption maxima at 335 and 380 nm which have been attributed to $\pi \rightarrow \pi^*$ and $n \rightarrow \pi^*$ transitions, respectively, of the >C=N chromophore.[110] On complexation to diphenyllead(IV), to give the complex $Ph_2Pb(ONN)$, the former transition appeared at 365 nm due to polarisation of the >C=N bond resulting from π-electron interaction between the lead and the ligand.

Charge transfer bands and secondary absorptions for the benzene ring in di- and triphenyltin(IV) complexes of semi- and thiosemicarbazones have been assigned to bands in the 344 - 397 nm region.[78,81] Organotin(IV) and organolead(IV) complexes of Schiff bases derived from S-benzyldithio-carbazate prepared by Degaonkar *et al.* exhibited a new band at 450 nm which was attributed to ligand-to-metal charge transfer.[82] Another new band at 426 nm was also observed in their continuing studies on other R_2ML complexes, where R = Cl, Me, Et, *n*-OBu, *i*-OPr or Ph, M = Pb, Ti or Sn and L = new dibasic tridentate ONS donor Schiff base dithiocarbazate ligands.[108] This was also attributed to LMCT.

A number of workers have observed sharp absorptions in the 240 - 273 nm region of the electronic spectra of organotin(IV) complexes of various ligand types.[10,86,87,160,149] These have been assigned to charge transfer due to the formation of σ bonds and $d_\pi\text{-}p_\pi$ (or $p \rightarrow d$) bonds as a result of the interaction between the *p* orbitals of the O and S ligand donor atoms and the vacant $5d$ orbitals of tin. Although this bonding model for organometal complexes has been employed by the workers mentioned above we believe that the molecular orbital diagram represented in Figure 2.3 is more suitable in representing the possible electronic transitions in these types of complexes.
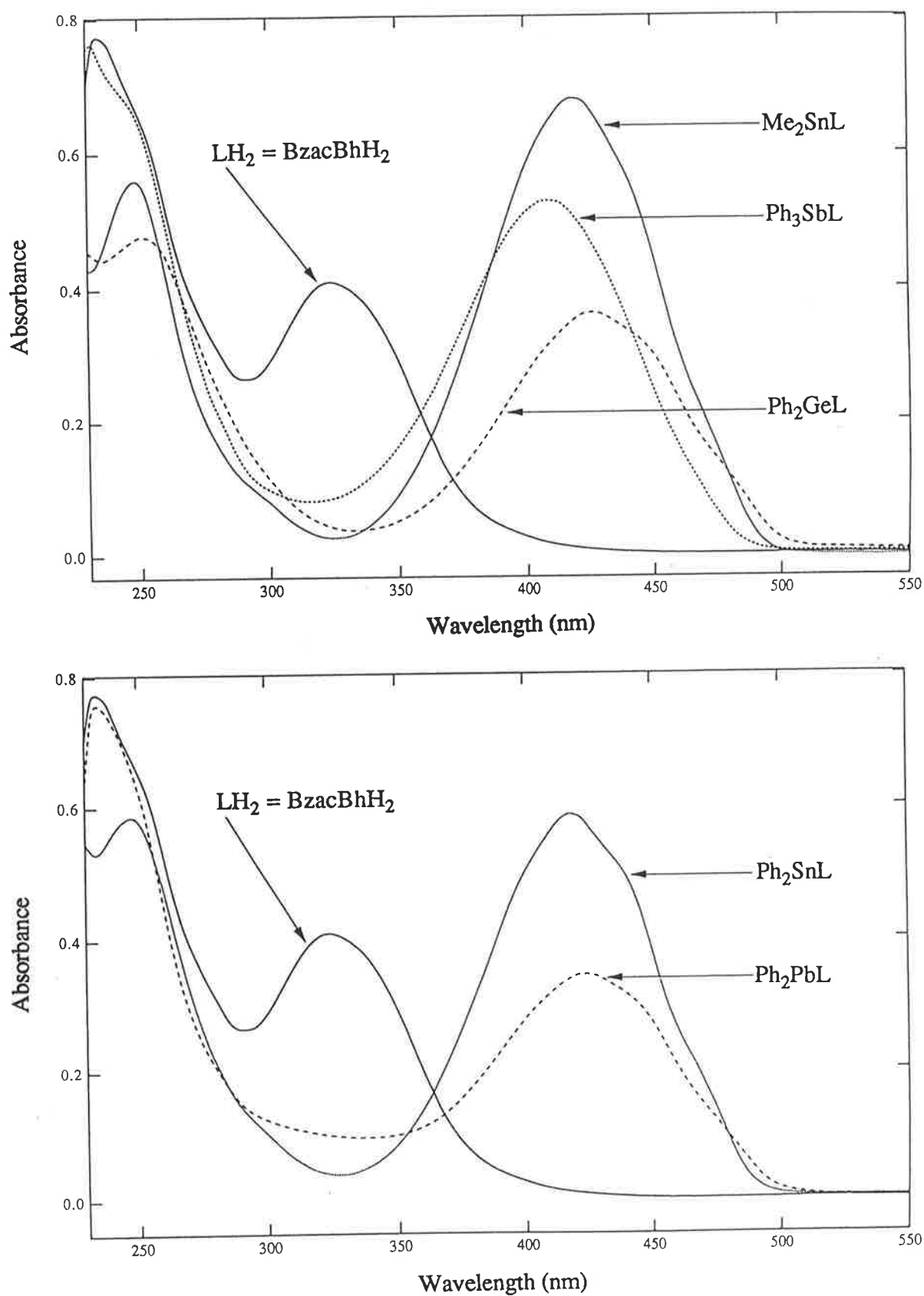
Figure 2.6: *Overlay of the electronic spectra of BzacBhH₂ (LH₂), Ph₂GeL, Me₂SnL, Ph₂SnL, Ph₂PbL and Ph₃SbL in dichloromethane.*
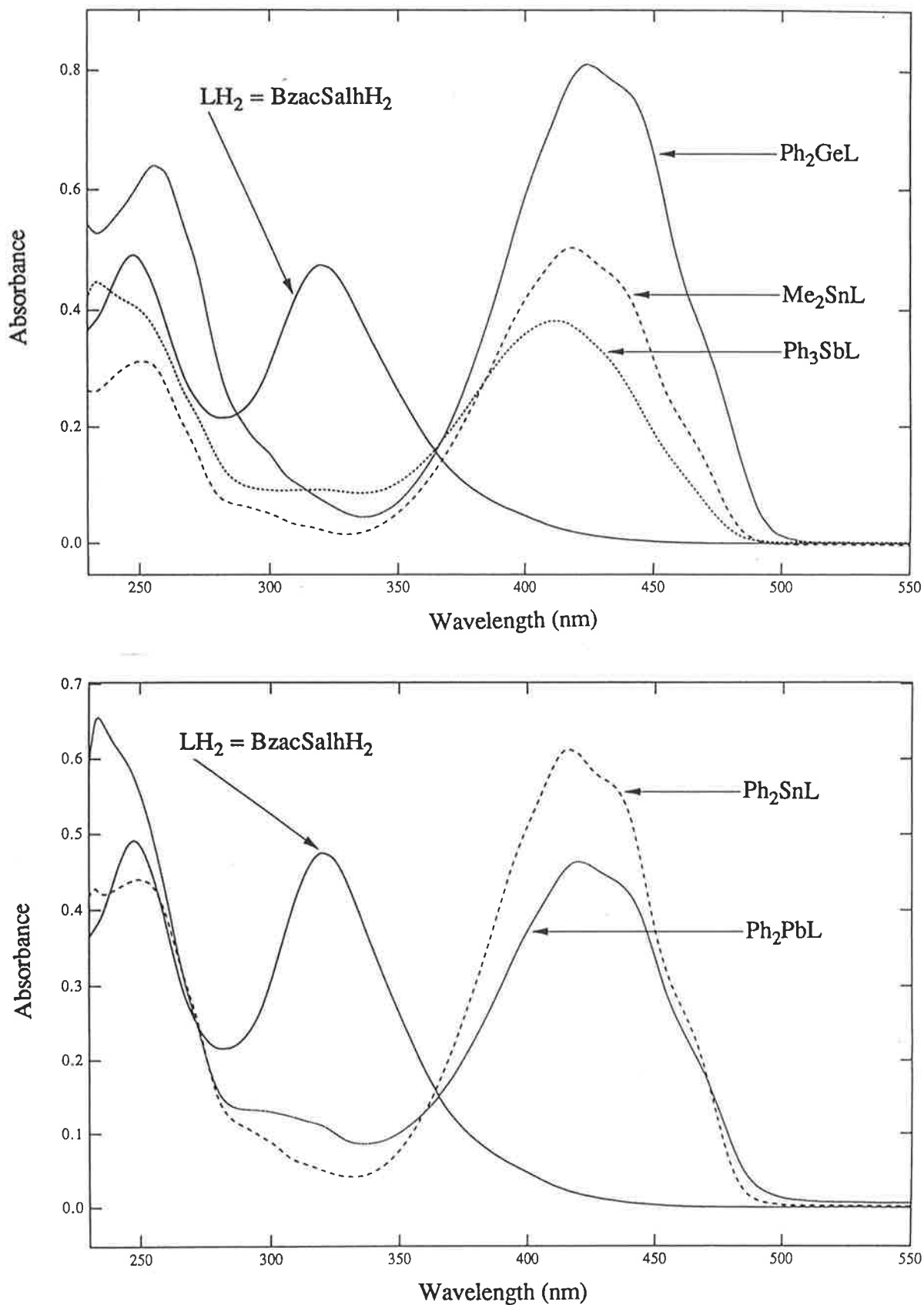
Figure 2.7: *Overlay of the electronic spectra of BzacSalhH$_2$ (LH$_2$), Ph$_2$GeL, Me$_2$SnL, Ph$_2$SnL, Ph$_2$PbL and Ph$_3$SbL in dichloromethane.*
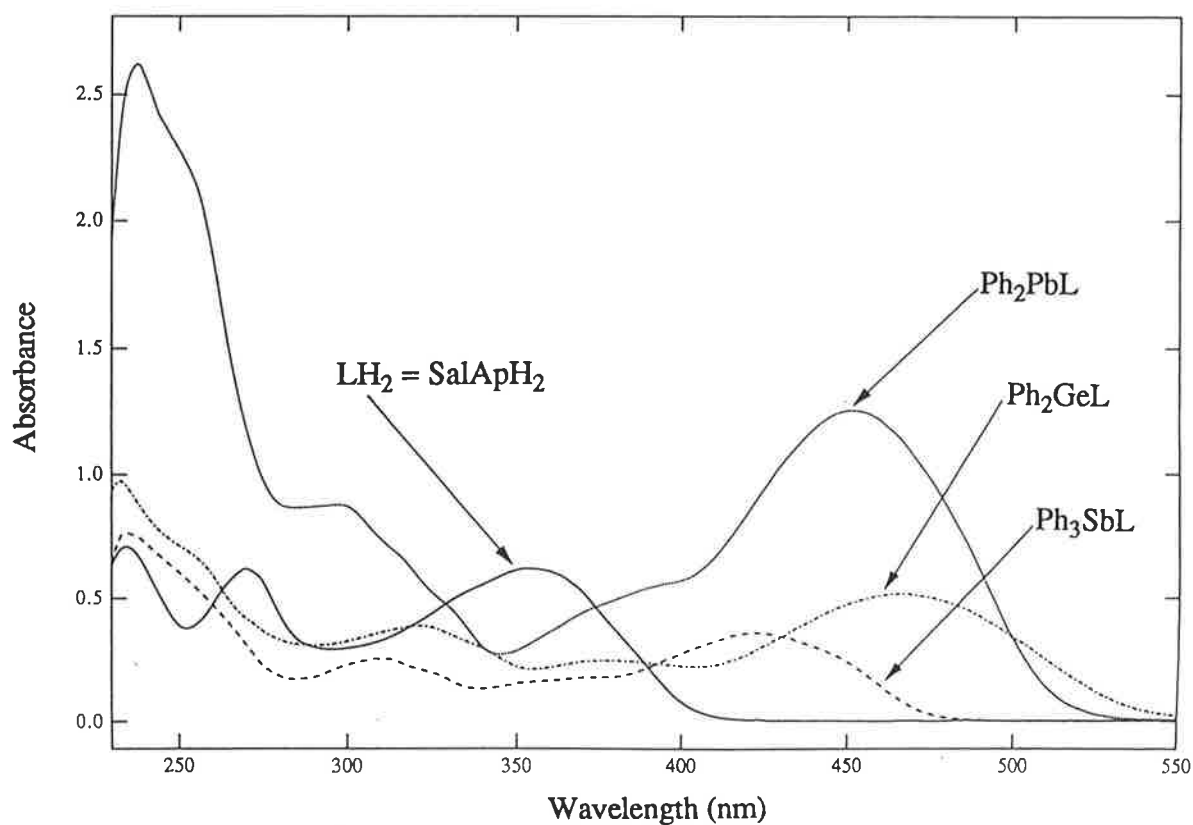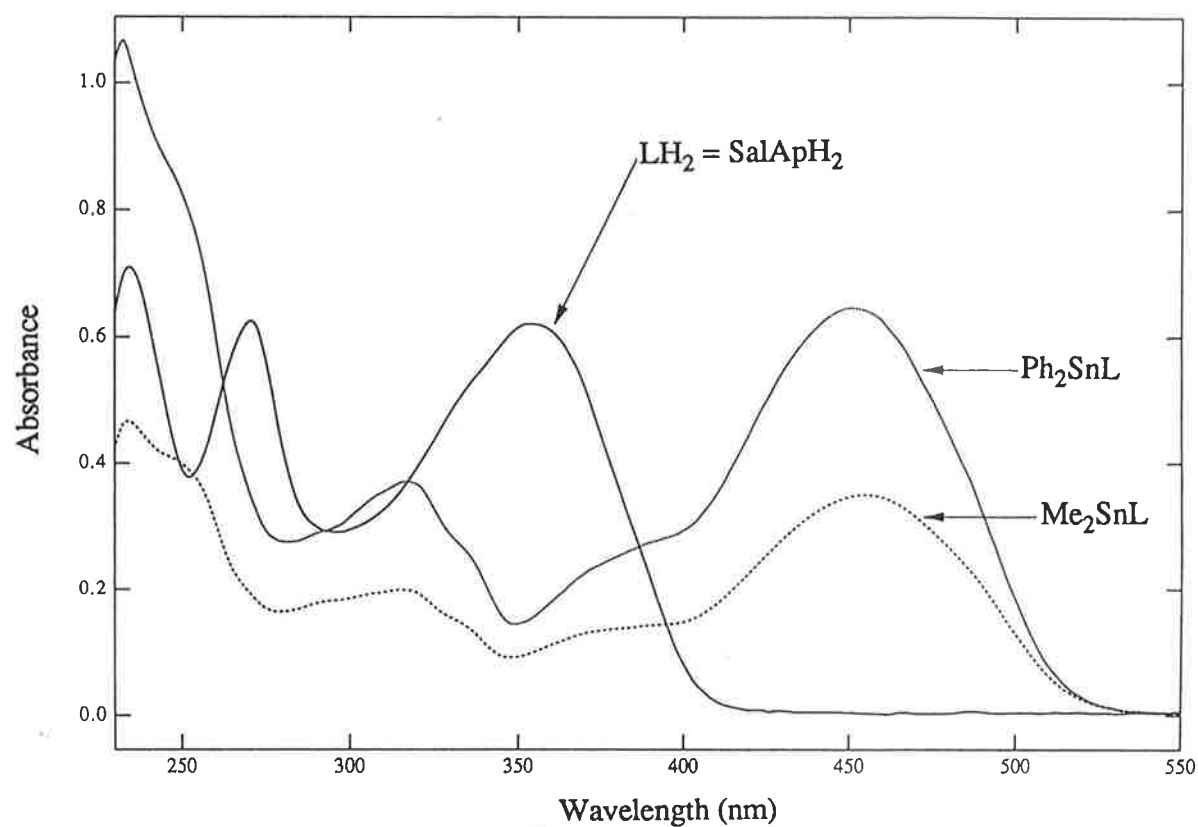
Figure 2.8: *Overlay of the electronic spectra of SalApH$_2$ (LH$_2$), Ph$_2$GeL, Me$_2$SnL, Ph$_2$SnL, Ph$_2$PbL and Ph$_3$SbL in dichloromethane.*
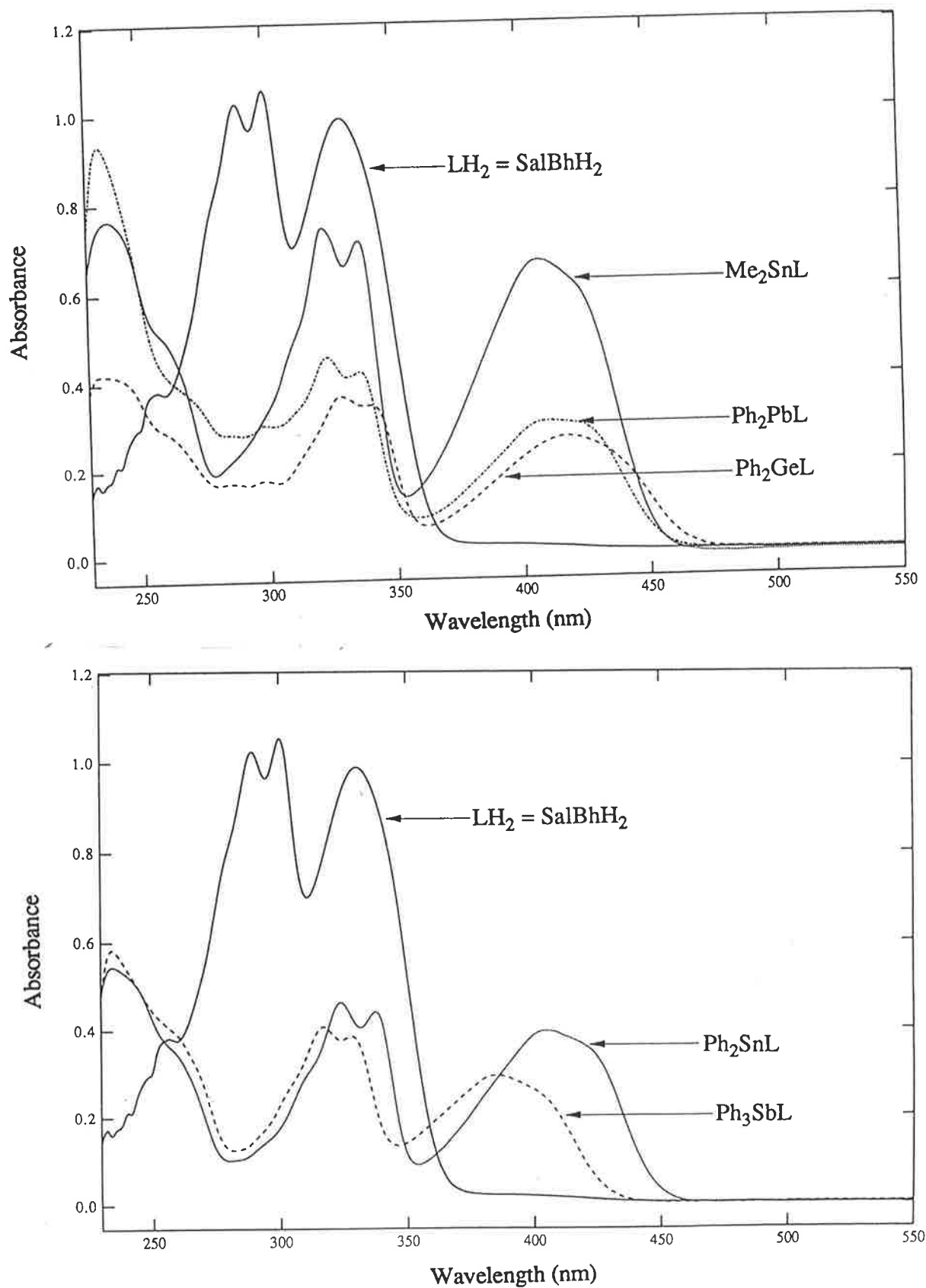
Figure 2.9: *Overlay of the electronic spectra of SalBhH2 (LH2), Ph2GeL, Me2SnL, Ph2SnL, Ph2PbL and Ph3SbL in dichloromethane.*
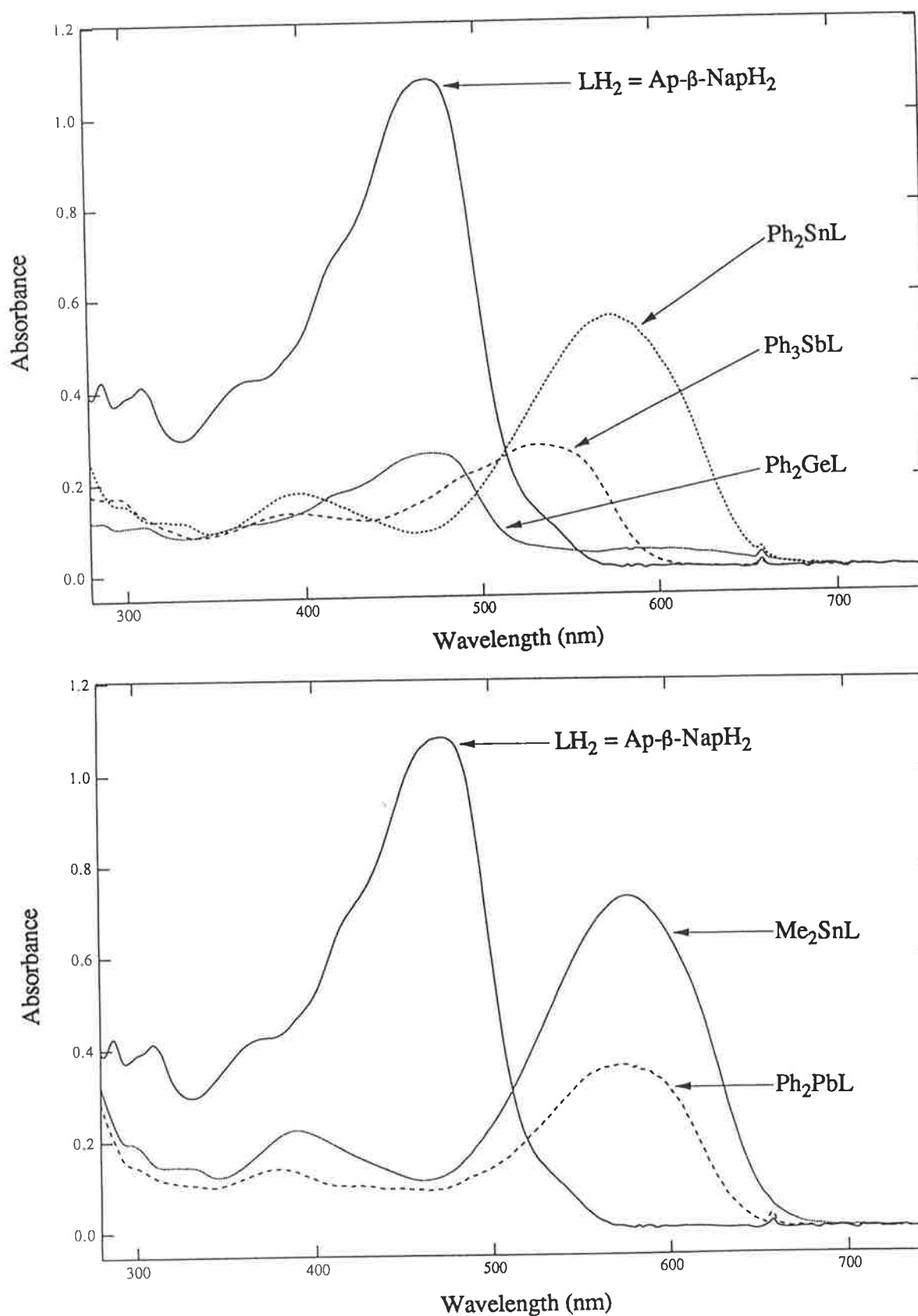
Figure 210: *Overlay of the electronic spectra of Ap-β-NapH₂ (LH₂), Ph₂GeL, Me₂SnL, Ph₂SnL, Ph₂PbL and Ph₃SbL in dichloromethane.*
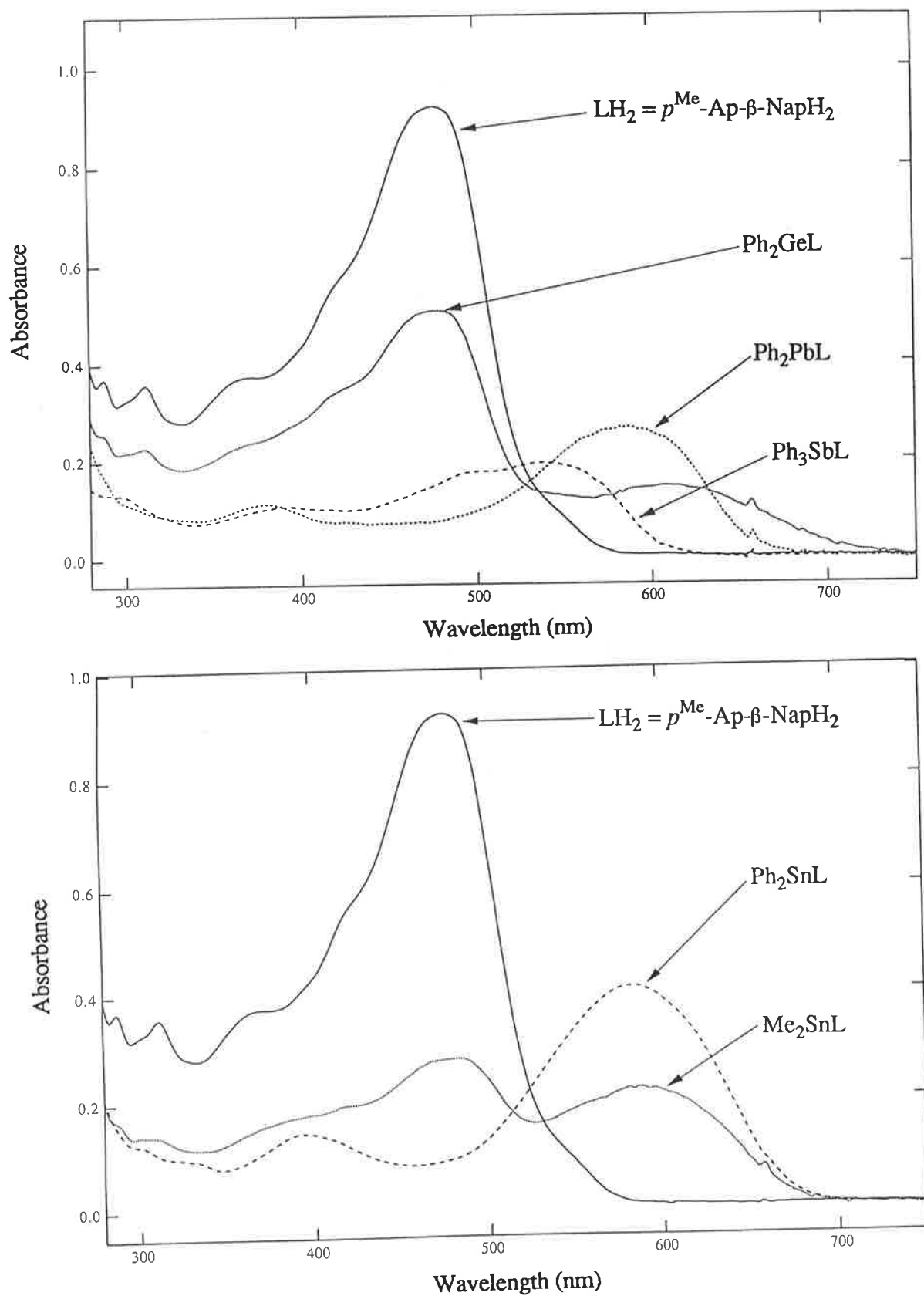
Figure 2.11: *Overlay of the electronic spectra of pMe-Ap-β-NapH2 (LH2), Ph2GeL, Me2SnL, Ph2SnL, Ph2PbL and Ph3SbL in dichloromethane.*

Table 2.10: Electronic Spectral Data for Organometal Complexes in Dichloromethane.

Ligand/ Complex	Wavelength (nm) [log ε]				
	CT(2)	CT(1)	ILT(3)	ILT(2)	ILT(1)
LH$_2$ = BzacBhH$_2$:				324 [3·81]$^{T(2)}$	
Ph$_2$GeL		426 [4·02]			252 [4·14]
Me$_2$SnL		420 [4·15]		hidden by	248 [4·06]
Ph$_2$SnL	434 sh	418 [4·21]		CT	248 [4·21]
Ph$_2$PbL	444 sh	424 [4·05]		bands	256 sh
Ph$_3$SbL		410 [4·19]			246 sh
LH$_2$ = BzacSalhH$_2$:				320 [3·96]$^{T(2)}$	248 [3·98]$^{T(1)}$
Ph$_2$GeL	438 sh	424 [4·39]			256 [4·29]
Me$_2$SnL	436 sh	418 [4·13]		hidden by	252 [3·92]
Ph$_2$SnL	436 sh	416 [4·35]		CT	250 [4·20]
Ph$_2$PbL	440 sh	420 [4·31]		bands	246 sh
Ph$_3$SbL		412 [4·20]			248 sh
LH$_2$ = SalApH$_2$:				354 [4·11]$^{T(2)}$	270 [4·12]$^{T(1)}$
Ph$_2$GeL		466 [4·05]		380 [3·73]	322 [3·92]
Me$_2$SnL		454 [4·02]		394 sh	316 [3·77]
Ph$_2$SnL		450 [4·13]		396 sh	318 [3·90]

Ph$_2$PbL		450 [4.12]		398 sh	298 [3.96]
Ph$_3$SbL		424 [4.00]		372 sh	310 [3.85]
LH$_2$ = SalBhH$_2$:			328 [4.08] T(3)	296 [4.24] T(2)	286 [4.27] T(1)
Ph$_2$GeL	436 sh	418 [3.90]		340 [4.02]	328 [4.05]
Me$_2$SnL	422 sh	408 [4.14]		336 [4.17]	322 [4.19]
Ph$_2$SnL	422 sh	406 [4.08]		338 [4.13]	324 [4.15]
Ph$_2$PbL	426 sh	410 [4.09]		336 [4.23]	324 [4.26]
Ph$_3$SbL	404 sh	384 [4.05]		328 [4.17]	316 [4.20]
LH$_2$ = Ap-β-NapH$_2$:			474 [4.21] T(3)	425 sh T(2)	377 sh T(1)
Ph$_2$GeL	586 [3.09]	474 [3.86]			382 sh
Me$_2$SnL	576 [4.20]				388 [3.69]
Ph$_2$SnL	574 [4.26]	hidden by CT(2)		hidden by CT bands	394 [3.76]
Ph$_2$PbL	572 [4.10]				380 [3.69]
Ph$_3$SbL	530 [4.00]				394 [3.69]
LH$_2$ = p^{Me}-Ap-β-NapH$_2$:			476 [4.20] T(3)	425 sh T(2)	372 sh T(1)
Ph$_2$GeL	608 [3.70]	476 [4.23]			398 sh
Me$_2$SnL	582 [3.79]	486 [3.88]		hidden by CT bands	400 sh
Ph$_2$SnL	582 [4.09]	hidden by CT(2)			394 [3.64]
Ph$_2$PbL	582 [4.01]				380 [3.64]
Ph$_3$SbL	536 [3.92]	504 [3.88]			390 [3.66]

¥ Label for this transition is only for the complexes. T(1), T(2), and T(3) refer to transitions in the protonated ligands. sh = shoulder.

2.7 Nuclear Magnetic Resonance Spectra

2.7.1 Introduction

The ^{1}H-NMR spectra of several organogermanium(IV), organotin(IV), organolead(IV) and organoantimony(V) complexes of Schiff base and azo dye ligands were recorded in CDCl$_3$ using TMS as the internal standard. In addition, the ^{1}H-NMR spectra of the ML$_2$ complexes of germanium and tin were recorded in CDCl$_3$/TMS. Due to insufficient solubility of SalHbaH$_2$ in chloroform the ^{1}H-NMR spectrum of this ligand and its tin complex were recorded in (CD$_3$)$_2$SO/TMS. Comparisons were made with the ^{1}H-NMR spectra of the protonated ligands in the same solvent/reference system. Although the Schiff base SalBhH$_2$ was also insufficiently soluble in CDCl$_3$, for comparison purposes complexes of this ligand were studied in CDCl$_3$. Particular interest was paid to the signals due to the hyroxyl protons and the signals due to the -C$\underline{H}$=N- or >C=C$\underline{H}$- protons, as the disappearance of the former and the shift in the latter of these signals upon complexation of the Schiff base or azo dye ligands would provide an indication as to whether coordination of the ligands had taken place. The ^{1}H-NMR spectra of the Schiff bases can be complicated due to keto-enol tautomerism. Often resonances due to protons of hydroxyl groups are so broad that they are not observed. Results are summarised in Table 2.11. Literature data for some identical and some related SalAp and SalBh organometal complexes prepared and studied by other workers are also given in Table 2.11 (in bold and italic).[9,123,161]

2.7.2 Results

Signals for the hydroxyl protons in the Schiff base SalHbaH$_2$ were observed at δ13.69 and δ9.65 ppm. The intensity of these signals was lower than in the ligand and their position shifted downfield slightly (δ13.71 and δ9.70 ppm, respectively) upon complexation to tin. However, absence of these signals is expected as an indication of deprotonation and coordination of the Schiff base. This could be attributed to the tridentate ligand coordinating through the protonated form. The remaining chemical shift signals characteristic for Ar-$\underline{H}$, -C$\underline{H}$=N- and =N-C$\underline{H}_2$- were all observed at the same positions after complexation of SalHbaH$_2$.

Signals for the hydroxyl protons in the azo dye Ap-β-NapH$_2$ were observed at δ14·53 and δ12·45 ppm and those in the azo dye pMe-Ap-β-NapH$_2$ were observed at δ14·59 and δ12·26 ppm. The absence of these resonances in the spectra of their complexes (R$_n$ML and ML$_2$) is indicative of deprotonation and complexation of the phenolic oxygen atoms to the metal.

Ligands BzacBhH$_2$ and BzacSalhH$_2$ would both exhibit a signal due to hydroxyl protons if they exist in the enol tautomer. Indeed the ^{1}H-NMR spectra of these ligands showed them to favour the enol tautomer in deuterated chloroform as no signal due to an -N<u>H</u>- proton was observed in the spectrum of either. However, only BzacSalhH$_2$ showed a signal due to a hydroxyl proton, at δ11·26 ppm. Three hydroxyl protons are present in the enol tautomer of this ligand, each in a different enviroment. Integration of this spectrum showed that the singlet in the δ(O<u>H</u>) region was due to one proton only. This hydroxyl proton resonance was assigned to the phenolic hydroxyl function (the other two are enolic hydroxyls) which did not take part in coordination since it appeared in the spectra of its complexes (except that of Ph$_2$Pb(BzacSalh)). A downward shift for this signal (δ12·35 - 11·51 ppm) upon complexation lends support to the coordination of BzacSalhH$_2$ through the diketone and hydrazide functions of the ligand.

The methyne proton (-C<u>H</u>=C<) signals of the Schiff bases BzacBhH$_2$ and BzacSalhH$_2$ were observed at δ5·44 and δ5·29 ppm, respectively. The presence of these signals is further evidence that these ligands favoured the enol tautomer. In the corresponding complexes, these signals appeared in the ranges δ5·88 - 5·56 ppm and δ5·94 - 5·59 ppm, respectively, showing that the enolic form was also adopted when the ligand complexed. The shift observed for these signals was greatest in the germanium complexes and least in the lead complexes. Similar results have been reported by other workers. For example, signals due to -C<u>H</u>=C< protons in Schiff base and β-diketonate complexes of tin, lead and antimony have been observed in the δ6·56 - 5·40 ppm,[58,161] δ5·67 - 5·05 ppm[105] and δ6·40 - 5·01 ppm[116,119,124] regions, respectively.

A singlet was observed for the methyl protons C<u>H</u>$_3$C=N- in BzacBhH$_2$ and BzacSalhH$_2$ at positions δ2·08 ppm and δ2·15 ppm, respectively. These singlets were shifted downfield (δ2·58 - 2·21 ppm) upon complexation suggesting coordination through the azomethine nitrogen atom. Similar observations have been made in numerous other studies on tin,[85,153,161-163]

lead[105] and antimony[124,125] complexes of Schiff base ligands of the donor type ON, ONO, NS, ONS and tetraaza (N_4) macrocycles.

The free Schiff base SalApH$_2$ contains no diketone or hydrazide moieties. The oxygen donor atoms in this ligand are phenolic oxygens. The azomethine proton (-C$\underline{H}$=N-) resonance appeared at $\delta 8.69$ ppm. In the ^{1}H-NMR spectra of the R$_2$M(SalAp) complexes, where R = Me, *n*-Bu or Ph and M = germanium, tin or lead, and the Ph$_3$Sb(SalAp) complex this azomethine proton resonance was observed in the $\delta 8.69$ - 8.16 ppm region. This resonance in the Ph$_2$Ge(SalAp) and R$_2$Sn(SalAp) (R = Me, *n*-Bu or Ph) complexes appeared at the higher chemical shift end of this range. A greater shift upfield in the azomethine proton signal was observed in the lead and antimony complexes. The general shift upfield for this signal is indicative of coordination by the azomethine nitrogen atom.[126,140] In the dimethyl- and diphenyltin complexes of SalApH$_2$ the chemical shift of the azomethine proton resonance agrees well with literature data on the same compounds.[161] Owing to the insufficient solubility of SalBhH$_2$ in chloroform, a spectrum for this ligand was not recorded. Organometal complexes of this ligand displayed the azomethine proton resonance in the $\delta 8.83$ - 8.08 ppm region.

The organo groups, especially the aliphatic ones, further supported the R$_n$ML formulation (n = 2 or 3). Resonances due to the Sn-C$\underline{H}_3$ protons were observed as a sharp singlet in the $\delta 0.85$ - 0.78 ppm region consistent with data reported in the literature.[9,59,87,164-166] On the sides of this singlet double satellite resonances appeared which were approximately 6 - 8% the intensity of the central resonance. This is due to coupling of the methyl protons with the ^{117}Sn and ^{119}Sn isotopes.[82,108,164]

Resonances due to methyl (C$\underline{H}_3$-) and methylene (-C$\underline{H}_2$-) protons of the *n*-butyl groups attached to tin were assigned to resonances in the $\delta 0.92$ - 0.84 ppm and $\delta 1.82$ - 1.25 ppm regions, respectively, consistent with that found in di-*n*-butyltin and tri-*n*-butyltin complexes of carboxylate ligands.[167] As in these reports, the methylene resonances of the *n*-butyl groups could not be individually located. Muralidhara *et al.* could not resolve them at even at 200 MHz.[167] Chandler *et al.*, on the other hand, have assigned resonances at $\delta(0.79$ ppm; t), $\delta(1.30$ ppm; m), $\delta(1.43$ ppm; m) and $\delta(3.75$ ppm; t), $\delta(3.49$ ppm; t) to C$\underline{H}_3$, γ-C$\underline{H}_2$, β-C$\underline{H}_2$ and α-C$\underline{H}_2$ protons respectively, where t = triplet and m = multiplet.[168]

In the ^{1}H-NMR spectra of the diphenyl metal complexes, the multiplet observed in the aromatic region was quite complicated, hence it was difficult to differentiate between the resonances due to the aromatic protons of the Schiff base or azo dye ligands and those due to the protons of the phenyl organo groups directly attached to the metal atoms. Some workers have attempted to distinguish between the two enviroments.[81] For example, Nath *et al.* assigned the resonances in the ranges $\delta 7.67 - 6.90$ ppm and $\delta 7.98 - 7.20$ ppm to the aromatic protons in the ligands and the protons on the phenyl groups directly attached to tin, respectively, in di- and triphenyltin(IV) complexes of semi- and thiosemicarbazones.[81] ^{1}H-NMR studies on complexes in which the only aromatic protons present are those due to phenyl groups directly attached to antimony report a range of $\delta 8.40 - 7.10$ ppm.[169]

Table 2.11: ^{1}H-NMR Spectral Data for the ML$_2$ and the Organometal Complexes.

Ligand/ Complex	Chemical Shift in ppm (Integration)				
	-N-H/-O-H	Ar-H	>C=CH-/ -CH=N-	-C-CH$_3$	Sn-R (R = Me or n-Bu)
LH$_2$ = BzacBhH$_2$	–	7·95 - 7·26 (m; 10H)	5·44 (s; 1H)	2·08 (s; 3H)	--
Ph$_2$GeL	–	8·18 - 7·03 (m; 20H)	5·88 (s; 1H)	2·58 (s; 2H)	--
Me$_2$SnL	--	8·07 - 7·37 (m; 10H)	5·63 (s; 1H)	2·55 (s; 3H)	0·78 (s; 5H)
n-Bu$_2$SnL	--	8·21 - 7·37 (m; 8H)	5·62 (s; 1H)	2·54 (s???)	1·78 - 1·25 (m; 12H), 0·92 (t; 6H)
Ph$_2$SnL	–	8·25 - 7·38 (m; 20H)	5·80 (s; 1H)	2·55 (s; 3H)	--
Ph$_2$PbL	–	8·25 - 7·36 (m; 20H)	5·56 (s; 1H)	2·49 (s; 3H)	--
Ph$_3$SbL	--	8·14 - 7·18 (m; 25H)	5·57 (s; 1H)	2·30 (s; 3H)	--
LH$_2$ = BzacSalhH$_2$	11·26 (s; 1H)	8·44 - 6·89 (m; 10H)	5·29 (s; 1H)	2·15 (s; 3H)	--
Ph$_2$GeL	11·51 (s; 1H)	8·10 - 6·96 (m; 19H)	5·94 (s; 1H)	2·50 (s; 3H)	--
Me$_2$SnL	12·22 (s; 1H)	7·89 - 6·86 (m; 10H)	5·67 (s; 1H)	2·46 (s; 3H)	0·83 (s; 6H)
n-Bu$_2$SnL	12·35 (s; 1H)	8·10 - 6·90 (m; 9H)	5·66 (s; 1H)	2·45 (s; 3H)	1·82 - 1·25 (m; 13H), 0·88 (t; 7H)
Ph$_2$SnL	12·07 (s; 1H)	8·22 - 6·98 (m; 19H)	5·84 (s; 1H)	2·46 (s; 3H)	--
Ph$_2$PbL		8·19 - 6·97 (m; 19H)	5·59 (s; 1H)	2·37 (s; 3H)	--
Ph$_3$SbL	12·00 (s; 1H)	8·29 - 6·94 (m; 24H)	5·61 (s; 1H)	2·21 (s; 3H)	--
LH$_2$ = SalApH$_2$	--	7·45 - 6·97 (m; 18H)	8·69 (s; 1H)	--	--
Ph$_2$GeL	--	8·03 - 6·73 (m; 18H)	8·69 (s; 1H)	--	--
Me$_2$SnL	--	7·43 - 6·69 (m; 8H)	8·68 (s; 1H)	--	0·78 (s; 6H)
Me$_2$SnL^a	–	*7·60 - 6·50*	*8·60*	--	*0·75*
n-Bu$_2$SnL	--	7·41 - 6·66 (m; 8H)	8·66 (s; 1H)	--	1·68 - 1·26 (m; 12H), 0·84 (t; 6H)
Ph$_2$SnL	--	8·05 - 6·71 (m; 18H)	8·69 (s; 1H)	--	--
Ph$_2$SnL^a	--	*8·20 - 6·40*	*8·60*	--	--
Ph$_2$PbL	--	7·92 - 6·57 (m; 18H)	8·42 (s; 1H)	--	--
Ph$_2$PbL^b	--	*8·0 - 6·2*	*8·25*	--	--
Me$_2$PbL^b	--	*7·3 - 6·3*	*8·20*	--	2·05
Ph$_3$SbL	--	7·61 - 6·71 (m; 23H)	8·16 (s; 1 H)	--	--
Me$_3$SbL^c	Remaining data not given for this complex in the literature				1·15
LH$_2$ = SalBhH$_2$	Not recorded due to insufficient solubility				
Ph$_2$GeL	--	8·20 - 6·81 (m; 19H)	8·83 (s; 1H)	--	--

	-O-H	Ar-H	-CH=N-	=N-CH₂-	Sn-R (R = Me or n-Bu)
Me₂SnL	--	8·08 - 6·72 (m; 10H)	8·76 (s; 1H)	--	0·84 (s; 6H)
Me₂SnL[d]	--	*8·07 - 6·75*	*8·76*	--	*0·84*
n-Bu₂SnL	--	8·09 - 6·70 (m; 8H)	8·75 (s; 1H)	--	1·69 - 1·25 (m; 12H), 0·86 (t; 6H)
Ph₂SnL	--	8·26 - 6·76 (m; 19H)	8·76 (s; 1H)	--	--
Ph₂PbL	--	8·24 - 6·63 (m; 19H)	8·47 (s; 1H)	--	--
Ph₃SbL	--	8·15 - 6·77 (m; 24H)	8·08 (s; 1H)	--	
LH₂ = Ap-β-NapH₂	14·53 (s;1H), 12·45 (s; 1H)	8·25 - 7·08 (m; 10H)	--	--	--
Ph₂GeL	--	8·26 - 7·06 (m)	--	--	--
Me₂SnL	--	8·60 - 6·80 (m; 10H)	--	--	0·85 (s; 6H)
n-Bu₂SnL	--	8·60 - 6·75 (m; 10H)	--	--	1·70 - 1·25 (m; 12H), 0·85 (t; 6H)
Ph₂SnL	--	8·60 - 6·81 (m)	--	--	--
Ph₂PbL	--	8·56 - 6·67 (m)	--	--	--
Ph₃SbL	--	8·63 - 6·79 (m)	--	--	--
GeL₂	--	8·80 - 6·73 (m)	--	--	--
SnL₂	--	8·81 - 6·91 (m)	--	--	--
LH₂ = p^Me-Ap-β-NapH₂	14·59 (s; 1H), 12·26 (s; 1H)	8·26 - 6·99 (m;9H)	--	2·40 (s; 3H)	--
Ph₂GeL	--	8·56 - 6·99 (m; 19H)	--	2·36 (s; 3H)	--
Me₂SnL	--	8·61 - 6·75 (m; 10H)	--	2·37 (s; 3H)	0·83 (s; 6H)
n-Bu₂SnL	--	8·62 - 6·76 (m; 9H)	--	2·36 (s; 3H)	1·67 - 1·29 (m; 12H), 0·84 (s; 6H)
Ph₂SnL	--	8·61 - 6·68 (m; 19H)	--	2·35 (s; 3H)	--
Ph₂PbL	--	8·57 - 6·90 (m; 19H)	--	2·34 (s; 3H)	--
Ph₃SbL	--	8·64 - 6·98 (m; 24H)	--	2·29 (s; 3H)	--
LH₂ = Ap-p^Cl-PhenolH₂					
GeL₂	--	8·05 - 6·66 (m)	--	--	--
	-O-H	**Ar-H**	**-CH=N-**	**=N-CH₂-**	**Sn-R (R = Me or n-Bu)**
LH₂ = SalHbaH₂	13·69 (s; 1H), 9·65 (s; 1H)	7·47 - 6·74 (m; 8H)	8·63 (s; 1H)	4·71 (s; 2H)	--
Sn(SalHba)₂	13·71 (s, 0·5H), 9·70 (s; 0·5H)	7·47 - 6·74 (m; 8H)	8·63 (s; 1H)	4·71 (s; 2H)	--

s = singlet, t = triplet and m = multiplet.
[a] Reference 161; [b] Reference 105; [c] Reference 123; [d] Reference 9.

2.8 Crystal Structures of Some Organometal Complexes

Crystal structures were determined for a series of representative complexes, namely Ph_2GeL, Ph_2SnL, Ph_2PbL and Ph_3SbL, where L = SalAp. In these structures, a distorted trigonal bipyramid geometry was found for the germanium and tin complexes, and a distorted octahedral geometry was found for the lead and antimony complexes. During the course of this investigation we became aware that the crystal structures of $Ph_2Sn(SalAp)$,[170] the analogous dimethyltin complex $Me_2Sn(SalAp)$[171] and the trimethylantimony complex $Me_3Sb(SalAp)$[123] had been determined. The two crystal structures of $Ph_2Sn(SalAp)$ are not isomorphous, however, apart from some small differences, the preexisiting structure of $Ph_2Sn(SalAp)$[170] was essentially the same as that determined by us. Evidence for disorder in the Ph_2GeL, Ph_2SnL and Ph_3SbL structures was found in that there were two sites for the C=N atoms (each site was assigned 50% occupancy). In the diagrams the disorder is illustrated but in the relevant Tables only one set of contacts is listed; in the Appendix all bond distances and angles are listed.

2.8.1 Introduction

In discussing the coordination geometry of organotin complexes it is convenient to consider the tin atom together with its organo substituents as a coordination centre to which anionic or neutral donors can be attached. In this way coordination numbers greater than the group valency of four are easily achieved.[172] Many coordination geometries may be acquired by organotin complexes, either as neutral or ionic species, in which the tin atom possesses a coordination number of four, five, six, seven and, in some cases, eight have been found. Triorganotin derivatives which are pentacoordinate are well known, but less well known are examples of hexacoordinate tin. On the other hand, both penta- and hexacoordinate diorganotin complexes are known.[172] The former include diorganotin halide oxinates and diorganotin halide carboxylates, and the latter include diorganotin bis(chelates) (e.g. carboxylate and acetylacetonate chelates). In most of the hexacoordinate diorganotin complexes, the two alkyl organo groups are positioned approximately *trans* to each other.[172] Relatively little work has been carried out on monoorganotin derivatives, however examples of hexacoordinate (e.g. $[(acac)XRSn(OCH_3)]_2$, where X = halide and R = Me, Et or *n*-Bu[173]) and

heptacoordinate (e.g. phenyltin tris(tropolonate)[174]) monoorganotin derivatives are known.

The first pentacoordinate tin structure published in 1962 was that of the pyridine complex of trimethyltin(IV) chloride, $Me_3Sn(Cl)py$.[175] The methyl groups were found to occupy the equatorial positions of a trigonal bipyramid and the chlorine and nitrogen atoms occupied the axial positions. This arrangement of atoms in the first coordination sphere of tin has been found to be a common feature of pentacoordinated triorganotin complexes. A trigonal bipyramidal geometry agrees well with the valence shell electron pair repulsion theory according to which a trigonal bipyramidal geometry is favoured for five valence electron pairs, with the bonding pairs from the more electronegative ligands taking up the axial positions.[172] Thus, in triorganotin complexes, the carbon atoms through which the organo groups are attached would be coplanar with the central metal atom, and the more electronegative donors would occupy the axial positions. This is an example of Bent's rule.[98b,117,161] and is illustrated in Figure 2.12.
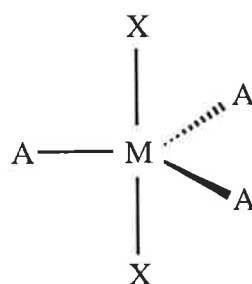
Figure 2.12: *Trigonal bipyramidal coordination around the metal M, where donor atom X is more electronegative than donor atom A.*

A trigonal bipyramidal arrangement which produces a non-linear C-Sn-C moiety (C = carbon donor atoms from the organo groups) is also found in the diorganotin complexes. Examples of di- and triorganotin complexes exhibiting this arrangement include Ph_2SnL, where L = ONO or ONS donor ligands,[170,176] $\{[Me_2Sn(O_2CC_4H_3S)]_2O\}_2$[60] $[(cyclo-C_6H_{11})_2NH_2][Bu_3-Sn(O_2CC_6H_4-2-SO_3],$[177] $R_2Sn(Cl)L$, where R = Me or Ph and L = O, S or OS donor ligands,[178-181] R_3SnL, where R = Ph and L = RCO_2,[182]

β-diketonate[183] or the anion of N-benzoyl-N-phenylhydroxylamine,[184] and [Bu$_4$N][Me$_2$SnCl(Dmit)],[185] where Dmit = dianion of 4,5-dimercapto-1,3-dithiole-2-thione.

Intermolecular bonding in organotin complexes, by ligands acting as bridging groups, has resulted in the formation of dimeric structures.[66,171] For example, two individual Me$_2$Sn(SalAp) molecules which each form a distorted trigonal bipyramid, form a weakly associated dimer containing hexacoordinate tin atoms as depicted in Figure 2.13.[171]
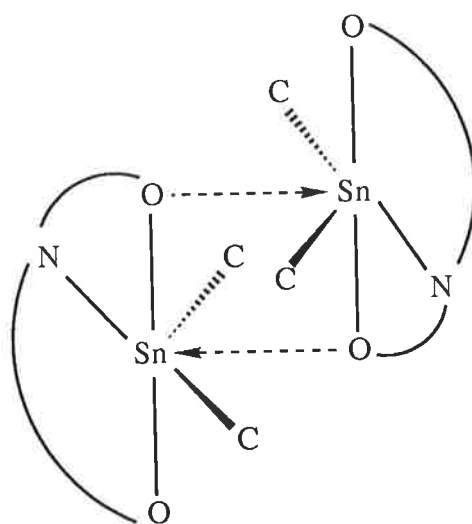
Figure 2.13: *Representation of the dimerisation of two molecules of Me$_2$Sn(SalAp) via an oxygen atom of each tridentate ONO donor ligand, giving hexacoordinate tin. C = the carbon atom of a methyl group.*

Bent's rule has also been observed in the pentacoordinate triorganoantimony complexes, R$_3$SbX$_2$, where R = Me or Ph and X = F, Cl, Br, NCS or R'CO$_2$.[122,186,187] In addition, hexacoordinate di- and triorganoantimony complexes which display octahedral geometries have been found.[116,122,123] Examples include Ph$_2$Sb(acac)Cl$_2$ and Me$_3$SbL, where L = a dinegative tridentate ligand.[116,118,123] In the diorganoantimony complex just mentioned, the organo groups were *trans* to each other and this agreed with the conclusions reached from NMR experiments. Similar conclusions on the position of the organo groups, based on NMR and Mössbauer studies, have

been made for other diorganoantimony complexes, such as R_2SbX_2L, where R = Me or Ph, X = Cl or Br and L = acac, dpm (*tert*-BuCOCHCO-*tert*-Bu) or pac (*tert*-BuCOCHCOMe),[116-118,122] and $Me_2SbL(Cl)$, where L = the dinegative tridentate ligand SalAp.[188] A feature of all the triorganoantimony complexes is a T-shaped C_3Sb moiety (C = carbon donor atoms of the organo groups). From NMR and Mössbauer measurements, this structure was reasonably assumed for other complexes such as $Ph_3Sb(acac)Cl$[116] and Ph_3SbL, where L = a dinegative tridentate Schiff base.[122] Dimerisation has also been proposed in organoantimony complexes. For example, octahedral coordination around antimony in $R_2Sb(OMe)_3$, where R = alkyl, due to dimerisation has been suggested.[122]

Trigonal bipyramidal and octahedral geometries have been proposed by Dixit *et al.* for the diorganolead(IV) complexes $R_2Pb(L)Cl$ and R_2PbL_2, respectively, where L = a bidentate thiosemicarbazone.[109] These conclusions were reached from spectroscopic and X-ray powder diffraction studies. It was suggested that the two phenyl groups occupied the axial positions in the trigonal bipyramid geometry and *trans* positions in the octahedral geometry.

Cefalú *et al.* used structural aspects to discuss the bonding between tin and rigid planar configurations such as Schiff bases.[161] X-ray structures of pentacoordinate organotin complexes of ONO and ONS donor Schiff bases, R_2SnL, where R = Me,Bu or Ph and L = the ONO or ONS donor Schiff base, reveal that the carbon atoms of the organo groups and the nitrogen atom of the Schiff base azomethine group are positioned in a trigonal plane. Thus, tin can be considered to be nearly sp^2 hybridised to a carbon in each of the organo groups and to a nitrogen atom in the Schiff base.[161] O-Sn-O or O-Sn-S bonds are formed between the remaining tin(IV) p orbital and the O and/or S atoms orbitals of the appropriate symmetry. Quasi (trigonal) bipyramidal structures are the result. This model is consistent with a review by Muetterties and Schunn in 1966 who stated "there appear to be no pentacoordinated species, whose structure is known with reasonable certainty, in which the more electronegative ligands do not occupy the axial sites."[161]

2.8.2   Crystal structure of Ph₂Ge(SalAp)

A single crystal of Ph₂Ge(SalAp) suitable for crystal structure was obtained from a benzene solution of the compound. The molecular structure is shown in Figure 2.14 and selected bond lengths and bond angles, based on the atomic numbering used in this Figure, are listed in Tables 2.12 and 2.13, respectively. All of the crystallographic data for the crystal structure determination of Ph₂Ge(SalAp) are given in Tables A.1 and A.2 in the Appendix.

The structure is molecular, there being no significant intermolecular contacts in the lattice. Trigonal bipyramidal coordination about the germanium atom was observed in this complex. The first coordination sphere of the germanium atom was made up of two phenyl carbon atoms and a SalAp nitrogen donor atom in the equatorial positions, and two SalAp oxygen donor atoms in the axial positions of the trigonal bipyramid. The $C(121)$-Ge-$C(111)$, $C(121)$-Ge-$N(1)$ and $C(111)$-Ge-$N(1)$ bond angles were almost at the ideal trigonal angle of 120°. The Schiff base azomethine nitrogen atom, $N(1)$, was not quite coplanar with the Ge, $C(111)$ and $C(121)$ atoms. It deviated from the equatorial plane towards the Schiff base five-membered ring. Distortion of the $O(1)$-Ge-$O(2)$ bond from linearity is consistent with the bites of the chelate rings which precludes a $O(1)$-Ge-$O(2)$ bond angle of 180°. The $C(7)$-$N(1)$ distance (1·31(4) Å) clearly indicated double bond character in this bond. Furthermore, the Ge-$O(1)$ and Ge-$O(2)$ bond distances were virtually identical and the Ge-$N(1)$ distance was slightly longer than these consistent with the formation of a Ge→N dative bond.
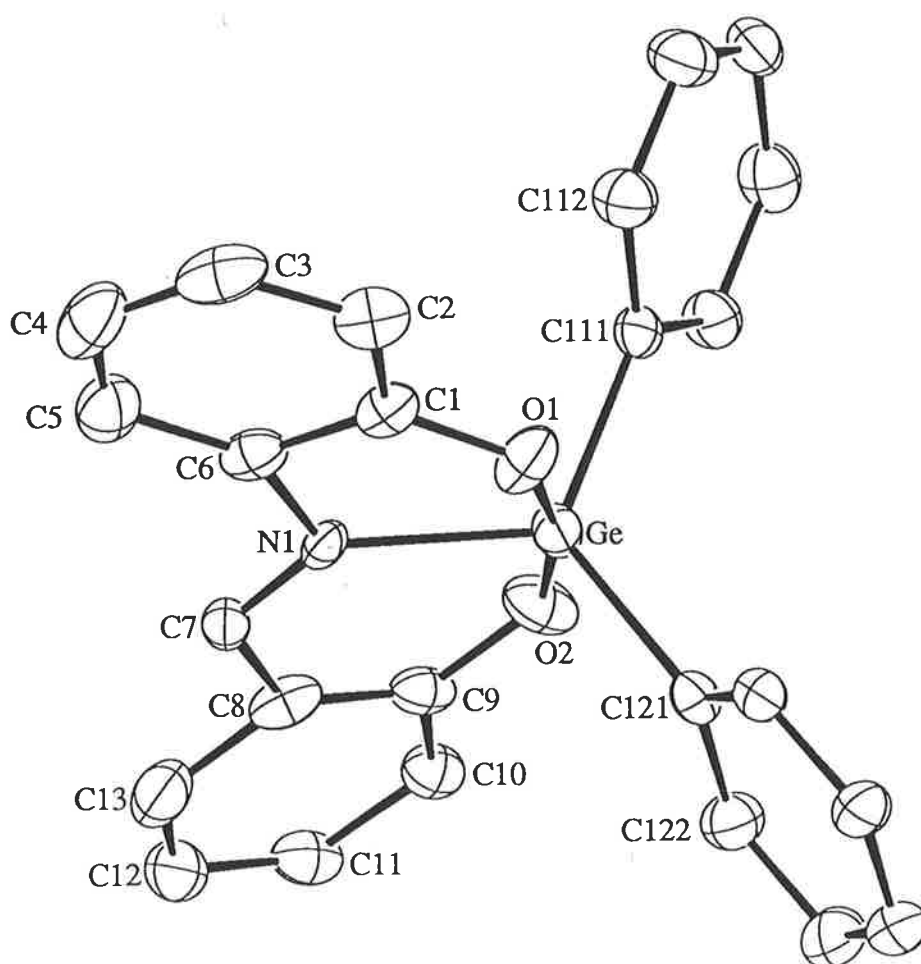
Figure 2.14: *The molecular structure of Ph₂Ge(SalAp).*

Table 2.12: Bond Distances (Å) in the Primary Coordination Sphere of Germanium in $Ph_2Ge(SalAp)$.

O(1)	--- Ge	1·921(4)
O(2)	--- Ge	1·918(4)
N(1)	--- Ge	2·04(2)
C(111)	--- Ge	1·945(4)
C(121)	--- Ge	1·946(5)

Table 2.13: Bond Angles (Degrees) in the Primary Coordination Sphere of Germanium in $Ph_2Ge(SalAp)$.

O(2)	- Ge -	O(1)	167·6(2)
N(1)	- Ge -	O(1)	72·6(7)
N(1)	- Ge -	O(2)	95·0(7)
C(111)	- Ge -	O(1)	93·5(2)
C(111)	- Ge -	O(2)	91·7(2)
C(111)	- Ge -	N(1)	116·9(4)
C(121)	- Ge -	O(1)	92·3(2)
C(121)	- Ge -	O(2)	94·6(2)
C(121)	- Ge -	N(1)	120·6(3)
C(121)	- Ge -	C(111)	121·2(2)

2.8.3   Crystal Structure of Ph$_2$Sn(SalAp)

Orange crystals of Ph$_2$Sn(SalAp) were obtained by the vapour diffusion of hexane into a dichloromethane solution of the compound. The molecular structure is depicted in Figure 2.15 and selected bond lengths and bond angles, based on the atomic numbering in this Figure, are listed in Table 2.14 and Table 2.15, respectively. All of the crystallographic data for the crystal structure of Ph$_2$Sn(SalAp) is given in Tables A.3 and A.4 in the Appendix.

The crystal lattice is comprised of discrete molecules of Ph$_2$Sn(SalAp). The first coordination sphere of the tin atom was made up of a SalAp nitrogen donor atom and two phenyl carbon atoms, which define the equatorial plane of a trigonal bipyramidal geometry, and the two SalAp oxygen donor atoms in the axial positions. The C(111)-Sn-N(1) bond angle deviated from the ideal trigonal angle of 120° more than the C(111)-Sn-C(121) and C(121)-Sn-N(1) bond angles. Furthermore, this bond angle deviated from 120° more than the corresponding bond angle in Ph$_2$Ge(SalAp) [116·9(4)°]. The axial O(1)-Sn-O(2) bond deviated from linearity more than the corresponding bond in Ph$_2$Ge(SalAp) because the greater size of the tin atom did not allow it to fit inside the chelate rings as well as the germanium atom. As a consequence the Sn-N(1) bond (2·220(6) Å) was greater than the analogous bond (Ge-N(1) = 2·04(2) Å) in Ph$_2$Ge(SalAp). No intermolecular Sn-O bridges exists in Ph$_2$Sn(SalAp) unlike in the analogous dimethyl complex, Me$_2$Sn(SalAp), which exists as a dimer (Figure 2.13).[171]

The Sn-O distances in the five- and six-membered chelate rings (2·081(3) and 2·067(4) Å) and the Sn-N distance (2·220(6) Å) were similar to those quoted by Preut *et al.*[170] for the same complex (2·103(8) and 2·085(8) Å for Sn-O and 2·24(1) Å for Sn-N) and were comparable to the analogous bond distances in the Me$_2$Sn(SalAp) complex (2·105(8) and 2·118(9) Å for Sn-O, and 2·23(1) Å for Sn-N).[171] The C(7)-N(1) distance [1·23(1) Å] was indicative of double bond character and it was comparable to the corresponding bond distances in Me$_2$Sn(SalAp) and Ph$_2$Sn(Sat),[176] where Sat = the dianion of 2-(*o*-hydroxyphenyl)benzothiazoline (1·26(2) and 1·287(5) Å, respectively). A closer comparison of bond lengths and bond angles is made in Section 2.8.6.
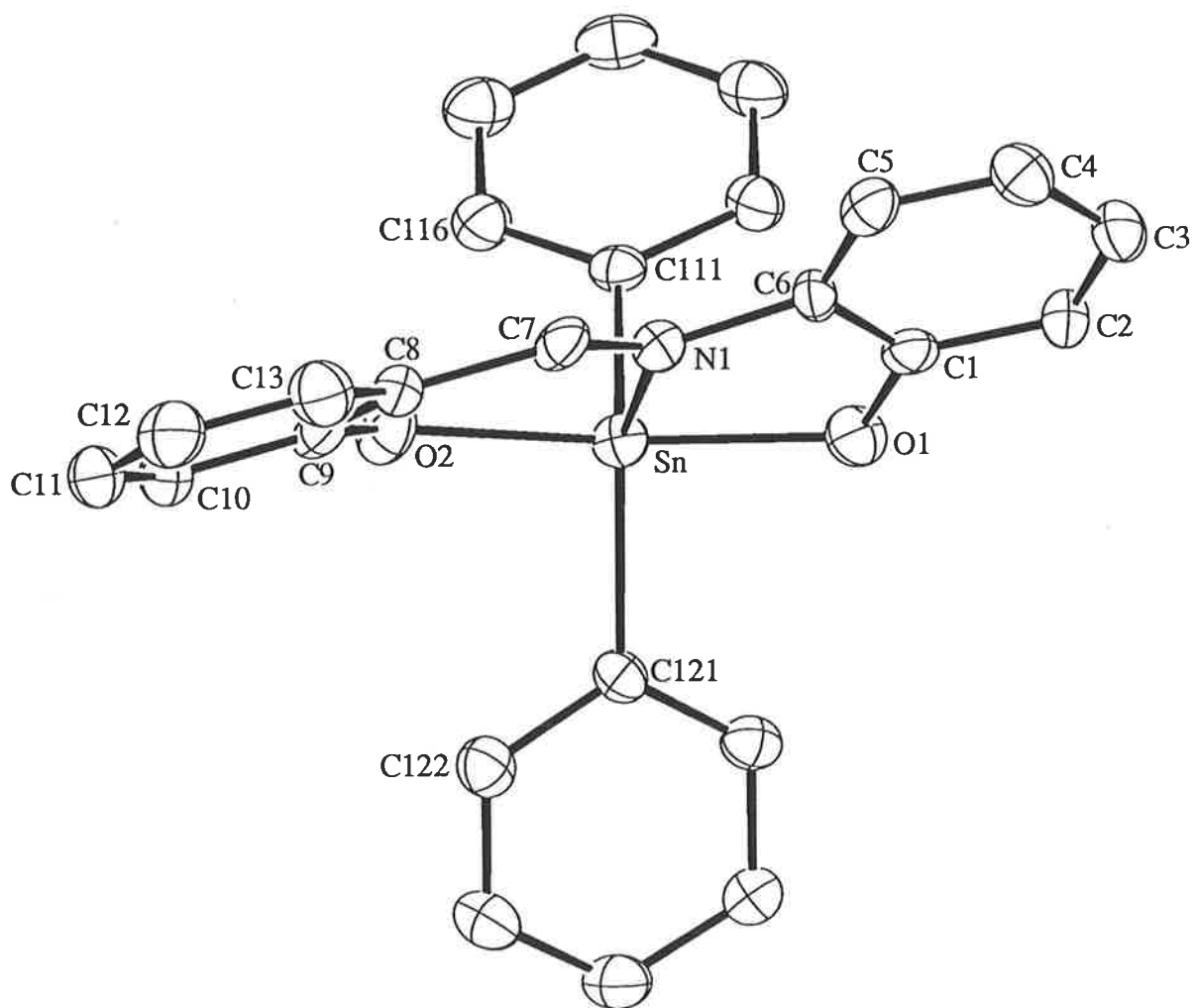
Figure 2.15: *The molecular structure of Ph₂Sn(SalAp).*

Table 2.14: Bond Distances (Å) in the Primary Coordination Sphere of Tin in Ph$_2$Sn(SalAp).

O(1)	--- Sn	2·081(3)
O(2)	--- Sn	2·067(4)
N(1)	--- Sn	2·220(6)
C(111)	--- Sn	2·118(5)
C(121)	--- Sn	2·111(5)

Table 2.15: Bond Angles (Degrees) in the Primary Coordination Sphere of Tin in Ph$_2$Sn(SalAp).

O(2)	- Sn -	O(1)		159·8(2)
N(1)	- Sn -	O(1)		74·1(2)
N(1)	- Sn -	O(2)		86·1(2)
C(111)	- Sn -	O(1)		95·4(2)
C(111)	- Sn -	O(2)		96·0(2)
C(111)	- Sn -	N(1)		113·2(2)
C(121)	- Sn -	O(1)		93·0(2)
C(121)	- Sn -	O(2)		95·4(2)
C(121)	- Sn -	N(1)		125·3(2)
C(121)	- Sn -	C(111)		120·9(2)

2.8.4 Crystal Structure of Ph₂Pb(SalAp)

A single crystal of this complex suitable for structure determination was obtained by the vapour diffusion of hexane into a dichloromethane solution of the compound. The molecular structure is depicted in Figure 2.16 and selected bond lengths and bond angles, based on the atomic numbering in this Figure, are listed in Tables 2.16 and 2.17, respectively. Only one half of the molecule was labelled as the data for the other half was identical. In the Tables primed atoms refer to the atoms in the other half of the molecule. All of the crystallographic data for this crystal structure is given in Tables A.5 and A.6 in the Appendix.

Unlike the previous two crystal structures, the coordination around the lead atom was a distorted octahedron due to the bridging of two Ph₂Pb(SalAp) units *via* the O(1) oxygen atoms of the Schiff bases. The two halves of the molecule are related to each other by a crystallographic centre a inversion. The equatorial plane of this dimeric structure is represented in Figure 2.17 from which it can be seen that the equatorial plane was soley occupied by the six Schiff base donor atoms. The two phenyl groups occupied the axial positions. The corresponding M-O bonds in the germanium and tin Ph₂M(SalAp) crystal structures were shorter than the Pb-O bonds in this structure consistent with the increasing size of the central metal atom.

The first coordination sphere of the lead atom was comprised of two phenyl carbon atoms, one nitrogen donor atom from the azomethine bridge in the tridentate SalAp ligand, and three oxygen donor atoms from two tridentate SalAp ligands. Two of the Pb-O bonds were intramolecular (Pb-O(1) = 2·246(4) Å and Pb-O(2) = 2·327(4) Å) and one was intermolecular (Pb-O(1') = 2·766(4) Å). The azomethine C(7)-N(1) bond distance (1·300(8) Å) clearly indicated double bond character in this bond.

The phenyl groups which occupied the axial (or *trans*) positions in the dimer were not colinear with the lead atoms and produced a C(111)-Pb-C(121) bond angle of 153·5(2)°. From the crystal structure in Figure 2.16 it can be seen that the phenyl groups are orientated away from the tridentate SalAp ligand such that they lie over the O(1)-Pb-O(2) angle. Furthermore, the O(1)-Pb-O(2) bond angle deviated even more from linearity than the analogous O(1)-M-O(2) bond angles in the Ph₂Ge(SalAp) and Ph₂Sn(SalAp) crystal structures due to lead being much larger in size than germanium and

tin. The larger size of lead allowed dimerisation *via* bridging oxygen atoms. A further consequence of the additional Pb$\cdots$O(1') interaction is an increase in steric pressure in the PbNO$_3$ basal plane which has the result of contracting the O(1)-Pb-O(2) angle relative to the analogous angles in the germanium and tin compounds.
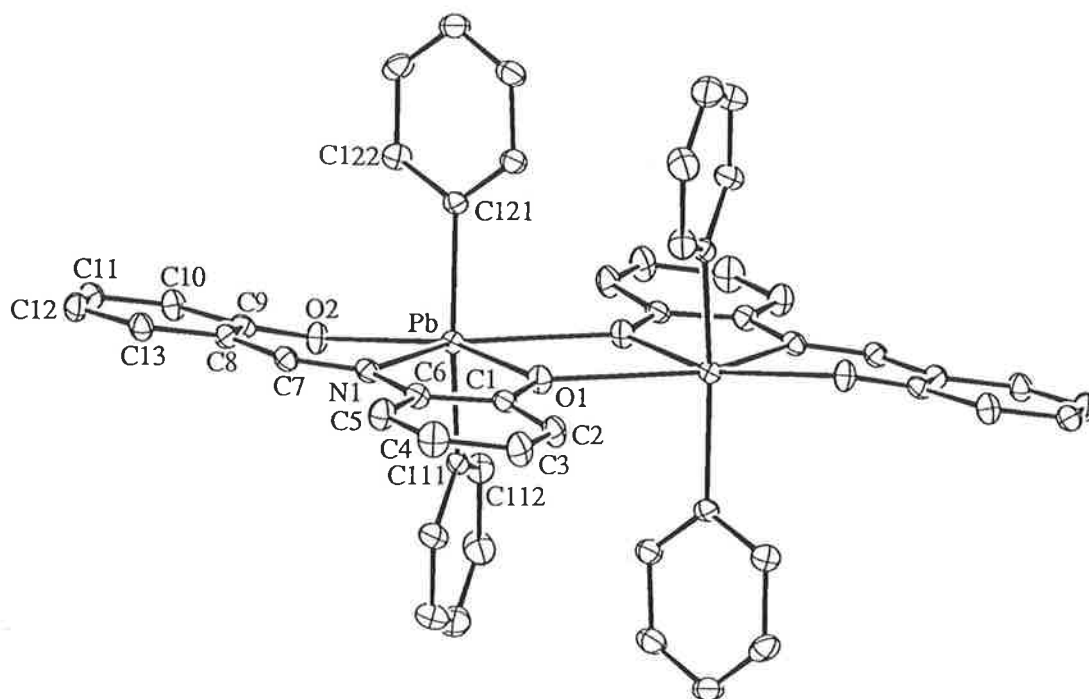
Figure 2.16: *The molecular structure of Ph₂Pb(SalAp).*
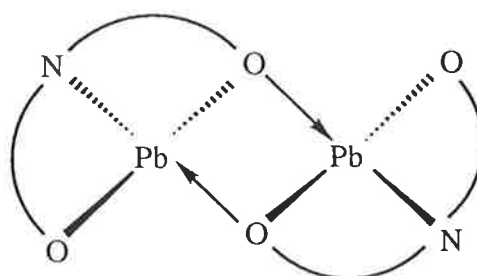
Figure 2.17: *Equatorial plane in the dimer of Ph₂Pb(SalAp).*

Table 2.16: Bond Distances (Å) in the Primary Coordination Sphere of Lead in Ph$_2$Pb(SalAp).

O(1)	--- Pb	2·246(4)
O(2)	--- Pb	2·327(4)
N(1)	--- Pb	2·337(5)
C(111)	--- Pb	2·151(6)
C(121)	--- Pb	2·166(6)
O(1')	--- Pb	2·766(4)

Table 2.17: Bond Angles (Degrees) in the Primary Coordination Sphere of Lead in Ph$_2$Pb(SalAp).

O(1)	- Pb -	O(2)	150·5(2)
O(1)	- Pb -	N(1)	72·9(2)
O(1)	- Pb -	C(111)	95·7(2)
O(1)	- Pb -	C(121)	102·4(2)
O(1)	- Pb -	O(1')	65·3(2)
O(2)	- Pb -	N(1)	79·0(2)
O(2)	- Pb -	C(111)	82·2(2)
O(2)	- Pb -	C(121)	90·7(2)
O(2)	- Pb -	O(1')	142·7(2)
N(1)	- Pb -	O(1')	138·1(2)
C(111)	- Pb -	N(1)	103·6(2)
C(111)	- Pb -	O(1')	84·1(2)
C(121)	- Pb -	N(1)	100·0(2)
C(121)	- Pb -	C(111)	153·5(2)
C(121)	- Pb -	O(1')	86·4(2)

2.8.5 Crystal Structure of Ph₃Sb(SalAp)

A single crystal of Ph₃Sb(SalAp) was obtained by the vapour diffusion of hexane into a dichloromethane solution of the compound. The molecular structure is shown in Figure 2.18 and the bond distances and bond angles in the primary coordination sphere of antimony, based on the atomic numbering in this Figure, are listed in Tables 2.18 and 2.19, respectively. All of the crystallographic data for the crystal structure of Ph₃Sb(SalAp) are given in Tables A.7 and A.8 in the Appendix. The crystal structure analysis of Ph₃Sb(SalAp) revealed that the complex crystallised with two independant molecules in the cystallographic asymmetric unit. There were no significant differences between the two independant molecules and only one molecule is illustrated in Figure 2.18 and in the following discussion only details for molecule 1 are quoted.

The coordination sphere around antimony consisted of three phenyl carbon atoms, one nitrogen atom from the azomethine bridge in the tridentate SalAp ligand, and two oxygen donor atoms also from this ligand. The six donor atoms were in a distorted octahedral arrangement about the antimony atom in which the planar tridentate ligand, and the three phenyl carbon atoms occupied *meridional* positions. The structure is molecular with no significant intermolecular contacts in the crystal lattice.

The *trans* phenyl groups were not colinear with the central antimony atom such that the C(26)-Sb-C(14) bond angle was 168·6(5)°. Since the size of antimony is about the same as that of tin, the corresponding O(1)-M-O(2) bond angles were about the same in the crystal structures of Ph₃Sb(SalAp) and Ph₂Sn(SalAp). A bond distance of 1·31(7) Å for C(7)-N(1) indicated double bond character for the azomethine group in SalAp.

The crystal structure of Ph₃Sb(SalAp) was found to be very similar to the crystal structure of the analogous trimethyl complex, Me₃Sb(SalAp).[123] The bond angles O(1)-Sb-O(2), C(20)-Sb-N(1) and C(14)-Sb-C(26) were found to be 161·6(3)°, 170·6(9)° and 168·6(5)°, respectively, and the analogous bond angles in the crystal structure of Me₃Sb(SalAp) were found to be 159·8°, 164·7° and 165·3°, respectively (Estimated standard deviations for these parameters were not quoted in the original literature citation).
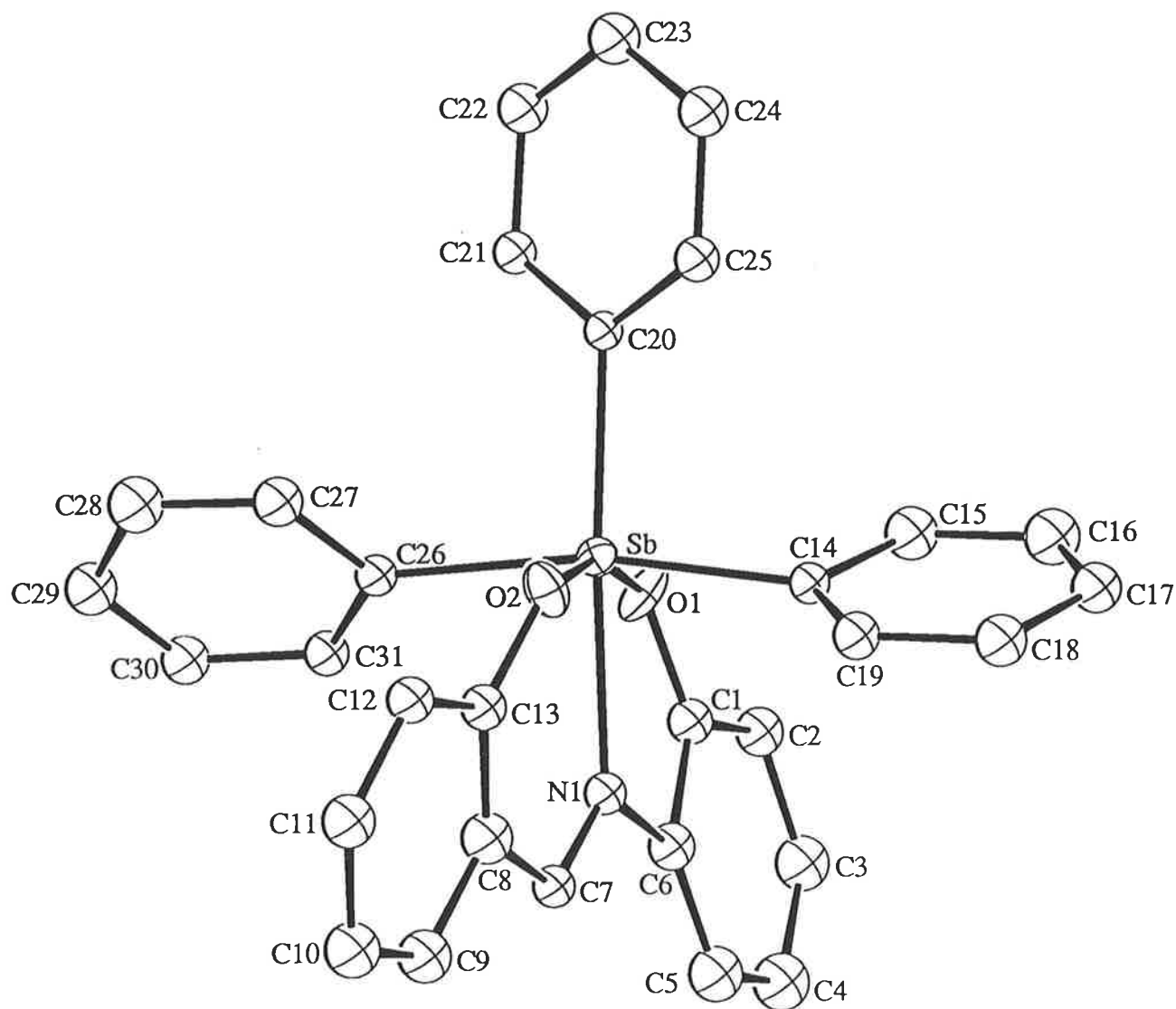
Figure 2.18: *The molecular structure of Ph3Sb(SalAp).*

Table 2.18: Bond Distances (Å) in the Primary Coordination Sphere of Antimony in Ph₃Sb(SalAp) (Details for molecule 1 only).

O(1)	--- Sb	2·065(8)
O(2)	--- Sb	2·033(9)
N(1)	--- Sb	2·26(2)
C(14)	--- Sb	2·11(1)
C(20)	--- Sb	2·153(8)
C(26)	--- Sb	2·15(1)

Table 2.19: Bond Angles (Degrees) in the Primary Coordination Sphere of Antimony in Ph₃Sb(SalAp) (Details for molecule 1 only).

O(2)	- Sb -	O(1)			161·6(3)
N(1)	- Sb -	O(1)			72·6(9)
N(1)	- Sb -	O(2)			89·1(9)
C(14)	- Sb -	O(1)			89·4(4)
C(14)	- Sb -	O(2)			89·7(4)
C(14)	- Sb -	N(1)			83·0(6)
C(20)	- Sb -	O(1)			98·1(5)
C(20)	- Sb -	O(2)			100·3(4)
C(20)	- Sb -	N(1)			170·6(9)
C(20)	- Sb -	C(14)			95·5(5)
C(26)	- Sb -	O(1)			88·4(4)
C(26)	- Sb -	O(2)			88·9(4)
C(26)	- Sb -	N(1)			85·7(6)
C(26)	- Sb -	C(14)			168·6(5)
C(26)	- Sb -	C(20)			95·8(5)

2.8.6 Comparison

The $Ph_2Ge(SalAp)$ and $Ph_2Sn(SalAp)$ complexes both exhibited trigonal bipyramidal geometries, whereas the $Ph_2Pb(SalAp)$ and $Ph_3Sb(SalAp)$ complexes both exhibited distorted octahedral geometries. Formation of a dimeric structure was only observed in the crystal structure of $Ph_2Pb(SalAp)$. The geometry of the complex changed from trigonal bipyramidal to distorted octahedral since the larger size made dimerisation via a bridging oxygen atom possible. Selected bond lengths and bond angles from these crystal structures together with bond lengths and bond angles from related crystal structures obtained from the literature are listed in Tables 2.20 and 2.21 below. From Tables 2.20 and 2.21 it can be seen that as the size of the group (IV) metal atom increased from germanium to lead the lengths of the M-O(1), M-O(2) and M-N(1) bonds increased. This indicated that optimal bonding distances between the ligand donor atoms and the central metal atom could not be obtained as the size of the metal increased. In other words, the germanium atom is coordinated more effectively than the tin and lead atoms. Furthermore, as the size of the group (IV) metal increased from germanium to lead the O(1)-M-O(2) bond angle increasingly deviated from linearity emphasing this point.

Table 2.20: Comparison of the Bond Lengths in the Determined Crystal Structures with Literature Data.

Complex	M-O(1)	M-O(2)	M-N(1)	C-O(1)	C-O(2)	C-N	N-C(Ar)
Ph$_2$Ge(SalAp)	1·921(4)	1·918(4)	2·036(15)	1·333(5)	1·310(5)	1·31(4)	1·49(2)
Ph$_2$Sn(SalAp)	2·081(3)	2·067(4)	2·220(6)	1·341(6)	1·331(6)	1·23(1)	1·482(8)
Ph$_2$Sn(SalAp)[a]	*2·103*	*2·085*	*2·24(1)*	*1·30(2)*	*1·32(1)*	*1·13(2)*	*1·55(2)*
Me$_2$Sn(SalAp)[b],[†]	*2·105(8)*	*2·118(9)*	*2·23(1)*	*1·32(1)*	*1·30(2)*	*1·26(2)*	*1·46(2)*
Ph$_2$Sn(Sat)[c]	*2·093(2)*	*--*	*2·217(3)*	*--*	*1·324(4)*	*1·287(5)*	*1·419(5)*
Ph$_2$Pb(SalAp)[*]	2·246(4)	2·327(4)	2·337(5)	1·327(7)	1·285(7)	1·300(8)	1·439(8)
Ph$_3$Sb(SalAp)[†]	2·065(8)	3·033(9)	2·26(2)	1·35(1)	1·34(1)	1·31(7)	1·55(3)
Me$_3$Sb(SalAp)[d],[‡]	*2·06*	*2·07*	*2·34*	*--*	*--*	*--*	*--*

Complex	M-C	M-C	M-C	Ar-C	Mean distances for C-C bonds in the aromatic ring for:		
					M-Ph	Sal ring	Ap ring
Ph$_2$Ge(SalAp)	1·945(4)	1·946(5)	--	1·46(3)	1·372(7) 1·378(7)	1·377(7)	1·374(8)
Ph$_2$Sn(SalAp)	2·118(5)	2·111(5)	--	1·478(9)	1·379(8) 1·382(7)	1·378(8)	1·375(7)
Ph$_2$Sn(SalAp)[a]	*2·13(1)*	*2·12(1)*	*--*	*1·48(2)*	*1·40(2) 1·40(2)*	*1·40(2)*	*1·40(2)*
Me$_2$Sn(SalAp)[b],[†]	*2·09(1)*	*2·14(1)*	*--*	*1·44(2)*	*--*	*1·40(2)*	*1·40(2)*
Ph$_2$Sn(Sat)[c]	*2·120(3)*	*2·126(3)*	*--*	*1·448(5)*	*1·391(6)*	*--*	*--*
Ph$_2$Pb(SalAp)[*]	2·151(6)	2·166(6)	--	1·425(9)	1·38(1) 1·39(1)	1·394(9)	1·39(1)
Ph$_3$Sb(SalAp)[†]	2·108(13)	2·153(8)	2·15(1)	1·42(3)	1·39(2) 1·38(2) 1·39(2)	1·39(2)	1·39(2)
Me$_3$Sb(SalAp)[d],[‡]	*2·10*	*2·19*	*2·14*	Data not given for these bond lengths in the literature		

[†] Data for molecule 1; [*] Dimer - data for the other half of the molecule is the same.

[‡] Estimated standard deviations for the various parameters in this complex were not quoted in the original literature citation.

[a] Reference 170; [b] Reference 171 ; [c] Reference 176; [d] Reference 123.

Sat = dianion of Schiff base 2-(o-hydroxyphenyl)benzothiazoline.

Table 2.21: Comparison of the Bond Angles in the Determined Crystal Structures with Literature Data.

Complex	O(1)-M-O(2)	N(1)-M-C(1)	N(1)-M-C(2)	C(1)-M-C(2)	O(1)-M-C(1)	O(1)-M-C(2)	O(1)-M-N(1)
Ph2Ge(SalAp)	167·6(2)	116·9(4)	120·6(3)	121·2(2)	93·5(2)	92·3(2)	72·6(7)
Ph2Sn(SalAp)	159·8(2)	113·2(2)	125·3(2)	120·9(2)	95·4(2)	93·0(2)	74·1(2)
Ph2Sn(SalAp)[a]	*159·5(3)*	*110·8(4)*	*127·3(4)*	*121·4(4)*	*97·2(4)*	*92·6(4)*	*74·0(4)*
Me2Sn(SalAp)[b],†	*158·6(4)*	*108·4(5)*	*112·4(5)*	*138·5(5)*	*97·7(4)*	*99·5(4)*	*75·0(4)*
Ph2Sn(Sat)[c]	*157·45(7)*	*112·4(1)*	*126·4(1)*	*120·5(1)*	*90·9(1)*	*91·0(1)*	*79·8(1)*
Ph2Pb(SalAp)*	150·5(2)	103·6(2)	100·0(2)	153·5(2)	95·7(2)	102·4(2)	72·9(2)
	O(2)-Sb-O(1)	C(20)-Sb-N(1)	N(1)-Sb-C(26)	N(1)-Sb-C(14)	C(14)-Sb-C(26)	C(20)-Sb-C(14)	C(20)-Sb-C(26)
Ph3Sb(SalAp)	161·6(3)	170·6(9)	85·7(6)	83·0(6)	168·6(5)	95·5(5)	95·8(5)
Me3Sb(SalAp)[d],‡	*159·8*	*164·7*	*80·2*	*85·8*	*165·3*	*96·8*	*95·5*

Complex	O(2)-M-C(1)	O(2)-M-C(2)	O(2)-M-N(1)	S(1)-Sn-C(1)	S(1)-Sn-C(2)	S(1)-Sn-N(1)	
Ph2Ge(SalAp)	91·7(2)	94·6(2)	95·0(7)	--	--	--	
Ph2Sn(SalAp)	96·0(2)	95·4(2)	86·1(2)	--	--	--	
Ph2Sn(SalAp)[a]	*96·0(4)*	*93·9(4)*	*86·6(4)*	--	--	--	
Me2Sn(SalAp)[b],†	*88·6(5)*	*88·9(4)*	*83·7(4)*	--	--	--	
Ph2Sn(Sat)[c]				*102·1(1)*	*97·91(9)*	*78·24(7)*	
Ph2Pb(SalAp)*	82·2(2)	90·7(2)	79·0(2)	--	--	--	
	C(20)-Sb-O(1)	C(20)-Sb-O(2)	C(26)-Sb-O(1)	C(26)-Sb-O(2)	O(2)-Sb-C(14)	O(1)-Sb-C(14)	O(2)-Sb-N(1)/ O(1)-Sb-N(1)
Ph3Sb(SalAp)†	98·1(5)	100·3(4)	88·4(4)	88·9(4)	89·7(4)	89·4(4)	89·1(9) / 72·6(9)
Me3Sb(SalAp)[d],‡	*98·7*	*100·7*	*88·0*	*95·3*	*90·2*	*82·2*	*94·3 / 66·6*

[a] Reference 170; [b] Reference 171 ; [c] Reference 176; [d] Reference 123.

† Data for molecule 1; * Dimer - data for the other half of the molecule is the same.

‡ Estimated standard deviations for the various parameters in this complex were not quoted in the original literature citation.

Chapter 3

AMIDE COMPLEXES

3.1 Introduction

As mentioned in the introductory Chapter highly electronegative ions such as fluoride ions and deprotonated phenol/enol oxygens are very effective donor atoms capable of achieving high oxidation states with many metals. Pearson's principle predicting the stability of complexes states that hard acids prefer to bind to hard bases and soft acids prefer to bind to soft bases.[98c] Transition metal ions, especially in the high oxidation state, come under the category of hard acids are coordinate to hard bases such as hydroxide and halide ions by σ- and π-donation. An obvious extension to these type of ligands would be a deprotonated amine nitrogen atom as depicted in Figure 3.1.
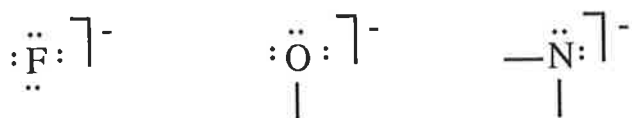
Figure 3.1: *Atoms capable of achieving high metal oxidation states.*

This is not easily achieved due to the low acidity of the -NH proton. However, if present as an amide function deprotonation is facilitated through resonance and inductive effects as shown below in Equation 3.1.[189a]

$$(3.1)$$
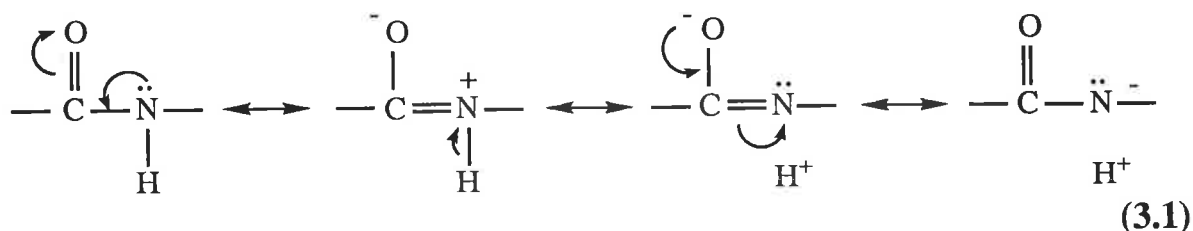
The presence of aromatic substituents on the amide group can enhance these effects. Thus, the design of ligands involving both amide and phenolic hydroxy groups and the examination of their ability to stabilise high metal oxidation states was initiated. Recent studies have shown that the deprotonated nitrogen of organic amides coordinates to metal ions (by σ- and π-donation) stabilising high metal oxidation states.[69,190-193] Examples from these studies include the osmium(IV) complex of 1,2-bis(3,5-dichloro-2-hydroxybenzamido)ethane[193] and the cobalt(IV) complex of 1,2-bis(3,5-dichloro-2-hydroxybenzamido)-4,5-dichlorobenzene,[190] in which both of these ligands coordinate in a tetradentate manner. N-(2-hydroxyphenyl)-salicylamide and derivatives of it have been found to form stable manganese(IV) and fairly stable manganese(V) complexes of the general formulas $[MnL_2]^{2-}$ and $[MnL_2]^-$, respectively,[96] as well as cobalt(IV) complexes of the general formula $K_3[CoL_2]$.[190] These amides function as trinegative tridentate chelating agents, coordinating through a deprotonated amide nitrogen atom and two deprotonated phenolic oxygen atoms as depicted in Figure 3.2.
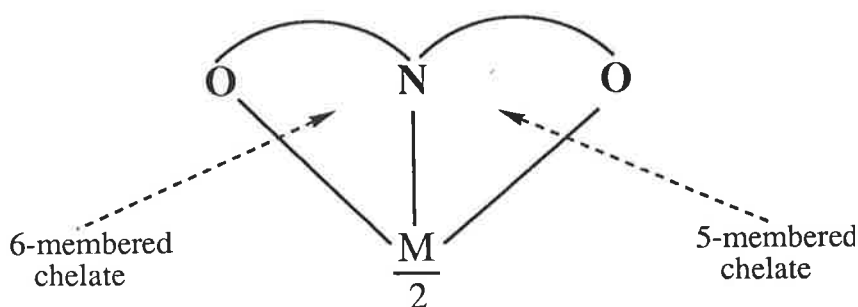
Figure 3.2 : *Coordination of a metal (M) by the oxygen and nitrogen donor atoms of the amide ligands resulting in the formation of five- and six-membered chelate rings.*

The ligands used in this study to complex manganese, titanium, vanadium and iron were secondary amides of the trinegative tridentate ONO donor type shown above. More specifically, N-(2-hydroxyphenyl)salicylamide, substitution derivatives of this parent amide, as well as some naphthol homologues were employed in this study.

3.2 Amide Ligands

An outline of the method used in the preparation of the amides is given in Reaction Scheme 3.1. The phenolic hydroxyl group of salicylic acid and its derivatives *(1a)* was protected by acetylation before being treated with thionyl chloride to form the corresponding acid chloride *(1c)*. Higher yields for the acid chlorides were obtained when the reaction solution was heated to 70°C rather than 30°C as suggested in the literature.[194] This was then reacted at room temperature with the *o*-hydroxy aromatic amine *(1d)* forming the acetylated amide *(1e)* with the elimination of hydrogen chloride. Acid hydrolysis of this product gave the desired dihydroxy amide *(1f)*. For N-(2-hydroxyphenyl)salicylamide, room temperature conditions were sufficient for the removal of the acetyl protecting group. All other amide ligands required heating of the dioxane/aqueous hydrochloric acid solutions close to reflux. The names, abbreviations and structures of the amide ligands prepared are presented in Table 3.1.

R₁ = H, 3-CH₃ or 5-Cl
R₂ = H, 5-Cl or

(i)   acetic anhydride (100°C; 7 hrs)
(ii) SOCl₂/urea (70°C; 5 hrs)
(iii) RT (1 hr) / H₂O
(iv) aqueous HCl
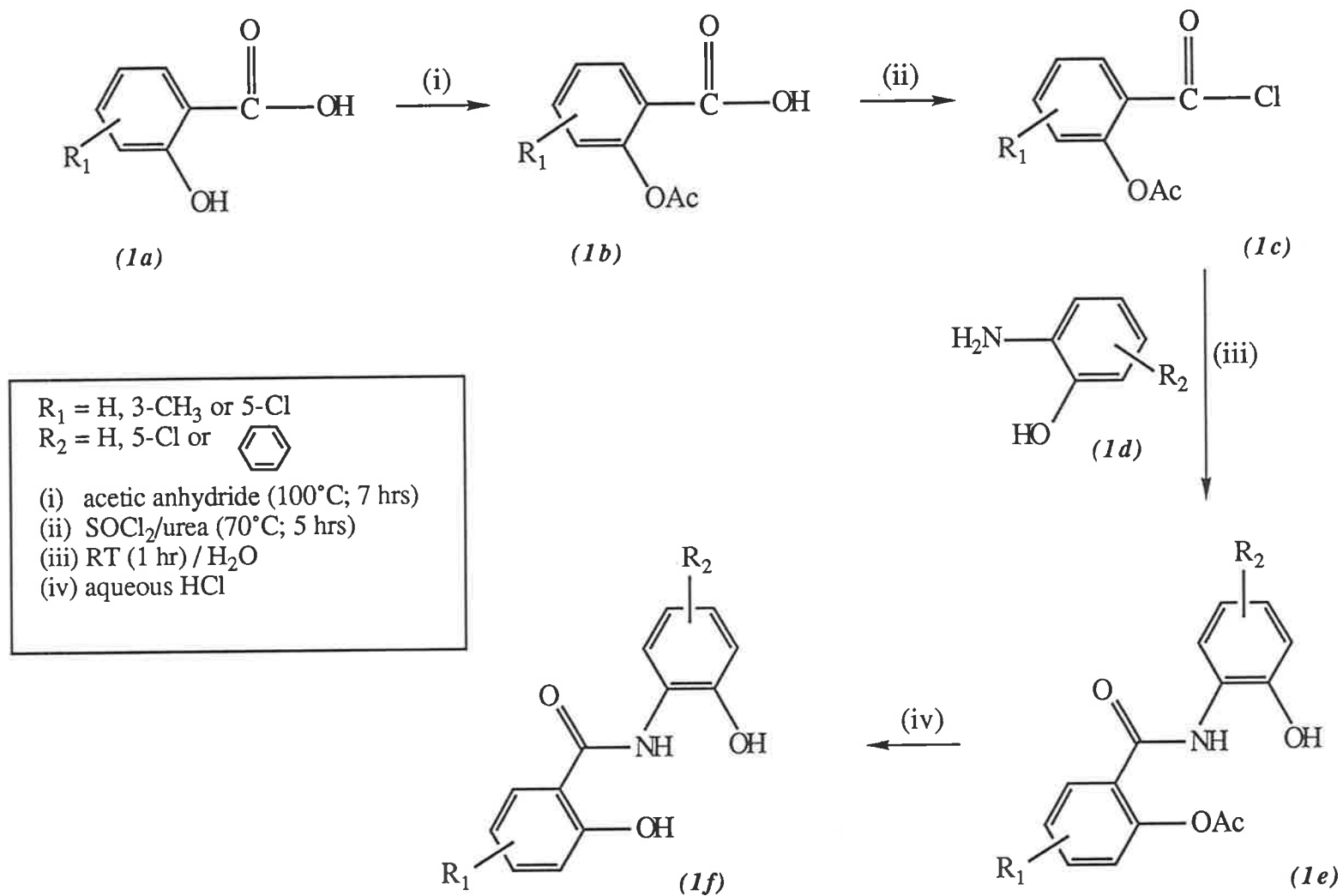
Reaction Scheme 3.1: *Method used for the preparation of the amide ligands.*

Table 3.1: Names, Abbreviations and Structures of Amide Ligands.
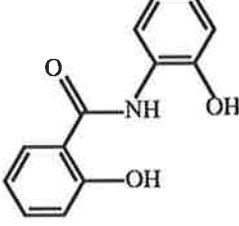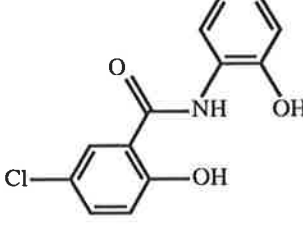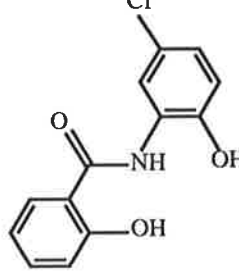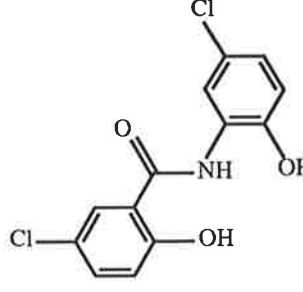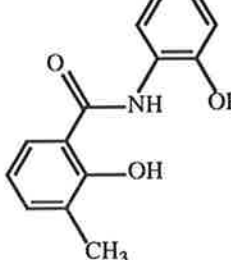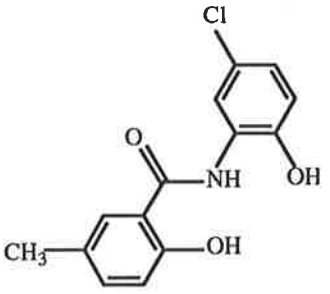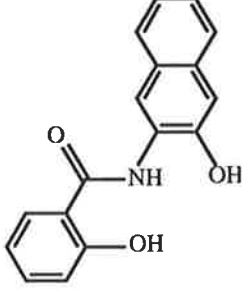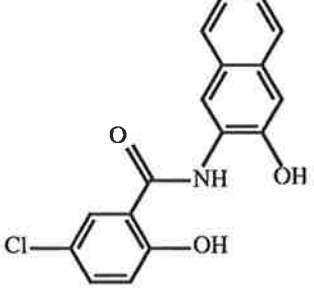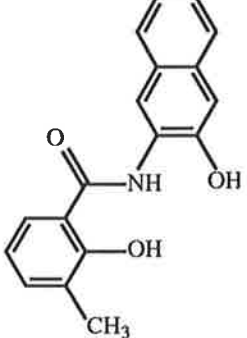
Name (Abbreviation)	Structure
N-(2-hydroxyphenyl)salicylamide (H_3L^1)	
N-(2-hydroxyphenyl)-5-chlorosalicylamide (H_3L^2)	
N-(5-chloro-2-hydroxyphenyl)salicylamide (H_3L^3)	
N-(5-chloro-2-hydroxyphenyl)-5-chlorosalicylamide (H_3L^4)	
N-(2-hydroxyphenyl)-3-methylsalicylamide (H_3L^5)	

Table 3.1: continued...

N-(5-chloro-2-hydroxyphenyl)-3-methylsalicylamide (H_3L^6)	
N-(2-naphthol)salicylamide (H_3L^7)	
N-(2-naphthol)-5-chlorosalicylamide (H_3L^8)	
N-(2-naphthol)-3-methylsalicylamide (H_3L^9)	

3.3 Preparation of Complexes

3.3.1 Complexes of Titanium and Manganese

3.3.1.1 Procedure

The amide ligands used in this study were assumed to behave as trinegative tridentate ligands capable of forming complexes with the formula $K_2[ML^n_2]$, containing the metal in oxidation state (IV) and coordination number six. Reactions of manganese and titanium with a range of amide ligands were performed at room temperature in methanol in the hope of obtaining crystalline products which were easily isolable.

Titanium complexes with the amide ligands were desirable benchmark compounds for oxidation state (IV). No higher oxidation state is possible for this element and Ti(III), because of its ease of oxidation, would be unlikely to interfere. Mole equivalent ratios for their preparation were calculated according to the $K_2[TiL^n_2]$ formulation. Titanium tetrabutoxide was chosen as the starting material for these complexes as it is a source of titanium(IV) as well as supplying four out of the six mole equivalent of base required for deprotonation of two mole equivalent of amide ligand. In addition, as a starting material it had desirable solubility properties and produced only butanol as a by-product. Two mole equivalent of base were supplied as potassium hydroxide. This also provided the potassium counter cations necessary for the formulation $K_2[TiL^n_2]$. The moisture sensitive nature of the titanium tetrabutoxide called for the application of Schlenk techniques and dry methanol.

Manganese complexes with the amide ligands were prepared using manganese diacetate tetrahydrate as the starting material. As well as being the source of manganese it supplied two mole equivalent of base in the form of acetate ions. The remaining amount of base was supplied as potassium hydroxide The reactions were performed under air to assist the oxidation of Mn(II). Similar techniques had been used with manganese,[94] ruthenium[93] and tin[97] in this laboratory.

3.3.1.2 Isolation of Products

Despite the large number of different ligands that were used, none of the titanium and manganese complex preparations produced solids even after

cooling the reaction solutions for two days. All reactions were performed in methanol. Concentrating the reaction solutions by removing some of the solvent under vacuum gave solids only in the syntheses of $K_2[MnL^n_2]$, where $n = 1, 2, 4, 5$ and 6. This was an effective method when the availability of the ligand made it possible to perform the complex syntheses on a large scale. In many other instances it proved necessary to work with the crude materials obtained after removing the solvent completely and relying on thorough washing to purify the resultant product. Although this is an unsatisfactory method for purifying the products, the spectroscopic and solution properties of these were still measured to determine whether these materials contained mainly the desired complex.

Microanalytical results for these products were poor and to a large extent because of water of hydration which probably accounts for the high solubility of these complexes. Carbon, hydrogen and nitrogen analyses were carried out for most crude samples, as well as potassium and manganese/titanium analyses for the $K_2[TiL^1_2]$ and $K_2[MnL^4_2]$ samples. In some cases, the C, H and N analyses were in close agreement with the expected values after assigning waters of hydration, and this is discussed later. However, results for the metal analyses were poor. Calculation of the product formula weight from the percentage of potassium or titanium/manganese found sometimes gave a value lower than that for the dehydrated formula $K_2[ML^n_2]$. These results are explained in more detail in Section 3.7.

3.3.2 Complexes of Vanadium and Iron

3.3.2.1 *Introduction*

Salam successfully prepared six coordinate vanadium(IV) VL_2 type complexes with dinegative tridentate ONO Schiff base ligands.[92] As an extension to that work, the formation of vanadium(IV) complexes with trinegative ligands containing the same donor atoms was investigated. Attempts were made to synthesise amide complexes of vanadium, $K_2[VL^n_2]$, as well as an ambitious attempt to synthesise the analogous complexes of iron which would require the uncommon Fe(IV) centre.

3.3.2.2 *Procedure and Isolation*

The only attempts to prepare V(IV) complexes were made using the ligand H_3L^1. Reactions were carried out using two different vanadium starting materials, namely bis(acetylacetonato)oxovanadium(IV) (VO(acac)$_2$) and vanadyl chloride (VOCl$_2$.2H$_2$O). Two mole equivalent of amide ligand was reacted with each of these vanadium starting materials in the presence of excess base, in methanol. For each vanadium starting material, a reaction was performed at room temperature and one under refluxing conditions. Furthermore, a reaction using VO(acac)$_2$ was also carried out under an inert dinitrogen atmosphere.

We endeavoured to prepare iron(IV) complexes of the type $K_2[FeL^n_2]$ with the amide ligands H_3L^1, H_3L^3 and H_3L^4. Tris(acetylacetonato)iron(III), (Fe(acac)$_3$), was reacted with two mole equivalent of amide ligand and three mole equivalent of potassium hydroxide in methanol, the remaining base being supplied by the acetylacetonate ions. These reactions were performed in the presence of air to facilitate the oxidation of iron(III).

As in the case of the titanium and manganese complexes, isolation of the products with the metals vanadium and iron was difficult. Since the products were highly soluble, the solutions had to be evaporated to dryness to obtain a solid. The spectroscopic and solution properties of the products obtained are discussed in the sections to follow.

After carrying out preliminary experiments with iron in our endeavours, studies by Koikawa *et al.*[35] on the synthesis and characterisation of iron(III) and iron(IV) complexes of N-(2-hydroxyphenyl)salicylamide (H_3L^1) and some of its derivatives was published. They reported the synthesis of the complex (NPr$_4$)$_2$[Fe(L^1)$_2$].2H$_2$O by oxidation of the iron(III) complex, $K_3[FeL^1_2]$.5H$_2$O, with cerium(IV). Using conditions similar to those employed in this study, the iron(IV) complex $K_2[Fe(L)_2]$.2·5H$_2$O, where L = L^1 with a methyl substituent in the 5-position on the 2-hydroxyphenyl moiety, was easily obtained. In addition, the Fe(III) complex (PBu$_4$)$_3$[Fe(L^3)$_2$] was obtained. However, the Fe(IV) complex with H_3L^3 could not be obtained, even after chemical oxidation.

3.4 Attempted Purification of Amide Complexes

Recrystallisation and column chromatography techniques were used to remove impurities from the products obtained from the titanium and manganese complex syntheses. Prior to the purification attempts, spectroscopic analyses indicated that the desired complexes were present in the crude products obtained. The solubility of all the products in methanol was high, therefore a second solvent was employed to initiate precipitation of the complexes. Column chromatography was performed on some of these products using alumina and/or florisil columns. Before purification of any of these products was attempted, freshly distilled methanol was added to all samples and the resultant solutions were filtered through a cotton wool plug before evaporating to dryness to regain the solids. This was done to ensure the removal of any insoluble MnO_2 or TiO_2. In almost all cases, the methanolic solutions showed no suspended matter. Mass spectroscopy and infrared spectroscopy were used to monitor the effectiveness of the purification procedures.

3.4.1 Recrystallisation

In general, recrystallistion produced mixed results. The recrystallisation attempt on $K_2[MnL^7_2]$ from methanol/chloroform saw no reprecipitation occurring. After the solvents were removed, infrared spectroscopy on the recovered material revealed the presence of a new peak at 1640 cm^{-1}. This absorption also appears in the spectrum of the protonated uncomplexed ligand (H_3L^7) suggesting some decomposition of the complex had occurred. Apart from some discrepancy around 880 cm^{-1}, the brown solid obtained from the recrystallisation (methanol/chloroform) of crude brown-black $K_2[MnL^8_2]$ yielded an infrared spectrum similar to that of the crude material. However, unlike the crude material, the mass spectrum did not support the correct formula weight. The $K_2[MnL^9_2]$ complex, on the other hand, showed a correct molecular ion peak in the mass spectrum of the crude material and a supportive mass spectrum was also obtained after recrystallisation from methanol/chloroform. Furthermore, a weak absorption at 1640 cm^{-1} in the infrared spectrum of the crude material due to some free amide had disappeared after recrystallisation. Disappointingly, elemental analysis on this complex was very poor.

Because of the negative results obtained with the manganese compounds, recrystallisation was only attempted on one titanium sample, $K_2[TiL^3_2]$. No solid could be precipitated out from methanol, not even after the dropwise addition of ether.

3.4.2 Column Chromatography

Since recrystallisation did not improve the purity of the amide complexes, column chromatography was then chosen as another method of purification of these products. Thin layer chromatography on the products obtained from the attempted preparation of manganese and titanium complexes showed one spot at the origin along with one or two spots just below the solvent front. Products $K_2[TiL^1_2]$ and $K_2[TiL^3_2]$ were passed through alumina/hexane columns and eluted with methanol. One band was collected in each case and another remained at the origin which was discarded. For both complexes, the product recovered from the methanol eluent had an identical infrared spectrum to that of the corresponding crude material. Microanalysis of the purified sample of $K_2[TiL^3_2]$ produced C and N analyses in support of the formulation $K_2[TiL_2].11H_2O$. The H analysis, however, was too low to support this formulation.

The $K_2[TiL^4_2]$ complex was passed through a column of florisil/ (95% $CHCl_3$:5% MeOH) and the polarity of this solvent mixture was gradually increased to 100% MeOH when eluting. A pale yellow band was first collected followed by an orange band. Beige and orange solids were respectively obtained when these eluents were evaporated to dryness. The infrared spectrum of the beige solid showed it to be protonated uncomplexed amide ligand (H_3L^4). Although the infrared spectrum of the orange solid supported the complexation of the amide ligand, the mass spectrum contained no molecular ion peak, or peak with m/e value corresponding to the complex anion. However, a molecular ion peak was observed in the mass spectrum of the crude material. These results suggested decomposition of the complex had taken place with the release of some amide ligand.

Similar results were obtained for the $K_2[TiL^2_2]$, $K_2[TiL^5_2]$ and $K_2[TiL^7_2]$ complexes on a florisil column. A conductance measurement on the latter sample after chromatography yielded a value of 85·1 ohm^{-1} cm^2 mol^{-1} in methanol suggesting a 1:1 electrolyte.[195] Passing a sample of $K_2[TiL^4_2]$

through an alumina/hexane column and eluting with methanol also produced a decomposition product, as no molecular ion was observed in the mass spectrum of this compound. A similar result was also obtained with the $K_2[MnL^2_2]$ sample. When another sample of $K_2[TiL^7_2]$ was passed through a column of alumina/hexane, a material with an infrared spectrum similar to that of the crude material was produced and microanalysis agreed with the formulation after the assignment of $7H_2O$.

We wish to mention here that contradictory infrared and mass spectral evidence as to the presence of the desired complexes may have been due to the unreliability of the mass spectral service available. Nevertheless, recrystallisation and column chromatography as methods of purification of the amide compounds could not be used with confidence.

3.5 Infrared Spectra

3.5.1 Introduction

Williams and Fleming report that N-H stretching absorptions for secondary amides -CONH- appear in the regions 3460 - 3400 cm^{-1} and 3100 - 3070 cm^{-1} and are of medium and weak intensities, respectively.[147c] In the former region, two bands appear due to the presence of two forms of N-H as shown below in Figure 3.3. In the amide carbonyl region, two bands are reported in the 1680 - 1630 cm^{-1} and 1570 - 1515 cm^{-1} regions, with the former generally more intense than the latter.

Figure 3.3: *The two forms of N-H present in secondary amides (Reference 147c).*

In their study on similar amides to those used in this study, Koikawa *et al.*[96] observed the amide vibrations at 1620 and 1560 cm^{-1} in the free ligand spectra shift to 1590 and 1520 cm^{-1}, respectively, in the corresponding manganese(IV) and manganese(V) complex spectra. These complexes, as well as the Co(III) and Co(IV) complexes of the same amide ligands, were all hydrated and accordingly exhibited a broad absorption around 3400 cm^{-1} due to the presence of this lattice water.[96,190]

The assignments of the peaks in the infrared spectra of the amide ligands and their complexes in this report were made by comparison of the infrared spectral data obtained to the data mentioned above. All of the infrared spectral data and assignments are summarised in Table 3.2.

Table 3.2: Infrared Spectral Data for Amide Ligands and their Complexes.

Ligand / Complex	Tentative Assignments (cm^{-1})				
	$\nu(H_2O)$	$\nu(NH)$	$\nu(OH\cdots N)$	$\nu(C=O)$	$\nu(C=C)$
H_3L^1	--	3261 s, 3133 m	2695 w, 2564 w	1616 s, 1559 s	1592 m
$K_2[TiL^1_2]$	3370 w, br	--	--	1596 s, 1524 s	1576 s
$K_2[MnL^1_2]$	3392 w, br	--	--	1594 s , 1537 s	1564 s
$K_2[VL^1_2]$	3353 w, br	--	--	1620 sh†, 1587 s, 1540 m	1558 m
$K_2[FeL^1_2]$	3340 w, br	--	2729 w	1593 s, 1525 s	1569 s
H_3L^2	--	3276 s	2723 w, 2675 w	1640 s, 1615 s, 1564 s	1593 s
$K_2[TiL^2_2]$	3370 w, br	--	--	1623 m, 1593 m, 1518 s	1565 m
$K_2[MnL^2_2]$	3370 s, br	--	--	1623 sh, 1595 s, 1527 sh	1559 s
H_3L^3	--	3270 s	2723 w, 2675 w	1618 s, 1604 sh, 1558 s	1592 s
$K_2[TiL^3_2]$	3370 s	--	--	1596 s, 1526 s	1575 s
$K_2[FeL^3_2]$	3338 w, br	--	--	1629 sh†, 1593 m, 1527 s	1565 m
H_3L^4	--	3287 s	2730 w, 2665 w	1649 s, 1608 m, 1551 s	1589 m
$K_2[TiL^4_2]$	3368 w, br	--	--	1635 sh, 1595 m, 1521 s	1570 m
$K_2[MnL^4_2]$	3400 w, br	--	--	1636 w, 1592 m, 1526 s	1574 m
$K_2[FeL^4_2]$	3338 w, br	--	--	1630 sh, 1593 sh, 1526 s	1573 m

H_3L^5	--	3397 s, 3202 s	2743 w, 2679 w	1628 s, 1616 s, 1556 s	1599 m
$K_2[TiL^5_2]$	3369 w, br	--	--	1593 s, 1529 s	1554 s
$K_2[MnL^5_2]$	3369 m, br	--	--	1589 m, 1524 s	1579 m
H_3L^6	--	3401 s, 3283 s	2728 w	1634 s, 1613 m, 1551 s	1602 m
$K_2[TiL^6_2]$	3392 w, br	--	--	1592 m, 1521 s	1536 s
$K_2[MnL^6_2]$	3350 w, br	--	--	1590 m, 1524 s	1564 w
H_3L^7	--	3216 m	2728 w	1633 sh, 1602 s, 1551 s	1591 s
$K_2[TiL^7_2]$	3368 w, br	--	--	1597 s, 1524 s	1575 s
$K_2[MnL^7_2]$	3370 w, br	--	--	1595 m, 1525 s	1568 s
H_3L^8	--	3288 m	2705 w, 2654 w	1647 m, 1622 s, 1566 s	1592 s
$K_2[TiL^8_2]$	3369 w, br	--	--	1617 m, 1594 m, 1522 m	1569 m
$K_2[MnL^8_2]$	3367 m, br	--	--	1595 sh, 1562 s	1537 sh
H_3L^9	--	3422 m, 3326 m	2726 w	1625 m, 1556 s	1597 m
$K_2[TiL^9_2]$	3367 m, br	--	--	1596 s, 1527 s	1534 s
$K_2[MnL^9_2]$	3367 m, br	--	--	1594 sh, 1529 s	1577 s

w = weak; m = medium; s = strong; br = broad; sh = shoulder.

† These absorptions were of higher frequency than the corresponding C=O absorptions in the protonated ligand. However, these were only observed as shoulders and therefore may be due to protonated uncomplexed H_3L^n.

3.5.2 Complexes of Titanium and Manganese

There is evidence of amide ligand coordination in all of the products obtained from the manganese and titanium syntheses. The N-H stretching frequencies which appeared in the 3422 - 3133 cm^{-1} region of the free amide spectra were absent in the spectra of all products. Two absorptions appearing in the 1649 - 1616 cm^{-1} and 1566 - 1551 cm^{-1} regions of the protonated ligand spectra were assigned to the carbonyl group of the amide. On complexation, these absorptions shifted to lower frequencies (1636 - 1589 cm^{-1} and 1537 - 1518 cm^{-1}, respectively). Shifts in the C=O stretching frequencies were not greater for any particular metal, sometimes a greater shift was observed after complexation to titanium while in other cases a greater shift was observed after complexation to manganese. For the ligands H_3L^n, where n = 2 - 8, another absorption appeared between these two carbonyl bands (1622 - 1602 cm^{-1}) which were also assigned to $v(C=O)$. In the case of $K_2[TiL^n_2]$, where n = 2 and 4 and $K_2[MnL^n_2]$, where n = 2 and 4, the highest frequency absorption in the carbonyl region may suggest the presence of a small amount of protonated uncomplexed ligand because of its low intensity.

A broad absorption due to lattice water was observed in the 3400 - 3350 cm^{-1} region of the manganese and titanium complex spectra. The medium or strong absorption observed between 1602 cm^{-1} and 1589 cm^{-1} in the free ligand spectra was attributed to aromatic ring stretching. This absorption also experienced a downward shift in frequency upon complex formation (1579 - 1534 cm^{-1}).

3.5.3 Complexes of Vanadium and Iron

On the basis of infrared spectroscopy, similar products were obtained from the reaction of H_3L^1 with either vanadium starting material, $VO(acac)_2$ or $VOCl_2.2H_2O$. Absorptions observed in the carbonyl region of the spectra were identical but those in the fingerprint region were slightly different. The spectra were comparable to those of the analogous manganese and titanium complexes. N-H stretching frequencies were absent and a shift to lower frequencies was observed for the carbonyl stretchings of the amide function (1587 and 1540 cm^{-1}) in the spectra of the vanadium complexes. This supported deprotonation and coordination of the amide ligand. The higher frequency C=O absorption contained a shoulder at 1620 cm^{-1} suggesting the

presence of some protonated uncomplexed amide. Performing the reaction under a dinitrogen atmosphere and using $VO(acac)_2$, a similar product was obtained on the basis of infrared spectroscopy. In all attempted complex formation reactions, the strong absorption near 1000 cm^{-1} in the spectrum of the vanadyl starting materials, due to $v(V=O)$, was absent in the spectra of the products indicating formation of non-oxo compounds and further lending support to the formation of the desired complex, $K_2[VL^1_2]$. The vanadium products were hydrated since a broad absorption due to lattice water was detected at 3353 cm^{-1}.

Products from the attempted preparations of $K_2[FeL^n_2]$, where n = 1, 3 and 4, produced infrared spectra similar to their analogous manganese, titanium and vanadium compounds. Absorptions in the ranges 1630 - 1593 cm^{-1} and 1527 - 1525 cm^{-1} were assigned to $v(C=O)$ of the coordinated amide function. The aromatic stretchings of the ligands appeared between 1573 and 1565 cm^{-1}. Both the C=O and aromatic C=C absorptions were lower in frequency in the complex spectra than in the free ligand spectra. Like the products obtained with the other metals, these products were also hydrated since an absorption due to lattice water observed around 3338 cm^{-1}.

Shifts in the amide C=O stretching frequencies upon complexation for the vanadium and iron products obtained were compared with those for the titanium and manganese products of the same ligand. These are shown in Table 3.3. The iron products compared well with the analogous titanium products, as did the vanadium products with the manganese products. These comparisons strengthen the idea that complexation of the amide ligands to vanadium and iron had occurred.

Table 3.3: Shifts in Amide C=O Vibrations (cm^{-1}) for Amide Compounds of Titanium, Manganese, Iron and Vanadium.

Amide Ligand	Amide Vibration in Ligand (cm^{-1})	Shift in cm^{-1} for the Compound of:			
		Ti	Mn	V	Fe
H$_3$L^1	1616	20	22	29	23
	1559	35	22	19	34
H$_3$L^3	1618	22	30‡	†	25
	1604	--	--	†	--
	1558	32	40‡	†	31
H$_3$L^4	1649	14	13	†	19
	1608	13	16	†	15
	1551	30	25	†	25

‡ Reference 96
† Synthesis was not attempted.

3.6 Mass Spectra

All products obtained from the reactions with the amide ligands were examined by mass spectroscopy. The findings are summarised in Table 3.4.

With all the amide ligands used, the postulated $K_2[ML_2]$ formulation was supported for M = titanium and manganese. A molecular ion peak characteristic of the anhydrous formula was observed in the mass spectra of these complexes, together with intense peaks characteristic of the fragments $K[ML_2]^-$ and $[ML_2]^{2-}$. By contrast, infrared spectra and microanalyses (see Section 3.7) showed the complexes to be heavily hydrated. Manganese has only one isotope (^{55}Mn, 100%) and titanium has one isotope which predominates (^{48}Ti, 73·7%). Thus, in the mass spectra of the titanium and manganese complexes of non-chlorine containing amide ligands (H_3L^1, H_3L^5, H_3L^7 and H_3L^9) the molecular ion peak was easily observed. Whereas in the mass spectra of complexes of the chlorine containing amide ligands the $^{35}Cl/^{37}Cl$ isotopic pattern was seen as indicated in Table 3.4. In some amide complexes of titanium and manganese, a peak at [Molecular ion + 39 (i.e. K)]$^+$, less intense than the molecular ion peak, also appeared in the spectra (Table 3.4). The presence of a $K_3[ML_2]$ species would suggest a lower oxidation state (M(III)) for the transition metals. However, manganese(III) is inconsistent with conductance (Section 3.10.2) and magnetic moment (Section 3.10.1) measurements. Since peaks at m/e values corresponding to [Molecular ion + K]$^+$ were obtained with the titanium complexes and formation of titanium(III) complexes is highly unlikely, we conclude that these spectral peaks are the result of a fortuitous ion association.

The various attempts to prepare the vanadium complex $K_2[VL^1_2]$ gave inconsistent mass spectra results as opposed to the infrared spectral data which suggested that the products were similar. Vanadium has only two isotopes, with the isotope ^{51}V (99·75%) being much more abundant. Thus, mass spectra of vanadium complexes are relatively simple. No peak characteristic of $K_2[VL^1_2]$ or $[VL^1_2]$ was observed in the mass spectra of the products obtained from the attempted preparations *(i)-(iii)* (Section 6.27.1). Only the product obtained from the experiment labelled method *(v)* showed a weak peak corresponding to $[K_2[VL^1_2] + 2H]^+$. In addition, more intense peaks were observed at $[K[VL^1_2] + 3H]^+$ and $[[VL^1_2] + 4H]^+$.

The mass spectra of the iron compounds exhibited a multiplet in the region where the molecular ion peak was expected. As the ^{56}Fe (91·8%) isotope predominates for this metal, the molecular ion peak in the mass spectrum of the complex with amide H_3L^1 was expected to be relatively simple. For the ligands H_3L^1, H_3L^3 and H_3L^4, the most intense peak in the multiplet was observed at 1H, 1H and 2H higher than the expected formula weight, respectively. A similar fragmentation pattern to that seen in the amide complexes of titanium and manganese was produced with the same ligand. That is, the successive loss of the two potassium ions was observed. In the spectrum of the products obtained with amides H_3L^3 and H_3L^4 an extra peak corresponding to [Molecular ion + K]$^+$ also appeared.

Table 3.4: Mass Spectral Data for Amide Complexes.

Complex (anhydrous)	F.W.	$\frac{m}{e}$ Found			
		[¥ + K]	K$_2$[ML$_2$]	K[ML$_2$]	[ML$_2$]
K$_2$[TiL$^1_2$]	578	‡	579	541	498
K$_2$[TiL$^2_2$]	647	--	647†	610†	573†
K$_2$[TiL$^3_2$]	647	686	646†	607†	568†
K$_2$[TiL$^4_2$]	716	756†	717†	679†	640†
K$_2$[TiL$^5_2$]	606	‡	607	568	528
K$_2$[TiL$^6_2$]	675	715	677†	640†	599†
K$_2$[TiL$^7_2$]	678	716	677	640	601
K$_2$[TiL$^8_2$]	747	‡	748†	710†	671†
K$_2$[TiL$^9_2$]	706	746	707	668	629
K$_2$[MnL$^1_2$]	585	‡	585	546	510
K$_2$[MnL$^2_2$]	654	--	652	613	575w
K$_2$[MnL$^4_2$]	723	762	723†	684†	645w
K$_2$[MnL$^5_2$]	613	652	613	575	537
K$_2$[MnL$^6_2$]	682	721	683†	644†	605†
K$_2$[MnL$^7_2$]	685	725	687	648	609
K$_2$[MnL$^8_2$]	754	‡	756†	717†	678w
K$_2$[MnL$^9_2$]	713	753	714	675	636
K$_2$[FeL$^1_2$] attempt	586	‡	587	551	512
K$_2$[FeL$^3_2$] attempt	655	694w	656w	618w	579w
K$_2$[FeL$^4_2$] attempt	724	764	726†	688†	651†

		$\frac{m}{e}$ Found
K$_2$[VL$^1_2$] attempts:		
(i)	581	537, 478, 460, 445, 345
(ii)	581	343, 306, 267, 230, 191, 131, 121, 93
(iii)	581	344, 305, 221, 207, 191, 169, 131, 113
(iv)	581	Not Recorded
(v)	581	583, 545(~¥-K), 507(~¥-2K), 471, 398, 306

† Isotopic pattern for ^{35}Cl/^{37}Cl was observed.
‡ Spectrum was not recorded up to these m/e values.
¥ = molecular ion corresponding to the anhydrous formula weight. w = weak; M = the appropriate transition metal; K = potassium

3.7 Microanalysis

Because of the failure to find a satisfactory way of purifying the products, not all the complexes were submitted for microanalysis. Those which were submitted were crude samples that had been carefully washed and dried and they were analysed for their C, N and H content, and in some cases, their metal content. In all samples the carbon and nitrogen content was lower than that for the anhydrous formula, and in all cases except the $K_2[MnL^5_2]$ sample, the content of hydrogen was higher than that for the anhydrous formula. The results appeared to be consistent with the presence of water, as detected by infrared spectroscopy and reported in the literature for similar complexes.[96] In addition, two complexes were analysed by atomic emission methods for their potassium and titanium or manganese contents. In this section the extent to which the titanium and manganese complexes were hydrated was examined.

By assigning $3 \cdot 5$ - $4 \cdot 5$ (=x) waters of hydration to the general formula $K_2[ML_2].xH_2O$, in some cases, the microanalytical results obtained supported the hydrated formulation. This is shown in Tables 3.5 and 3.6 for the titanium and manganese complexes, respectively. In each case, the C/N molar ratio and, where appropriate, the K/Ti and K/Mn molar ratios were determined and compared with the theoretical values. The greater than expected K/Ti and K/Mn molar ratios may suggest the presence of potassium containing impurities.

After assigning $3 \cdot 5$ H_2O to sample $K_2[TiL^1_2]$, although the content of carbon was high, good values were obtained for the hydrogen and nitrogen content. Similarly for other complexes, analyses on crude samples suggested the following formulations: $K_2[TiL^2_2].4 \cdot 5H_2O$, $K_2[TiL^4_2].4H_2O$, $K_2[TiL^7_2].4H_2O$, $K_2[MnL^2_2].3 \cdot 5H_2O$ and $K_2[MnL^4_2].3 \cdot 5H_2O$. In these formulas after taking into account the waters of hydration (xH_2O) there was at least one set of C, H and N microanalytical results for each sample where almost every analysis was at worst within the 86% limit of the calculated value. Results were so poor for the samples of $K_2[MnL^5_2].xH_2O$ and $K_2[MnL^6_2].xH_2O$ that no water of hydration could be assigned within reasonable error. Except for the sample $K_2[TiL^7_2].4H_2O$, the C/N molar ratios found were reasonably close (within 7% error) to the corresponding theoretical ratios.

Table 3.5: Tabulation of Microanalytical Results for Crude Titanium Compounds with Attempted Assignments of Water of Hydration.

	$K_2[TiL^n_2].xH_2O$						
	%C	%H	%N	%K	%Ti	C/N‡	K/Ti‡
n = 1							
calc. for x = 0	53·98	2·79	4·84	13·52	8·28	13·0	2·0
FOUND	**51·90**	**3·64**	**4·36**	**11·47**	**5·89**	**13·9**	**2·4**
calc. for x = 3·5	48·67	3·61	4·37	12·19	7·47	13·0	2·0
n = 2						--	--
calc. for x = 0	48·24	2·18	4·33	--	--	13·0	--
FOUND	**42·71**	**3·01**	**3·71**	--	--	**13·4**	--
calc. for x = 4·5	42·87	3·18	3·85	--	--	13·0	--
n = 4							
calc. for x = 0	43·60	1·69	3·91	--	--	13·0	--
FOUND I	**38·82**	**2·56**	**3·29**	--	--	**13·8**	--
FOUND II†	**38·89**	**2·61**	**3·29**	--	--	**13·8**	--
calc. for x = 4	39·61	2·56	3·55	--	--	13·0	--
n = 7							
calc. for x = 0	60·17	2·97	4·13	--	--	17·0	--
FOUND I	**51·01**	**3·80**	**3·03**	--	--	**19·6**	--
FOUND II†	**56·98**	**3·86**	**3·36**	--	--	**19·8**	--
FOUND III†	**56·51**	**3·65**	**3·22**	--	--	**20·5**	--
calc. for x = 4	54·40	3·76	3·73	--	--	17·0	--

‡ Molar ratios.

† Duplicate analysis or sample from another preparation.

Table 3.6: Tabulation of Microanalytical Results for Crude Manganese Compounds with Attempted Assignments of Water of Hydration.

	$K_2[MnL^n_2] \cdot xH_2O$						
	%C	%H	%N	%K	%Mn	C/N[‡]	K/Mn[†]
n = 2							
calc. for *x = 0*	47·72	2·16	4·28	--	--	13·0	2·0
FOUND	43·37	2·33	3·61	--	--	14·0	--
calc. for *x = 3·5*	43·52	2·95	3·90	--	--	13·0	--
n = 4							
calc. for *x = 0*	43·17	1·67	3·87	10·81	7·60	13·0	2·0
FOUND I	36·29	2·29	3·09	--	--	13·8	--
FOUND II[†]	36·70	2·88	2·62	17·11	8·53	16·3	2·8
FOUND III[†]	36·68	2·97	3·36	17·11	8·53	12·7	2·8
FOUND IV[†]	35·97	2·69	2·70	12·42	6·38	15·5	2·7
FOUND V[†]	39·63	2·14	3·27	18·74	5·92	14·1	4·4
calc. for *x = 3·5*	39·71	2·44	3·56	9·94	6·99	13·0	2·0
n = 5							
calc. for *x = 0*	54·81	3·29	4·57	--	--	14·0	2·0
FOUND I	43·48	2·78	3·13	--	--	16·2	--
FOUND II[†]	43·51	2·73	3·24	--	--	15·7	--
FOUND III[†]	46·20	3·27	3·27	--	--	16·4	--
	Poor agreement for *x = 0·5 - 10*						
n = 6							
calc. for *x = 0*	49·28	2·66	4·10	--	--	14·0	2·0
FOUND I	39·67	3·32	2·63	--	--	17·6	--
FOUND II[†]	37·95	2·93	2·24	--	--	19·8	--
FOUND III[†]	41·56	2·86	2·74	--	--	17·7	--
	Poor agreement *x = 0·5 - 10*						

‡ Molar ratios.

† Duplicate analysis or sample from another preparation.

Taking into account the "best-fit" value for the water of hydration (x) in some samples (Tables 3.5 and 3.6), the formula weight of these compounds were calculated based on the %C, %H and %N found in the microanalysis. These are shown in Table 3.7 for the titanium compounds and in Table 3.8 for the manganese compounds. For the two samples analysed by atomic emission, formula weights based on %K and %Ti or %Mn found were also calculated.

For all the titanium complexes, the formula weights calculated on the basis of the carbon and nitrogen analyses were higher than the anhydrous formula weight. For the sample $K_2[TiL^1_2].xH_2O$ its formula weight when $x = 3.5$ was not supported by the metal analyses (%K indicated $5.7H_2O$ and %Ti indicated $13H_2O$).

For the manganese complexes, the formula weights calculated on the basis of the carbon and nitrogen analyses were higher than the anhydrous formula weight. A value for x could only be assigned to the products obtained with H_3L^2 and H_3L^4. The C/N molar ratios found in these products had errors of 7.7% and 8.5% (for microanalysis FOUND V in Table 3.6)), respectively, when $x = 3.5$ was assigned to both. The hydrogen analysis for the compound $K_2[MnL^2_2].3.5H_2O$ gave a formula weight which was much higher than expected. Results obtained with the manganese compounds suggested that there was present some impurity other than water.

All measurements or methods of analysis used to further characterise these products obtained from these amide reactions were made on crude samples only.

Table 3.7: Formula Weights Calculated for the Titanium Compounds on the Basis of the Value of Water of Hydration (x) Determined from the Microanalytical Data.

F.W. Calc. Based on:	$K_2[TiL^n_2] \cdot xH_2O$			
	n = 1	**n = 2**	**n = 4**	**n = 7**
%C	602	731	804, 803[†]	717 - 801[†]
%H[‡]	637	770	772, 788[†]	731 - 773[†]
%N	643	755	851, 851[†]	834 - 925[†]
%K	682	--	--	--
%Ti	813	--	--	--
Calculated for $K_2[TiL^n_2] \cdot xH_2O$	641·58 ($x = 3.5$)	728·49 ($x = 4.5$)	788·37 ($x = 4$)	750·71 ($x = 4$)

[†] Results of several analyses.
[‡] Calculated including xH_2O.

Table 3.8: Formula Weights Calculated for the Manganese Compounds on the Basis of the Value of Water of Hydration (x) Determined from the Microanalytical Data.

F.W. Calc. Based on:	$K_2[MnL^n_2] \cdot xH_2O$			
	n = 2	**n = 4**	**n = 5**	**n = 6**
%C	720	788 - 861[†]	728 - 773[†]	809 - 886[†]
%H	909	645 - 895[†]	*	*
%N	7769	834 -1069[†]	857 - 896[†]	1022 - 1251[†]
%K	--	417	--	--
%Mn	--	928	--	--
Calculated for $K_2[MnL^n_2] \cdot xH_2O$	717·50 ($x = 3.5$)	786·40 ($x = 3.5$)	*	*

[†] Results of several analyses.
[‡] Calculated including xH_2O.
* Poor agreement.

3.8 Thermogravimetric Measurements

Microanalytical results confirmed that the amide complexes were hydrated. This was not an unexpected result as similar hydrated complexes of manganese and cobalt had been reported by other workers.[96,190] Attempts were therefore made to determine the number of waters of hydration thermogravimetrically. A comparison of these results with the microanalytical data of these compounds could then be made.

Crude samples of $K_2[TiL^n_2]$, where n=1, 2 and 4, and $K_2[MnL^4_2]$ were accurately weighed, dried under vacuum (35°C/~0·1 mmHg; over P_2O_5) and, after cooling under a dinitrogen atmosphere, reweighed. This was repeated until no further weight loss in these samples was produced. With some samples the experiment was performed in duplicate. The difference in weight was assumed to be entirely due to the loss of water, which was then calculated. Results are summarised in Table 3.9.

Table 3.9: Thermogravimetric *versus* Microanalytical Data for the Determination of the Waters of Hydration (x) in the Amide Complexes.

Complex	x (tga)	x (microanalysis)
$K_2[TiL^1_2].xH_2O$	4	3·5
$K_2[TiL^2_2].xH_2O$	2, 2·5*	4·5
$K_2[TiL^4_2].xH_2O$	3·5	4
$K_2[MnL^4_2].xH_2O$	3·5, 4*	3·5

* These results are from duplicate measurements.

The number of waters of hydration determined by the thermogravimetric measurements compared well with the hydrated formulations proposed from the microanalytical data, except $K_2[TiL^2_2].xH_2O$. The value for x determined

by Koikawa *et al.* ranged from *1 - 4·5* for a series manganese(IV) amide complexes,[96] *4 - 5* for a series of cobalt(III) amide complexes[190] and *1 - 5* for a series of Fe(III) and Fe(IV) amide complexes.[35]

In summary, for the titanium compounds analysed in this study, the number of waters assigned to the dehydrated formula, determined from thermogravimetric measurements, was in the range *2 - 4* and for the manganese compound it was *3·5* or *4*. The value of $x = 3·5$ or *4* for the manganese compound fell within the range of x determined by Koikawa *et al.* for a series manganese(IV) amide complexes.[96]

3.9 Electronic Spectra

3.9.1 Introduction

The solution properties of the amide complexes were studied by electronic spectroscopy. Electronic spectra for the amide complexes of titanium and manganese were recorded in dimethylformamide. In addition, the electronic spectra of the protonated ligands were recorded in the same solvent for comparison purposes. The solvent window in dimethylformamide had a lower wavelength limit of 270 nm. This solvent was employed since Koikawa *et al.* observed no spectral change with time when using this solvent in their studies.[96] They also found that the amide complex spectra were essentially the same in dimethylformamide and in fresh aqueous solution.

The d^3 manganese(IV) complexes would be expected to show absorptions due to (i) intraligand, (ii) ligand-to-metal charge transfer, and (iii) d-d transitions. Whereas the d^0-titanium(IV) complexes may show absorptions only due to intraligand and charge transfer transitions.

3.9.2 Types of Transitions

3.9.2.1 *Intraligand Transitions*

The amide ligands consist of amide functions with aromatic substituents on both the N and C atoms. Such structures would be expected to produce extensively delocalised π systems involving the amide bridge and both aromatic rings. Thus, the transitions possible are $\pi \rightarrow \pi^*$ and $n \rightarrow \pi^*$. These characteristic absorptions are generally observed in the ultraviolet region of the spectrum. Upon complex formation, the absorptions would be expected to shift to longer wavelengths and have increased intensities.[159]

3.9.2.2 *d-d Transitions*

Manganese(IV) has electronic configuration d^3 and would be expected to have three spin allowed transitions in octahedral coordination: ${}^4A_{2g}(F) \rightarrow {}^4T_{2g}(F)$, ${}^4A_{2g}(F) \rightarrow {}^4T_{1g}(F)$ and ${}^4A_{2g}(F) \rightarrow {}^4T_{1g}(P)$.[156b,196]

3.9.2.3   Ligand-to-Metal Charge Transfer

This study aims to investigate high oxidation states in metals stabilised by the formation of complexes with π-donating ligands. These properties of the metal and the ligand are the ones most likely to give rise to charge transfer transitions. Since the metal atom and the ligands are in such a close enviroment, a strong possibility of new transitions occurring exists. The high oxidation state of Ti(IV) and Mn(IV) and the nature of the amide ligands allows the transfer of an electron from the ligand to the metal (i.e. a metal-reduction charge transfer transition). Specifically, this would involve the high oxidation metal centres and the electron rich oxygen and nitrogen donor atoms in the chelate system, where promotion of electrons takes place from essentially ligand orbitals into empty essentially metal antibonding orbitals. Charge transfer (CT) processes are usually of higher energy than *d-d* transitions, appearing at the extreme blue end of the visible spectrum or in the ultraviolet region. Although, in the case where the metal is easily oxidised and the ligand is easily reduced, the charge transfer bands can occur at lower energies often extending into the visible region. The bands due to these transitions are of high intensity, as they are usually fully allowed transitions and possess molar extinction coefficient values of 10^3 - 10^4 dm^3 mol^{-1} cm^{-1} or more. Any forbidden CT transitions producing weak bands are rarely observed as they are hidden by the stronger CT bands.[6m] If we consider the coordination of an electron rich ligand such as a halide to a metal, then a simplified diagram of the ligand to metal charge transfer transitions can be illustrated by Figure 3.4.

3.9.3   Results

Diagrams which show the spectra of the free ligands overlayed with the spectra of their respective manganese and titanium crude complexes are shown in Figures 3.5 - 3.9 The wavelengths of the absorption maxima and other main features of the spectra and their corresponding molar extinction coefficients are given in Table 3.10.
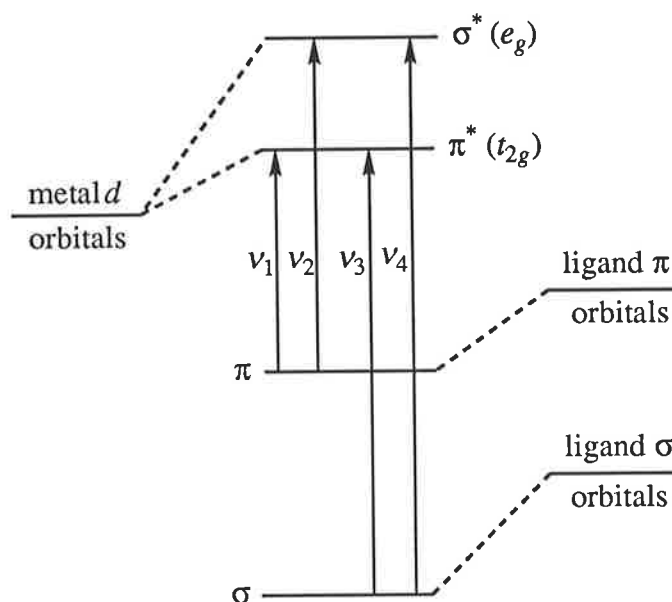
Figure 3.4: *The main classes of ligand-to-metal charge transfer transitions (Reference 6m).*

All of the amide ligands gave spectra containing an intense absorption in the range 304 - 318 nm. This absorption was associated with a well defined shoulder on the low energy side, which in some cases appeared as a distinct absorption in the 362 - 380 nm region. The ligands containing naphthyl rings (H_3L^7 - H_3L^9) contained a further absorption in the 338 - 344 nm region attributed to the presence of a second aromatic ring. The intense peak at 304 - 318 nm and the absorption just mentioned were assigned to $\pi \rightarrow \pi^*$ transitions and were labelled Band(1) and Band(2), respectively, in Table 3.10. Whereas the longer wavelength absorption in the 362 - 380 nm region , because of its lower intensity, was consistent with an $n \rightarrow \pi^*$ transition and labelled Band(3).

The transition labelled Band(1), which was observed as a peak in all of the protonated uncomplexed amide spectra, appeared at a longer wavelength in the spectra of the respective manganese and titanium complexes as a result of coordination having taken place.[159] In the case of the titanium complex spectra, the band was evident as a distinct peak (L^1 and L^6 - L^9) or as a

shoulder (L^2 - L^5), and in the case of the manganese complex spectra, the band always appeared as a distinct peak. Furthermore, the transition labelled Band(2) also appeared at a longer wavelength in the spectra of the respective manganese and titanium complexes.

In the 400 - 470 nm region of the titanium and manganese complex spectra a tail appeared suggesting the presence of a weaker absorption at a longer wavelength than the intraligand transitions. This band, which was less prominent in the complexes containing naphthyl rings, i.e. L^7, L^8 and L^9, was assigned to charge transfer (CT) from ligand to metal (Table 3.10).

In most of the manganese complex spectra two bands were observed in the 460 - 660 nm region, all of which had molar extinction coefficient values (ε) greater than 1×10^3 dm^3 mol^{-1} cm^{-1}. In related studies by other workers, absorptions in this region were attributed to ligand-to-metal charge transfer because they possessed wavelengths greater than that expected from the crystal field splitting of $[MnF_6]^{2-}$ (Δ_o = 21,750 cm^{-1} or 460 nm) and thus, could not be attributed to *d* - *d* transitions.[14,96] In the manganese complex spectra obtained in this study, although the absorptions in this wavelength range appeared at wavelengths too high to be *d* - *d* transitions, their absence in the analogous titanium complexes and their low energy suggested that they may in fact be *d* - *d* transitions. Lower values would be consistent with the destabilising effect of π-donation on the t_{2g} metal electron. Thus, some of these bands were recorded in Table 3.10 as such transitions. Although molar extinction coefficient values greater than 10^3 dm^3 mol^{-1} cm^{-1} are too high for *d-d* transitions the values were obtained from very low absorbances which were the tail end absorptions of dilute solutions and hence liable to a considerable uncertainty in their values. Absorptions labelled as charge transfer bands in the manganese complex spectra appeared at longer wavelengths (460 - 505 nm) than those observed in the titanium complex spectra (410 - 431 nm). This trend was expected for charge transfer bands as the energy of the 3*d* orbitals decreases along the transition series. We believe that the transfer is from the ligand phenolic oxygen orbitals to the metal *d* orbitals which would be the lowest unoccupied molecular orbitals (LUMO) in this case.

In several of the $K_2[TiL^n_2]$ complex spectra, where n = 1 - 6, and a couple of the $K_2[MnL^n_2]$ complex spectra, where n = 8 and 9, an absorption which sometimes coincided with Band(1) in the corresponding amide ligand was

observed. This absorption, labelled Band(0) in Table 3.10, could be fortuitous or it could mean that some decomposition of the complex had taken place in the solvent to give some free ligand in solution. Alternatively, it could imply that some free ligand was present in the crude samples. However, the fact that the absorption labelled Band(0) in the spectrum of $K_2[TiL^6{}_2]$ did not coincide with any free ligand absorption band led us to believe that this was a genuine intraligand band arising from a $\pi \rightarrow \pi^*$ transition in the ligand with a maximum beyond the wavelength range allowed by the solvent window. Complexation would lower their energy as observed for Band(1) and Band(2).

Results obtained in this electronic spectral study were in good agreement with findings made by Koikawa *et al.*[96] who observed intraligand transitions around 313 nm for similar manganese complexes. The same intraligand transition appeared around 286 nm in the free ligand spectra. Absorption bands found between 500 and 625 nm were assigned to ligand-to-metal charge transfer transitions.

The electronic spectra of some iron(III) and iron(IV) amide complexes, prepared by Koikawa *et al.*,[35] were studied in methanol. The iron(III) complexes showed an absorption band at 455 nm, with a value of ~5 $\times$ 10^3 dm^3 mol^{-1} cm^{-1} for the molar extinction coefficient, which was assigned to charge transfer. Intense absorptions appearing at wavelengths higher than 333 nm were attributed to intraligand transitions. The iron(IV) complexes exhibited similar spectra to the iron(III) complexes. An intense charge transfer band occurred at 476 nm. *d-d* Transitions in the iron(IV) complex spectra which were expected to be found at wavelengths lower than 400 nm were hidden by the intense charge transfer and intraligand absorptions.

Cobalt(III) complexes of amide ligands have also been examined by electronic spectroscopy in methanol.[190] Two spin-allowed *d-d* transitions are possible for cobalt(III) in an octahedral enviroment, namely $^1A_{1g} \rightarrow {}^1T_{1g}$ and $^1A_{1g} \rightarrow {}^1T_{2g}$. Koikawa *et al.* observed an intense intraligand transition at 342 nm in the spectra of these complexes. Bands appearing between 435 and 592 nm were too intense to be assigned to *d-d* transitions and were therefore believed to be due to charge transfer absorptions overlapping with *d-d* transition absorptions.
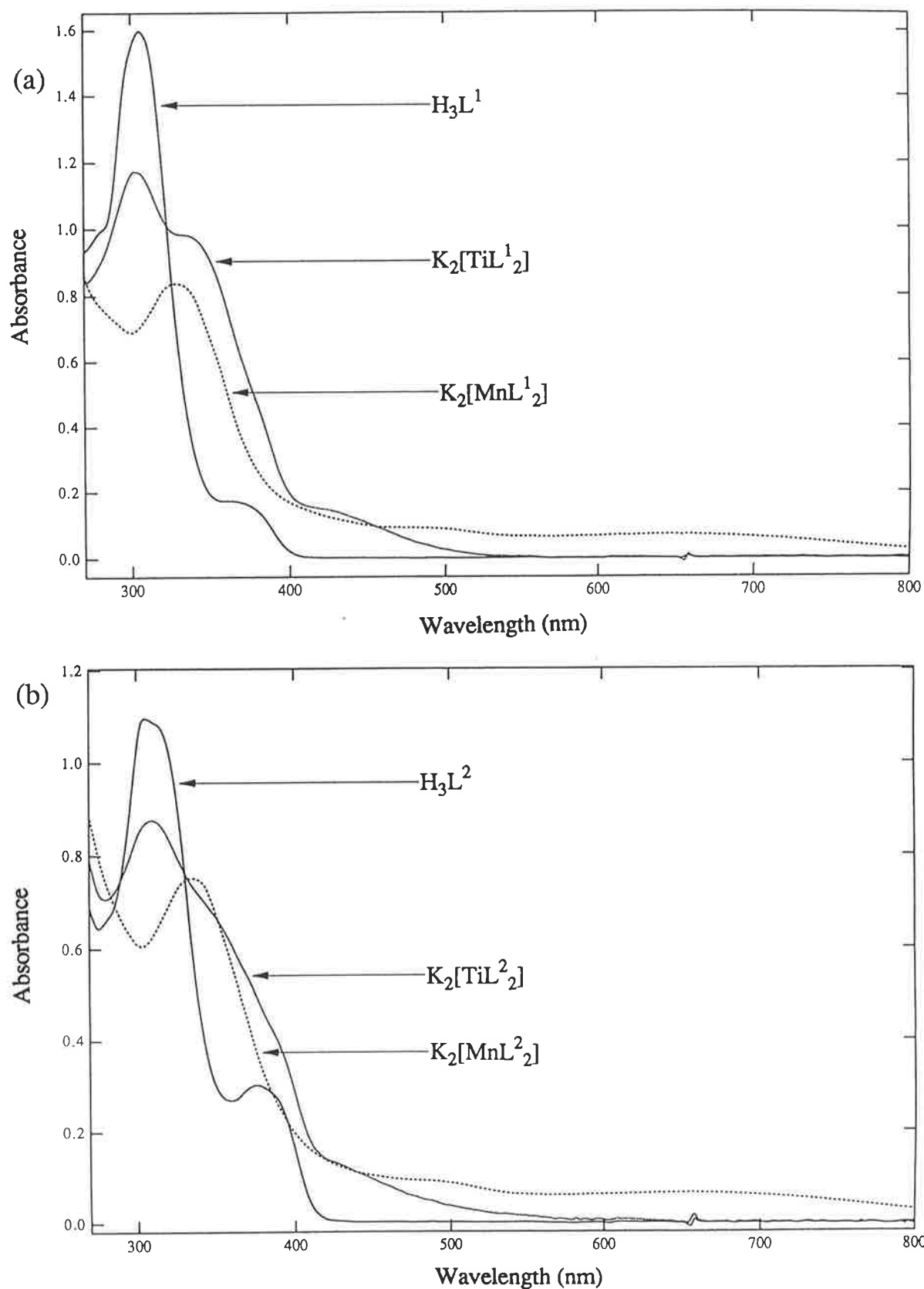
Figure 3.5: *(a) Overlay of the electronic spectra of N-(2-hydroxyphenyl)salicylamide* (H_3L^1), $K_2[TiL^1{}_2]$ *and* $K_2[MnL^1{}_2]$, *and (b) overlay of the electronic spectra of N-(2-hydroxyphenyl)-5-chlorosalicylamide* (H_3L^2), $K_2[TiL^2{}_2]$ *and* $K_2[MnL^2{}_2]$ *in dimethylformamide.*
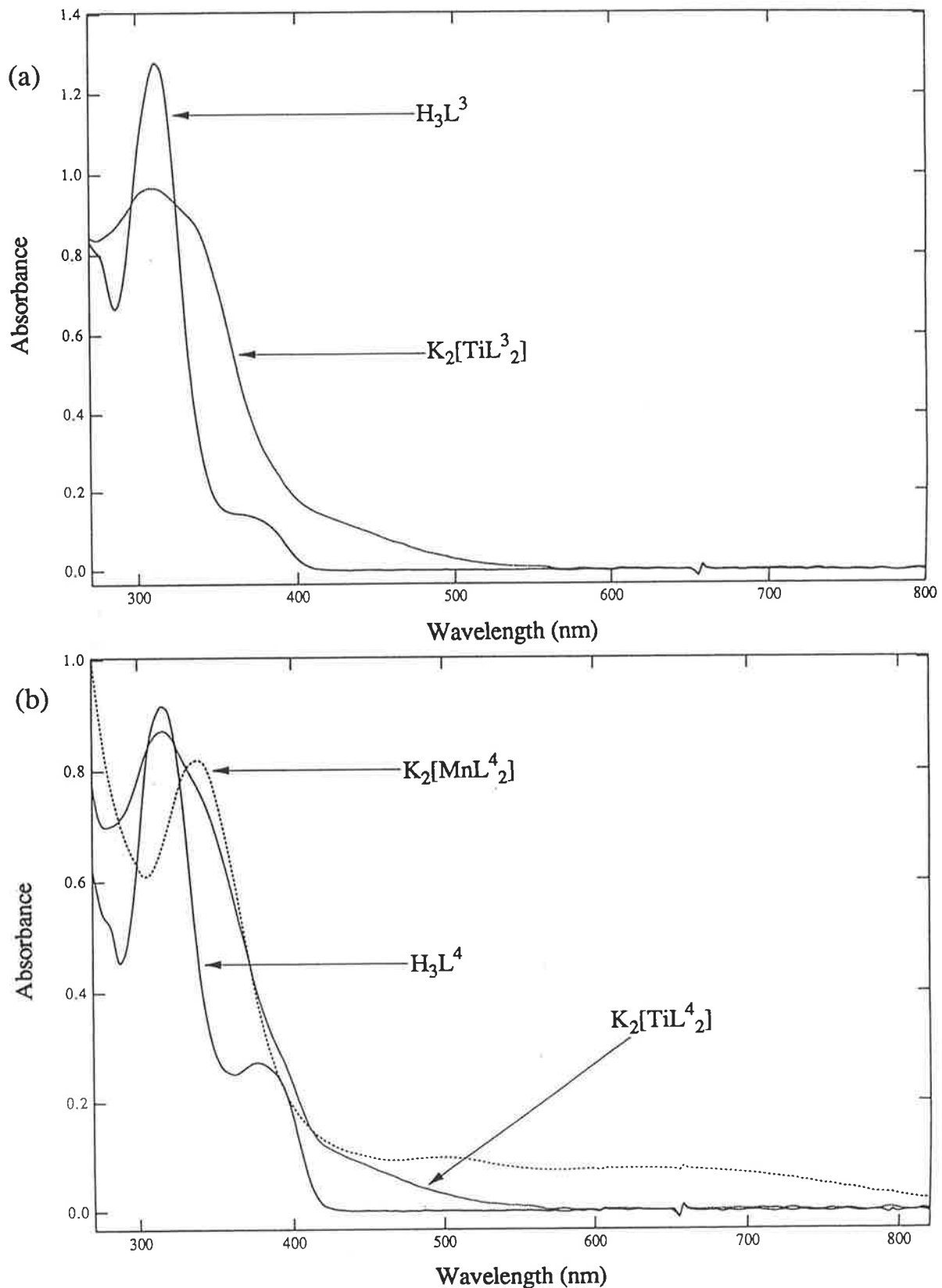
Figure 3.6: *(a) Overlay of the electronic spectra of N-(5-chloro-2-hydroxyphenyl)-salicylamide (H_3L^3) and $K_2[TiL^3{}_2]$, and (b) overlay of the electronic spectra of N-(5-chloro-2-hydroxyphenyl)-5-chlorosalicylamide (H_3L^4), $K_2[TiL^4{}_2]$ and $K_2[MnL^4{}_2]$ in dimethylformamide.*
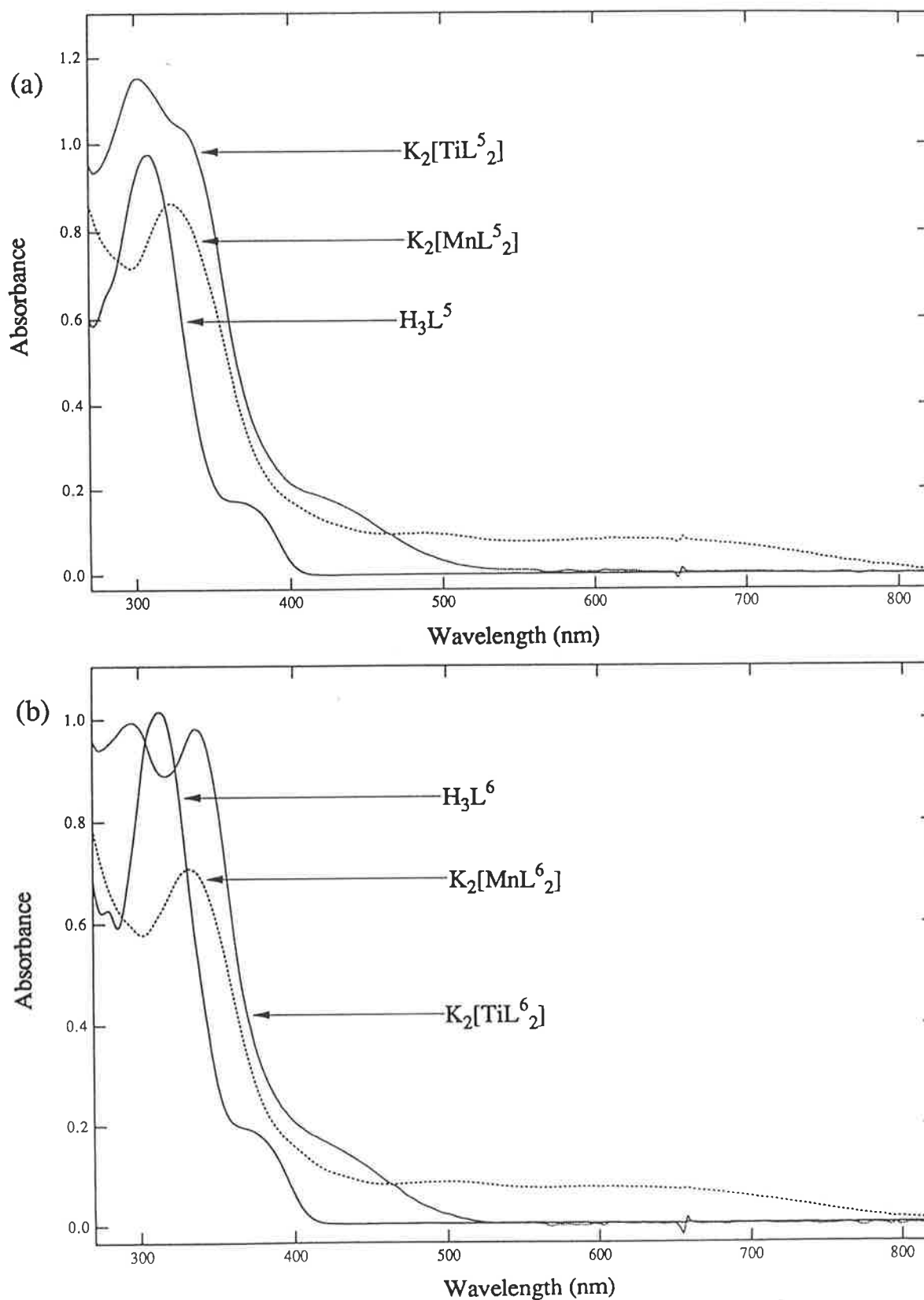
Figure 3.7: *(a) Overlay of the electronic spectra of N-(2-hydroxyphenyl)-3-methyl-salicylamide (H_3L^5), $K_2[TiL^5{}_2]$ and $K_2[MnL^5{}_2]$, and (b) overlay of the electronic spectra of N-(5-chloro-2-hydroxyphenyl)-3-methylsalicylamide (H_3L^6), $K_2[TiL^6{}_2]$ and $K_2[MnL^6{}_2]$ in dimethylformamide.*
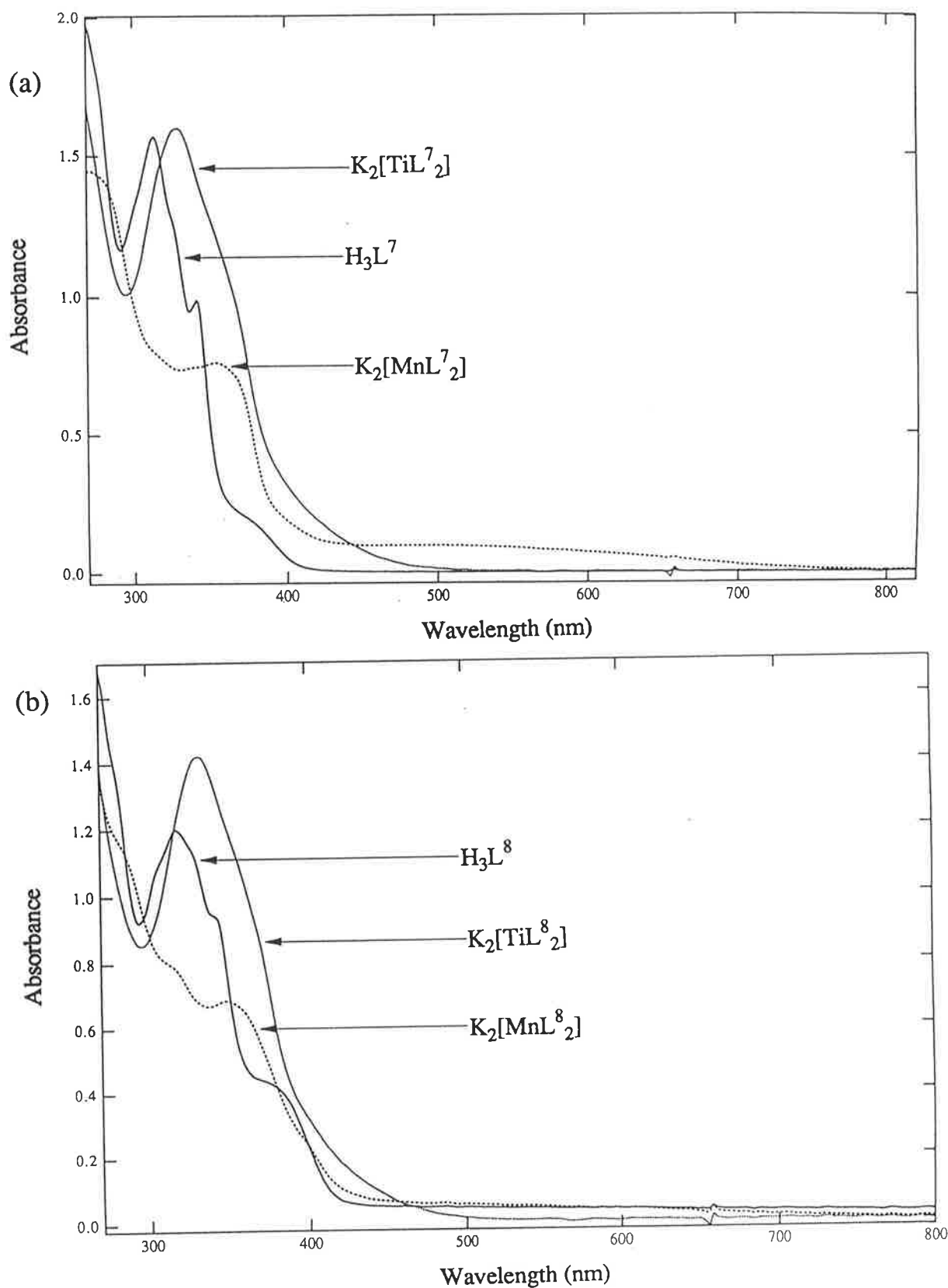
Figure 3.8: *(a) Overlay of the electronic spectra of N-(2-naphthol)salicylamide (H_3L^7), $K_2[TiL^7{}_2]$ and $K_2[MnL^7{}_2]$, and (b) overlay of the electronic spectra of N-(2-naphthol)-5-chlorosalicylamide (H_3L^8), $K_2[TiL^8{}_2]$ and $K_2[MnL^8{}_2]$ in dimethylformamide.*
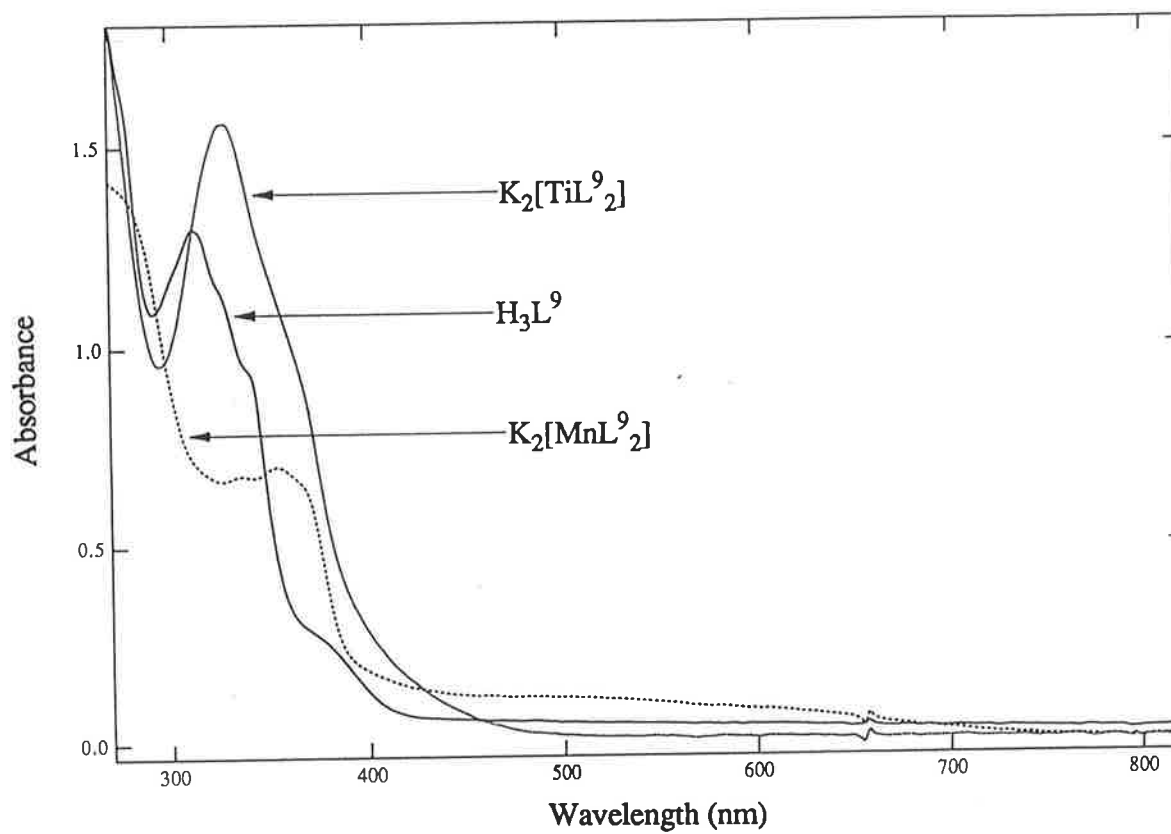
Figure 3.9: *Overlay of the electronic spectra of N-(2-naphthol)-3-methylsalicylamide* (H_3L^9), $K_2[TiL^9_2]$ *and* $K_2[MnL^9_2]$ *in dimethylformamide.*

Table 3.10: Electronic Spectral Data for Amide Complexes of Titanium and Manganese.

Ligand/ Complex	Wavelength (nm) [log ε]					
	d - d	CT	BAND(3)	BAND(2)	BAND(1)	BAND(0)
H_3L^1			364 [3·72]		304 [4·03]	
$K_2[TiL^1_2]$		412 sh			332 fl sh [4·29]	304 [4·37]
$K_2[MnL^1_2]$	658 [~3]	460 fl sh [3·32]			328 [4·29]	
$K_2[MnL^1_2]$	*637 sh*	*500 sh*			*325 [4·33]*	
H_3L^2			376 [3·43]		306 [3·99]	
$K_2[TiL^2_2]$		431 sh			343 sh	310 [4·29]
$K_2[MnL^2_2]$	656 [~3]	468 [3·34]			324 [4·13]	
H_3L^3			362 sh [3·15]		312 [4·10]	
$K_2[TiL^3_2]$		410 sh			330 sh	310 [4·36]
$K_2[MnL^3_2]^a$	*629 [3·48]*	*500 [3·55]*			*330 [4·39]*	
H_3L^4			378 [3·51]		318 [4·03]	
$K_2[TiL^4_2]$		422 sh			368 sh	318 [4·37]
$K_2[MnL^4_2]$	606 fl sh [~3]	500 [3·37]			330 [3·91]	
					340 [4·29]	

Compound						
H$_3$L^5			368 fl sh [3·85]		306 [3·96]	
K$_2$[TiL$^5_2$]		410 sh			326 sh [4·33]	302 [4·38]
K$_2$[MnL$^5_2$]	606 [~3]	486 [3·40]			324 [4·29]	
H$_3$L^6			368 [3·75]		314 [3·89]	
K$_2$[TiL$^6_2$]		418 sh			338 [4·39]	296 [4·39]
K$_2$[MnL$^6_2$]	590 fl sh [~3]	500 [3·37]			332 [4·28]	
H$_3$L^7			364 [3·68]	342 [3·90]	314 [3·98]	
K$_2$[TiL$^7_2$]				360 sh	328 [4·62]	
K$_2$[MnL$^7_2$]		486 [3·43]		354 [4·32]		
H$_3$L^8			380 [3·78]	344 [4·03]	316 [4·06]	
K$_2$[TiL$^8_2$]					332 [4·60]	
K$_2$[MnL$^8_2$]				348 [4·29]		310 sh [4·36]
H$_3$L^9			368 sh [3·52]	338 sh [4·03]	314 [4·17]	
K$_2$[TiL$^9_2$]					328 [4·58]	
K$_2$[MnL$^9_2$]		505 [3·51]		354 [4·27]		276 sh [4·57]

BANDS(0, 1 and 2) in the metal complexes correspond to intraligand transitions.

fl sh = flat shoulder; sh = shoulder.

[a] Reference 96.

3.10 Measurement of Solution Properties

In the case of the titanium and manganese amide compounds, it could be said from the microanalytical data obtained, that at least ~90% of the desired $K_2[ML^n_2]$ material was present. The consistency of the electronic spectra supported strongly the formulation and stability of these complexes at least in dimethylformamide solution. In an attempt to further characterise these compounds it was decided to perform magnetic moment and conductivity measurements on them.

All measurements were performed on crude samples which, in most cases, gave poor microanalyses. Compounds for which no microanalytical data was obtained or compounds for which the waters of hydration could not be assigned from the microanalytical data were all given a value of *3.5* for *x* and the corresponding formula weight was used in the conductance and magnetic moment calculations. To further confirm the conclusions reached about the extent of hydration from microanalytical and thermogravimetric measurements, and also because not all products had been examined by microanalysis thermogravimetric experiment, as well as using formula weights including *3.5*H_2O, magnetic moments and molar conductances (Section 3.10.2) were also calculated for a range of formula weights covering *1 - 5* waters of hydration (*x*). This demonstrates the dependance of the extent of hydration on the properties of the complexes.

3.10.1 Magnetic Moment Measurements

Mass spectral results mentioned earlier for the amide complexes suggested the possibility of oxidation states lower than (IV) for titanium, manganese and iron. Magnetic properties of transition metal atoms or ions which have unfilled *d* orbitals can provide valuable information on the structure and bonding of their complexes. The number of unpaired electrons is directly related to the arrangement and extent of the splitting of the *d* orbitals and decides the magnetic properties of a compound. The effective magnetic moments (Bohr Magnetons, B.M.) were calculated using the equation:

$$\mu_{eff} = 2.84\sqrt{X_{M(corr)} \times T} \qquad (3.2)$$

where $X_{M(corr)}$ = molar susceptibility corrected for any diamagnetic effects (c.g.s. units) and T = temperature (K).

The mass susceptibility of the manganese complexes was determined by the Evans method.[197] This method is convenient for determining the susceptibility in solution. The frequency at which a proton signal for a hydrogen containing solvent molecule resonates depends on the volume magnetic susceptibility of the solvent. This proton resonance, in a solution containing paramagnetic ions, is shifted from that in the pure solvent. The shift in the resonance frequency of the solvent proton is related to the volume susceptibility and can be used to calculate the mass susceptibility, X (c.g.s. units), of the dissolved paramagnetic substance, using Equation 3.3.

$$X = \frac{3\delta v}{2\pi v_o m} + X_o \qquad (3.3)$$

where δv = frequency shift (Hz),

        m = mass (g) of sample per 1 ml of solution,

        v_o = 60 MHz, and

        X_o = mass susceptibility of solvent.

The molar diamagnetic susceptibilities (X_M) of the amide ligands in the deprotonated form were calculated using Pascal's constants for the diamagnetism of the constituent atoms.[198a] For the ligands containing naphthyl rings the deviation from Pascals additivity rules was taken into consideration when determining X_M.[198b] Mass susceptibility measurements on the amide ligands were also carried out using a magnetic susceptibility balance to check for the absence of paramagnetic impurities (Section 6.32.3). However, due to a couple of inconsistent results obtained using the balance, the values calculated using Pascal's constants were used in all the magnetic moment calculations.

The mass susceptibility of the manganese and iron ions in the amide compounds were determined in methanolic solutions. Methanol has a mass susceptibility of -0.668×10^{-6} cm^3 g^{-1}.[13] The molar susceptibility ($= X \times$ F.W.) was then calculated and corrected for the diamagnetism of Mn(IV) (-8×10^{-6} c.g.s. units)[199] and the appropriate amide ligand. A value for the diamagnetic correction for Fe(IV) could not be found in the literature. However, a diamagnetic correction value of -8×10^{-6} c.g.s. units per mole was employed for the Fe(IV) ion in all calculations. This is because the diamagnetic corrections for the Mn(II) and Mn(III) ions are very similar to those for Fe(II) and Fe(III).[199] Thus, the diamagnetic correction for Mn(IV) was assumed to be similar to that for Fe(IV). As the potassium ions and the water of hydration are not present in the primary coordination sphere, the diamagnetic effect due to these can be neglected when using the Evans method.

For comparison purposes, a measurement was also carried out on the manganese complex of N-(2-hydroxyphenyl)salicylamide H$_3$L^1 which other workers have accurately characterised as K$_2$[MnL$^1_2$].3.5H$_2$O and have quoted a value of 4.06 B.M. for μ_{eff}.[96] The sample of K$_2$[MnL$^1_2$].3.5H$_2$O I prepared gave a μ_{eff} value of 3.97 B.M. indicating the validity of our experimental measurements.

In the manganese complexes, using the formula weight of K$_2$[ML$_2$].3.5H$_2$O to calculate the corrected molar susceptibility, X$_M$(corrected), gave magnetic moments in the range $3.70 - 4.31$ B.M. at T = 308.2 K (Table 3.11). These values are closest to the spin-only value of 3.87 B.M. for three unpaired electrons and thus, confirm the suggested formulation of these complexes as Mn(IV). Performing the calculations with formula weights which include *1 - 5* waters of hydration do not negate the agreement with the spin-only value of 3.87 B.M. The manganese(IV) complexes prepared by Koikawa *et al.* contained *1 - 4.5* waters of hydration gave μ_{eff} values in the range $3.67 - 4.06$ B.M..

Unlike the manganese complex with N-(2-hydroxyphenyl)salicylamide (H$_3$L^1), the vanadium product was insufficiently soluble in methanol and hence, its magnetic moment could not be measured by the Evans method.

As mentioned in Section 3.3.2, studies on complexes of iron with amide ligands, by Koikawa *et al.*, have recently been reported.[35] They found that iron(III) complexes of the amide ligands N-(2-hydroxyphenyl)salicylamide

and N-(2-hydroxy-5-chlorophenyl)salicylamide gave μ_{eff} values of 5·80 and 5·82 B.M., respectively, at room temperature characteristic of high-spin complexes (5 unpaired electrons). Iron(IV) complexes of the amide ligands N-(2-hydroxyphenyl)salicylamide and N-(2-hydroxy-5-methylphenyl)salicyl-amide gave μ_{eff} values of 4·99 and 2·84 B.M., respectively, at room temperature suggesting the former to be a high-spin complex (4 unpaired electrons) and the latter a low-spin complex (2 unpaired electrons).

Table 3.11: Effective Magnetic Moments for the Amide Complexes Determined at 308·2 K in Methanol.

Complex	μ_{eff} (B.M.)	
$K_2[MnL^n{}_2].xH_2O$:	$x = 3.5$	$x = 1 - 5$
n = 1	3·97 (4·06[†])	--
n = 2	3·89	3·78 - 3·96
n = 4	3·70	3·60 - 3·76
n = 5	3·89	3·76 - 3·96
n = 6	4·03	3·91 - 4·10
n = 7	3·78	3·68 - 3·84
n = 8	4·31	4·19 - 4·37
n = 9	4·15	4·04 - 4·22
$K_2[VL^1{}_2].xH_2O$ attempt:	Insoluble in methanol	
$K_2[FeL^n{}_2].xH_2O$ attempts:		
n = 1	4·57	4·42 - 4·67
n = 3	4·59	4·45 - 4·68
n = 4	4·54	4·41 - 4·61

† Reference 96 (using Evans method and Pascal's constants).

Summarised below in Table 3.12 are the results obtained by Koikawa *et al.*[35] as well as some other iron complex magnetic moment measurements found in the literature.[200]

Table 3.12: Experimental Magnetic Moments for Complexes of Iron in Different Oxidation States.

Oxidation State	Electronic Configuration	μ_{eff} (B.M.)
Fe(II)[a]	d^6, high spin	5·10 - 5·45
Fe(III)[a]	d^5, high spin	5·75 - 5·98
Fe(III)[a]	d^5, low spin	2·34 - 2·45
Fe(IV)[b]	d^4, high spin	4·99
Fe(IV)	d^4, low spin	2·84

[a] Reference 200; [b] Reference 35.

In this study, iron complexes of the amide ligands H_3L^1, H_3L^3 and H_3L^4 produced μ_{eff} values of 4·57, 4·59 and 4·54 B.M.,respectively, for the formula $K_2[FeL^n_2].3·5H_2O$. When comparing these values with the data in Table 3.12 the values agree best with their being compounds of Fe(IV). Although the values lie between μ_s (spin-only formula) values characteristic of three (3·87 B.M.) and four (4·90 B.M.) unpaired electrons, we are inclined to interpret the magnetic measurements as evidence for a d^4 high spin configuration which would be expected to show no contribution from the orbital angular momentum either in octahedral symmetry or the Jahn-Teller distorted tetragonal symmetry consistent with this configuration. Besides, the only alternatives for three unpaired electrons are the highly unlikely Fe(V) and high-spin Fe(I).

In the case of four unpaired electrons, high-spin Fe(II) and high-spin Fe(IV) complexes are possible, which suggests that the iron compounds obtained in this study are either of the type $K_2[Fe^{II}L_2]$ with the amide ligands

coordinating as dinegative bidentate ligands, or the proposed $K_2[Fe^{IV}L_2]$ type in which the amide ligands coordinate as trinegative tridentate ligands. The infrared spectra showed that the ligands were coordinated in the same way as in the corresponding titanium(IV) and manganese(IV) complexes. Moreover, the deviation in the magnetic moment for the d^6 octahedral configuration (Fe(II)), from the spin-only value of 4·90 B.M., would be even more pronounced due to the orbital angular momentum contribution. It should be mentioned that the complexes were prepared from an iron(III) starting material under oxidising conditions similar to those used by other workers who yielded Fe(III) compounds.

In case complexes analogous to those proposed above for iron (i.e. amides behaving as dinegative tridentate ligands) could be formed with titanium, a magnetic moment measurement in methanol was carried out on one sample, $K_2[TiL^1_2]$. A Ti(II) complex would exhibit 2 unpaired d electrons as opposed to Ti(IV) which would reveal no d electrons. This complex produced no frequency shift in the methyl proton signal of methanol thus, suggesting the presence of diamagnetic ions and confirming the formation of Ti(IV) amide complexes.

3.10.2   Conductance Measurements

Conductivity measurements are a useful means for obtaining structural information on a complex by determining its charge type. This technique involves measuring the electrical resistance of a solution of the complex at a particular constant temperature. The molar conductance (Λ_m) at infinite dilution, or at a stated concentration, can be used to determine the ionic composition of electrolytes. Λ_m is both temperature and solvent dependant. Ranges of conductances for several different charge type electrolytes are given in the review by Geary.[195]

The purpose of the conductance measurements in this study was to establish the formulation $K_2[MnL_2]$. Measurements were carried out at 25°C in methanol at concentrations near 10^{-3} mol dm^{-3} and the idealised formula $K_2[ML^n_2].x H_2O$ ($x = 3·5$) was used to calculate the molar conductance using Equation 3.4

$$\Lambda_m = \frac{1000\kappa}{C} \qquad\qquad (3.4)$$

where κ = specific conductance (ohm^{-1} cm^{-1}) and C = concentration (mol dm^{-3}).

The results are shown in Table 3.13. Also shown in Table 3.13 is a range of values calculated for $x = 1$ to $x = 5$. Geary reported the range 160 - 220 ohm^{-1} cm^2 mol^{-1} for 1:2 type electrolytes in methanol.[195] These measurements would not be able to determine the purity of the products obtained but would show whether the products were consistent with the proposed formulation.

The manganese complexes gave molar conductance values which were characteristic of 1:2 electrolytes. In all cases, the analogous titanium complexes produced lower Λ_m values. The molar conductances for the titanium complexes were lower than that reported by Geary but they were still well above the range 80 - 115 ohm^{-1} cm^2 mol^{-1} characteristic of a 1:1 electrolyte. The higher Λ_m values for the manganese complexes in comparison to those of the titanium complexes may suggest the presence of greater amounts of some potassium contaminant. This is consistent with findings from the elemental analyses where higher than expected values were found for the K/Mn ratio than the K/Ti ratio.

The products afforded from the attempted preparation of the $K_2[FeL^n_2]$ complexes, where n = 1, 3 and 4, assuming 3.5 waters of hydration, also gave Λ_m values characteristic of 1:2 electrolytes. However, it is not possible to differentiate between the $[Fe^{IV}L_2]^{2-}$ and $[Fe^{II}L_2]^{2-}$ which was one possible alternative suggested by the magnetic measurements.

The attempted preparation of the vanadium complex of N-(2-hydroxyphenyl)-salicylamide (H_3L^1) resulted in a product which was only partially soluble in methanol and hence, no conductance evidence could be obtained to confirm or reject the $K_2[VL_2]$ formulation.

Table 3.13: Conductance Measurements on Amide Complexes of Manganese, Titanium and Iron at 25°C in Methanol.

Complex	Λ_m (ohm^{-1} cm^2 mol^{-1})	
$K_2[MnL^n_2].xH_2O$:	$x = 3.5$	$x = 1 - 5$
n = 1	160 (159[†])	--
n = 2	161	151 - 167
n = 4	171	161 - 177
n = 5	182	170 - 189
n = 6	182	172 - 189
n = 7	205	193 - 213
n = 8	192	181 - 198
n = 9	191	180 - 198
$K_2[TiL^n_2].xH_2O$:		
n = 1	151	140 - 157
n = 2	150	141 - 156
n = 3	160*	150 - 166*
n = 4	141	133 - 146
n = 5	172	161 - 179
n = 6	139	130 - 144
n = 7	167*	157 - 174*
n = 8	152	143 - 157
n = 9	164	154 - 170
$K_2[FeL^n_2].xH_2O$ attempts:		
n = 1	169	157 - 176
n = 3	210	197 - 218
n = 4	194	183 - 201

[†] Reference 96.
* Value or range recorded as the the mean of several measurements.

3.11   An Assessment of the Experimental Evidence Presented in Chapter 3, Concerning the Structure of the Amide Complexes

In investigating the coordination complexes of the trinegative tridentate amide ligands a serious disadvantage has been the difficulty in obtaining materials of the purity required to produce unambiguous microanalytical support for the proposed formulations. The inability to obtain the materials either as crystalline, or at least as solids separating from a reaction mixture, confined us to working with crude products which undoubtedly contained impurities. The best purification procedure used was thorough washing, as attempts to purify by chromatography or recrystallisation of certain compounds were either unsuccessful or led to decomposition.

The difficulty in obtaining well characterised solids was due to their high solubility, which in itself was the result of the complexes being heavily hydrated. Similar results have been observed by other workers and it is very unfortunate that no suitable crystal structures exist for such complexes, as the association of the amide ligand with water molecules is a characteristic feature of the ligand and one that persists through a large number of structural variants in the ligands and with all the different metals used by us. The strategy of using many structural variants of the ligand in the hope of obtaining crystalline products, a strategy that has been successful in previous studies in this laboratory (e.g. Salam[92]), failed because of what we believe is this very specific interaction between the amide and the waters of hydraion. This interaction does not hold under the conditions of obtaining FAB mass spectra.

Although in many cases the microanalytical results could be improved by allowing for a number of water molecules in the $K_2[ML^n_2]$ formulation, many of the analytical results were still outside the limits of what is normally the acceptable in synthetic chemistry. Nonetheless, there is sufficient evidence from spectroscopic and other physical measurements to predicate that the bulk of the materials isolated by us conform with the proposed coordination of the amide ligand in trinegative tridentate form, giving rise to $K_2[ML^n_2]$ type complexes. Infrared studies showed the loss of protons attached to O and N with consistent shifts in the vibrational frequencies of the amide function. Electronic spectra and conductivities showed similarity between the various compounds. Solution magnetic moments supported the

high oxidation state (IV) in the manganese compounds and was a postive alternative in the iron compounds. Electrochemical measurements showed many of the compounds to be similar (Chapter 5) and were in agreement with the few, well documented, cases reported by other workers. There is little doubt in our mind that the crude materials prepared contained the complexes of the suggested formulations in high percentages, but that unavoidable impurities have interfered with the microanalytical results and put the outside the nrmally accepted values. In hindsight, our strategy of structural variation in the ligand in the hope of obtaining a crystalline product that could be used as a benchmark to validate all the other proposed structures was unsuccessful. An alternative strategy would have been to use large scale preparations, hoping that precipitation conditions would have favoured the isolation of crystalline materials. This alternative was considered less appropriate because of the amount of work associated with the preparation of the ligands on a large scale.

Chapter 4

NEW CHELATING LIGANDS

4.1 Introduction

It was seen in Chapter 2 that the Schiff base ligands used were capable of stabilising the high oxidation states in numerous metals. Our research included a ligand of the type shown in Figure 4.1, capable of forming five- and six-membered rings with the metal which are the optimum size for the formation of stable chelate rings with transition metal ions.[201] Stabilisation was achieved through π-donation from the aromatic oxo functions and the delocalised π orbitals of the conjugated ligand system.

6-membered ring   5-membered ring
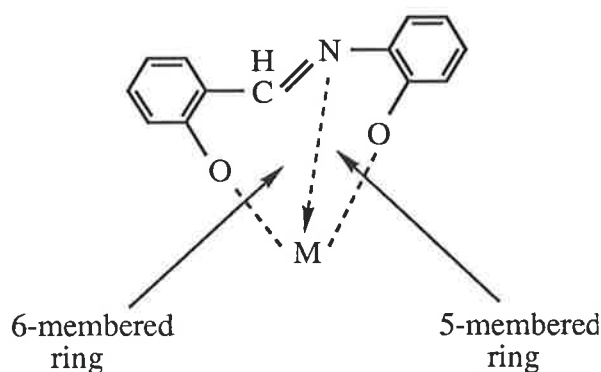
Figure 4.1: *The sought after chelation by Schiff base ligands, where M represents a metal.*

As well as extending work in the Schiff base ligand area it was interesting to consider what effect various modifications to the general structure of this particular Schiff base ligand would have on its ability to form complexes and on the properties of any complexes formed (structure, redox behaviour etc.). In particular, we decided to retain the aromatic oxo functions and replace the azomethine -CH=N- function with other bridges, such that the overall structure was maintained and also an electron donating site in the bridging

position was provided. The type of organic compounds we tried to prepare are listed in Figure 4.2.

X	Y	Type of Compound
$-CH=N-$		Schiff Base (Chapter 2)
$-N=N-$		Azo Dye (Chapter 2)
$-CH=CH-$		Alkene
$-CH_2-O-$		Ether
$-\overset{\overset{\displaystyle O}{\|\|}}{C}-O-$		Ester
$-\overset{\overset{\displaystyle O}{\|\|}}{C}-N-$		Amide (Chapter 3)
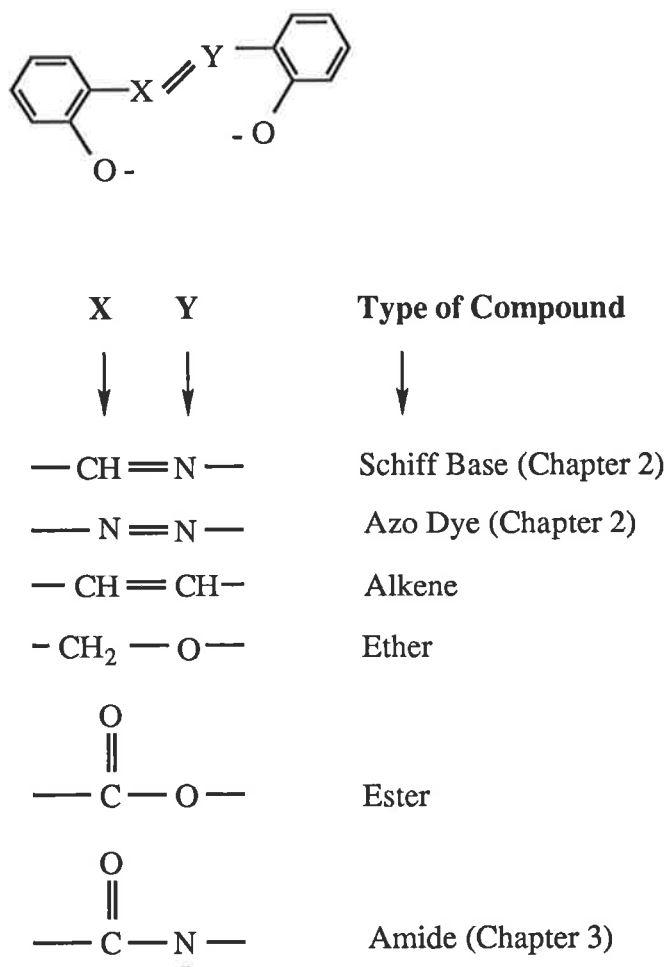
Figure 4.2: *General structure of the ligands of interest, along with the functional groups which were to be varied.*

In these bridges, the varied Y function can be considered as being isoelectronic with the azomethine $=N-$ in the Schiff bases. The azo compounds and amide compounds together with their resultant complexes have already been discussed, in Chapters 2 and 3 respectively, and were observed to function in a way similar to the Schiff bases. Our aim now was to investigate 2,2'-dihydroxystilbene ($-XY- = -CH=CH-$), 2,2'-dihydroxybenzyl-phenyl ether ($-XY- = -CH_2O-$) and 2-hydroxyphenyl salicylate ($-XY- = -CO_2-$), and some of their derivatives, as possible ligands for stabilising higher oxidation states of metal ions.

4.2　2,2'-Dihydroxybenzylphenyl Ether

4.2.1　Introduction

The Williamson synthesis of ethers is commonly used because of its versatility: it can be used to prepare unsymmetrical as well as symmetrical ethers. It involves nucleophilic substitution of halide ion by an alkoxide ion.

$$R^1X \ + \ M^{+\,-}OR^2 \ \longrightarrow \ R^1OR^2 \ + \ MX \tag{4.1}$$

In the preparation of an unsymmetrical ether, a choice in the starting materials arises. The danger of elimination, resulting in the formation of an olefin, competing with the desired substitution must also be considered. Tertiary and aryl halides are generally too unreactive, while secondary halides would result in low yields.[189b,202a,203a] Thus the first synthetic route tried for the preparation of 2,2'-dihydroxybenzylphenyl ether was to treat 2-hydroxybenzyl bromide *(1a)* with the alkali salt of catechol *(1b)* as shown in Reaction Scheme 4.1.
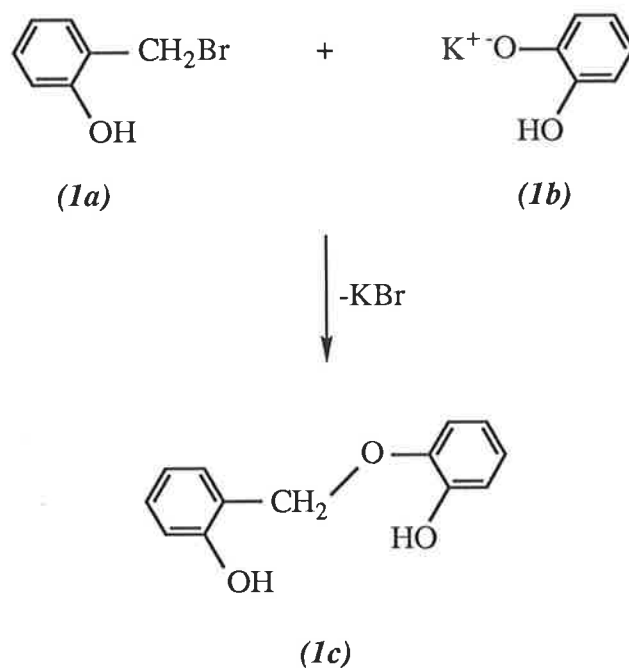
Reaction Scheme 4.1

However, a synthesis for the required starting material 2-hydroxybenzyl bromide could not be found in the literature. Attempts to prepare 2-hydroxybenzyl bromide *via* bromination of *o*-cresol with N-bromo-succinimide produced an oil as the product, which thin layer chromatography and NMR spectroscopy revealed the presence of a large amount (87%) of unreacted *o*-cresol and no 2-hydroxybenzyl bromide. The inability to obtain the bromide starting material may be due to its instability according to Equation 4.2.

$$CH_2 \longrightarrow Br \qquad \qquad CH_2 \qquad + \qquad HBr \qquad \qquad (4.2)$$
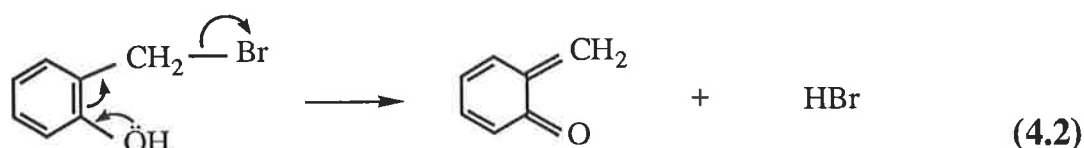
A strong absorption was observed in the carbonyl region of the infrared spectrum of the oily product, lending support to this theory. The unstable nature of the 2-hydroxybenzyl bromide led us to believe that it was essential to modify the hydroxyl group.

When selecting a protecting group, requirements are that the group can be easily attached and easily removed, under conditions that will not affect other functional groups in the molecule. Furthermore, while attached to the molecule, it must be resistant to the planned reaction pathway. A range of ethers and esters can be used for the protection of the hydroxyl function,[204] a common choice being the tetrahydropyranyl ether (THP) protecting group. As the compound of interest is also an ether (2,2'-dihydroxybenzylphenyl ether), it was decided not to use an ether for protection in case its removal interfered with the new benzyl-phenyl ether linkage. A literature search on the general formula (2-OR)ArCH$_2$Br yielded numerous alkyl- and aryloxybenzyl bromides. The simplest, 2-bromomethylphenyl acetate *(2a)* was chosen as the starting halide for the preparation of 2,2'-dihydroxybenzylphenyl ether, and an outline of the synthesis is shown in Reaction Scheme 4.2.
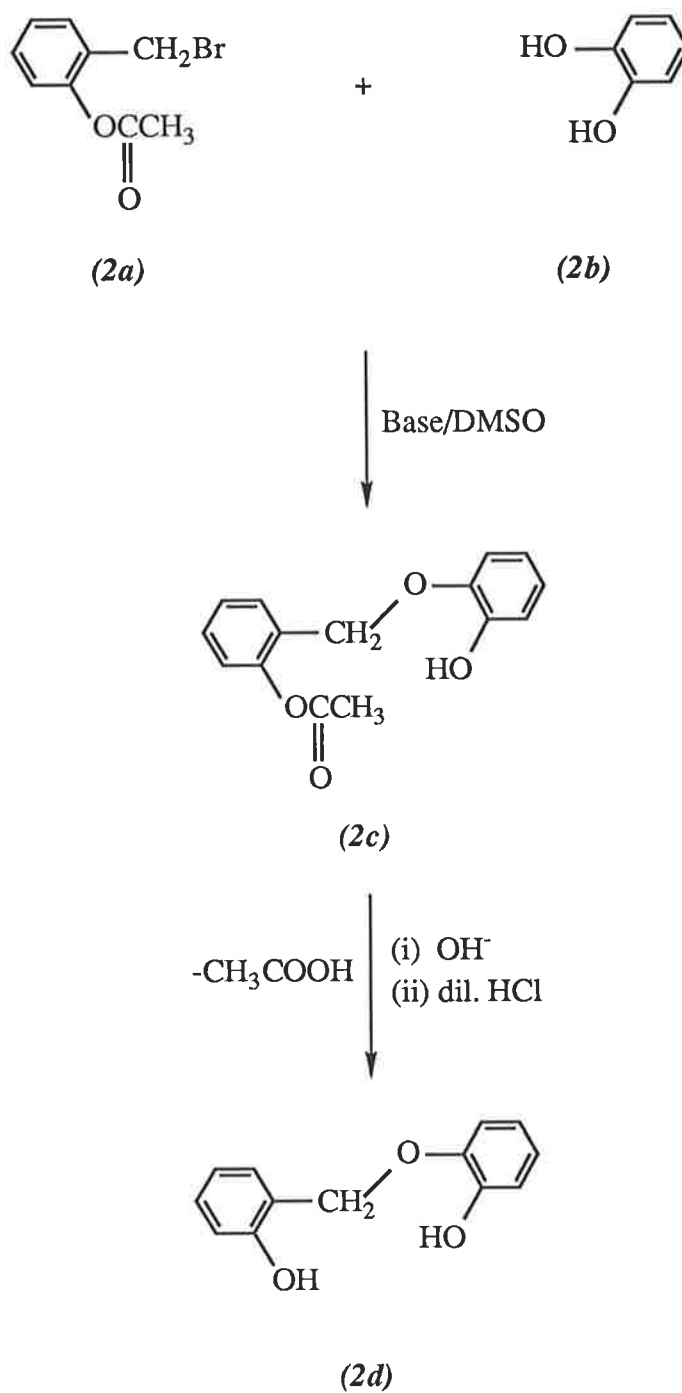
Reaction Scheme 4.2

4.2.2 Synthesis of 2,2'-Dihydroxybenzylphenyl Ether using an Acetyl Protecting Group

4.2.2.1 Procedure

Numerous experiments were performed in an attempt to prepare 2,2'-dihydroxybenzylphenyl ether from the reaction between 2-bromomethylphenyl acetate (2a) and catechol (2b) in the presence of base in solvent dimethylsulphoxide. Various reaction conditions were employed and these are summarised in Table 4.1. They include the use of different bases, temperatures, reaction times and mole ratios of the starting materials and base.

Table 4.1: The Different Reaction Conditions Employed in the Attempted Preparations of 2,2'-Dihydroxybenzylphenyl Ether using an Acetyl Protecting Group.

Reaction	Base	ROH : BrR Mole Ratio	ROH : Base Mole Ratio	Temp. (°C)
A	CH_3O^- Na^+	1:1	1:1	RT
B	KOH	1:1	$1:(1+x)^*$	RT
C	KOH	1:1	1:2	RT
D	KOH	1:1	$1:(1+1)^*$	60 - 70
E	KOH	1:2	1:4	RT
F[†]	KOH	1:1	1:1·5	RT
G[†]	KOH	1:1	$1:(1+1)^*$	85
H[†]	KOH	1:1	1:4	30
I[†]	KOH	1:1	1:4	80 - 100

RT implies room temperature conditions.
ROH = catechol; BrR = 2-bromomethylphenyl acetate.
* one mole equivalent was added initially and after reacting for some time another one mole equivalent or an unknown amount, x, was added such that base was in excess of catechol.
† Reaction mixtures which were acidified.

Solid KOH in dimethylsulphoxide was used as the base in reactions *B - I*. This system has been used by many workers as an easy, fast and mild procedure for the alkylation of phenols, amides, acids, alcohols and ketones.[205-207] The alkylating agent *(2a)* and substrate *(2b)* are simply added to a mixture of powdered KOH in dimethylsulphoxide at room temperature. The solubility of KOH in dimethylsulphoxide is poor allowing only surface reactivity, which makes the mixture suitable as a base for nucleophilic displacement reactions.[206] In the case of reaction *A*, using sodium methoxide as base, the monosodium salt of catechol was prepared and isolated before reacting with the halide starting material.

In other studies on the synthesis of ethers using the KOH/dimethylsulphoxide system, a substrate to KOH ratio of 1:4[205] and 1:1·7[207] have been used. A catechol to base ratio of 1:1 was initially employed in our research for three reasons:

   (i)   to avoid the formation of the dialkali salt of catechol,

   (ii) to avoid competitive hydrolysis of the acetate group in 2-bromomethylphenyl acetate. More base could be added later if it was required,[208]

   (iii) to avoid premature hydrolysis so that the acetylated ether (Reaction Scheme 4.2 *(2c)*) could be isolated as an intermediate product. The acetyl protecting group could then be removed by further hydrolysis in a solvent such as alcohol.[208]

The general procedure for the preparation of 2,2'-dihydroxybenzylphenyl ether was to add the catechol to the KOH/dimethylsulphoxide or $CH_3O^-Na^+$/dimethylsulphoxide system, followed by 2-bromomethylphenyl acetate after stirring at room temperature for two minutes. As a precaution, the reactions were carried out under an atmosphere of dinitrogen. After allowing the reaction to proceed at the desired temperature, attempts to isolate the acetylated ether were made by water drownout and subsequent extraction from the reaction mixture with diethyl ether (reaction *A*) or dichloromethane (reactions *B - I*). The extracts were then dried and the solvent removed under vacuum. All products were isolated as oils. The products of the reaction were examined for the presence of the desired ether by ^{1}H-NMR spectroscopy and, on occasions, mass spectroscopy and infrared spectroscopy. The relevant regions examined in the ^{1}H-NMR spectra were: $\delta(CH_3CO_2-)$ as evidence of the acetylated ether (Reaction Scheme 4.2 *(2c)*), $\delta(-CH_2O-)$ as evidence of the

sought after bond formation and unreacted starting materials. Replacement of acidic protons by D_2O was used to detect the presence of aromatic hydroxyl groups. In some cases an attempt to purify the product was made.

4.2.2.2 *Results*

Inspite of the many variations in the conditions used we were unable to maximise the formation of the desired product which probably was formed in a small yield amongst other related products. Presented below is a summary of the results obtained from attempts to prepare 2,2'-dihydroxybenzylphenyl ether. The ^{1}H-NMR data is given in the Experimental Chapter.

Attempts to prepare the ether with an initial catechol to base ratio of 1:1 and one mole equivalent of 2-bromomethylphenyl acetate always resulted in a product whose ^{1}H-NMR spectrum contained peaks in the expected regions (i.e. aromatic, -C$\underline{H}_2$O- and C$\underline{H}_3$CO$_2$-). In some cases starting materials were detected by ^{1}H-NMR (reaction *B*) and by TLC (reaction *D*). In all cases, multiple peaks were observed in the -C$\underline{H}_2$O- region (δ5·2 - 4·9 ppm) easily distinguished from any peaks due to hydroxyl protons from unreacted catechol, which also resonate in this area (δ5·05 ppm). This showed that a mixture of compounds containing a -C$\underline{H}_2$O- group were present. The presence of more than one compounds was also confirmed by the presence of more than one peak in the C$\underline{H}_3$CO$_2$- region. Only reaction *A* gave a product which contained a single peak in this region. Addition of excess base, at a later stage in the synthesis, as expected saw the elimination of the peaks in the C$\underline{H}_3$CO$_2$- region and the appearance of aromatic hydroxyl groups (reaction *B*). In another case, when treating the reaction mixture with excess base at elevated temperatures (60 - 70°C), multiple peaks were still observed in both δ(-C$\underline{H}_2$O-) and δ(C$\underline{H}_3$CO$_2$-) regions of the ^{1}H-NMR spectrum (reaction *D*). It was considered that one of the peaks in the δ(C$\underline{H}_3$CO$_2$-) region could be due to the methyl protons of acetic acid, formed by the hydrolysis of the acetylated ether and which is expected to resonate in this region (δ2·05).[147d] Integration of the spectral peaks showed that even if one of the peaks was due to the acetylated ether then this was only a minor product.

The multiple peaks observed in the δ(-C$\underline{H}_2$O-) region of the ^{1}H-NMR spectra suggested that even at a 1:1 catechol to base ratio some hydrolysis occurred resulting in the production of some diol ether (Reaction Scheme 4.2 *(2d)*).

This prompted the use of excess base from the beginning of the synthesis in an attempt to ensure the complete hydrolysis of the acetylated intermediate, and the recovery of only a single product, the diol ether. With a 1:2 and 1:4 catechol to base mole ratio, at or near room temperature, the results were no different to those obtained with a 1:1 ratio.

In one case, at room temperature using excess base, a 1:2 catechol to 2-bromomethylphenyl acetate mole ratio was used(reaction *E*). The ^{1}H-NMR spectrum of the yellow precipitate obtained suggested the presence of some acetylated ether as a minor product. However, the overall yield would be less than 2%. The presence of this product was also confirmed by mass spectroscopy. In addition, the mass spectrum contained a more intense peak corresponding to the formula weight of the diol ether. However, this peak may also have been due to a fragmentation product of the acetylated ether. The ^{1}H-NMR spectrum of the product showed several -CH_2O- containing compounds suggesting that the product could not be a mixture of only protected and diol ethers.

Variations in the procedure for isolating the product were also carried out. The reaction mixture was acidified after the use of excess base to favour the formation of the diol ether. Using a 1:1·5 mole ratio for catechol to base at room temperature, and extracting the product in the usual manner before acidification in ethanol yielded a product similar to that obtained in earlier attempts. Although the ^{1}H-NMR spectrum contained resonances in the expected regions, those in the δ(-C$\underline{H}_2$O-) and δ(C$\underline{H}_3$CO$_2$-) regions were multiple peaks suggesting several CH$_3$O- and -CH$_2$O- containing compounds were present (e.g. reaction *F*). Similar observations were made even when the amount of excess base was increased (crude material from reaction *I* and second extract from reaction *H*), and when the reaction mixture was heated and acidified before extraction of the product (*G*). In one case, no peaks at all were observed in the δ(C$\underline{H}_3$CO$_2$-) region of the ^{1}H-NMR spectrum (first extract; reaction *H*) but the integrated spectrum did not support the formation of diol ether. The third extract from this reaction showed no peaks in the expected δ(-C$\underline{H}_2$O-) region, showing that no ether formation had taken place.

For two of the above reactions above (*G* and *I*), attempts were made to purify their product by column chromatography. Not only did chromatography show no improvement in the purity of the products, but it seemed to introduce decomposition products. Integration of the ^{1}H-NMR spectra did not support a

mixture of acetylated and diol ethers without much impurity. In the case of reaction G, for example, the product obtained by elution with dichloromethane exhibited multiple peaks in the $\delta(-C\underline{H}_2O-)$ and $\delta(C\underline{H}_3CO_2-)$ regions with additional peaks in between these regions and upfield from the $\delta(C\underline{H}_3CO_2-)$ region.

The lack of success of the synthesis of 2,2'-dihydroxybenzylphenyl ether following Reaction Scheme 4.2 suggested more than one type of ether forming from side-reactions. The possibility that this was due to the two hydroxyl groups present in catechol prompted the use of 2-acetyloxyphenol (Figure 4.3(i)) as a replacement for catechol in Reaction Scheme 4.2. Under these conditions the reaction between 2-bromomethylphenyl acetate and 2-acetyloxyphenol in dimethylsulphoxide, using NaH as the base and room temperature conditions, yielded a cloudy yellow oil whose ^{1}H-NMR spectrum contained multiple peaks in the expected $\delta(C\underline{H}_3CO_2-)$ and $\delta(-C\underline{H}_2O-)$ regions. The presence of 2,2'-diacetyloxybenzylphenyl ether (Figure 4.3(ii)) was also suggested but as a minor product. This was not investigated any further.

At this point it was decided to consider that our original choice of protecting group was not stable enough in the KOH/dimethylsulphoxide system used, and investigated whether ether protecting groups would provide better results.

(i)　　　　　　　　　　　　　　　(ii)
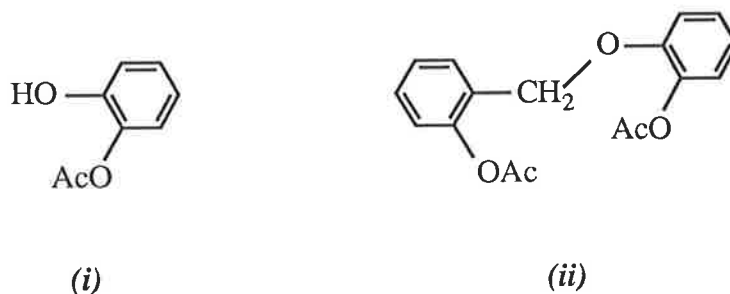
Figure 4.3: (i) 2-Acetyloxyphenol and (ii) 2,2'-diacetyloxybenzylphenyl ether (where Ac = CH₃CO).

4.2.3 Methyl Protecting Group

To determine if the problems encountered in Section 4.2.2 were due to the acetyl protecting group, the synthesis shown by Reaction Scheme 4.3 was designed. The reaction between equimolar amounts of 2-methoxybenzyl bromide *(3a)*, successfully prepared from 2-methylanisole, and readily available guaicol *(3b)* in KOH/dimethylsulphoxide produced 2,2'-dimethoxy-benzylphenyl ether *(3c)* in 46% yield. ^{1}H-NMR and mass spectral data supported this (see Experimental Chapter).
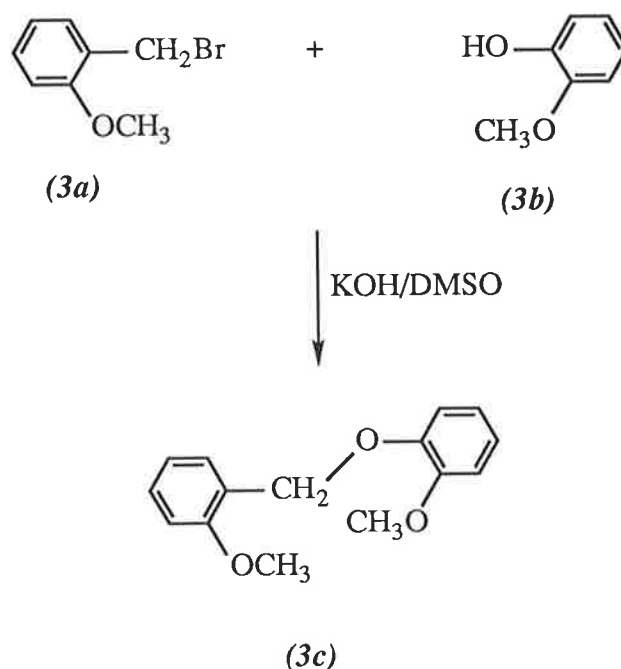
Reaction Scheme 4.3

The formation of this aryl ether in a reasonable yield confirmed that our initial choice for protection of the hydroxyl group (i.e. the acetyl protecting group) had led to complicating side-reactions.

There are numerous reagents which selectively remove methyl groups which are protecting hydroxyl groups (demethylation) in the presence of various

other functional groups within the molecule.[203b,209-212] However, they also split the benzyl-phenyl ether linkage.[213] An attempt was made to try and remove this protection following a similar method to that successfully used by Salam used in the synthesis of the azo dye Ap-p^{Cl}-PhenolH$_2$, where the methyl protecting group was removed using AlCl$_3$/benzene (Chapter 2).[92] However, this procedure used on 2,2'-dimethoxybenzylphenyl ether cleaved the benzyl-phenyl ether linkage as there was no evidence of a peak in the δ(-C$\underline{H}_2$O-) region.

4.2.4 2-Methoxypropane Protecting Group

2-Methoxypropene *(4b)* was considered as an alternative protecting group as very mild conditions (20% aqueous acetic acid) would be required to remove it.[214] This synthesis would require the preparation of 2-methoxypropane-benzyl bromide *(4d)* as a starting material, the outline of which is shown in Reaction Scheme 4.4. Once synthesised, this product could then be reacted with catechol or similarly-protected catechol.
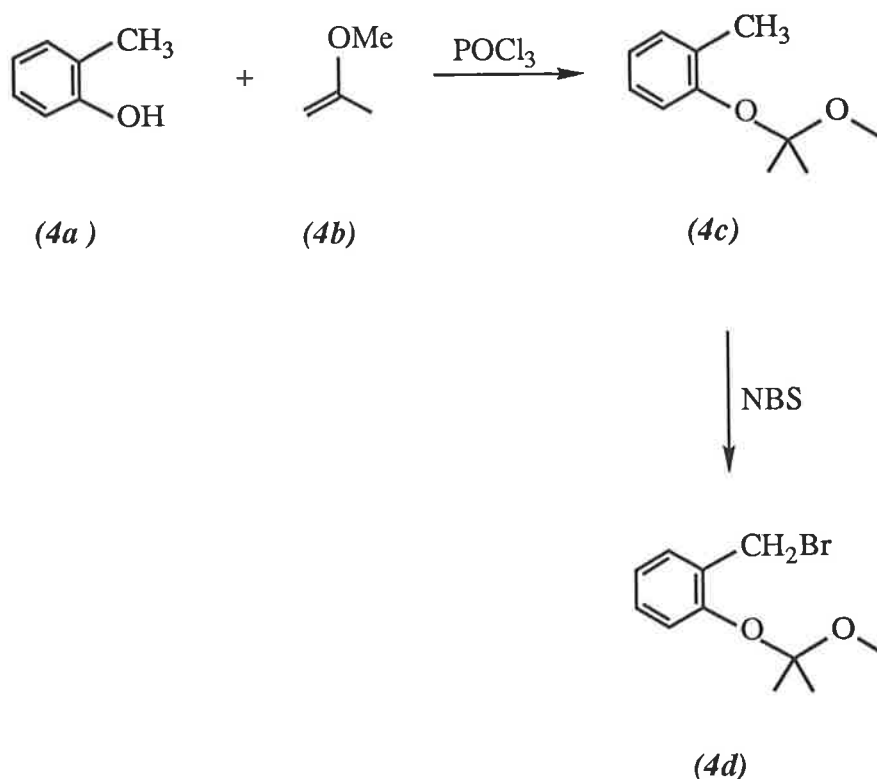
Reaction Scheme 4.4

The formation of the intermediate product *(4c)* was successful, however attempts to form its bromide *(4d)*, by NBS bromination, were less successful. The ^{1}H-NMR spectrum of the final product showed that the protecting group was too unstable under these conditions, as the signal for its >C(CH$_3$)$_2$ protons, observed at $\delta 1 \cdot 44$ ppm in the starting material, had disappeared. Thus, this was not pursued any further.

4.2.5 Trimethylsilyl Protecting Group

As a final attempt to prepare 2,2'-dihydroxybenzylphenyl ether, a trimethylsilyl protecting group for the hydroxyl function was used as another alternative.[215] This synthesis would require the preparation of 2-(trimethyl-silyloxy)benzyl bromide (*5d*) as a starting material. The pathway followed is shown in Reaction Scheme 4.5. If successfully synthesised, this product could then be reacted with catechol or similarly-protected catechol.
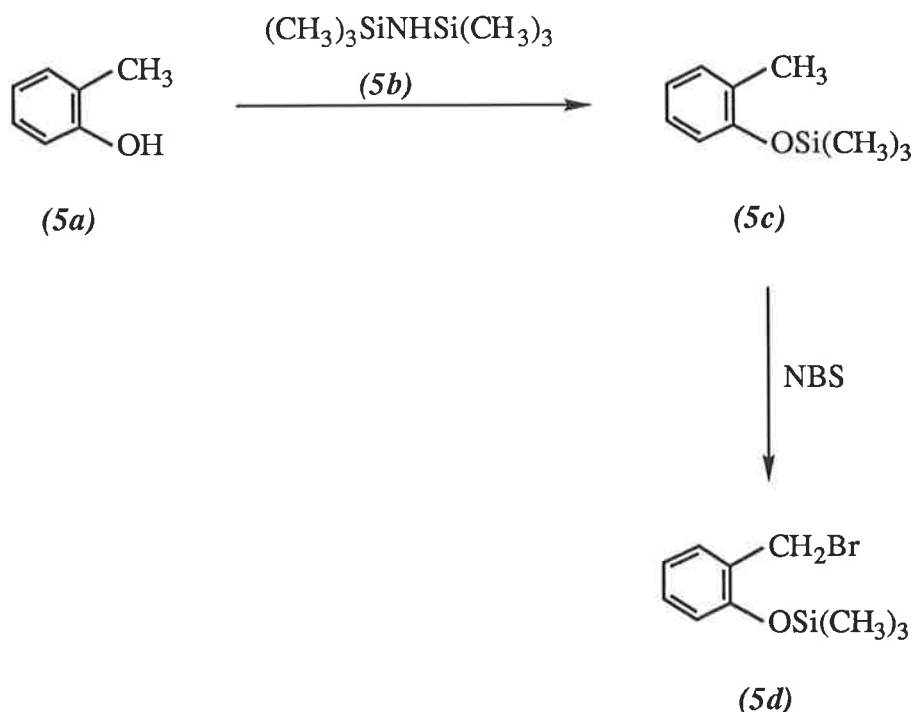
Reaction Scheme 4.5

The intermediate product *(5c)* was successfully formed by heating hexamethyldisilazane *(5b)* with two mole equivalent of *o*-cresol *(5a)*. Several bromination attempts with N-bromosuccinimide were carried out, giving a product which contained 90% unreacted starting material *(5c)*. Hence, this synthetic route was not pursued any further.

4.2.6 Investigation of Complex Formation

As many of the preparations in Section 4.2.2 showed that some of the ether (free or protected) could be present in the products, it was decided to investigate complex formation of one of the products from these reactions. Assuming that the product from reaction *B* contained some of the desired 2,2'-dihydroxybenzyl-phenyl ether in the product, we decided to attempt complex formation with titanium(IV). Titanium tetrabutoxide was reacted with a portion of the oil from reaction *B* and four mole equivalent of base (lithium acetate) in ethanol, under refluxing conditions. The infrared spectrum of the precipitate obtained from this reaction contained only a few absorptions which were mostly broad and some of which were in the v(O-H) region (3700 - 3000 cm^{-1}). If complex formation had occurred, then no absorptions were expected in the v(O-H) region since the ligand would be deprotonated. Mass spectroscopy also did not support the sought after complex, TiL$_2$, where L = the dianion of 2,2'-dihydroxybenzylphenyl ether. The m/e values 371 (EI mass spectrum) and 258 (FAB mass spectrum) were lower than the desired value of 476.

4.3 2-Hydroxyphenyl Salicylate

4.3.1 Introduction

The ester of the basic structure that would conform with the criteria in Figure 4.2, where -XY- = -CO_2-, was 2-hydroxyphenyl salicylate. Various methods exist for the preparation of esters. A common pathway is from carboxylic acids and alcohols. The esterification process is an acid catalysed reaction. Sulphuric and hydrochloric acids are common choices as catalysts because they also possess water-binding properties, however phosphoric and arenesulphonic acids have also been used. Because of its acidity, a carboxylic acid must be able to catalyse its own esterification, such that an ester can be produced merely by heating together the carboxylic acid and the alcohol.[202b]

4.3.2 Strategy

The obvious first route to take in the synthesis of 2-hydroxyphenyl salicylate was that shown below in Reaction Scheme 4.6.

Simply mixing solutions of salicylic acid *(6a)* with excess catechol *(6b)* in chloroform for several hours saw no reaction take place. Only starting materials were detected by thin layer chromatography. The addition of concentrated sulphuric acid and refluxing of the mixture yielded the same result. The infrared spectrum of the product obtained was identical to that of a mixture of the acid and alcohol starting materials.
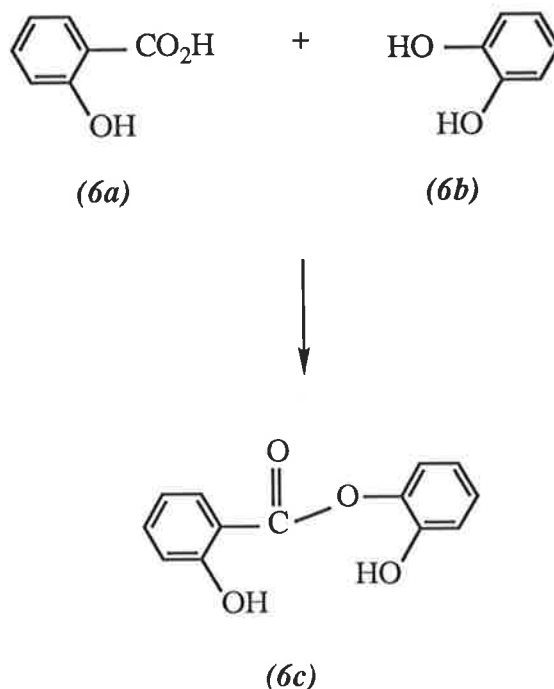
Reaction Scheme 4.6

The lack of success of the procedure just mentioned was put down to the structures of the salicylic acid and the alcohol which determine the rate of esterification. Firstly, it is known that primary alcohols are esterified faster than secondary or tertiary alcohols. Secondly, in the aromatic series, the rate of esterification can be reduced by steric effects. For example, *ortho*-substituted carboxylic acids are known to react with difficulty.[202b] Kanaoka *et al.* reported that aryl esters were not attained by the common process of esterification of carboxylic acids.[216] In other studies, Kanaoka *et al.* reported that phenols were usually not acylated with carboxylic acids in the presence of an acidic catalyst, because of the rather low nucleophilicity of the phenols.[217]

Another problem with the procedure shown in Reaction Scheme 4.6, for the preparation of the ester directly from the acid, is that the reaction is reversible and generally reaches equilibrium when there are significant quantities of both reactants and products present. However, preparation of esters from acid

chlorides are essentially reactions which are irreversible and therefore go to completion. Consequently, many aryl esters are prepared by reacting activated derivatives of carboxylic acids, such as acid halides, with alcohols.[216] The preparation of 2-hydroxyphenyl salicylate (Reaction Scheme 4.7, *(7d)*) would therefore require 2-hydroxybenzoyl chloride as starting material. We know, from the syntheses of the amide ligands (Chapter 3), that this acid chloride of salicylic acid could not be prepared without first protecting the hydroxyl group. As described in Chapter 3, the starting material used in those syntheses was 2-acetyloxybenzoyl chloride *(7a)* (i.e. an acetyl protecting group). However, the use of this as a starting material for the preparation of 2-hydroxyphenyl salicylate *(7d)*, following pathway 1 in Reaction Scheme 4.7, would not be suitable because on removal of the acetyl protecting group, cleavage could occur in the wrong position, as shown by pathway 2, yielding products *(7e)* and *(7f)*.
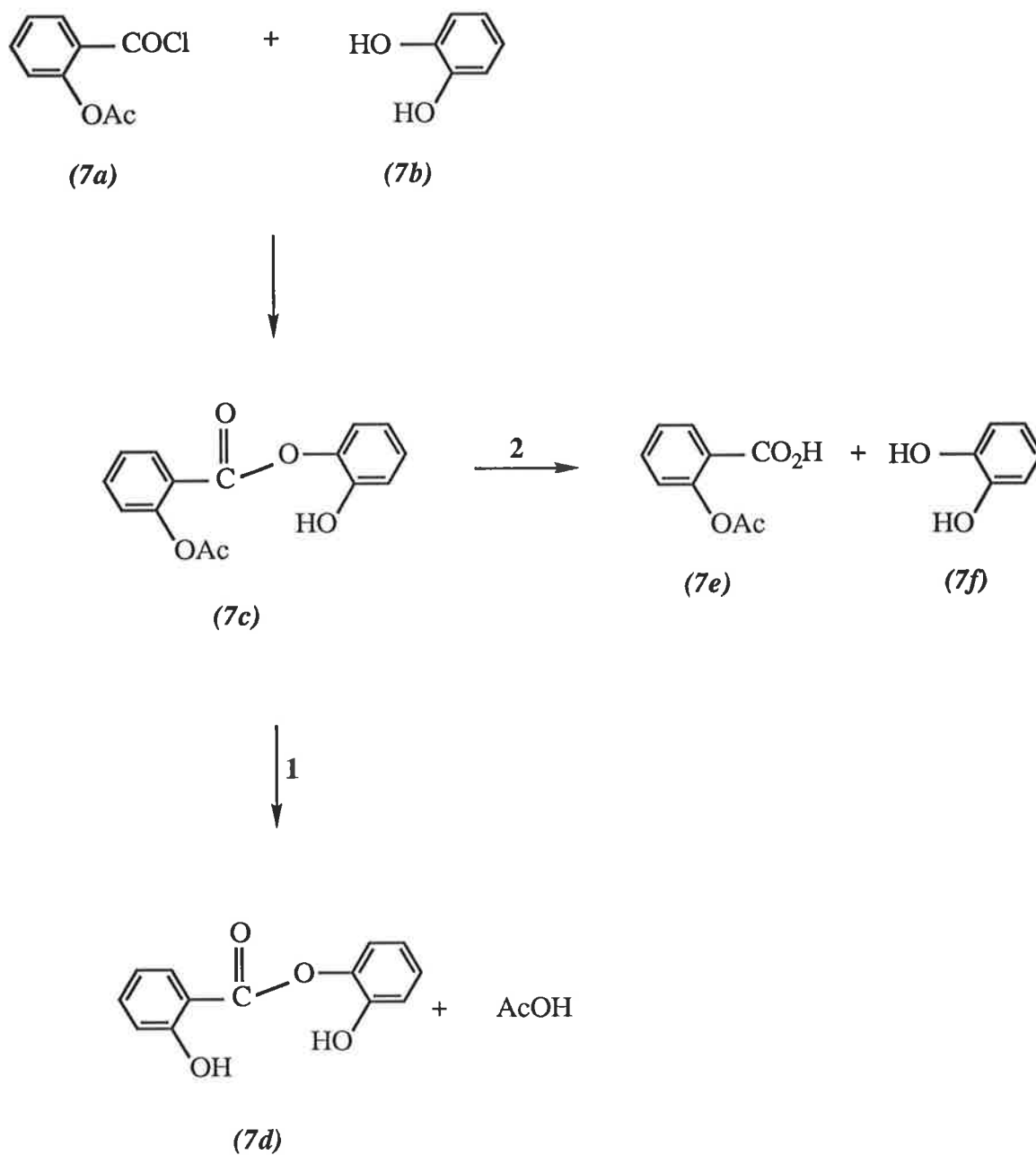
Reaction Scheme 4.7

4.3.3 Attempted Reactions

Alternative synthetic routes to acid catalysed esterification were sought for the preparation of 2-hydroxyphenyl salicylate. A thorough study by Kanaoka *et al.*, on the functions of polyphosphate ester (PPE), showed it to be an efficient agent for various condensation reactions.[217] It was demonstrated that aryl esters could be prepared from carboxylic acids and phenols under mild conditions using PPE as a condensing agent. Upon mixing excess PPE with equimolar amounts of benzoic acid and phenol in chloroform, then either refluxing the mixture for 30 minutes or allowing it to stand at room temperature for 24 hours, yielded phenyl benzoate in 83 or 90% yield, respectively.[216] Under the refluxing conditions just mentioned, these workers obtained phenyl salicylate in 63% yield from salicylic acid and phenol.

Following the procedure described by Kanaoka *et al.*,[217] using PPE as a condensing agent for the reaction between salicylic acid and catechol in chloroform, proved unsuccessful in the synthesis of 2-hydroxyphenyl salicylate. Although a product was observed by thin layer chromatography, the formula weight peak for 2-hydroxyphenyl salicylate, which was observed in the mass spectrum (231; Molecular ion + H), was very weak with more intense peaks appearing at higher m/e values.

Whilst carrying out a literature search on the desired ester, a citation by Patolia and Trivedi on the synthesis of xanthone derivatives was found.[218] These workers discovered that when ethyl salicylate was refluxed with various phenol derivatives in diphenyl ether, the corresponding phenyl salicylate derivatives were obtained. This system did not require the use of a condensing agent. In one case, they found that heating catechol with ethyl salicylate in diphenyl ether for 12 hours gave 2-hydroxyphenyl salicylate (m.p. 80 - 81°C), while prolonged refluxing (19 - 21 hours) gave 4-hydroxy-xanthone in low yield. However, no mention was made on the pressure conditions used to bring diphenyl ether to its boiling point (259°C; 1 atm). Attempts to prepare the ester from the brief experimental outline described by these workers proved most frustrating. Refluxing diphenyl ether was achieved under vacuum (oil bath) as well as at atmospheric pressure (heating mantle). Yet, in both cases, catechol starting material precipitated out of solution upon cooling. The reaction in which the ether was refluxed under atmospheric conditions was repeated several times. However, the result was the same, with the recovery of catechol ranging from 20 to 73%. In all cases, the filtrate was

brown-black in colour. The infrared spectrum recorded of the neat filtrate revealed the presence of predominantly ethyl salicylate and obviously diphenyl ether. Although, a second carbonyl stretching absorption (1715 cm^{-1}) of medium intensity was observed at a higher frequency than that for ethyl salicylate (1677 cm^{-1}), which was possibly due to the desired ester. Removal of almost all the diphenyl ether by distillation under vacuum, and cooling of the remaining residue still did not yield any expected solid.

4.4 2,2'-Dihydroxystilbene

4.4.1 Introduction

Although the alkene functional group is found as a ligand mainly in organometallic compounds and other low oxidation metals it was thought that the stabilising effect of two chelate rings on both sides of alkene functional group may act as a suitable ligand for the formation of complexes analogous to those of Schiff base ligands. The alkene compound of interest was 2,2'-dihydroxystilbene, or 1,2-bis(2-hydroxyphenyl)ethene. A literature search on this compound revealed that the well known use of metals in reductive coupling reactions for carbon-carbon bond formation could be employed in its synthesis. Whilst studying the syntheses and structures of stilbene cycles, Tirador-Rives *et al.* isolated 2,2'-dihydroxystilbene (Reaction Scheme 4.8, *(8e)*) in 74% yield.[219] More precisely, they isolated 2,2'-dihydroxystilbene while attempting the ring closure of the aromatic bis(carbonyl) ether *(8c)*.
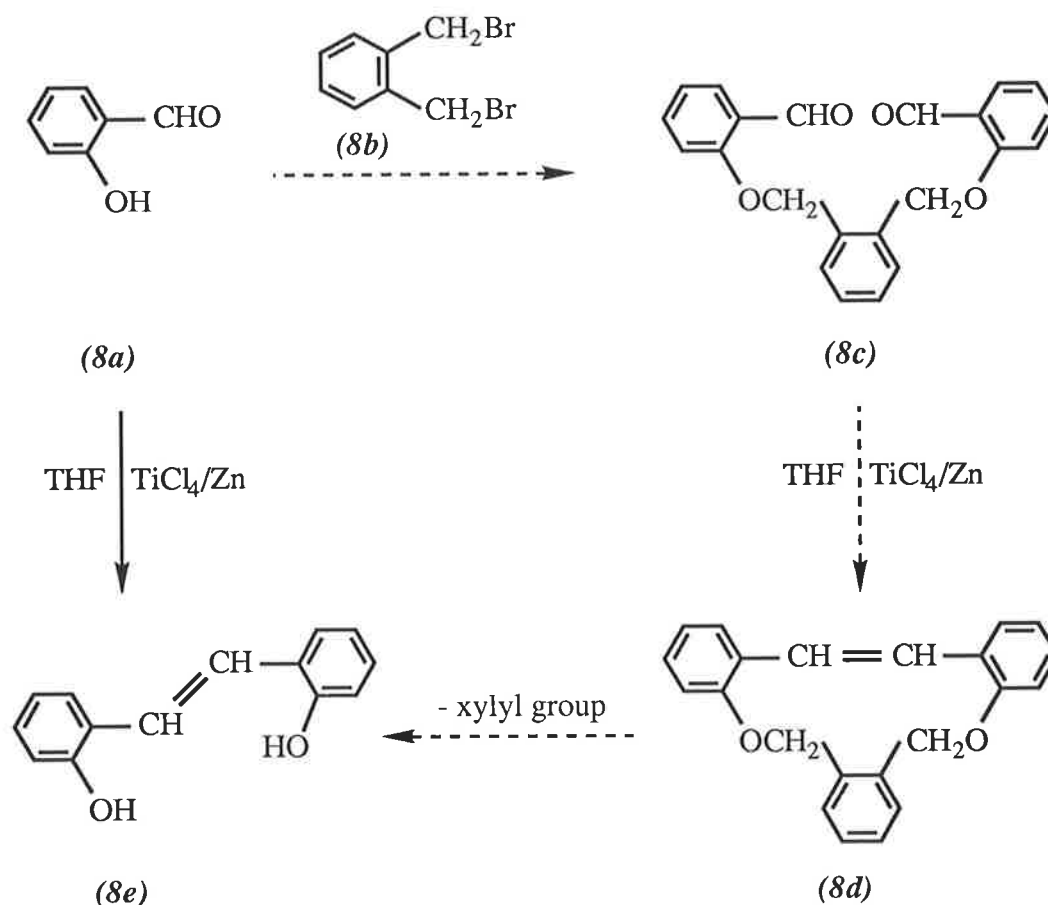
Reaction Scheme 4.8

The synthetic route carried out by these workers is indicated by the broken arrows in Reaction Scheme 4.8. Salicylaldehyde *(8a)* was reacted with the electrophile α,α'-dibromo-*o*-xylene *(8b)*. After the reductive coupling reaction with $TiCl_4/Zn$, and subsequent cyclisation steps, the xylyl moiety was lost giving the *trans* dihydroxyalkene *(8e)*. As our interest was in the formation of the alkene and not the cyclised compound *(8d)*, we decided to treat salicylaldehyde directly with $TiCl_4/Zn$ in tetrahydrofuran, followed by the extraction using the same experimental procedure as Tirador-Rives *et al.*[219] The desired material was isolated, but in a lower yield (9%) than that obtained by the above mentioned workers. However, this was sufficient quantity to perform some exploratory complex formation experiments

4.4.2　Investigation of Complex Formation

Preliminary work was carried out with 2,2'-dihydroxystilbene to test its ability to stabilise high oxidation states in transition metals. Complexation attempts were only made with titanium(IV). The titanium starting material, titanium tetrabutoxide or titanium tetrachloride, was reacted with approximately two moles equivalent of 2,2'-dihydroxystilbene and four mole equivalent of base. The products from the reactions were analysed by infrared and mass spectroscopy.

Both of the titanium starting materials produced no reaction with the alkene in ethanol using lithium acetate as the base. In tetrahydrofuran, using sodium ethoxide as the base, the reaction between the titanium tetrachloride and the alkene produced a product whose infrared spectrum showed some evidence of complexation. A strong absorption at 1593 cm^{-1} with a shoulder of medium intensity at 1610 cm^{-1} was exhibited by this product. This was unlike the alkene itself which absorbs strongly at both 1610 and 1593 cm^{-1} due to the -C=C- and aromatic ring, respectively. Also, the strong absorption at 3340 cm^{-1}, characteristic for the protonated alkene, appeared very weak in the spectrum of the product. The rest of the spectrum, however, contained relatively few peaks dissimilar to those of 2,2'-dihydroxystilbene. The mass spectrum of the product exhibited a molecular ion peak at m/e 504 which was higher than that expected for the desired $Ti(OC_6H_4CH=CHC_6H_4O)_2$ compound (m/e 468). A possibility here is the formation of TiL(LH)Cl, where L = the dianion of 2,2'-dihydroxystilbene, $OC_6H_4CH=CHC_6H_4O$.

Chapter 5

ELECTROCHEMISTRY

5.1 Introduction

The stability of the high oxidation states achieved by the metals can be explored electrochemically. Electron transfer (oxidation-reduction) reactions between stable metal oxidation states can occur and such processes can be reversible, quasi-reversible or irreversible. The electrochemistry of several group (IV) and group (V) metal complexes of Schiff base and azo dye ligands and amide complexes of manganese and titanium were studied to determine their electron transfer characteristics.

Cyclic voltammograms of ML_2 complexes of Schiff base and azo dye ligands revealed two quasi-reversible steps attributed to M(IV)/M(III) and M(III)/M(II). The organometal(IV) and organoantimony(V) complexes of Schiff base and azo dye ligands revealed a large wave assigned to the M(IV)/M(III) and M(V)/M(IV) couples, respectively. Results for the amide complexes of manganese were consistent with those reported in the literature for similar complexes.[96] Three waves due to the couples Mn(VI)/Mn(V), Mn(V)/Mn(IV) and Mn(IV)/Mn(III) were exhibited by these complexes. Analogous titanium complexes showed a wave due to the Ti(IV)/Ti(III) redox couple at a more negative potential.

5.2 Application of Electrochemical Techniques

Electrochemistry experiments can provide useful information about redox reactions. The energy which is needed to add an electron to, or subtract an electron from, an electrode surface can be represented in terms of the potential of the electron transfer. In voltammetry, a three-electrode system is employed where a potential is applied between the reference and working electrodes, and the current flow between the working and counter electrodes is measured. A supporting electrolyte is present to repress the migration of the charged reactants and products. The current flowing at an electrode is measured as a function of the potential applied to the electrode. Application of different voltage waveforms to the electrode produces different voltammograms (current-potential curves), each of which has its usefulness.[220]

Cyclic voltammetry is an easy and direct method used to characterise a redox system.[221,222] In this technique, the potential of the working electrode is changed linearly with time between two potential limits. More than one electrode reaction may take place as many electrochemical processes produce an intermediate which then undergoes further chemical reaction. These processes can also be studied. The peak resulting from the reduction of a species is called the cathodic peak and that resulting from the oxidation of a species is called the anodic peak. These two peaks are characterised by several parameters: the cathodic (E_{pc}) and anodic (E_{pa}) peak potentials and the cathodic (i_{pc}) and anodic (i_{pa}) peak currents. One of the various tests for checking the reversibility of a redox process is the ratio of peak currents, i_{pa}/i_{pc}. If the ratio is equal to 1·00 then the process can be said to be reversible. When both the oxidised and reduced species are stable and rapidly exchange electrons with the working electrode in the time scale of the experiment the process is said to be reversible and cyclic voltammetry can then be used to calculate the reduction or half-wave potential of the half reaction using Equation 5.1.[221,222] The reduction potential ($E_{1/2}$) is exactly midway between E_{pa} and E_{pc}.

$$E_{1/2} = \frac{E_{pa} + E_{pc}}{2} \hspace{3cm} (5.1)$$

The number of electrons (n) transferred during a reversible electrode reaction can be determined from the difference between the cathodic and anodic peak potentials as shown by Equation 5.2.[222]

$$\Delta E_p = E_{pa} - E_{pc} = \frac{0.058}{n} \qquad (5.2)$$

Often however, electrode reactions are irreversible and the number of electrons transferred cannot be determined from Equation 5.2. Bulk electrolysis, also known as controlled potential electrolysis, can be employed to determine n in this case. In this technique, a fixed potential is applied to a working electrode of large surface area to minimise electrolysis time. The number of electrons transferred is then calculated from the charge transferred and the number of moles of sample under investigation.

Electrochemical pulse techniques such as differential pulse voltammetry (DPV), normal pulse voltammetry (NPV) and Osteryoung square wave voltammetry (OSWV) are commonly used for quantitative analysis.[222] Depending on the technique, detection limits in the range 10^{-6} - 10^{-9} mol dm^{-3} are possible for many heavy metals and organic compounds. In DPV, the potential waveform is made up of small amplitude pulses which are superimposed on a staircase waveform.[222,223] The current is measured before and after each pulse and the output observed is the current difference *versus* the base potential. In NPV, the waveform consists of increasing potential pulses. The output produced is the current sampled at the end of each pulse *versus* the base potential. Faradaic current, which is a direct measure of the rate of the electrochemical reaction taking place, flows when the potential at the electrode is close to the reduction potential ($E_{1/2}$) of the reaction. Thus, this method is useful for measuring the reduction potential, $E_{1/2}$, of a reaction. Sampled direct current polarography is another technique which can be used to obtain this information.[222] OSWV produces a similar output to that obtained from DPV. The potential waveform consists of a pulse train of square waves superimposed on a staircase waveform.[222-224] The potential is initially set at a value, say E_0, and then stepped directly (pulsed) to a second value, say E_1. Current samples are taken before and after each pulse. The time of sampling is such that any background current arising, because the electrode

is a capacitor,[223] is minimised and the current detected is due mostly to the electrochemical reaction taking place. The output is the current difference *versus* the base potential. The peak potential is related to the half-wave potential as shown by Equation 5.3. Since OSWV and DPV measure current differences, any background current which is unrelated to the reaction of the material under investigation, makes a negligible contribution to the current measured.[223] Thus, these techniques are more sensitive than cyclic voltammetry which measures the total current.

$$E_p = E_{1/2} - \frac{\text{pulse amplitude}}{2} \tag{5.3}$$

The electrochemical techniques mentioned above are useful in correlating the effect of the ligand on the reduction potential of a metal. Salam observed that for different VL_2 complexes with Schiff bases of varying amino and constant ketonic groups, $-E_{1/2}$ for the V(IV)/V(III) couple was observed in the order: K-Salh < K-Bh < K-Ap, where K = the ketonic part of the Schiff base.[92] Thus, the K-Ap ligands were found to be more electron-releasing. For the p^X-substituted ligand p^X-Ap-β-Nap, $-E_{1/2}$ for the V(IV)/V(III) couple in VL_2 complexes was observed in the order: X = Cl < X = H < X = Me.[92]

5.3 Previous Related Work

5.3.1 Schiff Base and Azo Dye Complexes

Electrochemical studies on VL_2 type non-oxo vanadium(IV) complexes with the same Schiff base and azo dye ligands used in this research have been carried out by Salam.[92] Cyclic voltammograms obtained in dimethylsulphoxide with tetraethylammonium tetrafluoroborate (Et_4NBF_4) as the supporting electrolyte on a platinum working electrode showed V(IV)/V(III) and V(III)/V(II) redox couples in the regions -0·05 to -0·40 volts and -1·50 to -1·80 volts, respectively, *versus* a saturated calomel electrode (SCE). In some cases, the V(III)/V(II) couple was not observed as it occurred at a potential more negative than the cathodic reduction limit of the medium. The one-electron transfer of the V(IV)/V(III) couple was confirmed by bulk electrolysis.

Similar neutral bis(tridentate) titanium(IV) complexes (TiL_2), also prepared by Salam, were studied in the same medium as the VL_2 complexes mentioned above.[92] The Ti(IV)/Ti(III) redox couple was observed in the region -0·47 to -0·98 volts and the Ti(III)/Ti(II) couple in the region -1·63 to -1·79 volts, *versus* a SCE. The TiL_2 complexes were found to be more difficult to reduce than the corresponding VL_2 complexes, as expected from their positions in the first row transition series (the energy of the $3d$ orbital which is accepting the electron decreases along the first transition series).

GeL_2 and SnL_2 complexes with Schiff base ligands have been studied electrochemically on a platinum working electrode in dimethylsulphoxide using tetrabutylammonium tetrafluoroborate (Bu_4NBF_4) as the supporting electrolyte.[97] Each showed two redox couples attributed to M(IV)/M(III) and M(III)/M(II). The M(IV)/M(III) redox couples appeared in the regions -1·46 to -1·76 volts and -1·41 to -1·70 volts for the germanium and tin complexes, respectively, and the corresponding M(III)/M(II) couples appeared in the regions -1·83 to -2·17 volts and -1·83 to -1·98 volts. These potentials were relative to a Ag/Ag^+ (dimethylsulphoxide) reference electrode. The reduction potentials for the GeL_2 complexes were more negative than the reduction potentials for the analogous SnL_2 complexes.

5.3.2 Amide Complexes

Koikawa *et al.* have carried out electrochemical measurements on manganese complexes of amide ligands in dichloromethane using 1,4,7,10,13,16-hexa-cyclooctadecane (18-crown-6) to dissolve the amide complexes.[96] Cyclic voltammetry and differential pulse voltammetry were used to determine the redox potentials. Three redox couples were observed and considered irreversible based on the separation between the cathodic and anodic peaks. They were assigned to Mn(VI)/Mn(V), Mn(V)/Mn(IV) and Mn(IV)/Mn(III) as shown below.

$$[Mn^{VI}L_2]^0 \underset{-e^-}{\overset{+e^-}{\rightleftharpoons}} [Mn^{V}L_2]^- \underset{-e^-}{\overset{+e^-}{\rightleftharpoons}} [Mn^{IV}L_2]^{2-} \underset{-e^-}{\overset{+e^-}{\rightleftharpoons}} [Mn^{III}L_2]^{3-} \qquad (5.4)$$

Redox potentials for the Mn(VI)/Mn(V), Mn(V)/Mn(IV) and Mn(IV)/Mn(III) couples were observed in the regions 1·09 to 0·59 volts, 0·75 to 0·09 volts and -0·65 to -0·89 volts *versus* a SCE, respectively, and were dependent on the substituents on the ligands. Substituents on the 2-hydroxyphenyl moiety of the amide ligands exercised an electronic effect on the metal complexes by modifying the electron-releasing/withdrawing behaviour of the ligand donor atoms. The higher oxidation states of manganese were stabilised when an electron-releasing substituent was present. The same observation was made by Okawa *et al.* from their electrochemical study of manganese(IV) complexes prepared by the oxidation of binuclear manganese(II) complexes of salicylideneamino-*o*-hydroxybenzene derivatives.[14] Two redox couples were observed and assigned to the processes shown below.

$$Mn(IV) \underset{-e^-}{\overset{+e^-}{\rightleftharpoons}} Mn(III) \underset{-e^-}{\overset{+e^-}{\rightleftharpoons}} Mn(II) \qquad (5.5)$$
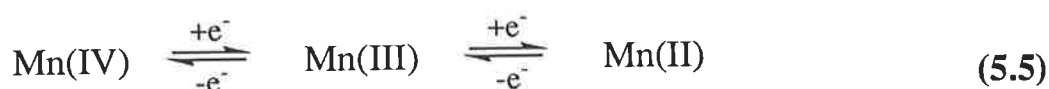
The first process appeared in the range 0·21 to -0·10 volts and the second in the range -0·49 to - 0·79 volts *versus* a hygrogen electrode. These results showed that the oxidation state Mn(IV) was more stable with the trinegative

tridentate amide ligands than the dinegative tridentate Schiff base ligands since the reduction potential of the Mn(IV)/Mn(III) redox couple in the amide complexes was more negative than that of the Schiff base complexes.

Koikawa *et al.* have also extended their studies with the complexation of the amide ligands to cobalt, forming Co(III) products of the general formula $K_3[CoL_2]$.[190] Two redox potentials were observed between 0·6 and -0·4 volts *versus* a SCE, and were assigned to Co(V)/Co(IV) and Co(IV)/Co(III) after confirmation by bulk electrolysis measurements. These cobalt (III) complexes were easily oxidised to cobalt(IV) by chemical or electrochemical means.

5.4 Electrochemical Experiments

Complexes of Schiff base and azo dye ligands were studied in dimethyl-sulphoxide using 0.10 mol dm^{-3} tetraethylammonium perchlorate (Et_4NClO_4) as the supporting electrolyte. Complexes of amide ligands were studied in dichloromethane solution using 0.05 mol dm^{-3} Et_4NClO_4 as the supporting electrolyte since it was less soluble in this solvent. This electrolyte was chosen for its electrochemical inertness over a wide potential range. The amide complexes were solubilised with the crown ether 1,4,7,10,13-pentaoxa-cyclopentadecane (15-crown-5).

The electrochemical properties of the compounds prepared were examined by cyclic voltammetry and Osteryoung square wave voltammetry at room temperature on a glassy-carbon working electrode and using an aqueous saturated calomel electrode (SCE) as the reference electrode. For comparison purposes, electrochemical analysis of some samples was also carried out on a platinum working electrode using a Ag/Ag^+ (dimethylsulphoxide) reference electrode and tetrabutylammonium tetrafluoroborate as the supporting electrolyte. In all the electrochemical experiments carried out, except for those on the amide complexes, a small amount of ferrocene was added to the solutions to check for any potential drift by the reference electrode. The oxidation/reduction of ferrocene is a model system of an essentially reversible process which has been recommended as a standard for use in electroanalytical voltammetry.[225] The $E_{1/2}$ of the ferrocene couple could also be used as a reference for the potential of the SCE in this medium which, because of the junction between the different solvents used in the electrode and the medium containing the complex, would have a large contribution from the junction potential.

Normal pulse voltammetry was performed on a solution containing known concentrations of $V(BzacBh)_2$ and $Sn(Ap-\beta-Nap)_2$ and on a solution containing known concentrations of $V(BzacBh)_2$ and $Ph_2Ge(BzacSalh)$ on a glassy-carbon working electrode. These experiments were carried out in an attempt to determine the number of electrons transferred in the reductive steps of the ML_2 and organometal complexes prepared in this study. As mentioned earlier, in this electrochemical technique no faradaic current flows until the potential at the electrode is close to the reduction potential for the process occurring. The current is proportional to the concentration of the species in solution and the number of electrons transferred using the same electrode.[223]

Therefore, for a solution containing more than one electrochemically active species at equal concentration, the ratio of the currents produced in the different processes is therefore proportional to the number of electrons transferred in each process. If the number of electrons transferred for one process is known then the number of electrons transferred in other processes can be determined.

5.5 Results

5.5.1 Bis(Dinegative Tridentate) Complexes

All GeL_2 and SnL_2 complexes produced two quasi-reversible waves when studied by cyclic voltammetry. To determine the number of electrons transferred in each wave, normal pulse voltammetry was performed on a solution containing 1.04×10^{-3} mol dm^{-3} Sn(Ap-β-Nap)$_2$ and 1.06×10^{-3} mol dm^{-3} V(BzacBh)$_2$. Scanning towards negative potential, two reduction steps were observed for the Sn(Ap-β-Nap)$_2$ complex, at -0.54 volts and -0.84 volts *versus* a SCE, corresponding to the two waves observed in its cyclic voltammogram. The V(BzacBh)$_2$ complex showed one reduction process in the electrochemical window available in these experiments which was due to the V(IV)/V(III) couple, that is, a one electron transfer took place.[92] The reduction potential for the V(IV)/V(III) couple was observed at -0.30 volts *versus* a SCE and this compared well with that determined by Salam (-0.35 volts *versus* a SCE) in cyclic voltammetry experiments.[92] The ratio of the currents produced by this couple and the two processes observed in the SnL$_2$ complex was approximately 1:1:1. Thus, the two waves observed in the cyclic voltammogram of Sn(Ap-β-Nap)$_2$ were both one electron processes. This result was assumed to occur also with the Ge(Ap-β-Nap)$_2$, Ge(Ap-p^{Cl}-Phenol)$_2$ and Sn(SalHba)$_2$ complexes. Scanning towards the negative potential, the first wave in the cyclic voltammogram for these ML$_2$ complexes was assigned to the M(IV)/M(III) couple and the second wave to the M(III)/M(II) couple. The cyclic voltammograms together with the corresponding Osteryoung square wave voltammograms showing the half-wave potentials for the processes in some of these complexes are shown in Figures 5.1 and 5.2. Anodic and cathodic reduction potentials for these complexes and data for complexes with similar ligands complexed to other metals are summarised in Table 5.1.

Reduction potentials for the ML$_2$ complexes of azo dye ligands were more positive than those found for the ML$_2$ complexes of Schiff base ligands with these metals.[97] Reduction potentials for the M(IV)/M(III) and M(III)/M(II) couples in the azo dye complexes appeared in the ranges -0.33 to -0.52 volts and -0.74 to -0.88 volts, respectively, *versus* a SCE. The Schiff base complex Sn(SalHba)$_2$ showed these couples at -1.58 volts and -1.91 volts, respectively, *versus* a SCE. A similar observation was made by Salam upon comparing the reduction potentials of Schiff base and azo dye ML$_2$ complexes,[92] and

suggested that the azo dye ligands were more electron-withdrawing and the lowest unoccupied molecular orbital in the complexes, into which the electron is being placed upon reduction of the complex, was at lower energy.
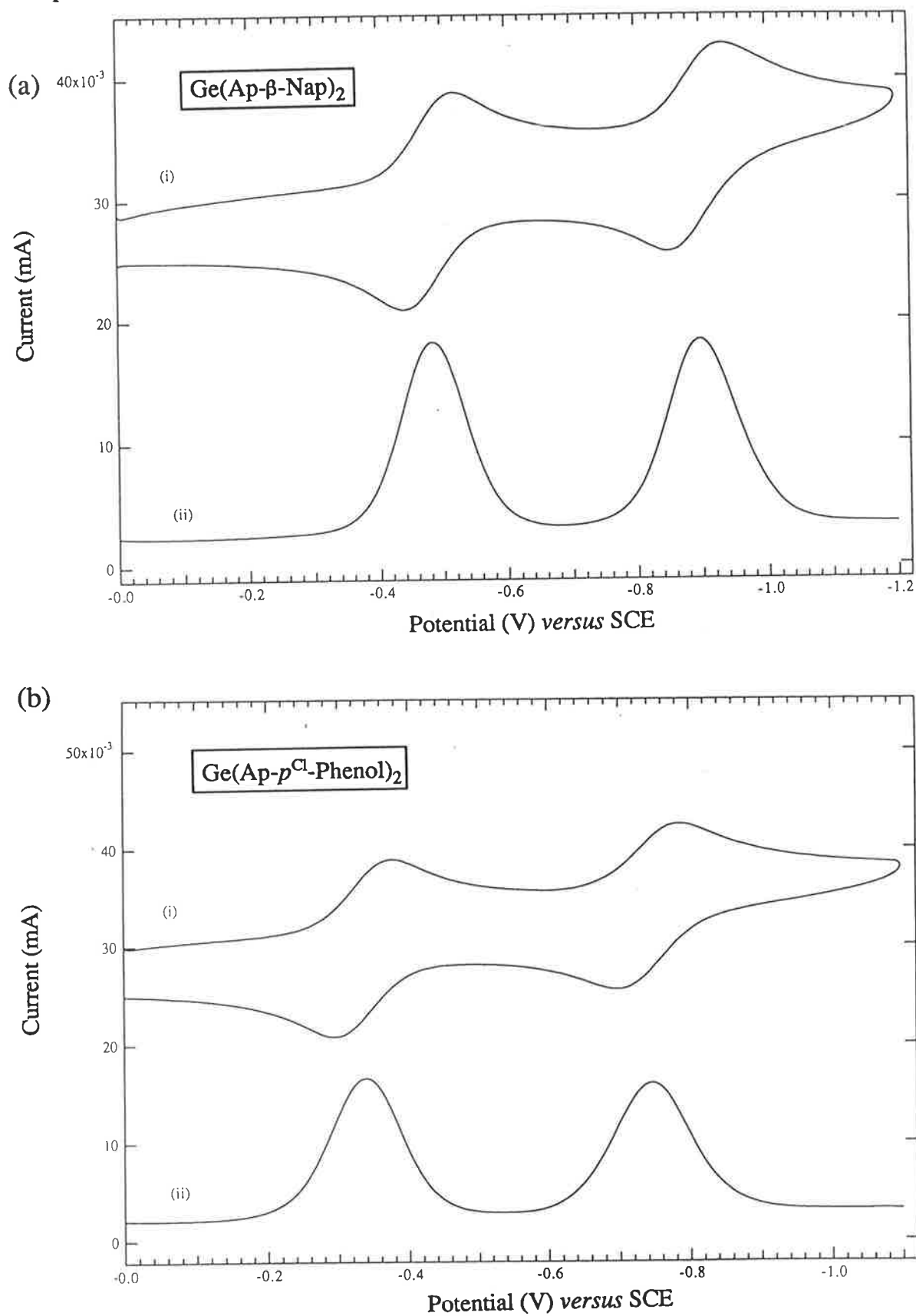
Figure 5.1: *Electrochemistry of (a) Ge(Ap-β-Nap)₂ and (b) Ge(Ap-p^Cl-Phenol)₂ in DMSO/0·10 mol dm⁻³ Et₄NClO₄/GC. (i) Cyclic voltammograms at scan rate 100 mV s⁻¹, and (ii) Osteryoung square wave voltammograms at scan rate 60 mV s⁻¹.*
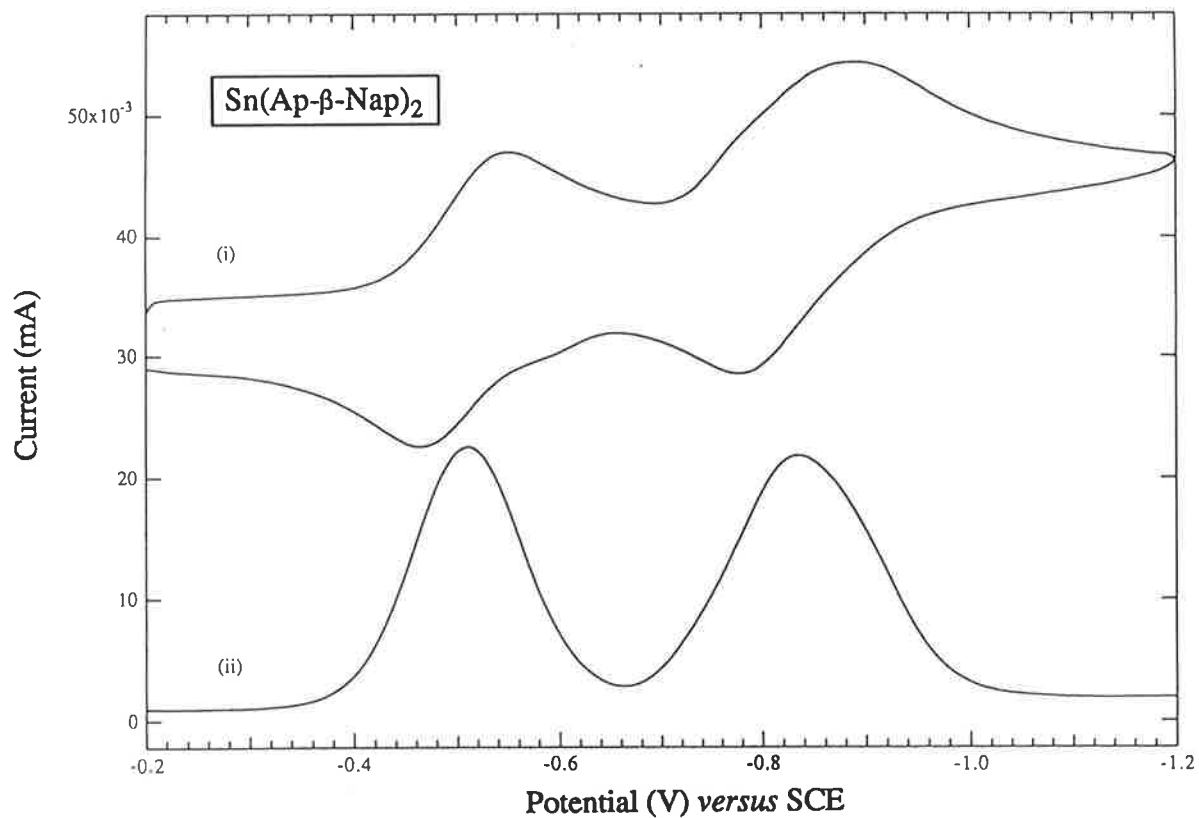
Figure 5.2: *Electrochemistry of Sn(Ap-β-Nap)$_2$ in DMSO/0·10 mol dm^{-3} Et$_4$NClO$_4$/GC. (i) Cyclic voltammogram at scan rate 100 mV s^{-1}, and (ii) Osteryoung square wave voltammogram at scan rate 60 mV s^{-1}.*

Table 5.1: Electrochemical Data for the ML_2 Complexes on a Glassy-Carbon Working Electrode in Dimethylsulphoxide using $0 \cdot 10$ mol dm^{-3} Et$_4$NClO$_4$ as the Supporting Electrolyte.

Complex	E_{pa}[†]	E_{pc}[†]	$E_{1/2}$[‡]	ΔE_p	i_{pa}/i_{pc}
			(Volts)		
Ge(Ap-β-Nap)$_2$	-0·46	-0·54	-0·51	0·08	1·07
	-0·87	-0·96	-0·88	0·09	0·86
Sn(Ap-β-Nap)$_2$	-0·47	-0·56	-0·52	0·09	0·84
	-0·79	-0·90	-0·85	0·11	0·96
V(Ap-β-Nap)$_2$[*]	+0·06	0·00	+0·03	0·06	1·17
Ge(Ap-p^{Cl}-Phenol)$_2$	-0·28	-0·36	-0·33	0·08	1·06
	-0·68	-0·78	-0·74	0·10	0·92
Sn(SalAp)$_2$[#]	--	-1·24	-1·20		--
	-1·60	-1·76	-1·64		0·85
Sn(SalHba)$_2$	--	-1·65	-1·58		--
	--	-1·95	-1·91		--

All potentials measured *versus* a SCE.

[†] Data from cyclic voltammetry using a scan rate of 100 mV s^{-1}.

[‡] Data from Osteryoung square wave voltammetry using a scan rate of 60 mV s^{-1}.

[*] Reference 92.

[#] Reference 97- corrected for SCE as the reference.

In the electrochemical system used ferrocene has E_{pa} = +0·53 volts, E_{pc} = +0·36 volts and $E_{1/2}$ = +0·41 volts.

From OSWV measurements, reduction potentials for the Sn(IV)/Sn(III) and Sn(III)/Sn(II) couples in Sn(SalHba)$_2$ were more negative than those observed for Sn(SalAp)$_2$. Sn(SalHba)$_2$ was therefore found to be more stable, or harder to reduce, than Sn(SalAp)$_2$. This was expected as the introduction of a methylene group between the aromatic ring and the azomethine nitrogen atom would make the ligand more electron donating due to the positive inductive effects of the methylene group. Also, SalHba is a less conjugated system than SalAp and the donation of electrons from the nitrogen atom of SalHba to the metal would be greater than that from the nitrogen atom of SalAp to the metal.

Manganese(IV) complexes with other Schiff bases and azo dyes are currently being studied by electrochemical methods in this laboratory.[94]

5.5.2 Organometal(Dinegative Tridentate) Complexes

Electrochemistry was performed only on the methyl and/or phenyl derivatives of germanium, tin, lead and antimony. The cyclic voltammograms obtained for the R_2ML (R = Me and/or Ph and M = Ge, Sn and Pb) and the triphenylantimony(V) complexes of Schiff base ligands were dominated by one large wave (Table 5.2). For most complexes, this wave was irreversible as shown in Figures 5.3 - 5.5 for the complexes $Ph_2Ge(SalAp)$, $Ph_2Ge(SalBh)$, $Me_2Sn(SalBh)$, $Ph_2Sn(SalBh)$, $Ph_2Pb(BzacBh)$ and $Ph_3Sb(SalBh)$, however in a few cases it did appear quasi-reversible as shown in Figures 5.6 - 5.8 for the complexes $Ph_2Ge(BzacBh)$, $Ph_2Ge(BzacSalh)$, $Me_2Sn(BzacBh)$, $Me_2Sn(BzacSalh)$, $Ph_2Sn(BzacSalh)$ and $Ph_3Sb(BzacBh)$. In most cyclic voltammograms, one or two less prominent peaks were observed at a more positive potential relative to the dominant wave. These extraneous peaks appeared anodic (e.g. Figures 5.3 and 5.4) or cathodic (e.g. Figures 5.7 and 5.8a). Some complexes produced a cathodic peak in their cyclic voltammogram, at a more negative potential relative to the large wave. Usually this was very near the cathodic limit of the medium and was therefore not tabulated as breakdown of the medium could be producing this peak.

To determine the number of electrons transferred in the dominant wave observed in the cyclic voltammograms, normal pulse voltammetry on a glassy-carbon working electrode was performed on a solution containing 1.77×10^{-3} mol dm^{-3} $Ph_2Ge(BzacSalh)$ and 1.75×10^{-3} mol dm^{-3} $V(BzacBh)_2$. This organogermanium(IV) complex was chosen because it produced no extraneous peaks which could contribute to the faradaic current due to the redox reaction in $V(BzacBh)_2$. One reduction step was observed for the $Ph_2Ge(BzacSalh)$ complex at -0.94 volts *versus* a SCE, corresponding to the large reversible wave observed in its cyclic voltammogram. The reduction potential for the V(IV)/V(III) couple in $V(BzacBh)_2$ was observed at -0.32 volts *versus* a SCE. The ratio of the currents produced by this couple and the processes observed in the $Ph_2Ge(BzacSalh)$ complex was approximately 1:1. Thus, the large wave observed in the cyclic voltammogram for the $Ph_2Ge(BzacSalh)$ complex was a one electron process. This result was assumed for all the organometal complexes. The large wave in the cyclic voltammograms was attributed to the processes $M(IV) + e^- \rightleftharpoons M(III)$ and $M(V) + e^- \rightleftharpoons M(IV)$ for the organometal(IV) complexes and organoantimony(V) complexes, respectively. The reduction potentials

corresponding to these processes, determined by Osteryoung square wave voltammetry, appeared in the range -1·17 to -1·78 volts for the Schiff base complexes and in the range -0·76 to -1·06 volts for the azo dye complexes, *versus* a SCE. Results are summarised in Table 5.2.

As observed with the ML_2 complexes, the azo dye organometal complexes generally produced waves at less negative potentials compared to the Schiff base organometal complexes. Thus, two one electron processes (M(IV)/M(III) and M(III)/M(II) for the group (IV) metals and M(V)/M(IV) and M(IV)/M(III) for the organoantimony complexes) were also observed in these complexes. In some of the voltammograms of the azo dye complexes, the presence of extraneous peaks made assignment of the couples difficult (Figure 5.9 and 5.10). The data for these complexes is also summarised in Table 5.2.

For the Schiff base organogroup (IV) metal complexes, the organogermanium complexes were easier to reduce and the organolead complexes were harder to reduce. The triphenylantimony complexes were sometimes easier (for the ligand BzacSalh) and other times harder (for the ligands BzacBh, SalAp and SalBh) to reduce than the analogous diphenyltin complexes. With every metal except lead, the Schiff base $SalApH_2$ produced organometal complexes which were the easiest to reduce and the Schiff base $BzacBhH_2$ produced organometal complexes which were the hardest to reduce.

The extraneous cathodic and anodic peaks which appeared in the regions -0·19 to -0·60 volts and -0·05 to -0·74 volts, respectively, probably arise from the slow disproportionation reactions. These peaks were not tabulated as in some cases their redox potential was not detected by OSWV. Disproportionation of an intermediate oxidation state is thermodynamically possible if the reduction potential of the intermediate and lower oxidation state couple (e.g. M(III)/M(II) in the group (IV) metals) is more positive than the reduction potential of the intermediate and higher oxidation state couple (e.g. M(IV)/M(III) in the group (IV) metals).[226] When beginning cyclic voltammetry experiments, the group (IV) metals are present in oxidation state (IV) and as the potential becomes more negative reduction of the species begins. One electron is transferred from the electrode to give the M(III) species, which is unstable for group (IV) metals. Upon sweeping the potential in the anodic direction, if the rate of disproportionation of M(III) to M(II) and M(IV) was slower than the rate of electron transfer at the electrode surface,

then the extraneous anodic peaks could be due to some oxidation of M(II) to M(III) at a more positive potential. In cases where a second extraneous anodic peak was observed, this could be due to the subsequent oxidation of M(III) to M(IV). Any M(III) surviving long enough could be reduced to M(II) at a more positive potential than M(IV)/M(III) when sweeping the potential in the cathodic direction again. Similar disproportionation processes could also be occurring to Sb(V) in the voltammograms of the triphenylantimony(V) complexes.
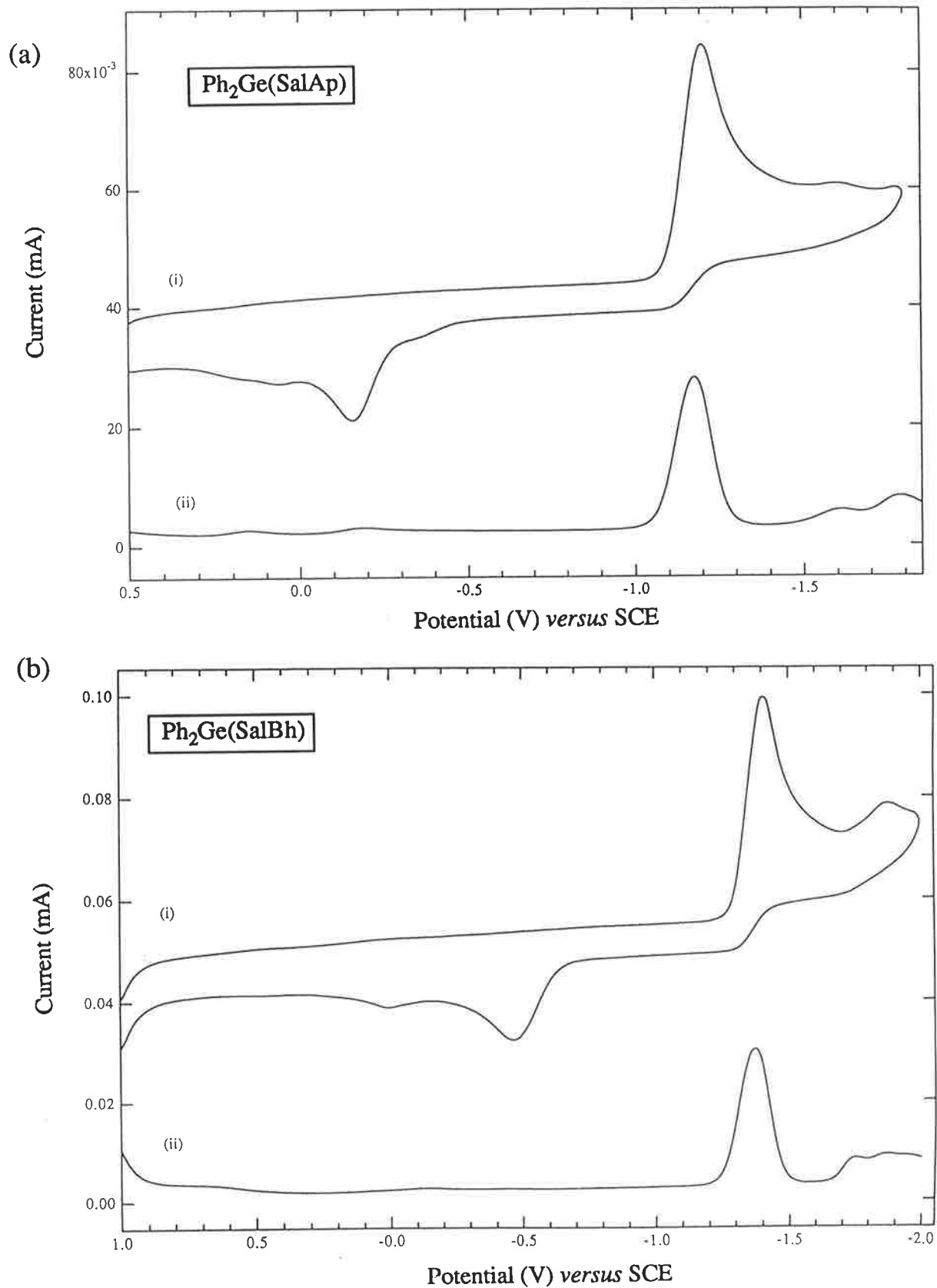
Figure 5.3: *Electrochemistry of (a) Ph$_2$Ge(SalAp) and (b) Ph$_2$Ge(SalBh) in DMSO/0·10 mol dm^{-3} Et$_4$NClO$_4$/GC. (i) Cyclic voltammograms at scan rate 100 mV s^{-1}, and (ii) Osteryoung square wave voltammograms at scan rate 60 mV s^{-1}.*
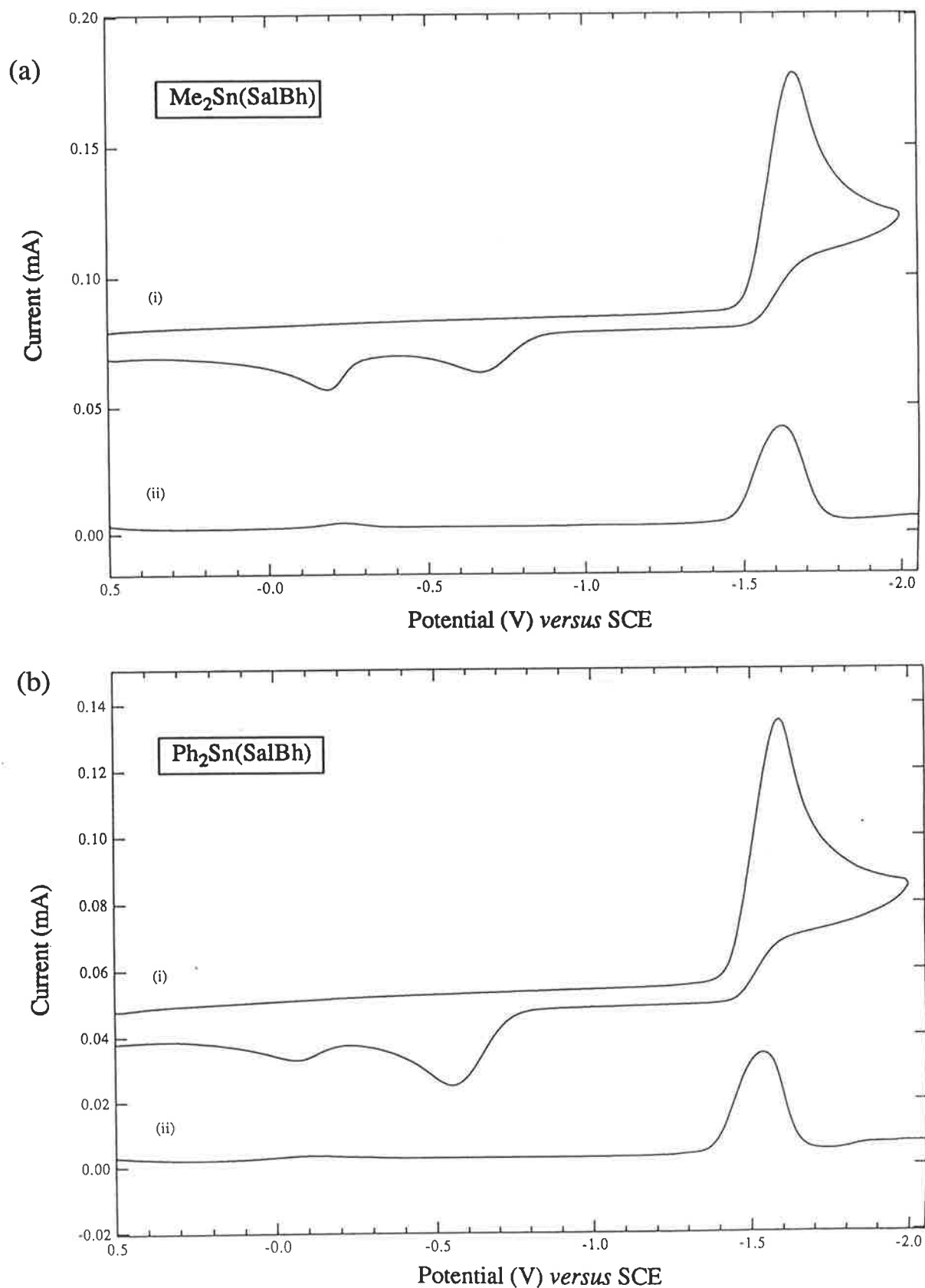
Figure 5.4: *Electrochemistry of (a) Me$_2$Sn(SalBh) and (b) Ph$_2$Sn(SalBh) in DMSO/0·10 mol dm^{-3} Et$_4$NClO$_4$/GC. (i) Cyclic voltammograms at scan rate 100 mV s^{-1}, and (ii) Osteryoung square wave voltammograms at scan rate 60 mV s^{-1}.*
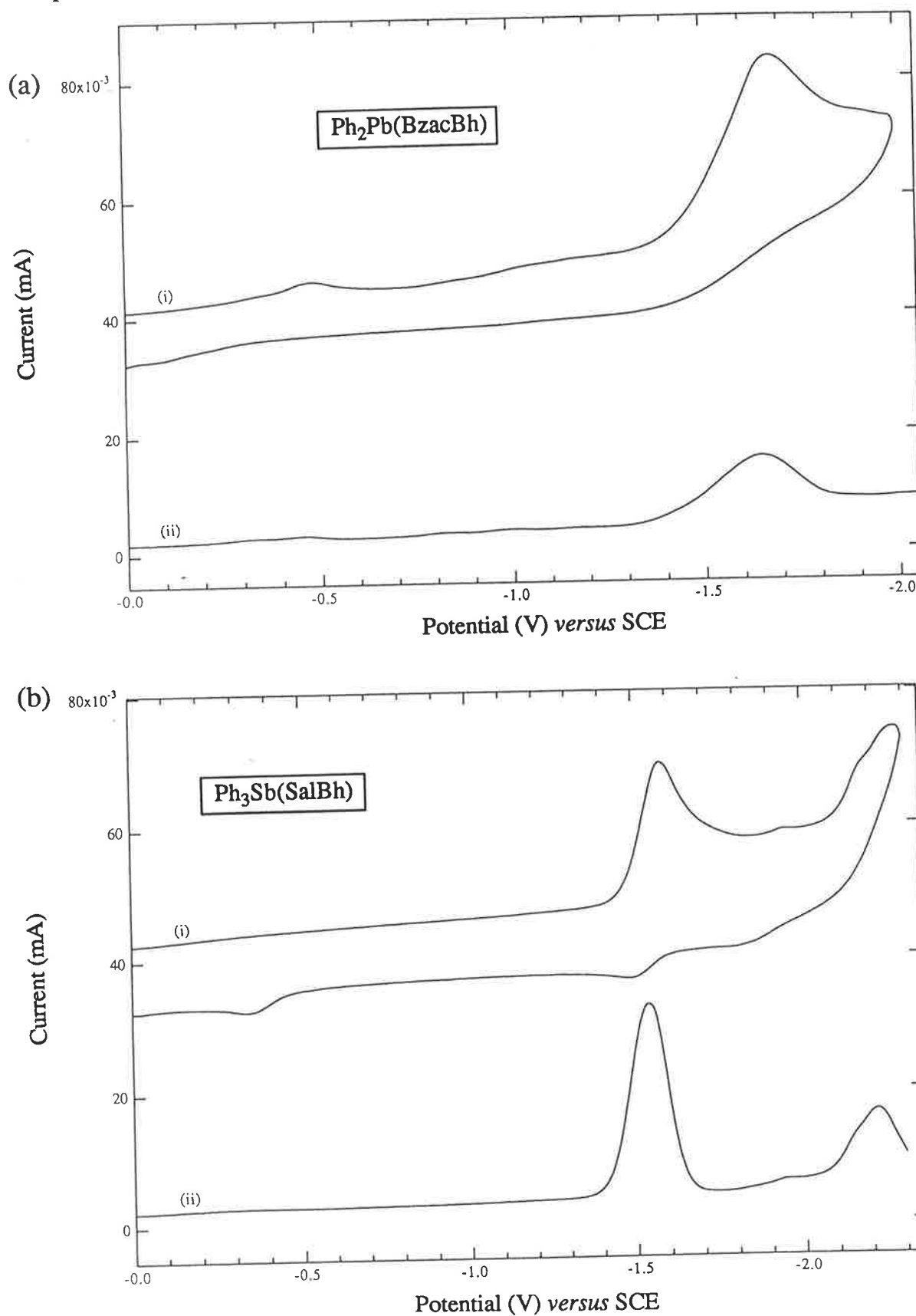
Figure 5.5: *Electrochemistry of (a) $Ph_2Pb(BzacBh)$ and (b) $Ph_3Sb(SalBh)$ in DMSO/ 0·10 mol dm^{-3} Et$_4$NClO$_4$/GC. (i) Cyclic voltammograms at scan rate 100 mV s^{-1}, and (ii) Osteryoung square wave voltammograms at scan rate 60 mV s^{-1}.*
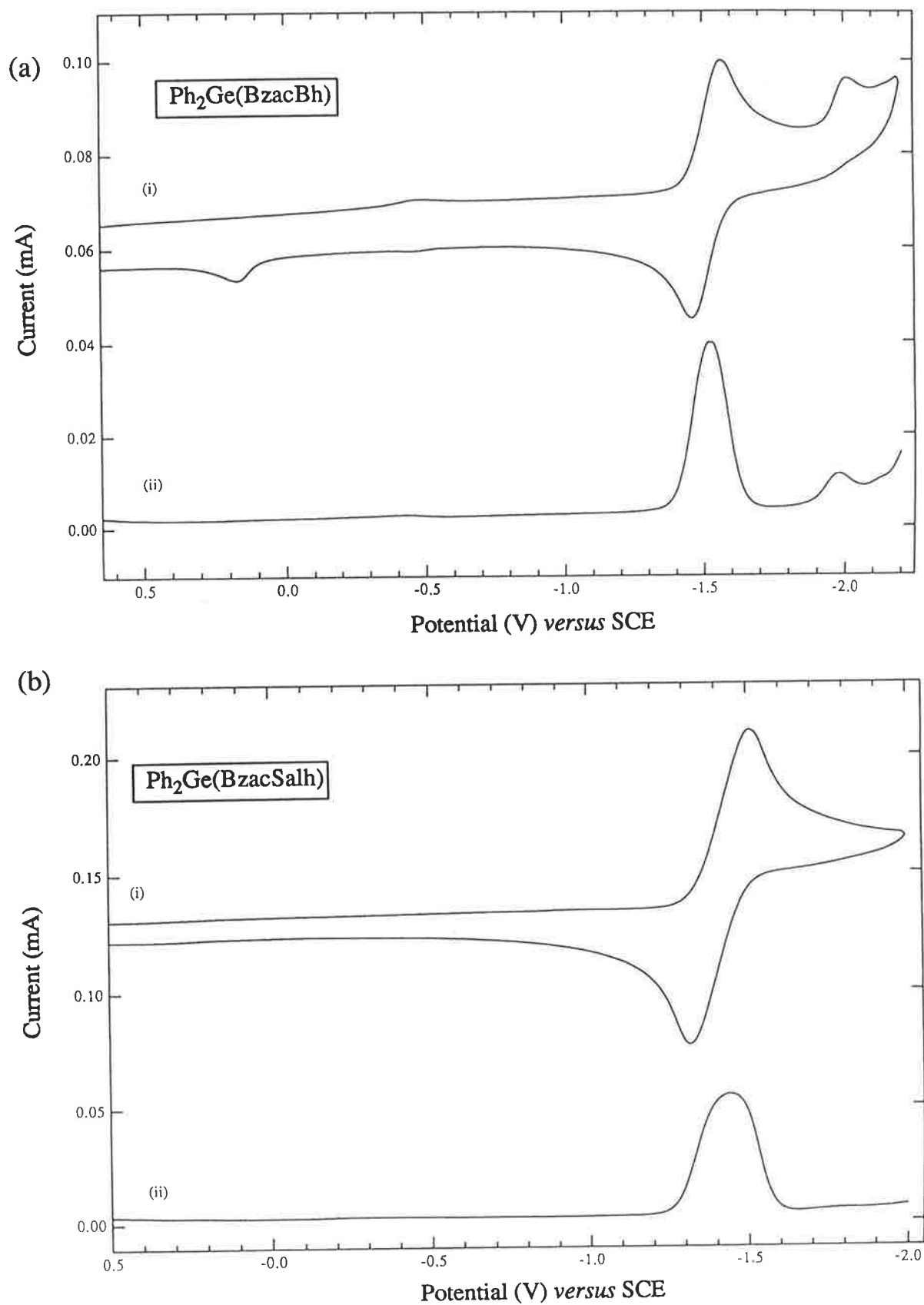
Figure 5.6: *Electrochemistry of (a) Ph₂Ge(BzacBh) and (b) Ph₂Ge(BzacSalh) in DMSO/ 0·10 mol dm⁻³ Et₄NClO₄/GC. (i) Cyclic voltammograms at scan rate 100 mV s⁻¹, and (ii) Osteryoung square wave voltammograms at scan rate 60 mV s⁻¹.*

(a)

(b)
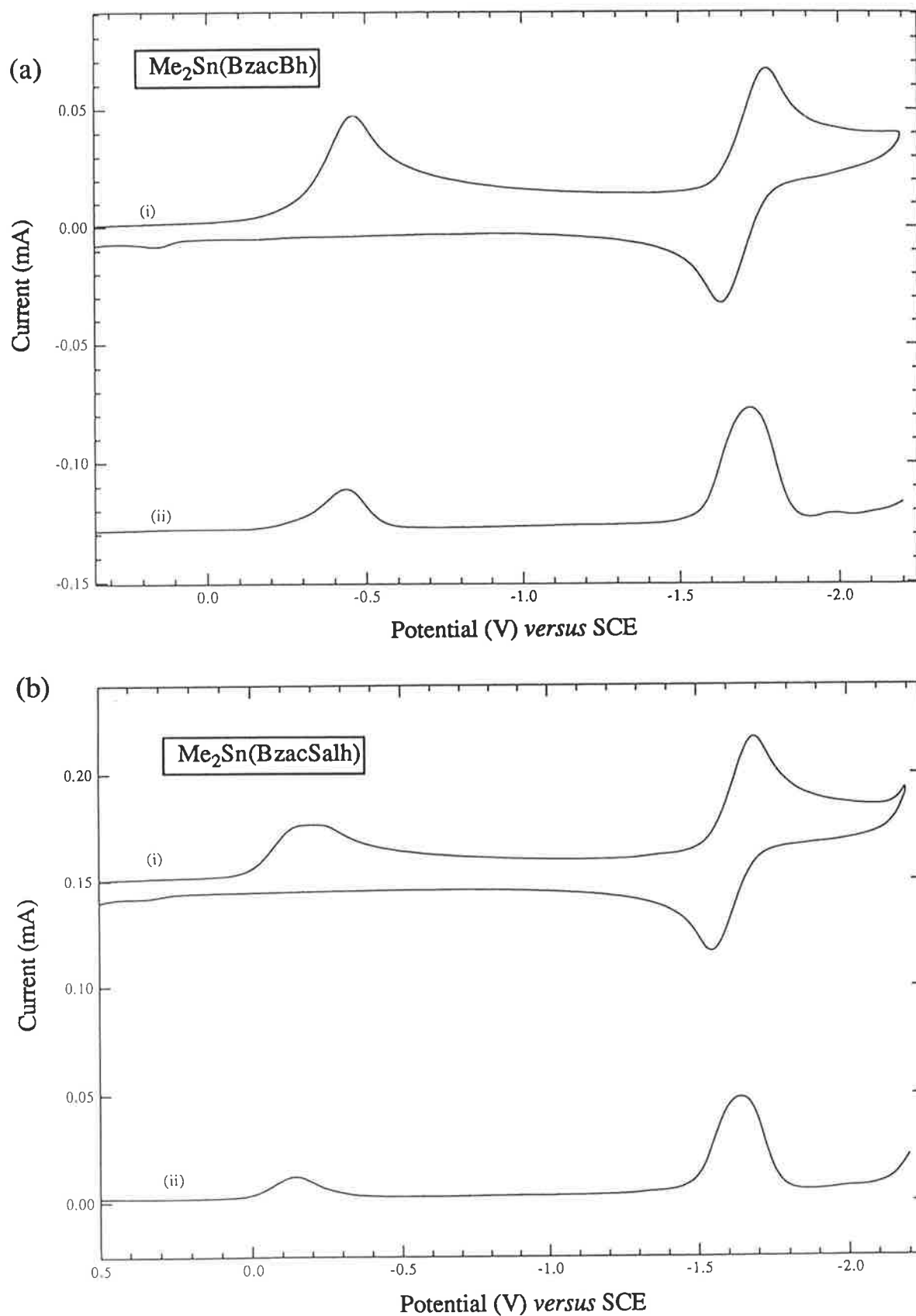
Figure 5.7: *Electrochemistry of (a) Me₂Sn(BzacBh) and (b) Me₂Sn(BzacSalh) in DMSO/0·10 mol dm⁻³ Et₄NClO₄/GC. (i) Cyclic voltammograms at scan rate 100 mV s⁻¹, and (ii) Osteryoung square wave voltammograms at scan rate 60 mV s⁻¹.*
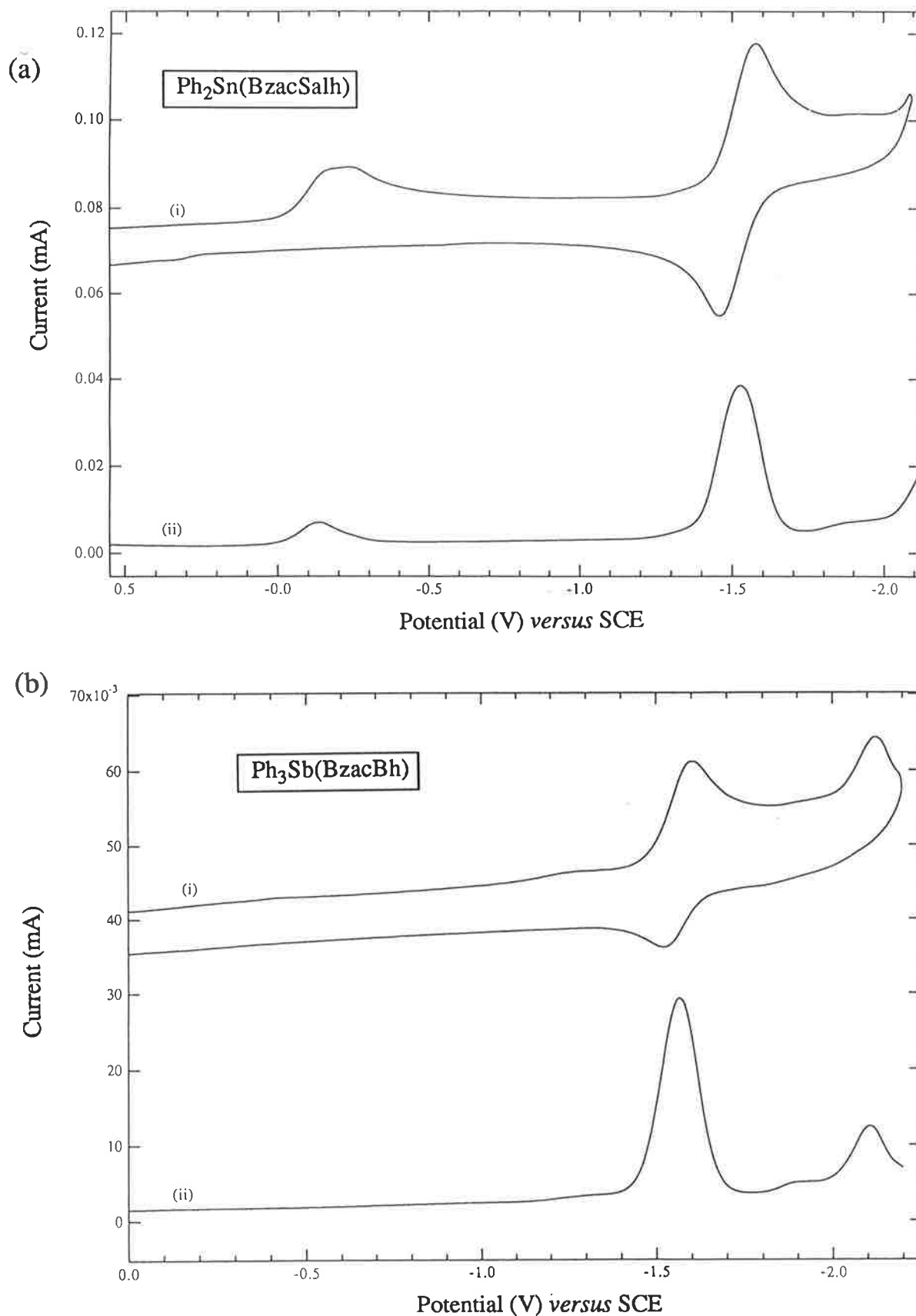
Figure 5.8: *Electrochemistry of (a) Ph₂Sn(BzacSalh) and (b) Ph₃Sb(BzacBh) in DMSO/
0·10 mol dm⁻³ Et₄NClO₄/GC. (i) Cyclic voltammograms at scan rate 100 mV s⁻¹, and (ii)
Osteryoung square wave voltammograms at scan rate 60 mV s⁻¹.*
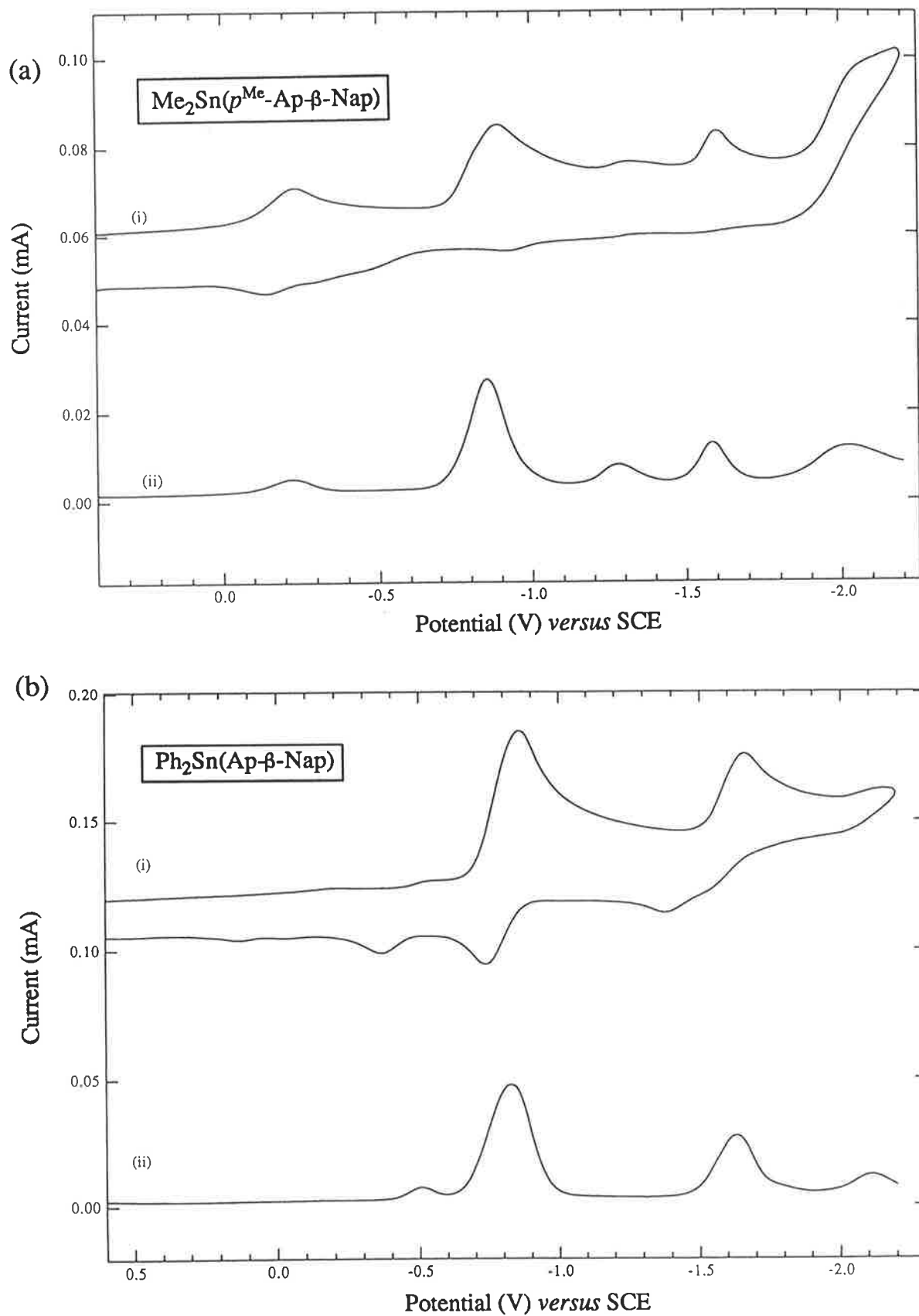
Figure 5.9: *Electrochemistry of (a) Me₂Sn(pᴹᵉ-Ap-β-Nap) and (b) Ph₂Sn(Ap-β-Nap) in DMSO/ 0·10 mol dm⁻³ Et₄NClO₄/GC. (i) Cyclic voltammograms at scan rate 100 mV s⁻¹, and (ii) Osteryoung square wave voltammograms at scan rate 60 mV s⁻¹.*
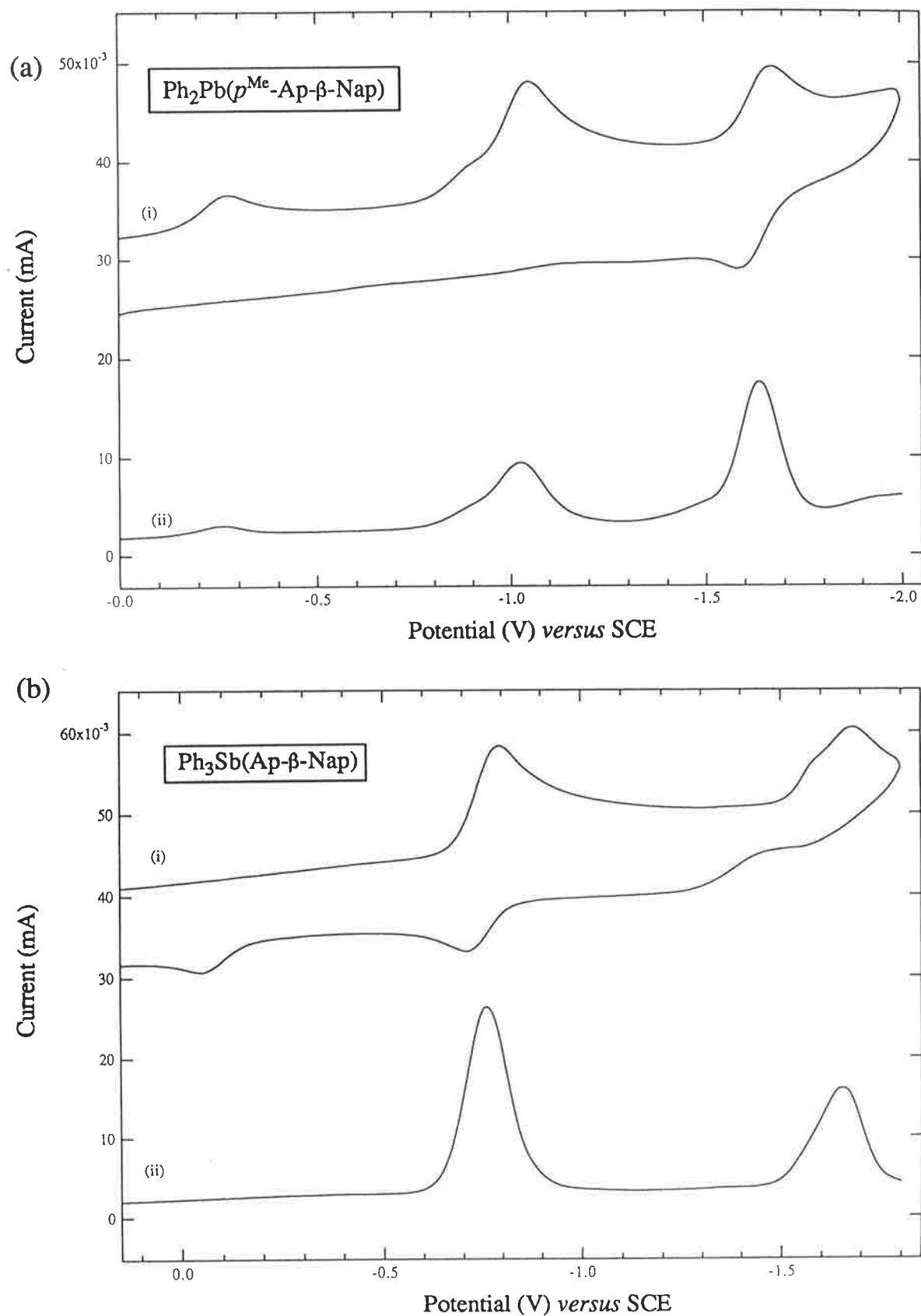
Figure 5.10: *Electrochemistry of (a) Ph₂Pb(pᴹᵉ-Ap-β-Nap) and (b) Ph₃Sb(Ap-β-Nap) in DMSO/0·10 mol dm⁻³ Et₄NClO₄/GC. (i) Cyclic voltammograms at scan rate 100 mV s⁻¹, and (ii) Osteryoung square wave voltammograms at scan rate 60 mV s⁻¹.*

Table 5.2: Electrochemical Data for Organometal Complexes on a Glassy-Carbon Working Electrode in Dimethylsulphoxide using 0.10 mol dm^{-3} Et_4NClO_4 as the Supporting Electrolyte.

Complex	E_{pa}[†]	E_{pc}[†]	$E_{1/2}$[‡] (Volts)	ΔE_p	i_{pa}/i_{pc}
$Ph_2Ge(BzacBh)$	-1·45	-1·56	-1·51	0·11	0·90
$Me_2Sn(BzacBh)$	-1·64	-1·79	-1·73	0·15	0·97
$Ph_2Sn(BzacBh)$	-1·54	-1·63	-1·59	0·09	0·82
$Ph_2Pb(BzacBh)$	--	-1·75	-1·71	--	--
$Ph_3Sb(BzacBh)$	-1·55	-1·63	-1·60	0·08	0·48
$Ph_2Ge(BzacSalh)$	-1·33	-1·52	-1·45	0·19	0·98
$Me_2Sn(BzacSalh)$	-1·53	-1·68	-1·62	0·15	0·95
$Ph_2Sn(BzacSalh)$	-1·45	-1·58	-1·53	0·13	0·95
$Ph_2Pb(BzacSalh)$	--	-1·86	-1·78	--	--
$Ph_3Sb(BzacSalh)$	-1·42	-1·52	-1·49	0·10	0·13
$Ph_2Ge(SalAp)$	--	-1·19	-1·17	--	--
$Me_2Sn(SalAp)$	--	-1·43	-1·39	--	--
$Ph_2Sn(SalAp)$	--	-1·37	-1·34	--	--
$Ph_2Pb(SalAp)$	--	-1·61	-1·58	--	--
$Ph_3Sb(SalAp)$	-1·33	-1·42	-1·39	0·09	0·32
$Ph_2Ge(SalBh)$	--	-1·41	-1·38	--	--
$Me_2Sn(SalBh)$	--	-1·64	-1·61	--	--
$Ph_2Sn(SalBh)$	--	-1·56	-1·52	--	--
$Ph_2Pb(SalBh)$	--	-1·88	-1·78	--	--
$Ph_3Sb(SalBh)$	-1·48	-1·58	-1·54	0·10	0·17

$Ph_2Ge(Ap-\beta-Nap)$	--	-1·01	-0·99	--	--
	--	-1·39	-1·31	--	--
$Me_2Sn(Ap-\beta-Nap)$	-0·81	-0·92	-0·88	0·11	0·34
	--	-1·70	-1·67	--	--
$Ph_2Sn(Ap-\beta-Nap)$	-0·72	-0·86	-0·81	0·14	0·46
	--	-1·66	-1·62	--	--
$Ph_2Pb(Ap-\beta-Nap)$	--	-1·07	-1·05	--	--
	-1·57	-1·67	-1·63	0·10	0·83
$Ph_3Sb(Ap-\beta-Nap)$	-0·72	-0·80	-0·76	0·08	0·45
	--	-1·68	-1·65	--	--
$Ph_2Ge(p^{Me}-Ap-\beta-Nap)$	--	-1·01	-0·97	--	--
	--	-1·51	-1·40	--	--
$Me_2Sn(p^{Me}-Ap-\beta-Nap)$	-0·84	-0·91	-0·88	0·07	0·17
	--	-1·64	-1·61		--
$Ph_2Sn(p^{Me}-Ap-\beta-Nap)$	-0·76	-0·89	-0·84	0·13	0·45
	-1·55	-1·71	-1·67	0·16	0·23
$Ph_2Pb(p^{Me}-Ap-\beta-Nap)$	--	-1·08	-1·06	--	--
	-1·60	-1·69	-1·66	0·09	0·70
$Ph_3Sb(p^{Me}-Ap-\beta-Nap)$	-0·74	-0·83	-0·78	0·09	0·51
	--	-1·67	-1·65	--	--

All potentials measured *versus* a SCE.

[†] Data from cyclic voltammetry using a scan rate of 100 mV s^{-1}.

[‡] Data from Osteryoung square wave voltammetry using a scan rate of 60 mV s^{-1}. In this electrochemical system ferrocene has E_{pa} = +0·53 volts, E_{pc} = +0·36 volts and $E_{1/2}$ = +0·41 volts.

For the ligand $SalApH_2$ (LH_2), the diphenylgroup(IV) complexes were also studied on a platinum working electrode *versus* a Ag/Ag^+ (dimethyl-sulphoxide) reference electrode so that a comparison could be made with the corresponding ML_2 complexes.[97] These results are summarised in Table 5.3. Electrochemical data reveals that oxidation state (IV) becomes more stable down group (IV) for diphenyl complexes. The GeL_2 and Ph_2GeL complexes produced similar data, while Ph_2SnL appeared more stable than SnL_2. The unsuccessful synthesis of PbL_2 is in agreement with the greater stability of Ph_2PbL. Out of interest, $Pb(SalAp)$, the product obtained trying to synthesise $Pb(SalAp)_2$, was similarly electrochemically examined and one irreversible wave with a reduction potential -1·60 volts *versus* the Ag/Ag^+ electrode was observed.

Table 5.3: Comparison of Electrochemical Data for $M(SalAp)_2$ and $Ph_2M(SalAp)$ Complexes of Germanium, Tin and Lead on a Platinum Working Electrode in Dimethylsulphoxide using 0·10 mol dm^{-3} Bu_4NBF_4 as the Supporting Electrolyte.

Complex	E_{pa}[†]	E_{pc}[†] (volts)	$E_{1/2}$[‡]
$Ge(SalAp)_2$[a]	--	-1·49	-1·46
	-1·95	-2·09	-2·01
$Ph_2Ge(SalAp)$	--	-1·47	-1·44
$Sn(SalAp)_2$[a]	--	-1·43	-1·41
	-1·79	-1·95	-1·86
$Ph_2Sn(SalAp)$	--	-1·60	-1·57
$Pb(SalAp)_2$	Could not be synthesised		
$Pb(SalAp)$	--	-1·65	-1·60
$Ph_2Pb(SalAp)$	--	-1·75	-1·69

All potentials *versus* a Ag/Ag^+ (DMSO) reference electrode.
[†] Data from cyclic voltammetry using a scan rate of 100 mV s^{-1}.
[‡] Data from Osteryoung square wave voltammetry using a scan rate of 60 mV s^{-1}.
[a] Reference 97.
In this system ferrocene has E_{pa} = +0·22 volts, E_{pc} = +0·13 volts and $E_{1/2}$ = +0·17 volts.

5.5.3 Amide Complexes

All amide complexes of manganese and titanium prepared were studied electrochemically to examine the effect of the ligand and metal on the redox properties. Koikawa *et al.* had earlier reported these types of amide complexes to be unstable on platinum or glassy-carbon working electrode surfaces in dimethylformamide.[96] For this reason the compounds were solubilised in dichloromethane by addition of a crown ether. Various attempts were made by us to use a solvent in which these compounds were readily soluble. However, in acetonitrile no activity was observed on a platinum working electrode using a Ag/Ag^+ (acetonitrile) reference electrode, and in methanol the cathodic reduction limit of the medium only allowed measurement up to -0·40 volts. Voltammograms on freshly prepared dimethylsulphoxide solutions gave results similar to those on dichloromethane/crown ether solutions. The dichloromethane/crown ether system was found to be the best system to use since the dimethylsulphoxide solutions gave irreproducible results on standing. The macrocyclic polyether 15-crown-5 was found to be capable of solubilising all of the amide complexes of manganese and titanium in dichloromethane. No ferrocene was added to the solutions in these experiments as its redox couple coincided and interfered with one of those for the manganese complexes.

Results obtained for the manganese compounds were similar to that reported.by Koikawa *et al.* for similar compounds.[96] Typical outputs are shown in Figures 5.11 and 5.12 for compounds $K_2[MnL^5{}_2]$ and $K_2[MnL^6{}_2]$, respectively. In most cases, three waves were observed in the cyclic voltammograms which were assigned to Mn(VI)/Mn(V), Mn(V)/Mn(IV) and Mn(IV)/Mn(III) couples. Half-wave potentials for these waves were observed in the regions 0·84 to 0·71 volts, 0·57 to 0·40 volts and -0·60 to -0·82 volts, respectively, *versus* a SCE. Complexes of the amide ligands containing naphthyl rings (i.e. L^7, L^8 and L^9) gave clear results only for the M(IV)/M(III) couple. Electrochemical information on the manganese compounds is given in Table 5.4.
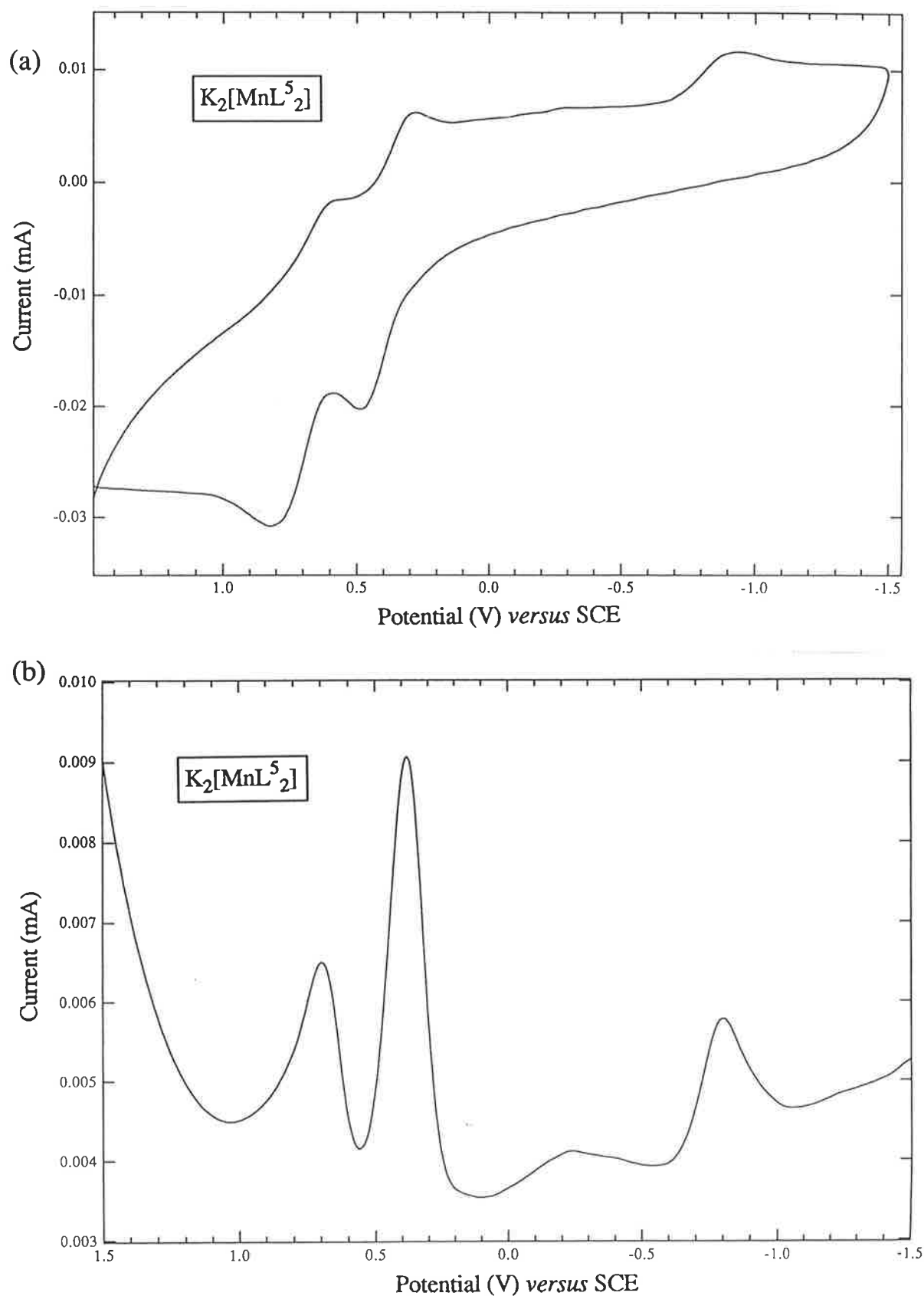
Figure 5.11: *Electrochemistry of $K_2[MnL^5{}_2]$ in $CH_2Cl_2/0·05$ mol dm^{-3} Et_4NClO_4/GC. (a) Cyclic voltammogram at scan rate 80 mV s^{-1}, and (b) Osteryoung square wave voltammogram at scan rate 60 mV s^{-1}.*
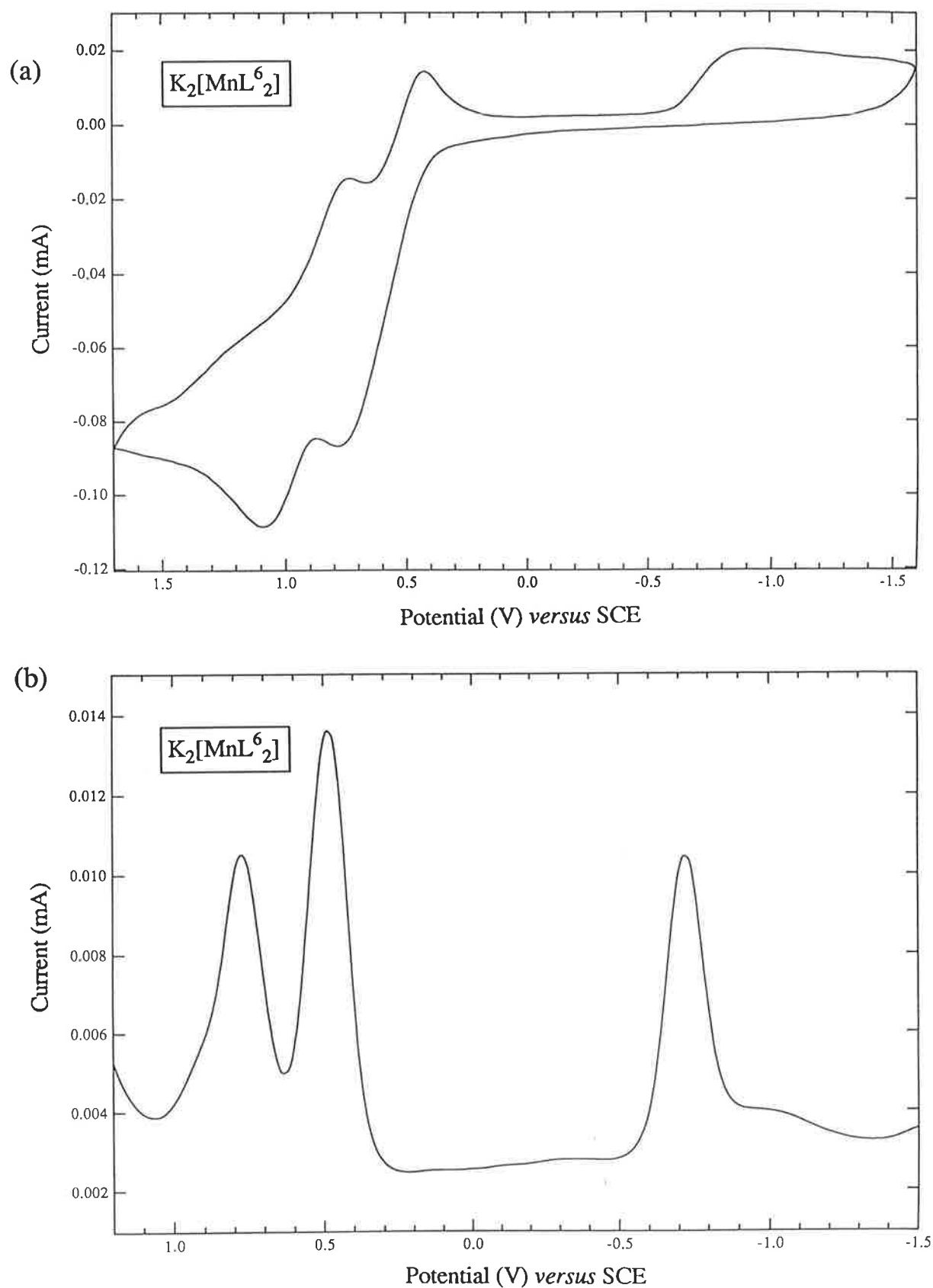
**Figure 5.12:** *Electrochemistry of $K_2[MnL^6{}_2]$ in $CH_2Cl_2/0.05$ mol dm^{-3} Et_4NClO_4/GC. (a) Cyclic voltammogram at scan rate 80 mV s^{-1}, and (b) Osteryoung square wave voltammogram at scan rate 60 mV s^{-1}.*

Table 5.4: Electrochemical Data for the Amide Complexes of Manganese on a Glassy-Carbon Working Electrode in Dichloromethane using 0.05 mol dm^{-3} Et$_4$NClO$_4$ as the Supporting Electrolyte.

Complex	E_{pa}[†]	E_{pc}[†]	$E_{1/2}$[‡] (Volts)	ΔE_p	i_{pa}/i_{pc}[¥]
$K_2[MnL^1_2]$	$+1.26$	--	*	--	
	$+0.78$	--	*	--	
	--	-1.06	-1.01	--	
$K_2[MnL^2_2]$	$+0.96$	$+0.75$	$+0.80$	0.21	
	$+0.68$	$+0.29$	$+0.51$	0.39	
	--	-0.77	-0.65	--	
$K_2[MnL^4_2]$	$+0.91$	$+0.75$	$+0.84$	0.16	
	$+0.65$	$+0.51$	$+0.57$	0.14	1.18
	--	-0.65	-0.60	--	
$K_2[MnL^5_2]$	$+0.82$	$+0.60$	$+0.71$	0.22	
	$+0.49$	$+0.29$	$+0.40$	0.20	0.98
	--	-0.93	-0.78	--	
$K_2[MnL^6_2]$	$+0.84$	$+0.68$	$+0.77$	0.16	
	$+0.55$	$+0.41$	$+0.48$	0.14	1.27
	--	-0.79	-0.72	--	
$K_2[MnL^7_2]$	--	-0.80	-0.82	--	
$K_2[MnL^8_2]$	--	-0.60	-0.61	--	
$K_2[MnL^9_2]$	--	-0.79	-0.80	--	

All potentials *versus* a SCE.
† Data from cyclic voltammetry using a scan rate of 80 mV s^{-1}.
‡ Data from Osteryoung square wave voltammetry using a scan rate of 60 mV s^{-1}.
* Peaks in OSWV were not well resolved.
¥ Current ratios calculated for few samples only.

The titanium complexes exhibited one wave in their cyclic voltammograms with a half-wave potential in the region -1·60 to -2·04 volts *versus* a SCE which was assigned to the Ti(IV)/Ti(III) couple. Examples are shown in Figures 5.13 and 5.14 for the compounds $K_2[TiL^7_2]$ and $K_2[TiL^8_2]$, respectively. As there is no difficulty in achieving the oxidation state (IV) with titanium, and because the energy of the lowest unoccupied orbital at which reduction is taking place is higher than that in manganese, these complexes were expected to be harder to reduce than the corresponding manganese(IV) compounds. Therefore, more negative half-wave potentials were expected for the Ti(IV)/Ti(III) couple compared to the Mn(IV)/Mn(III) couple. This in fact was observed for all of the titanium and manganese complexes of all the amide ligands. The Ti(IV)/Ti(III) was the one of greatest interest because it permitted comparisons with the half-wave potentials of related Mn(IV) complexes. Also, potentials more negative than those for the TiL_2 Schiff base complexes studied by Salam[92] were expected because it was observed that amide complexes of manganese gave more negative reduction potentials than Schiff base complexes of manganese.[14] Such considerations led us to assign half-wave potentials to the couple Ti(IV)/Ti(III). The Ti(III)/Ti(II) couple was not observed before the cathodic reduction limit of the medium. This was not surprising as similar findings were reported by Salam for Schiff base complexes of titanium.[92] Potential data for these complexes are summarised in Table 5.5.

In the case of the manganese complexes, as the electron-releasing character of the amide ligand increased so did $-E_{1/2}$ of the complex. Apart from some discrepancies, this trend was also shown in the titanium complexes. This is represented in Table 5.6 for the manganese complexes and in Table 5.7 for the titanium complexes.

(a)

$K_2[TiL^7{}_2]$

Current (mA)

Potential (V) *versus* SCE

(b)

$K_2[TiL^7{}_2]$

Current (mA)

Potential (V) *versus* SCE
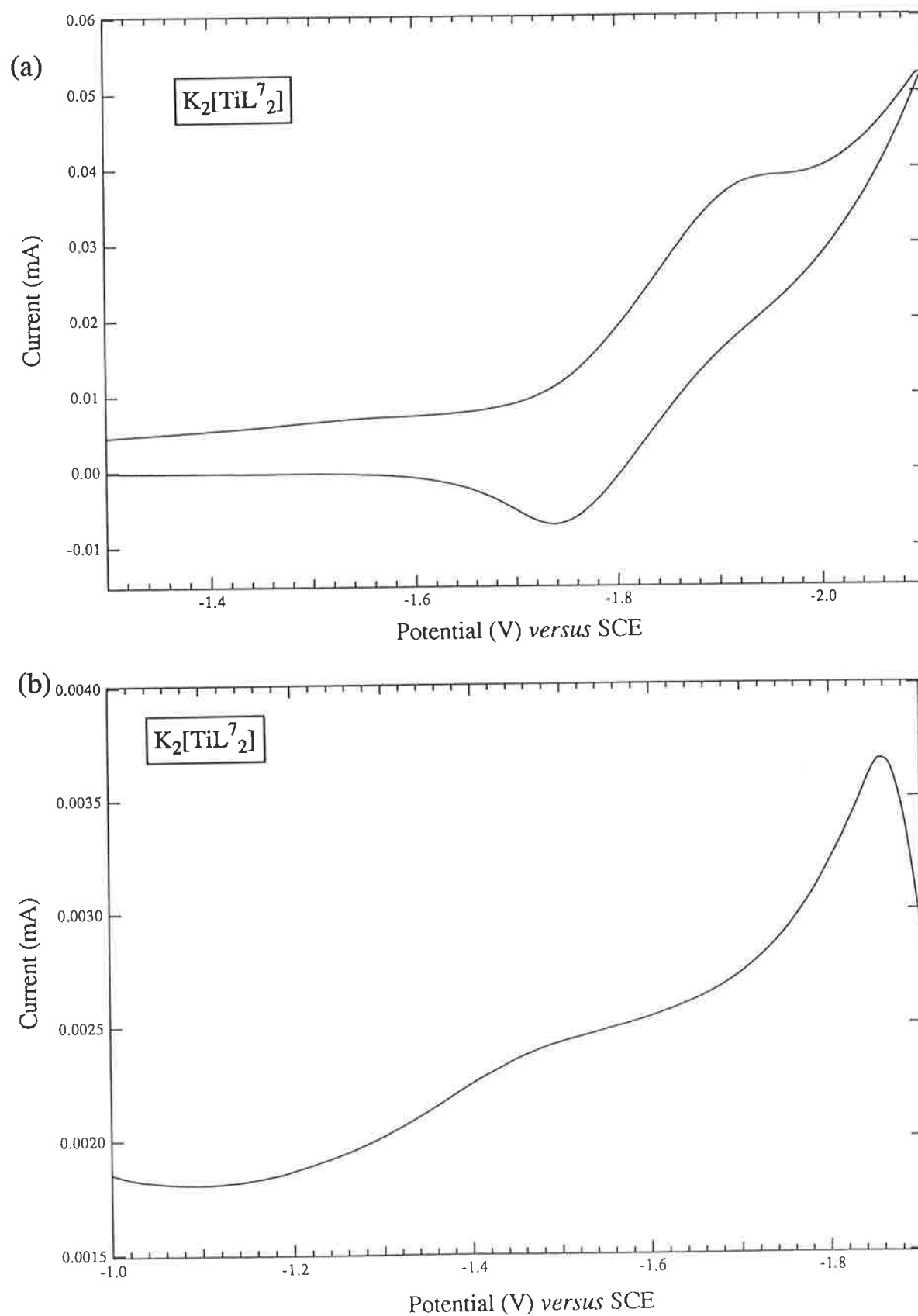
Figure 5.13: *Electrochemistry of $K_2[TiL^7{}_2]$ in $CH_2Cl_2/0.05$ mol dm^{-3} Et_4NClO_4/GC.*
(a) Cyclic voltammogram at scan rate 80 mV s^{-1}, and (b) Osteryoung square wave voltammogram at scan rate 60 mV s^{-1}.

(a)

(b)
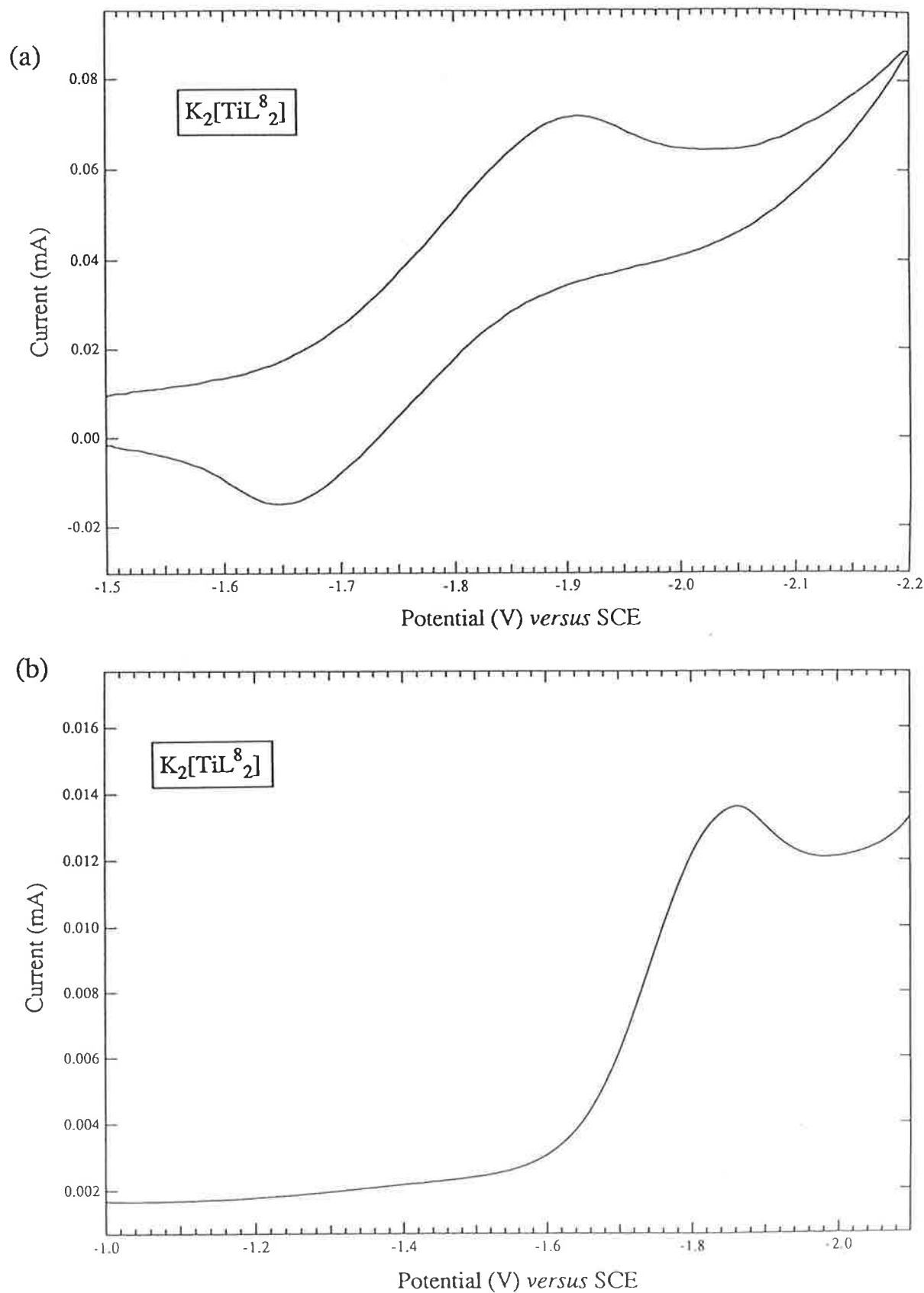
Figure 5.14: *Electrochemistry of $K_2[TiL^8{}_2]$ in $CH_2Cl_2/0\cdot05$ mol dm^{-3} Et_4NClO_4/GC. (a) Cyclic voltammogram at scan rate 80 mV s^{-1}, and (b) Osteryoung square wave voltammogram at scan rate 60 mV s^{-1}.*

Table 5.5: Electrochemical Data for the Amide Complexes of Titanium on a Glassy-Carbon Working Electrode in Dichloromethane using 0·05 mol dm^{-3} Et$_4$NClO$_4$ as the Supporting Electrolyte.

Complex	E_{pa}[†]	E_{pc}[†]	$E_{1/2}$[‡] (Volts)	ΔE_p	i_{pa}/i_{pc}[¥]
K$_2$[TiL$^1_2$]	-1·81	-2·04	-1·94	0·23	
K$_2$[TiL$^2_2$]	-1·72	-1·92	-1·83	0·20	
K$_2$[TiL$^3_2$]	-1·70	-2·08	-1·92	0·38	
K$_2$[TiL$^4_2$]	-1·68	-1·90	-1·83	0·22	0·75
K$_2$[TiL$^5_2$]	--	--	-1·60	--	
K$_2$[TiL$^6_2$]	-1·85	-2·13	-2·04	0·28	
K$_2$[TiL$^7_2$]	-1·74	-1·93	-1·86	0·19	
K$_2$[TiL$^8_2$]	-1·65	-1·91	-1·86	0·26	1·52
K$_2$[TiL$^9_2$]	-1·80	-1·98	-1·82	0·18	

All potentials *versus* a SCE.

[†] Data from cyclic voltammetry using a scan rate of 80 mV s^{-1}.

[‡] Data from Osteryoung square wave voltammetry using a scan rate of 60 mV s^{-1}.

[¥] Current ratios calculated for two samples only.

Table 5.6: Reduction Potential Data for the Mn(IV)/Mn(III) Couple in the $K_2[MnL^n_2]$ Complexes.

Ligand L^n, where n =	4	8	2	6	5	9	7	1
Substituent on salicylamide moiety	5-Cl	5-Cl	5-Cl	3-Me	3-Me	3-Me	-	-
Substituent on aminophenol/naphthol moiety	5-Cl	*	--	5-Cl	--	*	*	-
Reduction potential for Mn(IV)/Mn(III) couple				Increasingly negative				→

* Amide ligand derived from naphthol.

Table 5.7: Reduction Potential Data for the Ti(IV)/Mn(III) Couple in the $K_2[TiL^n_2]$ Complexes.

Ligand L^n, where n =	4	2	7	8	3	1	6
Substituent on salicylamide moiety	5-Cl	5-Cl	--	3-Me	--	--	3-Me
Substituent on aminophenol/naphthol moiety	5-Cl		--	*	5-Cl	--	5-Cl
Reduction potential for Ti(IV)/Ti(III) couple				Increasingly negative			→

* Amide ligand derived from naphthol.

Chapter 6

EXPERIMENTAL

6.1 Solvents

6.1.1 For synthetic work

Solvents ethanol and methanol were dried and purified according to the methods detailed by Vogel.[227a,b]

Dry tetrahydrofuran was obtained by distilling the LR grade solvent over sodium/benzophenone and under dinitrogen before use.[228a]

Dry chloroform was obtained by distilling the AR grade solvent over calcium chloride under an atmosphere of dinitrogen.[228b] For the preparation of the polyphosphate ester the distilled chloroform was shaken with P_2O_5, filtered through glass wool and then used immediately.[217]

Dry benzene was obtained by storing the AR grade solvent over calcium chloride overnight before distilling under an atmosphere of dinitrogen and storing over 4Å molecular sieves.

AR dimethylsulphoxide, HPLC grade dimethylsulphoxide, AR carbon tetrachloride, AR diethyl ether and AR dioxane were stored over 4Å molecular sieves before use in any synthesis requiring dry solvent.

All other solvents used were LR grade.

6.1.2 For purification and some physical measurements

LR grade solvents were used for chromatography, recrystallisations, magnetic moment measurements, conductance measurements and recording of electronic spectra. LR grade solvents were used for washing the solid products, except in the case of hexane where AR grade was used.

Deuterated chloroform, dimethylsulphoxide, methanol and deuterium oxide were obtained from Cambridge Isotope Laboratories. Trimethylsilane was obtained from Aldrich Chemical Co. Inc.

6.1.3 For electrochemistry

A similar procedure to that described by Perrin *et al.*[228c] was followed to prepare dry dichloromethane
LR dichloromethane was washed twice with conc. sulphuric acid (1/4 × volume), allowing the solvent-acid mixture to stir overnight each time. The solvent was then washed once with aqueous 5% potassium hydroxide (1/4 × volume) followed by water. After filtering through an alumina pad and stirring overnight over calcium hydride the solvent was fractionally distilled under an atmosphere of dinitrogen and stored over 4Å molecular sieves.

HPLC grade dimethylsulphoxide was stored over 4Å molecular sieves before use.

6.2 Gases

High purity dinitrogen, dioxygen and argon were obtained from Commonwealth Industrial Gases Ltd.

6.3 Starting Materials

6.3.1 Purchased starting materials

Benzoylacetone, 2-aminobenzyl alcohol, guaiacol, 3-amino-2-naphthol, 3-methylsalicylic acid, 5-chlorosalicylic acid, 5-chloro-2-hydroxyanaline, silicon tetrachloride, lead tetraacetate, 2-amino-*p*-cresol, *p*^{Cl}-phenol, 2-methoxypropene, hexamethyldisilazane, potassium antimonyl tartrate hydrate, titanium tetrabutoxide, 15-crown-6 and N-bromosuccinimide were obtained from Aldrich Chemical Co Inc. Catechol was also obtained from Aldrich Chemical Co. Inc., but purified by sublimation before use.

o-Aminophenol, acetylacetone, vanadyl chloride solution, urea, lead nitrate, β-naphthol, potassium hydroxide, anhydrous sodium sulphate, anhydrous magnesium sulphate, calcium chloride (8 - 16 mesh) and pyridine were obtained from British Drug House Chemicals Pty Ltd.

Diphenylgermanium dichloride, dimethyltin dichloride, *n*-dibutyltin dichloride, diphenyltin dichloride, triphenyllead chloride and triphenyl-

antimony dichloride were obtained from Johnson Matthey GMBH Alfa Products.

Antimony tribromide and salicylaldehyde were obtained from Hopkins and Williams Ltd.. The former was dried under vacuum over P_2O_5 before use.

Thionyl chloride, dimethylsulphate, hydrochloric acid, sodium hydroxide and salicylic acid were obtained from Ajax Chemicals Ltd.

Triethylamine, chromatographic alumina (100 - 125 mesh) and germanium tetrachloride were obtained from Fluka AG.

Anhydrous aluminium chloride was obtained from Merck-Schuchardt.

Sodium and sulphuric acid were obtained from the Analytical and Research Chemical Company.

6.3.2 Diphenyllead dichloride

Hydrochloric acid (1 mol dm^{-3}; 4·7 ml; $4·7 \times 10^{-3}$ mol) was added to a mixture of Ph_3PbCl (2·00 g; $4·22 \times 10^{-3}$ mol) in dry ethanol (75 ml). The mixture was heated under reflux for 5 hours during which time a colourless solution formed followed by precipitation of a white solid. The mixture was allowed to stand overnight. The white solid was collected and washed with cold ethanol (3 × 5 ml). Yield 1·21 g ($2·80 \times 10^{-3}$ mol; 66%). F.W.: calc. for $C_{12}H_{10}Cl_2Pb$, 432·31; found *(mass spectrum)*, 433.

6.3.3 Bis(acetylacetonato)oxovanadium(IV), VO(acac)$_2$

This compound was prepared following the procedure described in the literature.[229]

6.3.4 *o*-Cresyl acetate

This compound was prepared following the literature method.[230] A solution of *o*-cresol (30·0 ml; 0·29 mmol) in acetic anhydride:pyridine (84·0 ml; 1:1) was allowed to stir at room temperature for 24 hours. The solvents were removed by vacuum distillation followed by vacuum distillation of the residue to obtain the colourless ester. Yield 36·2 g (0·24 mmol; 83%), b.p. 101·5°C/18 mm Hg (Lit.[230] 105°C/20 mm Hg).

6.3.5 2-Methoxypropanetoluene

The compound was prepared following a similar procedure to that used by Kluge *et al.* for the protection of a hydroxyl group of an alcohol with 2-methoxypropene.[214] 2-Methoxypropene (7·97 ml; 83·2 mmol) was added to *o*-cresol (2·03 ml; 19·7 mmol) forming a yellow solution. A trace of phosphorus oxychloride, in a capillary tube, was introduced into the reaction flask. The flask was stoppered and allowed to stand at room temperature for 2·5 hours before adding triethylamine (2 drops). The course of the reaction was followed by TLC (90% dichloromethane:10% hexane). Excess 2-methoxypropene was removed by vacuum distillation leaving behind a yellow oil. Yield 2·85 g (15·8 mmol; 80%). *^{1}H-NMR (CDCl$_3$/TMS):* δ7·10 - 6·53 (m; 4H, Ar<u>H</u>), 3·32 (s; 3H, C<u>H</u>$_3$O), 2·13 (s; 3H, C<u>H</u>$_3$Ar) and 1·44 ppm (s; 6H, >C(C<u>H</u>$_3$)$_2$). The material was used as such.

6.3.6 2-Methylanisole

The experimental procedure described in Vogel for the preparation of anisole from phenol[227d] was followed to prepare this compound using *o*-cresol (27·0 g; 0·25 mol), NaOH (10·5 g; 0·26 mol) in water (100 ml) and dimethyl sulphate (23·5 ml; 0·25 mol). Yield 18·4 g (0·15 mol; 60%), b.p. 170 - 172°C (Lit.[13] 171-172°C). *^{1}H-NMR (CDCl$_3$/TMS):* δ7·02 - 6·42 (m; 4H, Ar<u>H</u>), 3·58 (s; 3H, OC<u>H</u>$_3$) and 2·12 ppm (s; 3H, ArC<u>H</u>$_3$). Material was used as such.

6.3.7 2-(Trimethylsilyloxy)toluene

o-Cresol (2·90 ml; 28·1 mmol) and hexamethyldisilazane (3·00 ml; 14·2 mmol) were refluxed under an atmosphere of dinitrogen for 2·5 hours forming an orange solution. After standing overnight, the solution was distilled under vacuum collecting a colourless distillate (78°C/~7 mm Hg). Yield 4·23 g (23·5 mmol; 83%). F.W.: calc. for C$_{10}$H$_{16}$OSi, 180·32; found *(mass spectrum)*, 154. *^{1}H-NMR (CDCl$_3$/TMS):* δ7·11 - 6·53 (m; 4H, Ar<u>H</u>), 2·14 (s; 3H, ArC<u>H</u>$_3$) and 0·24 ppm (s; 9H, Si(C<u>H</u>$_3$)$_3$). Material was used as such.

6.3.8 2-Acetyloxyphenol

This compound was prepared using a modification of the procedure given in the literature for *o*-cresyl acetate.[230] A solution of catechol (2·00 g; 18·2 mmol) in pyridine:acetic anhydride (2·0 ml; 1:1) solvent mixture was stirred under dinitrogen at room temperature for 4 hours. Excess solvent was removed by vacuum distillation (60°C/15-20 mm Hg) leaving behind a dark

yellow oil. Yield 1·97 g (12·9 mmol; 71%). F.W.: calc. for $C_8H_8O_3$, 152·15; found *(mass spectrum)* 153. *1H-NMR (CDCl3/TMS):* δ7·21 - 6·56 (m; 4H, Ar<u>H</u>); 6·34 (s; 1H, Ar<u>OH</u>; disappeared upon addition of D_2O) and 2·22 ppm (s; 3H, $O_2CC\underline{H}_3$). *Lit. (CDCl3):* δ7·2 (broad s; 4H) and 2·1 ppm (s; 3H)[231] *Infrared spectrum:* 3431 s, 1766 s, 1598 s and 1510 s cm^{-1}. *Lit.(CDCl3):* 3560, 1760, 1605 and 1500 cm^{-1}.[231]

6.3.9 Polyphosphate ester (PPE)

This viscous, slightly brown syrup was prepared by the literature method [217]

6.3.10 Tin dichloride

Tin dichloride dihydrate, $SnCl_2.2H_2O$, was dehydrated with acetic anhydride, as described by Brauer.[232]

6.3.11 Tris(acetylacetonato)iron(III), Fe(acac)3

A solution of acetylacetone (2·0 ml; 19 mmol) in ethanol (10 ml) was added to a solution of $FeCl_3.6H_2O$ (1·4 g; 5·2 mmol) in water (30 ml). The resultant red-black solution was heated on a steam bath before adding a warm solution sodium acetate (3·0 g, 22 mmol) in water (20 ml). A brick red precipitate formed which was collected, recrystallised from ethanol/water and dried. Yield 1·6 g (4·4 mmol; 87%). M.p. 183 - 184°C (Lit.[13] 184°C).

Derivatives of Benzyl Bromide

6.3.12 Attempted preparation of 2-hydroxybenzyl bromide

N-Bromosuccinimide (1·73 g; 9·72 mmol) was added, in portions, to a cold solution of *o*-cresol (1·0 ml; 9·7 mmol) in carbon tetrachloride. The pale yellow solution was heated under reflux till succinimide appeared on the surface of the solution (~10 minutes).[233] The mixture was allowed to cool and the succinimide was filtered off. The orange filtrate was evaporated to dryness affording an orange oil. TLC (90% ethanol:10% hexane) showed strong presence of starting material along with a very faint spot. *1H-NMR (CDCl3/TMS):* δ7·18-6·28 (m; 48H), 5·47 (s; 10·5H, disappeared upon addition of D_2O), 2·54 (s; 4·5H) and 2·17 ppm (s; 34H).

6.3.13 2-Bromomethylphenyl acetate

This compound was prepared by the literature method.[230]

o-Cresyl acetate (20·0 g;0·13 mmol) in carbon tetrachloride (AR; 65 ml) was heated under reflux for 1 hour with NBS (23·8 g; 0·13 mmol) and dibenzoyl peroxide (0·34 g). The mixture was allowed to stand for 1 hour before cooling in an ice-bath and removing the succinimide by vacuum filtration. The filtrate was evaporated to dryness affording a pale yellow oil which was distilled under vacuum yielding a very pale yellow oil. Yield 18·0 g (78·6 mmol; 59%), b.p. 72°C/0·05 mm Hg (Lit. 82°C/0·02 mm Hg,[230] 83°C/0·1 mm Hg[234]). F.W.: calc. 229·08; found *(mass spectrum)*, 230 and 228.

6.3.14 Attempted preparation of 2-methoxypropanebenzyl bromide

Using 2-methoxypropanetoluene (2·83 g; 15·7 mmol) and NBS (2·80 g; 15·7 mmol) in carbon tetrachloride (AR; 15 ml), and following the experimental procedure described in 6.3.12, a black viscous material was obtained. Yield 3·07 g. *^{1}H-NMR (CDCl$_3$/TMS):* δ7·23 - 6·40 (m; 45H), 5·12 (m; 13H), 3·14 and 3·11 (d; 9H) and 2·15 (s; 40H).

6.3.15 2-Methoxybenzyl bromide

This bromide was prepared following a similar procedure to that in the literature.[235]

2-Methylanisole (10·2 ml; 82·2 mmol), NBS (7·32 g; 41·1 mmol), and dibenzoylperoxide (0·21 g; initiator) in carbon tetrachloride (AR; 50 ml) were refluxed under dinitrogen. After 1 hour, more initiator (0·21 g) was added and refluxing continued till succinimide appeared on the surface of the solution (~1 hour). The succinimide was filtered off and the solvent removed with a rotary evaporator leaving behind an orange liquid. The product was fractionally distilled under vacuum yielding unreacted 2-methylanisole (6·71 g; 67% recovery) at 69-72°C/15 mm Hg and a fraction at 128°C/ 15 mm Hg (2·06 g). *^{1}H-NMR (CDCl$_3$/TMS):* δ7·50 - 6·47 (m; 4H, Ar<u>H</u>), 4·49 (s; 0·1H, ArC<u>H</u>$_2$Br), 3·70 (s; 3H, ArOC<u>H</u>$_3$) and 2·15 ppm (s; 3H, ArC<u>H</u>$_3$). The weak peak at δ4·49 ppm indicated that only a small amount of bromide had formed. The remaining peaks were characteristic of the starting material.

Repeating the above experiment using 2-methylanisole (5·00 ml; 40·3 mmol), NBS (3·59 g; 20·2 mmol) and dibenzoyl peroxide (two portions of 0·11 g) in carbon tetrachloride (40 ml; AR) and longer refluxing (7 hours; N$_2$) produced

an orange-red liquid. 2-Methylanisole (0·88 g; 18%) was recovered by distillation (70°C/15 mm Hg). The residue was then distilled and collected in two fractions (0·94 g + 1·54 g). On cooling, each of these solidified into a white solid. ^{1}H-NMR showed both fractions to be mixtures of the starting material and the desired product with the first fraction containing ~64% bromide and the second ~83% bromide. *^{1}H-NMR (CDCl$_3$/TMS):* δ7·36 - 6·46 (m; Ar$\underline{H}$, contains starting material), 4·47 (s; ArC$\underline{H}_2$Br), 3·79 (s; ArOC$\underline{H}_3$), 3·70 (s; ArOC$\underline{H}_3$)* and 3·13 ppm (s; ArC$\underline{H}_3$)*.
*Indicates starting material.

The first fraction above was passed through a column (florisil/hexane) eluting initially with dichloromethane/hexane (1:1) and gradually increasing the polarity to 100% dichloromethane. One long yellow band was observed which was collected as 5 × 10 ml samples. These samples were shown to be identical by TLC (100% dichloromethane) and were combined. Removal of the solvent by rotary evaporation yielded an off-white solid. *^{1}H-NMR (CDCl$_3$/TMS):* δ7·38 - 6·50 (m; Ar$\underline{H}$, contains starting material) 4·53 (s; ArC$\underline{H}_2$Br), 3·84 (s; ArOC$\underline{H}_3$), 3·75 (s; ArOC$\underline{H}_3$)* and 2·16 ppm (s; Ar$\underline{H}$)*. The sample was found to be a mixture of the starting material and the desired product (23 and 77%, respectively, from the integrated ^{1}H-NMR spectrum). *Indicates starting material.

The fraction from column chromatography (containing 77% bromide) and the earlier portion collected from the distillation (containing 83% bromide) were used as such, making allowances for the presence of starting material.

6.3.16 Attempted preparation of 2-(trimethylsilyloxy)benzyl bromide

2-(Trimethylsilyloxy)toluene (2·45 g; 13·6 mmol), NBS (2·41 g; 13·5 mmol), dibenzoyl peroxide (70 mg), carbon tetrachloride (AR; 20 ml), and following the same experimental procedure described in 6.3.13 refluxing under dinitrogen for 2 hours, yielded a red-brown oil. *^{1}H-NMR (CDCl$_3$/TMS):* δ7·63 - 6·80 (m; 4H, Ar-$\underline{H}$), 4·80 (s; 0·1H; C$\underline{H}_2$Br), 2·60 (s; 3H, Ar-C$\underline{H}_3$) and 0·80 ppm (s; 8H; Si(C$\underline{H}_3$)$_3$). This was shown to be mostly unreacted starting material (~90%), with some evidence of the desired product. F.W.: calc. for C$_{10}$H$_{15}$OBrSi, 259·22; found *(mass spectrum)*, 213 [BrCH$_2$ArOSi].

Repeating the reaction several times with varying conditions such as longer reflux, more dibenzoyl peroxide initiator, azoisobutyronitrile as initiator, or irradiating with a 250 watt Hg lamp[236] while refluxing, gave similar results.

Derivatives of Salicylic Acid

6.3.17 2-Acetyloxysalicylic acid

This compound was prepared by the literature method.[194] Salicylic acid (20·0 g; 145 mmol) in acetic anhydride (35 ml; 0·37 mol) was heated at 100°C for 7 hours, with stirring. The resultant pale yellow solution was allowed to cool to room temperature before cooling overnight (8°C). A white crystalline solid was collected and washed with petroleum spirit (5 × 20 ml). Yield 18·0 g (100 mmol; 69%), m.p. 126 - 130°C (Lit.[13] 135°C). *Infrared spectrum:* identical to that of authentic sample.

6.3.18 2-Acetyloxy-5-chlorosalicylic acid

Using 5-chlorosalicylic acid (10·0 g; 57·9 mmol) in acetic anhydride (19 ml; 0·20 mol), and following the experimental procedure described in 6.3.17, a white solid was obtained. Yield 8·90 g (41·5 mmol; 72%), m.p. 139 - 141°C. F.W.: calc for $C_9H_7O_4Cl$, 214·60; found *(mass spectrum)*, 217 and 215 (for ^{37}Cl and ^{35}Cl, respectively).

6.3.19 2-Acetyloxy-3-methylsalicylic acid

Using 3-methylsalicylic acid (10·0 g; 65·7 mmol) in acetic anhydride (15·5 ml; 164 mmol), and following the same experimental procedure described in 6.3.17, a white solid was obtained. Yield 3·46 g (17·8 mmol; 27%), m.p. 105 - 108°C. F.W: calc. for $C_{10}H_{10}O_4$, 194·19; found *(mass spectrum)*, 194.

Derivatives of Benzoyl Chloride

6.3.20 2-Acetyloxybenzoyl chloride

This compound was prepared following a slightly modified procedure to that described in the literature.[194]
2-Acetyloxysalicylic acid (10·0 g, 55·5 mmol) was reacted with thionyl chloride (6·0 ml; 82 mmol) and urea (0·11 g; 1·8 mmol) for 5 hours at 70°C, using a HCl gas absorption trap.[227e] The resultant yellow-orange liquid was distilled under vacuum to yield a colourless liquid which quickly crystallised. Yield 9·81 g (49·4 mmol; 89%), m.p. 46 - 49°C (Lit.[194] 49 - 50°C), b.p.

76°C/~0·2 mm Hg (Lit.[194] 86°C/0·01 mm Hg). F.W.: calc. for $C_9H_7O_3Cl$, 198·61; found *(mass spectrum)*, 163 (Molecular ion less ^{35}Cl).

6.3.21   2-Acetyloxy-5-chlorobenzoyl chloride

Using 2-acetyloxy-5-chlorosalicylic acid (10·0 g; 46·6 mmol), and following the experimental procedure described in 6.3.20, yielded a white solid. Yield 9·04 g (38·8 mmol; 83%), m.p. 80 - 95°C, b.p. 92°C/~0·2 mm Hg. F.W.: calc. for $C_9H_6O_3Cl_2$, 233·05; found *(mass spectrum)*, 197 (Molecular ion less ^{35}Cl).

6.3.22   2-Acetyloxy-3-methylbenzoyl chloride

Using 2-acetyloxy-3-methylsalicylic acid (9·04 g; 46·6 mmol), and following the experimental procedure described in 6.3.20, yielded a white solid. Yield 8·39 g (39·5 mmol; 85%), m.p. 34 - 36°C, b.p. 82°C/0·12 mm Hg. F.W.: calc. for $C_{10}H_9O_3Cl$, 212·63; found *(mass spectrum)*, 214 and 212 (for ^{37}Cl and ^{35}Cl, respectively).

6.4   Dinegative Tridentate Ligands

6.4.1   Schiff Bases

Protonated ligands 4-phenylbutane-2,4-dionebenzoylhydrazone (BzacBhH₂), 4-phenylbutane-2,4-dionesalicyloylhydrazone (BzacSalhH₂), 2-hydroxy-acetophenonebenzoylhydrazone (HapBhH₂), salicylideneamino-*o*-hydroxy-benzene (SalApH₂), salicylaldehydebenzoylhydrazone (SalBhH₂) and salicylaldehydesalicylloylhydrazone (SalSalhH₂) were prepared by methods described by Salam.[92] N-Salicylidene-*o*-hydroxybenzylamine (SalHbaH₂) was prepared by Jones.[94]

6.4.2   Azo Dyes

Protonated ligands *o*-hydroxybenzeneazo-β-naphthol (Ap-β-NapH₂), *p*-methyl-*o*-hydroxybenzeneazo-β-naphthol (*p*^Me^-Ap-β-NapH₂) and *o*-hydroxybenzeneazo-*p*-chlorophenol (Ap-*p*^Cl^-PhenolH₂) were prepared by methods described by Salam.[92]

6.5 Trinegative Tridentate Ligands

The infrared spectral data for all the amide lignds is given in Section 3.5 (Table 3.2).

6.5.1 N-(2-Hydroxyphenyl)salicylamide, H_3L^1

The amide was prepared following a similar experimental procedure to that in the literature.[96]

o-Acetyloxybenzoyl chloride (3·00 g; 15·1 mmol) was dissolved by heating in dioxane (AR; 5 ml). This solution was added, dropwise and under stirring, to a mixture of o-aminophenol (1·65 g; 15·1 mmol) in dioxane (AR; 8 ml). The o-aminophenol slowly dissolved forming a red-brown solution. Stirring was continued at room temperature for 1 hour before adding water (16·5 ml) to dissolve any o-aminophenol hydrochloride. The red-black solution which formed was stirred at room temperature for 6 hours and then cooled overnight (8°C). A light pink precipitate was collected and washed with petroleum spirit (5 × 5ml), and the filtrate concentrated affording a second crop of N-(2-hydroxyphenyl)-2-acetyloxybenzamide. Yield 3·13 g.

To a portion (1·24 g; 4·57 mmol) of the crude product obtained above a mixture of dioxane (LR; 10 ml) and aqueous HCl (35%; 10 ml) was added. The resultant deep red solution was stirred for 24 hours at room temperature. The solution was evaporated to dryness leaving behind a flesh coloured solid which was recrystallised from methanol:water (80:20). Yield 0·94 g (4·10 mmol; 90%), m.p. 163 - 166°C (Lit.[96] 165 - 166°C).

6.5.2 N-(2-Hydroxyphenyl)-5-chlorosalicylamide, H_3L^2

The N-(2-hydroxyphenyl)-2-acetyloxy-5-chlorobenzamide was prepared following a slightly modified experimental procedure to that described in 6.5.1, using 2-acetyloxy-5-chlorobenzoyl chloride (9·04 g; 38·8 mmol) and o-aminophenol (4·23 g; 38·8 mmol). During the hydrolysis of the acetyloxy derivative the mixture was heated at ~90°C to dissolve this amide. The solution was then heated close to reflux for 1 hour and allowed to cool to room temperature. A small amount of beige coloured solid appeared. The mixture was concentrated to ~30 ml, on a rotary evaporator, producing more solid. A brown-grey solid was collected and washed with water (5 × 10ml). Methanol:water (80:20; 80 ml) was added and the mixture heated at 60°C for 1 hour. Any insoluble material was removed by filtration and the brown

filtrate concentrated till the amide began to precipitate. A beige solid was obtained. Yield 4·37 g (16·6 mmol; 43%), m.p. 184 - 185°C. Analysis required for $C_{13}H_{10}NO_3Cl$: C, 59·22; H, 3·82; N, 5·31%. Found: C, 58·35; H, 3·96; N, 5·18%. F.W.: calc., 263·68; found *(mass spectrum)*, 265 and 263 (for ^{37}Cl and ^{35}Cl, respectively).

6.5.3 N-(5-Chloro-2-hydroxyphenyl)salicylamide, H_3L^3

Using 2-acetyloxybenzoyl chloride (2·60 g; 13·1 mmol) and 5-chloro-2-hydroxyanaline (1·88 g; 13·1 mmol), and following the experimental procedure described in 6.5.2, a light pink solid was obtained. Yield 1·22 g (4·63 mmol; 35%), m.p. 187 - 189°C (Lit.^{96} 189 - 191°C). F.W.: calc. for $C_{13}H_{10}NO_3Cl$, 263·68; found *(mass spectrum)*, 265 and 263 (for ^{37}Cl and ^{35}Cl, respectively).

6.5.4 N-(5-Chloro-2-hydroxyphenyl)-5-chlorosalicylamide, H_3L^4

Using 2-acetyloxy-5-chlorobenzoyl chloride (3·02 g; 13·0 mmol) and 5-chloro-2-hydroxyanaline (1·86 g; 13·0 mmol), and following the experimental procedure described in 6.5.2, an almost colourless solid was obtained. Yield 1·63 g (5·47 mmol; 42%), m.p. 226 - 228°C. Analysis calc. for $C_{13}H_9NO_3Cl_2$: C, 52·38; H, 3·04; N, 4·70%. Found: C, 52·21; H, 3·03; H, 4·65%. F.W.: calc., 298·13; found *(mass spectrum)*, 300 and 298 (for ^{37}Cl and ^{35}Cl, respectively).

6.5.5 N-(2-Hydroxyphenyl)-3-methylsalicylamide, H_3L^5

Using 2-acetyloxy-3-methylbenzoyl chloride (4·00 g; 18·8 mmol) and *o*-aminophenol (2·05 g; 18·8 mmol), and following the experimental procedure described in 6.5.2, a light beige solid was obtained. During the hydrolysis of the N-(2-hydroxyphenyl)-2-acetyloxy-3-methylbenzamide a dark brown oil formed. Under vigorous stirring a beige solid was produced. Yield 1·42 g (5·84 mmol; 31%), m.p. 149 - 152°C. Analysis calc. for $C_{14}H_{13}NO_3$: C, 69·12; H, 5·39; N, 5·76%. Found: C, 68·64; H, 5·42; N, 5·65%. F.W.: calc. 243·26; found *(mass spectrum)*, 243.

6.5.6 N-(5-Chloro-2-hydroxyphenyl)-3-methylsalicylamide, H_3L^6

Using 2-acetyloxy-3-methylbenzoyl chloride (4·31 g; 20·3 mmol) and 5-chloro-2-hydroxyanaline (2·91 g; 20·3 mmol), and following the experimental procedure described in 6.5.2, a beige solid was obtained. Yield

1·87 g (6·73 mmol; 33%), m.p. 193 - 195°C. Analysis calc. for $C_{14}H_{12}NO_3Cl$: C, 60·55; H, 4·36; N, 5·04%. Found: C, 60·53; H, 4·44; N, 5·05%. F.W.: calc., 277.71; found *(mass spectrum)*, 279 and 277 (for ^{37}Cl and ^{35}Cl, respectively).

6.5.7 N-(2-Naphthol)salicylamide, H_3L^7

Using 2-acetyloxybenzoyl chloride (1·25 g; 6·28 mmol) and 3-amino-2-naphthol (1·00 g; 6·28 mmol), and following the experimental procedure described in 6.5.2, a yellow-brown solid was obtained. Yield 0·36 g (1·29 mmol; 21%), dec. ~164°C. Analysis calc. for $C_{17}H_{13}NO_3$: C, 73·11; H, 4·69; N, 5·02%. Found: C, 71·29; H, 4·79; N, 4·81%. F.W.: calc, 279·30; found *(mass spectrum)*, 280.

6.5.8 N-(2-Naphthol)-5-chlorosalicylamide, H_3L^8

Using 2-acetyloxy-5-chlorobenzoyl chloride (1·01 g; 4·33 mmol) and 3-amino-2-naphthol (0·68 g; 4·27 mmol), and following the experimental procedure described in 6.5.2, a beige solid was obtained. Yield 0·45 g (1·43 mmol; 34%), m.p. 224 - 226°C. Analysis calc. for $C_{17}H_{12}NO_3Cl$: C, 65·08; H, 3·86;N, 4·46%. Found: C, 64·39; H, 3·93; N, 4·37%. F.W.: calc., 313·74; found *(mass spectrum)*, 316 and 314 (for ^{37}Cl and ^{35}Cl, respectively).

6.5.9 N-(2-Naphthol)-3-methylsalicylamide, H_3L^9

Using 2-acetyloxy-3-methylbenzoyl chloride (1·34 g; 6·30 mmol) and 3-amino-2-naphthol (1·00 g; 6·28 mmol), and following the experimental procedure described in 6.5.2 with 3 hours refluxing during the hydrolysis, a beige solid was obtained. Yield 0·42 g (1·4 mmol; 23%), m.p. 149 - 152°C. F.W.: calc. for $C_{18}H_{15}NO_3$, 293·32; found *(mass spectrum)*, 293.

6.6 Attempted Preparations of 2,2'-Dihydroxybenzyl-phenyl Ether

Glassware was flame-dried and cooled under dinitrogen. All manipulations were carried out under dinitrogen.

6.6.1 Reaction *A*

Sodium metal (78 mg; 3·4 mmol) was dissolved in dry methanol (15 ml). Catechol (0·37 g; 3·4 mmol) was added forming a blue solution which soon turned green then green-brown. The solvent was removed under vacuum and 2-bromomethylphenyl acetate (0·77 g; 3·4 mmol) in dimethylsulphoxide (HPLC grade; 5 ml) was added. The brown-black mixture was allowed to stir overnight at room temperature, becoming red in colour. The mixture was poured into icy water (100 ml) and the resultant brown mixture extracted with diethyl ether (3 × 100 ml). The organic extracts were combined and the yellow solution washed with water (3 × 50 ml), dried over MgSO$_4$, the solvent removed, and the orange-brown oil dried under vacuum. *^{1}H-NMR (CDCl$_3$/TMS):* δ7·13 - 6·40 (m; 8H), 4·95 - 4·87 (3 singlets; 2H) and 2·12 ppm (s; 0·5H). Assuming that the peak observed in the C$\underline{H}_3$CO$_2$- region is due to the acetylated ether this product could contain the desired diol ether with approximately 18% acetylated ether (calculated from the integration spectrum).

6.6.2 Reaction *B*

Catechol (0·50 g; 4·5 mmol) and 2-bromomethylphenyl acetate (1·04 g; 4·5 mmol) were added to powdered KOH (0·26 g; 4·6 mmol) in dry dimethylsulphoxide (9 ml). The pale yellow solution was stirred overnight at room temperature, during which time the solution became darker. The solution was poured into water (100 ml) forming a pale yellow mixture and extracted with dichloromethane (3 × 90 ml). The combined organic extracts were washed with water (5 × 50 ml), dried over MgSO$_4$, and the solvent removed affording a yellow oil. Attempts to crystallise using diethyl ether and dichloromethane/hexane failed. Yield 1·25 g. *Infrared:* 3440 s, 1765 s, 1745 s, 1600 s, 1500 s cm^{-1}. *^{1}H-NMR (CDCl$_3$/ TMS):* δ7·33 - 6·67 (m; 8H), 5·14 - 4·93 (4 singlets; 1·9H), 4·32 (s; 0·5H) and 2·29 - 2·20 ppm (3 singlets; 3H). 2-Bromomethylphenyl acetate was detected at δ4·32 (ArC$\underline{H}_2$Br) and 2·29 ppm (C$\underline{H}_3$CO$_2$-).

The oil was dissolved in methanol and excess KOH added till a colour change was observed. A red solution was formed. After cooling (8°C) overnight, a red-brown precipitate was collected and the filtrate evaporated to dryness giving a red oil.

Red-brown ppt.: yield 75 mg, mp >300°C. *Mass spectrum:* no evidence of the diol ether or the acetylated ether. An intense peak at m/e 110 was present, characteristic of the starting material catechol which is also however, a fragment of the expected product. *Infrared spectrum:* showed it not to be catechol but in fact mostly inorganic material.

In case this product contained some dipotassium salt of the ether, dilute HCl was added and the mixture extracted with dichloromethane. This only yielded the same material.

Red oil: yield 0·83 g. *^{1}H-NMR (CDCl$_3$/TMS):* δ7·35 - 6·52 (m; 8H), 5·17 (s; 0·8H) and 5·03 (s; 1·2H). Catechol was detected at δ6·80 (Ar$\underline{H}$) and 5·17 ppm (O$\underline{H}$; disappears on addition of D$_2$O).

6.6.3 Reaction *C*

In a two-arm tube (inverted "U" tube) fitted with a gas tap was placed KOH (0·52 g; 9·3 mmol) in dimethylsulphoxide (HPLC grade; 8 ml, degassed under vacuum) in one arm and catechol (0·51 g; 4·6 mmol) in the other. The arms were wrapped with aluminium foil protecting the catechol from light and the tube was evacuated before being filled with dinitrogen gas. The tube was then tilted so that the KOH/dimethylsulphoxide mixed with the catechol. A blue solution formed. 2-Bromomethylphenyl acetate (1·06 g; 4·63 mmol) in dimethylsulphoxide (HPLC grade; 1 ml) was then added forming an orange-brown solution which was stirred overnight, protected from light and air. The solution was then poured into an ice-water mixture (80 ml) forming a white mixture which later turned pale yellow. Extracted with dichloromethane (3 × 80 ml). The organic extracts were combined and the yellow solution washed with water (5 × 45 ml), dried over MgSO$_4$, and the solvent removed. The resultant orange oil was dried under vacuum. *^{1}H-NMR (CDCl$_3$/TMS):* δ7·38 - 6·42 (m; 8H), 5·02 - 4·95 (2 singlets; 1·7H), 3·33 (s; 0·3H) and 2·20 - 2·17 ppm (2 singlets; 1H). Integration of the peaks in the aromatic, -C$\underline{H}_2$O- and C$\underline{H}_3$CO$_2$- regions almost supports a 40:60 mixture of acetylated:diol ethers together with some acetic acid. Because of the extraneous peak appearing at δ3·33 ppm the product was not further analysed.

6.6.4 Reaction D

Catechol (0·50 g; 4·5 mmol) was added to a solution of KOH (0·26 g; 4·6 mmol) in dry dimethylsulphoxide (9 ml). 2-Bromomethylphenyl acetate (1·05 g; 4·6 mmol) was then added and the pale yellow solution was stirred under dinitrogen for 2 hours, becoming darker in colour. TLC (100% dichloromethane) showed presence of starting materials so stirring was continued overnight. The reaction still had not gone to completion so the solution was heated for 1 hour at 60 - 70°C. Once again TLC indicated strong presence of starting material. More KOH (0·15 g; 2·7 mmol) was added turning the yellow solution orange-brown. Later KOH (0·10 g; 1·8 mmol) was added. This produced no further change to the solution which was then stirred overnight. The pH of the solution was recorded (~7) before pouring it into water (100 ml). The pale yellow mixture was extracted with dichloromethane (3 × 100 ml). The organic layer was washed with water (5 × 50 ml), dried over MgSO4, and evaporated to dryness affording an orange oil. Yield 1·20 g. *Infrared:* 1770 s cm^{-1}. *Mass spectrum:* m/e found weak peak at m/e 258, characteristic of the acetylated ether, along with more intense peaks at m/e 214 and 216, characteristic of the desired diol ether. *^{1}H-NMR (CDCl3/TMS):* δ7·26 - 6·56 (m; 8H), 5·08 (s; 1·1H), 4·98 (s; 1·1H), 2·23 (m; 0·6H), 2·10 (s; 0·3H) and 2·02 ppm (s; 0·2H). The peak at δ2·02 ppm could be due to the methyl group in acetic acid as this is the product expected from the hydrolysis to remove the protecting group. Although peaks were observed in the correct regions, the integrated spectrum was not consistent with the presence of the desired product or of a mixture of the product with its acetylated form.

6.6.5 Reaction E

To a mixture of KOH (1·02 g; 18·2 mmol) in dry dimethysulphoxide (9 ml) was added catechol (0·50 g; 4·5 mmol) and 2-bromomethylphenyl acetate (2·1 g; 9·2 mmol). The mixture was stirred at room temperature for 1 hour, changing from yellow-brown to brown during this time, and then poured into water (90 ml) forming a pale yellow mixture. Extracted with dichloromethane (4 × 90 ml). The organic extracts were combined, washed with water (4 × 60 ml), dried over MgSO4, and the solvent removed affording an orange oil. The product was dissolved in a minimum amount of dichloromethane. Precipitation with hexane yielded a small amount of yellow solid which was collected. The filtrate when evaporated to dryness afforded a red oil. Trituration in methanol gave a pink-brown precipitate which was collected.

<u>Yellow ppt.</u>: yield 25 mg, m.p. 155°C. *Infrared spectrum:* 3440 w, 1770 m, 1745 m, 1612 s, 1595 s, 1502 s cm^{-1}. *Mass spectrum:* a weak formula weight peak at m/e 258 in the mass spectrum of this crop supports the acetylated ether. A more intense peak observed at m/e 214 for this compound, supports the diol ether, arising possibly from fragmentation of the acetylated ether. *^{1}H-NMR (CDCl$_3$/TMS):* δ7·40 - 6·53 (m; 8H), 5·12 (m; 2·7H) and 2·21 ppm (m; 0·7H). The integration of the peaks in the aromatic and -C$\underline{H}_2$O- regions for the yellow precipitate was almost correct for the desired ether, however the peak at δ5·12 ppm was broad with a few shoulders. The peak was shown by D$_2$O not to contain any unreacted catechol. The weak peak at δ2·21 was attributed to the presence of a small amount of acetylated ether. This was supported by a medium absorption in the carbonyl region of the infrared spectrum. Disappointingly, the yield from this reaction, for the intermediate product, would only be less than 2%.

<u>Pink-brown ppt.</u>: yield 20 mg. *Infrared spectrum:* 3393 m, 1737 m, 1607 s, 1590 s, 1499 s cm^{-1}. *^{1}H-NMR (CDCl$_3$/TMS):* δ7·43 - 6·60 (m; 8H), 5·15 (m; 2·5H), 2·23 (s; 0·9H) and 1·27 ppm (s; 2·8H). The peak observed at δ1·27 ppm is too low to be attributed to C$\underline{H}_3$CO$_2$-, when compared to acetic acid or the starting material 2-bromomethylphenyl acetate, even though a medium absorption was observed in the carbonyl region of the infrared spectrum. Although integration of peaks in the aromatic and expected -C$\underline{H}_2$O- regions was almost correct the multiplet at δ5·15 ppm showed the presence of at least five separate products.

6.6.6 Reaction *F*

A mixture of KOH (0·17 g; 3·0 mmol) in DMSO (2 ml; AR) was stirred for 5 minutes at room temperature. Catechol (0·22 g; 2·0 mmol) was added forming a blue-green mixture. After further stirring for another 5 mins a solution of 2-bromomethylphenyl acetate (0·54 g; 2·4 mmol) in dry dimethylsulphoxide (4 ml) was added forming a brown solution immediately. Stirring, at room temperature was continued overnight. The solution was then poured into an ice-water mixture (40 ml) forming an off-white mixture with a small amount of yellow oil. Extracted with dichloromethane (3 × 60 ml). The organic extracts were combined, washed with water (5 × 10 ml), dried over MgSO$_4$, and evaporated to dryness affording a brown oil.

Dilute HCl (0·1 mol dm^{-3}; 1 ml) was added, followed by ethanol till the oil had dissloved. After stirring for 1 hour at room temperature, the solvents were

removed leaving behind an orange-brown oil. Dichloromethane (LR; 25 ml) was added and the yellow solution washed with water (5 × 10 ml), dried over $MgSO_4$, and evaporated to dryness affording an orange-brown oil with a very small amount of white solid. TLC (90% chloroform:10% hexane) on the oil showed presence of starting material and several products.

<u>Orange-brown oil</u>: *Infrared spectrum:* 3170 s, 1770 s, 1603 s cm^{-1}. *^{1}H-NMR (CDCl$_3$/TMS):* δ6·98 - 6·58 (m; 8H), 5·03 (m; 1·7H) and 2·25 - 2·18 ppm (3 singlets; 2·2H). Peaks were observed in the expected regions for the acetylated ether. However the multiple peaks in the -C<u>H</u>$_2$O- and C<u>H</u>$_3$CO$_2$- regions and their integration is not consistent with the presence of the desired product as the major component. Attempts were made to similarly analyse the white solid yielded from this reaction, but the available material produced a very weak non-informative spectrum.

6.6.7 Reaction *G*

Catechol (0·35 g; 3·2 mmol) and 2-bromomethylphenyl acetate (0·73 g; 3·2 mmol) were added to KOH (0·18 g; 3·2 mmol) in dry dimethylsulphoxide (6 ml). The yellow solution was heated at 85°C for 7·5 hours with stirring. No visible change was observed whilst heating. More KOH (0·18 g; 3·2 mmol) was added, the yellow solution turning yellow-brown immediately. Heating and stirring was continued for another 5.5 hours, during which time the solution turned orange-red. When poured into water (50 ml) a yellow cloudy solution, of pH 6·7, formed. Upon acidification to pH 5 (1 mol dm^{-3} HCl) a pale yellow solution and a brown oil were formed. Extracted with dichloromethane(2 × 60 ml). The organic extracts were combined and the yellow solution washed with water (5 × 25 ml), dried over $MgSO_4$, and the solvent removed affording an orange oil. Yield 0·47 g. *^{1}H-NMR (CDCl$_3$/TMS):* δ7·20 - 6·53 (m; 8H), 5·20 (s; 1·3H), 5·05 (s; 1·1H) and 2·15 - 2·08 ppm (2 singlets; 1·0H). If the peaks at δ2·08 and 2·15 ppm are due to the methyl in acetic acid and the methyl in the acetylated ether respectively, then integration of peaks was consistent with the presence of a mixture of the protected and diol ethers.

The oil was passed through a column (silica/hexane) eluting with dichloromethane. A yellow-orange band was collected. A stationary red band was removed eluting with methanol. The dichloromethane and methanol eluents were evaporated to dryness giving orange and red oils respectively.

Orange oil: yield 0·18 g. *^{1}H-NMR (CDCl$_3$/TMS):* δ9·57 (s;0·1H), 7·27 - 6·33 (m; 8H), 5·05 (s; 0·8H), 4·92 (s; 0·9H), 3·71 - 3·58 (2 singlets; 0·5H), 2·42 (s; 0·1H), 1·93 - 1·83 (2 singlets; 0·6H) and 1·15 ppm (s; 0·6H). If the peak at δ9·57 ppm is due to hydroxyl protons of the diol ether, the integration spectrum suggests this product to be present in very low yield (~3·5%). The two peaks in the expected -C$\underline{H}_2$O- region were shown not to be due to hydroxyl protons of unreacted catechol. Again, integration of these peaks and the multiple peaks in the aromatic region are not consistent with a mixture of the desired product and the acetylated ether as the main products.

Red oil: yield 0·21 g. *^{1}H-NMR (CD$_3$OD/TMS):* δ7·07 - 6·40 (m; 8H) and 4·84 ppm (br.s; 7H). The peak at δ4·84 ppm was shown by D$_2$O not to contain any hydroxyl protons (from either catechol or wet CD$_3$OD). Integration of peaks in the spectrum indicates a 1:1 ratio of aromatic:-C$\underline{H}_2$O- protons.

6.6.8 Reaction *H*

Catechol (0·47 g; 4·3 mmol) and 2-bromomethylphenyl acetate (0·97 g; 4·2 mmol) were added to KOH (0·95 g; 17 mmol) in dry dimethylsulphoxide (8 ml). The reaction was exothermic. The green mixture was stirred at room temperature, under dinitrogen, turning pale brown and then pink-brown. After stirring overnight the mixture developed a red tinge. TLC (100% dichloromethane) showed the presence of starting material, so the mixture was stirred for a further 24 hours at room temperature. Water (80 ml) was added to the mixture forming a red solution with a basic pH. Upon acidification to pH 4 (1 mol dm^{-3} HCl) the mixture turned yellow-orange, and was extracted with dichloromethane (3 × 80 ml) keeping the extracts separate. Each extract was washed with water (5 × 15 ml), dried over MgSO$_4$, and evaporated to dryness affording a red, yellow and yellow oil from extracts one, two and three respectively.

First extract: *^{1}H-NMR (CDCl$_3$/TMS):* δ7·30 - 6·60 (m; 8H), 5·20 (s; 0·6H) and 5·07 ppm (s; 0·9H). No peaks were observed in the C$\underline{H}_3$CO$_2$- region. The singlets were shown by D$_2$O not to be due to hydroxyl protons. One may therefore be due to -C$\underline{H}_2$O- of the diol ether. Integration of peaks does not support the desired product as a major component.

Second extract: *^{1}H-NMR (CDCl$_3$/TMS):* δ7·20 - 6·58 (m; 8H), 5·22 (s; 0·6H), 5·07 (s; 1·4H), 2·92 (s; 0·3H), 2·58 (m; 0·3H) and 1·26 ppm (s; 0·2H). The yellow oil from the second extraction in this experiment showed a similar proton spectrum to that above with the addition of small peaks appearing in the C$\underline{H}_3$CO$_2$- region.

Third extract: ^1H-NMR (CDCl$_3$/TMS): δ7·17 - 6·57 (m), 2·90 (s) and 2·57 ppm (s). This oil was discarded, as no peak at all was observed in the expected -CH$_2$O- region.

6.6.9 Reaction *I*

Catechol (0·49 g; 4·5 mmol) and 2-bromomethylphenyl acetate (1·02 g; 4·5 mmol) were added to a mixture of KOH (1·00 g; 7·8 mmol) in dry dimethylsulphoxide (8 ml). The brown mixture was heated at 80-100°C, with stirring, for 1 hour, becoming yellow-black. Aqueous KOH (saturated solution; 10 ml) was added and the mixture heated again at 80 - 90°C for 1 hour. After cooling to room temperature the mixture was acidified to pH 2 (1 mol dm^{-3} HCl) forming a yellow-brown precipitate. After cooling (8°C) overnight, a black rubbery material had formed in a red solution. The solution was decanted and extracted with dichloromethane (3 × 50 ml). The organic extracts were kept separate and each was washed with water (4 × 15ml), the aqueous layer being strongly coloured in each case. After drying over MgSO$_4$, the solvent was removed from each extract affording an orange, yellow and pale yellow oil from extracts one, two and three, respectively. R$_f$ values (90% dichloromethane; 10% hexane) showed these oils to be identical and so they were combined. Yield not recorded. ^1H-NMR (CDCl$_3$/TMS): δ9·60 (s; 0·1H), 7·40 - 6·17 (m; 8H), 5·07 (s; 0·3H); 3·73 (s; 0·9H), 2·70 (s; 0·2H), 2·33 (s; 0·2H) and 2·05 ppm (s; 0·2H). The peak at δ5·07 ppm was shown not to contain hydroxyl protons of unreacted catechol. Integration of this peak and the aromatic multiplet showed that only approximately 16% diol ether and/or acetylated ether could be present.

Purification of this product was attempted by column chromatography (silica/hexane), eluting initially with 100% dichloromethane and increasing the polarity to 100% methanol. 5 × 10 ml fractions were collected. After TLC (90% dichloromethane:10% methanol), fractions 1 and 2 were combined as were fractions 3,4 and 5. The former combination produced a yellow oil when evaporated to dryness and the latter an orange-red oil. Yields were not recorded.

Yellow oil: ^1H-NMR (CDCl$_3$/TMS): weak spectrum with resonance only in aromatic region.

Orange-red oil: ^1H-NMR (CDCl$_3$/TMS): δ7·23 - 6·35 (m; 8H), 5·58 (br.s; 2·8H) and 2·12 ppm (s; 2·3H). The peak at δ5·58 ppm was so broad that it was only detected by the integration curve. The ratio of protons in the different

enviroments does not support the presence of the acetylated ether, or the diol ether.

The black rubbery material obtained in the preparation was dissolved in a minimum amount of dimethylsulphoxide (LR; 1 - 2 ml). Water (~20 ml) was then added and the mixture extracted with dichloromethane (2 × 50 ml). The combined extracts were treated as in previous attempts, producing a red oil. Yield not recorded. *1H-NMR (CDCl3/TMS):* δ7·40 - 6·33 (m; 8H) and 5·20 ppm (s; 1H). The integration curve revealed a 8:1 proton ratio for the aromatic and -CH₂O- enviroments respectively, inconsistent with the presence of the diol ether.

6.6.10   From 2,2'-Dimethoxybenzylphenyl ether

AlCl3 (0·17 g; 1·3 mmol) was added to a pale orange solution of 2,2'-dimethoxybenzylphenyl ether (0·16 g; 0·65 mmol) in dry benzene (20 ml). The solution turned pale yellow and cloudy. Refluxed under an atmosphere of dinitrogen for 5 hours and allowed to cool under dinitrogen. Removal of the solvent afforded an off-white solid to which dilute HCl (1 mol dm^{-3}; 20 ml) was added. The mixture was stirred at room temperature for 15 minutes before extracting with diethyl ether (3 × 40 ml). The combined ether extracts were washed with water (3 × 30 ml), dried over MgSO4, and the solvent removed affording a light brown solid, which infrared showed to be starting material. Yield 0·14 g (0·57 mmol; 88% recovery).

Repeating the above experiment using AlCl3 (0·69 g; 5.2 mmol) and 2,2'-dimethoxybenzylphenyl ether (0·15 g; 0·61 mmol) afforded a yellow-brown oil. Yield 0·10 g. *1H-NMR (CDCl3/TMS):* δ7·18 - 6·52 (m; 63H) and 3·72 ppm (m; 43H).

6.7   2,2'-Dimethoxybenzylphenyl Ether

Guaiacol (0·70 ml; 6·4 mmol) was added to a mixture of powdered KOH (0·37 g; 6·6 mmol) in dry dimethylsulphoxide (7 ml). The blue-green mixture was stirred at room temperature for 15 minutes becoming very dark green. 2-Methoxybenzyl bromide (1·28 g; 6·37 mmol) was then added and the mixture stirred overnight at room temperature, becoming orange-brown in colour. The mixture was poured into water (70 ml) forming a white emulsion and an orange oil which was then extracted with dichloromethane (3 × 70 ml).

The combined organic extracts were washed with water (6 × 30 ml), dried over Na_2SO_4, and the solvent removed affording an orange oil which, on standing, began to solidify. Petroleum spirit (LR; 20 ml) was added and the mixture stirred vigorously for ~1 minute. A pale orange solid was collected. Concentration of the filtrate gave a second crop of the same material. Yield 0·72 g (2·9 mmol; 46%), m.p. 91 - 93°C. F.W.: calc. for $C_{15}H_{16}O_3$: 244·29; found *(mass spectrum)*, 244. *^{1}H-NMR (CDCl$_3$/TMS):* δ6·81 (m; 8H), 5·14 (s; 2H), 3·81 (s; 3H) and 3·78 ppm (s; 3H). *Infrared spectrum:* 1589 s, 1506 s, 1495 s, 1255 s, 1226 s, 1128 s, 1112 s, 1041 s, 1027 s, 763 s and 738 s cm^{-1}.

6.8   2,2'-Diacetyloxybenzylphenyl Ether

2-Acetyloxyphenol (0·40 g; 2·6 mmol) was added to sodium hydride (51 mg; 2·1 mmol) in dry dimethylsulphoxide (1·0 ml), with stirring under dinitrogen, immediately forming a red-brown solution. 2-Bromomethylphenyl acetate (0·50 g; 2·2 mmol) was added and stirring was continued under dinitrogen. The reaction was slightly exothermic. The solution faded, becoming yellow-orange. As the presence of starting material was found to be present by TLC (100% chloroform) after stirring overnight the solution was stirred for a further 24 hours at room temperature. The resulting yellow-brown solution was poured into water (40 ml) forming a white mixture. It was extracted with dichloromethane (3 × 40 ml) and the combined extracts were washed with water (6 × 17 ml), dried over Na_2SO_4, and the solvent removed affording a cloudy yellow oil. Yield 0·56 g. ^{1}H-NMR (CDCl$_3$/TMS): δ7·52 - 6·68 (m; 6H), 5·63 (br s; 1H) 5·23 - 4·95 (3 singlets; 1H), 2·42 - 2·02 (4 singlets; 4H).

6.9   Attempted Preparation of 2-Hydroxyphenyl-salicylate

6.9.1   From Carboxylic Acid and Alcohol

Salicylic acid (0·50 g; 3·6 mmol) and catechol (0·80 g; 7·3 mmol) were dissolved in dry chloroform (30 ml) and the solution stirred overnight at room temperature. As TLC (90% dichloromethane:10% ethanol) showed only the presence of starting materials, concentrated H_2SO_4 (3 drops) was added and the mixture heated under reflux for 6 hours. After allowing to stand overnight, the chloroform layer had developed a pink tinge. Water (15 ml) was added

and the chloroform layer separated from the aqueous layer, dried over $MgSO_4$, and the solvent removed affording a white solid (0·68 g). It was shown by its infrared spectrum to be a mixture of the two starting materials.

6.9.2 From ethyl salicylate

Method (i)

A number of attempts were made to prepare the ester with reference to the literature method.[218] Catechol (2·00 g; 18·2 mmol) and ethyl salicylate (2·80 ml; 19·1 mmol) were refluxed under dinitrogen, at atmospheric pressure, for 12 hours in diphenyl ether (AR; 2·5 ml). The solution was then allowed to stand overnight, during which time a white-grey solid precipitated. The product was collected, washed thoroughly with hexane and analysed by infrared spectroscopy. Yield 1·00 g (9·08 mmol; 50% recovery of catechol).

Repeating the above procedure gave 18% recovery of catechol.

Method (ii)

Catechol (0·83 g; 7·72 mmol), ethyl salicylate (1·10 ml; 7·49 mmol), diphenyl ether (AR; 4·0 ml) were refluxed under vacuum (~0·18 mm Hg). Yield 0·61 g (5·54 mmol; 73% recovery of catechol). *Infrared (filtrate):* Mostly diphenyl ether with the presence of ethyl salicylate, however a carbonyl absorption at higher frequency (1715 cm^{-1}) than that observed for the ethyl salicylate starting material (1677 cm^{-1}) also appeared suggesting the presence of a new compound. The filtrate was distilled under vacuum to remove some of the diphenyl ether. No solid was afforded after cooling the residue.

6.9.3 From polyphosphate ester (PPE)

The experimental procedure described in the literature[216] was followed in an attempt to prepare the ester, using salicylic acid (0·86 g; 6·2 mmol), catechol (0·68 g; 6·2 mmol) and PPE (10·0 g; 92·6 mmol) in dry chloroform (13 ml). A cloudy yellow oil was afforded which began crystallising on standing. The precipitate was difficult to collect, as much viscous material was still present. Recrystallisation from ethanol/water gave a white waxy solid. TLC (100% chloroform) on this material showed absence of starting materials. Yield 0·40 g. F.W.: calc. for $C_{13}H_{10}O_4$, 230·22; found *(mass spectrum)* 291, 263, 231 [Molecular ion + H]. *Infrared spectrum:* 3224 s, 1688 s, 1585 s cm^{-1}.

6.10 2,2'-Dihydroxystilbene

All glassware was flame-dried and cooled under dinitrogen before use. All manipulations were carried out under dinitrogen.

A modified procedure to that in the literature was used to prepare this alkene.[219]
$TiCl_4$ (2·35 ml; 21·4 mmol) was added to a suspension of Zn (2·77 g; 42·4 mmol) in dry THF (20 ml). The thick green mixture was refluxed under an atmosphere of dinitrogen for 2·5 hours turning brown-black in colour. Salicylaldehyde (1·50 ml; 14·1 mmol) in dry THF (19 ml) was added, dropwise. The mixture was refluxed under an atmosphere of dinitrogen for 3 hours and allowed to stand overnight.

Aqueous K_2CO_3 (10% w/v; 110 ml) was added to the mixture which was then stirred, open to the atmosphere, till oxidation of titanium was complete (formation of yellow mixture). The TiO_2 was filtered off (celite pad). Exhaustive extraction on the filtrate and residue was carried out with diethyl ether. The ether extracts were combined, washed with brine (1 × 50 ml) and dried over $MgSO_4$. The solvent was removed giving a yellow oil. Trituration in chloroform yielded a white crystalline solid. Yield 0·14 g, m.p. 194 - 196°C (Lit.[219] 194·5 - 195·5°C for *trans* isomer). *Infrared spectrum:* 3340 s, 3290 s, 1610 s, 1590 s cm^{-1}. *^{1}H-NMR ($(CD_3)_2SO$/TMS):* δ7·47 - 6·34 (m; 10H, Ar<u>H</u>) and 9·29 ppm (s; 2H, ArO<u>H</u>). *UV-VIS (MeOH, λ (log ε)):* 331 (4·30), 280 (4·15), 232 (4·16) and 210 nm (4·43).

Bis(Dinegative Tridentate) Complexes

6.11 Attempted Preparations of Silicon(IV) Complexes

6.11.1 Si(BzacBh)$_2$

Method (i)

SiCl$_4$ (0·10 ml; 0·87 mmol) was added to a dark yellow solution of BzacBhH$_2$ (0·49 g; 1·7 mmol) and LiOAc.2H$_2$O (0·42 g; 4·1 mmol) in dry ethanol (25ml). The solution became almost colourless on addition of the tetrahalide. After heating under reflux for 4 hours the solution was allowed to stand overnight. The solution was concentrated, on a rotary evaporator till precipitation began, and the resultant mixture was cooled overnight (8°C). A white precipitate was collected. Yield 0·29g, m.p. 221 - 223°C. F.W.: calc. for C$_{34}$H$_{28}$N$_4$O$_4$Si, 584·71; found *(mass spectrum)*, 495, 481, 469, 423, 333. *Infrared spectrum:* 3130 m, 3100 m, 2618 s, 1615 s, 1596 s, 1536 m, 1294 s, 1268 s cm^{-1}. *^{1}H-NMR (CDCl$_3$/TMS):* δ7·93 - 7·27 (m; 5H); 6·39 (s; 1H) and 2·55 ppm (s; 3H).

Method (ii)

The experiment was repeated using SiCl$_4$ (0·87 mmol), BzacBhH$_2$ (1·7 mmol) and sodium ethoxide (3·4 mmol) as the base and refluxing for only 1 hour. NaCl, formed during the reaction, was filtered off and the filtrate concentrated affording a pale yellow solid. Yield 0·15 g, m.p. 221 - 223°C. *Infrared spectrum:* identical to that above. F.W.: found *(mass spectrum)*, 495, 481, 469, 423, 333.

Method (iii)

An identical product to that from method *(ii)*, based on infrared, was obtained under stringent conditions to exclude moisture, with overnight stirring at room temperature instead of refluxing.

Method (iv)

BzacBhH$_2$ (0·50 g; 1·8 mmol) was added to dichloromethane (25 ml; AR) cooled to 0°C (ice-bath), forming a yellow solution. SiCl$_4$ (0·10 ml; 0·87 mmol), also cooled (ice-bath), was added. The solution became slightly darker and was allowed to warm up to room temperature under stirring. A pH

measurement on the solution showed it to be acidic. Triethylamine was added, dropwise, till the solution recorded pH ~7. During this procedure white fumes appeared and a lemon yellow precipitate formed which was collected and washed with diethyl ether (3 × 4 ml). Yield 0·49 g. *Infrared spectrum:* 3380 w, 2604 s, 2496 s, 2359 m, no peaks in the region 2000 - 1470 cm^{-1}.

6.10.2 Si(SalAp)$_2$

SiCl$_4$ (0·10 ml; 0·87 mmol) was added, with stirring and under dinitrogen, to a solution of sodium metal (83 mg; 3·6 mmol) in dry ethanol (20 ml), forming a white mixture due to the formation of NaCl. SalApH$_2$ (0·37 g; 1·7 mmol) was added turning the mixture yellow in colour. The mixture was stirred under dinitrogen for 6 hours at 40 - 50°C. A yellow precipitate was collected and washed with diethyl ether (3 × 5 ml). Yield 0·49 g, dec. 213°C without melting. F.W.: calc. for C$_{26}$H$_{18}$N$_2$O$_4$Si, 450·53; found *(mass spectrum)*, 342, 264, 250. *Infrared spectrum:* 1645 s, 1610 s, 1583 s, 1284 s, 1231 s cm^{-1}.

Using a metal to ligand mole ratio of 1:1 an identical product to that above, based on infrared, was obtained .

6.11.3 Si(Ap-β-Nap)$_2$

All glassware was flame-dried and cooled under dinitrogen before use. Ap-β-NapH$_2$ (0·23 g; 0·87 mmol) was added to a solution of sodium metal (37 mg; 1·6 mmol) in dry ethanol (25 ml) forming a red-black solution. Upon addition of SiCl$_4$ (0·050 ml; 0·44 mmol) a red-burgundy mixture resulted. After stirring for 30 minutes at room temperature, and cooling overnight (8°C), a brown ppt. was collected. A portion was recrystallised from dichloromethane/hexane. Yield 0·31 g (crude), m.p.: 176 - 180°C (crude), 180 - 182°C (recrystallised). *Infrared spectrum (crude):* 3338 w, 1597 s, 1571 w, 1537 w, 1314 s cm^{-1}. *Infrared spectrum (recrystallised):* 1611 m, 1590 w, 1568 m, 1322 w cm^{-1}. F.W.: calc. for C$_{32}$H$_{20}$N$_4$O$_4$Si: 643·23; found *(mass spectrum; crude)*, 541, 507, 483, 471. The recrystallised material only produced peaks due to the background medium used to dissolve the product.

6.12 Germanium(IV) Complexes

The infrared and ^{1}H-NMR spectral data for the products obtained from these reactions are given in Section 2.5.3 (Table 2.6) and Section 2.7 (Table 2.11), respectively.

6.12.1 Ge(Ap-β-Nap)₂

Germanium tetrachloride (0·050 ml; 0·44 mmol) was added, under dinitrogen, to a solution of Ap-β-NapH₂ (0·23 g; 0·87 mmol) and LiOAc.2H₂O (0·18 g; 1·8 mmol) in dry ethanol (25 ml). The brown solution was refluxed under an atmosphere of dinitrogen for 30 minutes and allowed to stand overnight. A brown crystalline solid was collected, washed with petroleum spirit (3 × 3 ml) and recrystallised from dichloromethane/hexane. Yield 80 mg (0·13 mmol; 31%), m.p. >300°C. Analysis calc. for $C_{32}H_{20}N_4O_4Ge$: C, 64·37; H, 3·38; N, 9·38%. Found: C, 64·34; H, 3·51; N, 8·60%. F.W.: calc., 597·13; found *(mass spectrum)*, 598.

6.12.2 Ge(Ap-p^{Cl}-Phenol)₂

Using Ap-p^{Cl}-PhenolH₂ (0·22 g; 0·88 mmol), GeCl₄ (0·050 ml; 0·44 mmol) and LiOAc.2H₂O (0·18 g; 1·8 mmol), the experimental procedure described in 6.12.1 gave a purple solid. Yield 80 mg (0·14 mmol; 32%), m.p. >300°C. Analysis calc. for $C_{24}H_{14}N_4O_4Cl_2Ge$: C, 50·94; H, 2·49; N, 9·90%. Found: C; 54·76; H, 3·15; N, 8·58%. F.W.: calc., 565·90; found *(mass spectrum)*, 566.

6.13 Tin(IV) Complexes

The infrared and ^{1}H-NMR spectral data for the products obtained from these reactions are given in Section 2.5.3 (Table 2.6) and Section 2.7 (Table 2.11), respectively.

6.13.1 Sn(Ap-β-Nap)₂

Stannous chloride dihydrate (86 mg; 0·38 mmol) was added to a solution of Ap-β-NapH₂ (0·20 g; 0·76 mmol) and LiOAc.2H₂O (0·16 g; 1·57 mmol) in dry ethanol (30 ml). The red-brown solution was heated under reflux for 1 hour and allowed to cool to room temperature. Crystals formed and the

mixture was cooled overnight (8°C). A purple-brown solid was collected and recrystallised from dichloromethane/hexane to give a brown crystalline solid. Yield 0·12 g (0·19 mmol; 49%), m.p. >300°C. Analysis calc. for $C_{32}H_{20}N_4O_4Sn$: C, 59·75; H, 3·13; N, 8·71%. Found: C, 57·70; H, 3·18; N, 8·61%. F.W.: calc., 643·23; found *(mass spectrum)*, 644.

Further purification of this material was attempted by passing it through a column of alumina/hexane and eluting with 100% chloroform. However, the complex adhered strongly to the alumina. The polarity of the eluting solvent was increased to 80% chloroform:20% methanol, then 50% chloroform:50% methanol and eventually 100% methanol, but this was to no avail. In an attempt to recover the azo dye ligand, the column was eluted with 100% acetic acid. Slow evaporation of the acidic solution yielded burgundy coloured crystals suitable for X-ray analysis.

6.13.2 Sn(SalHba)₂

SnCl₂ (71 mg; 0·37 mmol) was added to a mixture of SalHbaH₂ (0·17 g; 0·71 mmol) and LiOAc.2H₂O (0·27 g; 2·6 mmol) in dry ethanol (25 ml). The yellow cloudy solution was heated under reflux for 4.5 hours with a silica-gel drying tube fitted to the condenser. After cooling overnight (8°C) the solution was evaporated to dryness leaving behind a yellow solid. Water (25 ml) was added to the solid and the mixture stirred at room temperature for 15 minutes to dissolve the excess LiOAc.2H₂O. A pale yellow solid was then collected and dried under a lamp. Yield 83 mg (0·15 mmol; 41%), m.p. ~140°C. Analysis calc. for $C_{28}H_{22}N_2O_4Sn$: C, 59·09; H, 3·90; N, 4·92%. Found: C, 60·05; H, 4·35; N, 4·79%. F.W.: calc., 569·18; found *(mass spectrum)* , 569.

6.14 Attempted Preparations of Lead(IV) Complexes

The infrared spectral data for the products obtained from these reactions is given in Section 2.5.3 (Table 2.6).

6.14.1 Pb(BzacBh)₂

A solution of lead nitrate (0·30 g; 0·91 mmol), BzacBhH₂ (0·50 g; 1·8 mmol) and LiOAc.2H₂O (0·79 g; 7·7 mmol) in dry ethanol (40ml) was heated under reflux for 5 hours and allowed to cool overnight. A yellow precipitate formed which was collected, washed with petroleum spirit (2 × 3 ml) and

recrystallised from dimethylsulphoxide/ethanol. Yield 0·18 g, dec. 288°C without melting. Analysis calc. for $C_{34}H_{28}N_4O_4Pb$: C,53·47; H, 3·70; N, 7·34%. Found: C, 42·65; H, 2·99; N, 5·82%. F.W.: calc., 763·81; found *(mass spectrum)*, 486.

An identical product was obtained when repeating this reaction with metal:ligand ratio 1:1. Yield 0·17 g (0·35 mmol; 39%), dec. ~265°C. Analysis calc. for $C_{17}H_{14}N_2O_2Pb$: C, 42·06; H, 2·90; N, 5·77%. Found: C, 41·48; 2·98; N, 5·58%. F.W.: calc.,485·50; found *(mass spectrum)*, 487.

6.14.2 Pb(SalAp)$_2$

Method (i)

Using SalApH$_2$ (0·50 g; 2·3 mmol), Pb(NO$_3$)$_2$ (0·39 g; 1·2 mmol) and LiOAc.2H$_2$O (0·80 g; 7·8 mmol), and following the experimental procedure described in 6.14.1, gave an orange precipitate. Yield 0·42 g, m.p. >300°C. Analysis calc. for $C_{26}H_{18}N_2O_4Pb$: C.49·60; H, 2·88; N, 4·45%. Found: C, 37·33; H, 2·21; N, 3·28% [Fits formulation Pb(SalAp): C, 37·32; H, 2·17; N, 3·35%]. F.W.: calc., 418·41; found *(mass spectrum)*, 412.

The reaction was repeated using sodium ethoxide as base and a metal:ligand mole ratio of 1:1. Yield 0·60 g. *Infrared spectrum:* similar to that of the material above. F.W.: calc, 418·41; found *(mass spectrum)*, 420.

Method (ii)

A solution of sodium metal (58 mg; 2·5 mmol) in dry ethanol (10 ml) was added to a solution of SalApH$_2$ (0·25 g; 1·2 mmol) in dry ethanol (10 ml). The resultant red-orange solution was stirred for 5 minutes at room temperature and then evaporated to dryness leaving the orange-brown sodium salt of SalApH$_2$. The solid was dried under vacuum, to ensure all traces of ethanol were removed, and then placed under dinitrogen. The reaction flask was then transferred into a dry box, previously flushed with dinitrogen gas, where dry dichloromethane (20 ml) was added. A yellow solution of Pb(OAc)$_4$ (0·26 g; 0·59 mmol) in dry dichloromethane (10 ml) was added, with stirring, to the above salt forming a brown mixture. Stirring was continued overnight at room temperature. A brown precipitate was collected and recrystallised from dimethylsulphoxide/ethanol. Yield 0·40 g, m.p. >300°C. Analysis found: C, 37·09; H, 2·38; N, 3·32% [in agreement with PbL]. F.W.: found *(mass spectrum)*, 420 [PbL + H].

Method (iii)

An orange precipitate was obtained when a solution of $Pb(OAc)_4$ (0·18 g; 0·41 mmol) in dry dichloromethane (7 ml) was added dropwise, over 2 hours to ensure the ligand was always in excess, to a mixture of $SalApH_2$ (0·18 g; 0·84 mmol) and triethylamine (0·25 ml; 1·8 mmol) in dry dichloromethane (10 ml). Recrystallised from dimethylsulphoxide/ethanol. Yield 44 mg, m.p. >300°C. Analysis found: C, 37·33; H, 2·25; N, 3·22% [in agreement with PbL]. F.W.: found *(mass spectrum)*, 420 [PbL + H].

Method (iv)

The reaction in method *(ii)* was repeated using dimethylsulphoxide instead of dichloromethane. Dimethylsulphoxide (AR; 2 ml) was added to the dry sodium salt of $SalApH_2$ forming a brown solution. The $Pb(OAc)_4$ in dimethylsulphoxide (AR; 2 ml) formed an orange solution which was added dropwise, over 1 hour, to the ligand solution. After stirring overnight, dry ethanol was added dropwise till the solution remained cloudy. A brown precipitate formed on cooling overnight (8°C). Yield 28 mg. Analysis found: C, 37·63; H, 2·47; N, 3·38% [in agreement with PbL].

Method (v) - *from Pb(SalAp)*

$SalApH_2$ (0·50 g; 0·23 mmol) was added to a solution of sodium metal (11 mg; 0·48 mmol) in dry ethanol (5 ml) forming a red solution, which later turned red-black. After stirring for 10 minutes at room temperature the solution was evaporated to dryness under vacuum. Pb(SalAp) (95 mg; 0·23 mmol) dissolved in hot dimethylsulphoxide (AR; minimum amount) was added to the disodium salt of the ligand. The resultant black solution was stirred for 30 minutes at room temperature and allowed to stand overnight. No precipitate formed. Oxygen gas was then bubbled through the solution, for 3 hours, which was then allowed to stand overnight again. No change to the solution took place. Ethanol was then added, dropwise, till the solution remained cloudy, and the mixture cooled overnight (8°C). A dark brown solid was collected and dried under vacuum. Yield 10 mg, m.p. >300°C. *Mass spectrum:* m/e found 481, 459.

6.14.3 Pb(BzacSalh)$_2$

Using $Pb(NO_3)_2$ (0·28 g; 0·85 mmol), $BzacSalhH_2$ (0·50 g; 1·7 mmol) and $LiOAc.2H_2O$ (0·40 g; 0·39 mmol), and following the experimental procedure

described in 6.14.1, a yellow precipitate was obtained. The crude material was recrystallised from dimethylsulphoxide/ethanol. Yield 0·39 g, dec. ~260°C without melting. Analysis calc. for $C_{34}H_{28}N_4O_6Pb$: C, 50·81; H, 3·51; N, 6·97%. Found: C, 40·71; H, 2·91; N, 5·53% [correct for Pb(BzacSalh), requiring: C, 40·71, H, 2·81; N, 5·59%]. F.W.: calc., 803·78; found *(mass spectrum)*, 503 [PbL = 501·50].

6.14.4 Pb(SalSalh)₂

Method (i)

Using Pb(NO₃)₂ (0·32 g; 0·97 mmol), SalSalhH₂ (0·50 g; 2·0 mmol) and LiOAc.2H₂O (0·55 g; 5·4 mmol), and following the experimental procedure described in 6.14.1, yielded a yellow precipitate. The crude material was recrystallised from dimethylsulphoxide/ethanol. Yield 0·42 g, m.p. >300°C. Analysis calc. for $C_{28}H_{20}N_4O_6Pb$: C, 46·99; H, 2·82; N, 7·83%. Found: C, 36·23; H, 2·46; N, 5·84% [correct for Pb(SalSalh), requiring: C, 36·44; H, 2·18; N, 6·07%]. F.W.: calc., 715·68; found *(mass spectrum)*, 462 [PbL = 461·44].

Method (ii)

Repeating the above experiment using sodium ethoxide as base gave an identical product. Analysis found: C, 36·23; H, 2·41; N, 5·86%.

Method (iii) - from Pb(SalSalh)

The procedure described in 6.14.2 (method *(v)*) was followed using sodium metal (17 mg; 0·74 mmol) dissolved in ethanol (8 ml), SalSalhH₂ (0·10 g; 0·39 mmol) in ethanol (8 ml) and Pb(SalSalh) (0·18 g; 0·39 mmol) dissolved in hot dimethylsulphoxide. A yellow precipitate was collected and dried under vacuum. Yield 95 mg, m.p. >300°C. Analysis found: C, 35·93; H, 2·35; N, 5·85% [correct for PbL]. F.W.: found *(mass spectrum)*, 460 [PbL].

6.14.5 Pb(HapBh)₂

Using Pb(NO₃)₂ (0·33 g; 1·0 mmol), HapBhH₂ (0·50 g; 2·0 mmol) and LiOAc.2H₂O (0·47 g; 4·6 mmol), and following the experimental procedure described in 6.14.1, yielded a lemon yellow precipitate. Yield 0·22 g, m.p. >300°C. Analysis calc. for $C_{30}H_{24}N_4O_4Pb$: C, 50·63; H, 3·40; N, 7·87%. Found: C, 39·17; H, 2·71; N, 6·03% [correct for Pb(HapBh), requiring: C,

39·21; H, 2·63; N, 6·10%]. F.W.: calc., 711·74; found *(mass spectrum)*, 461 [PbL = 459·46].

6.14.6 Pb(SalBh)$_2$

Using Pb(NO$_3$)$_2$ (0·35 g; 1·1 mmol), SalBhH$_2$ (0·50 g; 2·1 mmol) and LiOAc.2H$_2$O (0·46 g; 4·5 mmol), and following the experimental procedure described in 6.14.1, yielded a yellow precipitate. The crude material was recrystallised from dimethylsulphoxide/ethanol. Yield 0·17 g, m.p. >300°C. Analysis calc. for C$_{28}$H$_{20}$N$_4$O$_4$Pb: C, 49·19; H, 2·95; N, 8·20%. Found: C, 37·84; H, 2·50; N, 6·25% [correct for Pb(SalBh), requiring: C, 37·75; H, 2·26; N, 6·29%]. F.W.: calc., 683·68; found *(mass spectrum)*, 447 [PbL = 445·44].

6.15 Attempted Preparations of Antimony(V) Complexes

6.15.1 [Sb(SalAp)$_2$]Cl

Sodium metal (54 mg; 2·3 mmol) was dissolved in dry ethanol (20 ml) and the solution added, under dinitrogen, to SalApH$_2$ (0·17 g; 0·80 mmol) forming an orange-red solution. SbCl$_5$ (0·050 ml; 0·39 mmol) was then added turning the solution red-brown in colour. Refluxed under an atmosphere of dinitrogen for 1 hour and allowed to cool overnight. A brown precipitate was collected and washed with cold ethanol (3 × 3 ml). The filtrate was concentrated affording a second crop of brown solid.

First crop: yield 0·13 g. *Infrared spectrum:* showed it to be inorganic material. Second crop: yield 24 mg, dec. ~180°C. *Infrared spectrum:* 1605 s, 1592 sh, 1548 s, 1302 m cm^{-1}. Analysis calc. for C$_{26}$H$_{18}$N$_2$O$_4$ClSb: C, 53·87; H, 3·13; N, 4·83%. Found: C, 33·45; H, 2·26; N, 3·33%. F.W.: calc., 579·64; found *(mass spectrum)*, 630, 615, 582.

6.15.2 Sb(BzacBh)$_2$]Br

Method (i)

BzacBhH$_2$ (0·25 g; 0·89 mmol) was added to a solution of sodium metal (34 mg; 1·5 mmol) in dry ethanol (25 ml) forming a yellow solution. SbBr$_3$ (0·16 g; 0·44 mmol) turning the solution orange immediately. The solution was heated under reflux for 4 hours and allowed to stand overnight.

Concentration of the solution afforded an orange precipitate. Purification of the crude material was attempted: chloroform (AR; 25 ml) was added and after stirring for 10 minutes at room temperature an off-white insoluble solid was removed by filtering. The filtrate was evaporated to dryness affording a dark yellow solid.

<u>Orange solid</u>: yield 0·31 g. *Infrared spectrum:* 3548 m, 3470 m, 3402 s, 3231 m, 2727 w, 1637 s, 1616 s, 1590 s, 1537 s, 1305 s cm^{-1}.

<u>White solid</u>: yield not recorded. *Infrared spectrum :* showed it to be inorganic material.

<u>Yellow solid</u>: yield 0·25 g. *Infrared spectrum:* 1662 s, 1589 s, 1537 s, 130 7s, 3225 w cm^{-1}.

Method (ii)

Repeating method *(i)* with longer refluxing (24 hours) gave a yellow precipitate (first crop) and a dull orange solid (second crop).

<u>Yellow solid</u>: yield 25 mg. *Infrared spectrum:* showed it to be inorganic material.

<u>Orange solid</u>: yield 0·14 g. *Infrared spectrum:* 3392 s, 2728 w, 1636 m, 1616 m, 1590 m, 1559 m, 1539 s, 1306 m cm^{-1}.

6.16   Attempted Preparations of Antimony(III) Complexes

6.16.1   K[Sb(BzacBh)$_2$]

Method (i)

Potassium pyroantimonate (74 mg; 0·27 mmol) was dissolved in warm water (10 ml) and added to a cloudy yellow solution of BzacBhH$_2$ (0·15 g; 0·54 mmol) in ethanol (15 ml). The resulting dark yellow solution was heated under reflux for 16 hours. A white precipitate was collected and washed with cold ethanol (3 × 3 ml). The filtrate was concentrated, on a rotary evaporator, forming an off-white precipitate.

<u>First crop</u>: yield 0·31 g. *Infrared spectrum:* showed it to be inorganic material.

<u>Second crop</u>: yield 94 mg. *Infrared spectrum:* showed it to be unreacted BzacBhH$_2$.

Method (ii)

Sodium metal (28 mg; 1·2 mmol) was added to BzacBhH$_2$ (0·18 g; 0·64 mmol) in dry ethanol (20 ml). The bright yellow solution was evaporated to dryness and the yellow salt afforded dried under vacuum. Dry benzene (20 ml) and potassium antimonyl tartrate hydrate (0·10 g; 0·31 mmol) were added and the yellow mixture heated under reflux for 4 hours. After standing overnight, a dark yellow precipitate was collected and washed with cold benzene (3 × 5 ml) follwed by petroleum spirit (3 × 5 ml). Yield 0·24 g. *Infrared spectrum:* 3195 w, 1673 sh, 1622 m, 1594 m, 1536 s cm^{-1}.

Method (iii)

The reaction in method *(ii)* was repeated, this time by dissolving the potassium antimonyl tartrate hydrate (0·15 g; 0·46 mmol) in a minimum amount of water before adding to a solution of BzacBhH$_2$ (0·25 g; 0·89 mmol) and LiOAc.2H$_2$O (0·18 g; 1·8 mmol) in ethanol. The yellow mixture was stirred at room temperature overnight. A bright yellow precipitate was collected and washed with cold ethanol (3 × 3 ml). The filtrate was concentrated to give a second crop of very pale yellow precipitate.

First crop: yield 0·15 g. *Infrared spectrum:* 3584 w, 3401 mbr, 3225 s, 2728 w, 1662 s, 1602 s, 1581 s, 1556 s, 1535 s, 1316 s cm^{-1}. F.W.: calc. for C$_{34}$H$_{28}$N$_4$O$_4$KSb, 717·47; found *(mass spectrum)*, 567, 287, 280, 262.

Second crop: yield 98 mg. *Infrared spectrum:* 3354 s, 1620 s, 1574 s, 1493 m, 1319 s cm^{-1}.

Method (iv)

Potassium antimonyl tartrate hydrate (0·15 g; 0·46 mmol) was dissolved in water (minimum amount). BzacBhH$_2$ (0·25 g; 0·89 mmol) was dissolved in ethanol (LR; minimum amount) and added to the aqueous solution above. The resultant yellow mixture was heated under reflux for 3 hours and allowed to cool to room temperature. A white precipitate was collected and the yellow filtrate concentrated producing an off-white precipitate.

First crop: yield 0·10 g. *Infrared spectrum:* 3584 m, 3544 m, 3493 m, 3410 m, 1673 s, 1625 s, 1310 m cm^{-1}.

Second crop: yield 0·17 g *Infrared spectrum:* showed it to be unreacted BzacBhH$_2$.

6.16.2 Na[Sb(SalAp)₂]

Method (i)

To a solution of sodium metal (36 mg; 1·6 mmol) in dry ethanol (20 ml) was added SalApH$_2$ (0·15 g; 0·70 mmol) followed by SbCl$_3$ (80 mg; 0·35 mmol). The solution was stirred under dinitrogen (drybox) overnight at room temperature. An orange-brown precipitate was collected under dinitrogen using Schlenk techniques. The filtrate was concentrated yielding a second crop of orange-brown precipitate.

First crop: yield 0·11 g. *Infrared spectrum:* 3370 w, 1610 s, 1590 sh, 1540 m, 1300 m cm⁻¹. F.W.: calc. for C$_{26}$H$_{18}$N$_2$O$_4$NaSb, 567·18; found *(mass spectrum)*, 482, 460, 329.

Second crop: yield 43 mg. *Infrared spectrum:* showed it to be unreacted SalApH$_2$.

Method (ii)

The above procedure was repeated using SalApH$_2$ (0·19 g; 0·89 mmol), sodium metal (44 mg; 1·9 mmol), SbCl$_3$ (0·10 g; 0·44 mmol) and refluxing the solution under dinitrogen for 1 hour. After allowing to stand overnight, an orange precipitate was collected, washed free of any NaCl with water (3 × 3 ml), formed during the reaction, followed by ethanol (5 × 3 ml). The product was then dried under vacuum. Yield 97 mg, m.p. 272 - 273°C. Analysis calc.: C, 55·06; H, 3·20; N, 4·94%. Found: C, 56·23; H, 3·84; N, 4·61%. *Infrared spectrum:* 1603 s, 1579 m, 1559 m, 1537 s, 1315 s cm⁻¹. F.W.: found *(mass spectrum)*, 424, 412, 332.

6.16.3 Na[Sb(BzacBh)₂]

Using BzacBhH$_2$ (0·25 g; 0·89 mmol), Na (43 mg; 1·9 mmol) and SbBr$_3$ (0·17 g; 0·47 mmol), the procedure in Section 6.16.2 (method *(i)*) was followed with refluxing under dinitrogen for 4·5 hours. Bright yellow (first crop) and orange (second crop) solids were obtained.

First crop: yield 52 mg, m.p. 257 - 259°C. *Infrared spectrum:* 3468 w, 1589 s, 1559 s, 1537 s, 1307 s cm⁻¹. F.W.: calc. for C$_{34}$H$_{28}$N$_4$O$_4$NaSb, 701·36; found *(mass spectrum)*, 551 460 446, 399 [SbL].

Second crop: yield 0·42 g. *Infrared spectrum:* 3549 m, 3455 m, 3411 s, 2727 w, 1637 m, 1617 m, 1590 s, 1538 s, 1303 m cm⁻¹ (similar to that of the orange-brown solid yielded by method *(i)* in Section 6.16.2).

6.17 Attempted Preparations of Selenium(IV) Complexes

6.17.1 Se(BzacBh)₂

Method (i)

Triethylamine (0·60 ml; 4·3 mmol) was added to a yellow solution of BzacBhH₂ (0·25 g; 0·89 mmol) in dry dichloromethane (25 ml). The solution became darker yellow in colour and, after being flushed with dinitrogen, was transferred to a dry box previously flushed with dinitrogen gas. Selenium tetrachloride (0·11 g; 0·50 mmol) was added, the solution immediately turning red-brown. After refluxing under dinitrogen for 1 hour and cooling to room temperature, the solution was evaporated to dryness, on a rotary evaporator yielding a red-brown solid. This material was dissolved in a minimum amount of dichloromethane and reprecipitated with hexane. Yield 0·22 g, m.p. 263 - 265°C. F.W.: calc. for $C_{34}H_{28}N_4O_4Se$, 635·58; found *(mass spectrum)*, 240. *Infrared spectrum:* 2750 m, 2620 s, 2507 s, 1490 s, 1403 s, 1372 s, 1337 m, 1178 s, 1977 s, 1042 s, 856 s and 812 s cm^{-1}. No peaks were found in the v(C=N) region.

Method (ii)

The procedure above was repeated, this time in ethanol, obtaining a pale brown solid. Yield 97 mg, m.p. 267 - 269°C. F.W. found *(mass spectrum)*, 239. *Infrared spectrum:* identical to that for the product yielded above.

Control experiment

SeCl₄ (0·11 g; 0·49 mmol) was added to a solution of triethylamine (0·60 ml; 4·3 mmol) in dry dichloromethane (20 ml). The resultant red-brown solution was stirred at room temperature for 10 minutes and then heated under reflux for 1 hour. After cooling to room temperature the solution was concentrated under vacuum and a pink-brown precipitate produced on addition of hexane. Yield 0·24 g. *Infrared spectrum:* identical to that of the product obtained in method *(i)* above.

6.18 Attempted Preparations of Tellurium(IV) Complexes

6.18.1 Te(BzacBh)$_2$

Method (i)

Triethylamine (0·30 ml; 2·2 mmol) was added to a solution of BzacBhH$_2$ (0·20 g; 0·72 mmol) in dry ethanol (15 ml) forming a yellow solution. After transferring the solution to a dry box tellurium tetrachloride (0·10 g; 0·37 mmol) was added, producing a yellow precipitate. Yield 0·38 g, dec. ~115°C. *Infrared spectrum:* 3244 s, 2615 s, 2507 s, 1668 s, 1607 s, 1588 s cm^{-1}.

Method (ii)

A blue-grey solid was obtained when the above reaction was repeated using sodium ethoxide as base and heating the solution under reflux. Yield 0·11 g, m.p. >300°C. *Infrared spectrum:* showed it to be inorganic material.

6.18.2 Te(SalAp)$_2$

Method (i)

Tellurium oxide (0·10 g; 0·63 mmol) was dissolved in HCl (conc.; 5 ml) and then diluted with water (10 ml). The clear solution was then added to a solution of SalApH$_2$ (0·27 g; 1·2 mmol) and LiOAc.2H$_2$O (0·26 g; 2·5 mmol) in ethanol (20 ml; distilled). After extracting with dichloromethane (2 × 30 ml), the organic layer was washed with water (2 × 15 ml), dried over MgSO$_4$, and the solvent removed yielding a marone coloured solid. Yield 44 mg. *Infrared spectrum:* 3392 m, 3179 m, 2559 m, 1645 s, 1611 s and 1583 s cm^{-1}.

Method (ii)

An experiment was also carried out where a solution of Te(IV) in HCl was prepared, as described above in method *(i)*, and then attempts at neutralising it with an aqueous solution of NaOH (10%) were made. Precipitation occurred as the pH approached 7. After adding HCl (1 mol dm^{-3}) till the precipitate dissolved, the solution recorded a pH of 1 - 2. This solution was then added it to an ethanolic solution of SalApH$_2$ (0·27 g; 1·3 mmol) and sodium (68 mg; 3·0 mmol). After extracting with chloroform (3 × 50 ml), the organic layer was washed with water (2 × 25 ml), dried over MgSO$_4$, and evaporated to dryness yielding an orange solid. Yield 0·14 g (52% unreacted SalApH$_2$).

6.18.3 Te(Ap-p^{Cl}-Phenol)$_2$

TeO_2 (50 mg; 0·31 mmol) was dissolved in a minimum amount of conc. HCl. Aqueous NaOH (2 mol dm^{-3}) was added till the solution recorded pH 7. A white precipitate had formed. To this was added a solution of Ap-p^{Cl}-PhenolH$_2$ (0·16 g; 0·64 mmol) and KOH (70 mg; 1·2 mmol) in methanol (LR; 4 ml). After extracting with chloroform (3 × 60 ml) the combined organic extracts were washed with water (2 × 25 ml), dried over MgSO$_4$, and evaporated to dryness yielding a brown solid. Yield 0·15 g (94% unreacted Ap-p^{Cl}-PhenolH$_2$).

Organometal(Dinegative Tridentate) Complexes

The infrared and ^{1}H-NMR spectral data for the diorganogermanium(IV), -tin(IV), -lead(IV) and triphenylantimony(V) complexes of Schiff base and azo dye ligands obtained from these reactions are given in Section 2.5.4 (Table 2.8) and Section 2.7 (Table 2.11), respectively.

6.19 Diphenylgermanium(IV) Complexes

6.19.1 Ph$_2$Ge(BzacBh)

Sodium metal (15 mg; 0·65 mmol) was dissolved in dry ethanol (25 ml). BzacBhH$_2$ (91 mg; 0·33 mmol) was then added forming a yellow solution. After stirring for 10 minutes at room temperature, the solvent was removed under vacuum leaving behind the yellow sodium salt of the ligand. A solution of Ph$_2$GeCl$_2$ (97 mg; 0·33 mmol) in benzene (AR; 50 ml) was added to the salt under dinitrogen. The yellow mixture was refluxed under an atmosphere of dinitrogen for 4 hours, and allowed to cool to room temperature before further cooling overnight (8°C). NaCl formed during the reaction and unreacted ligand were removed by filtration. The filtrate was evaporated to dryness yielding a yellow solid.

The product was purified by adding dichloromethane (LR; 10 ml), removing any insoluble material by filtering the solution through a cotton wool plug, and evaporating the solution to dryness. A bright yellow solid was obtained which was washed thoroughly with hexane and dried under vacuum. Yield 86

mg (0·17 mmol; 52%), m.p. 170 - 175°C. Analysis calc. for $C_{29}H_{24}N_2O_2Ge$: C, 68·96; H, 4·79; N, 5·55%. Found: C, 69·95; H, 5·21; N, 6·27%. F.W.: calc., 505·11; found *(mass spectrum)*, 506.

6.19.2 Ph₂Ge(BzacSalh)

Using BzacSalhH₂ (0·22 g; 0·74 mmol), Ph₂GeCl₂ (0·22 g; 0·74 mmol) and Na metal (38 mg; 1·7 mmol), and following the experimental procedure described in section 6.19.1, a dark yellow solid was obtained. Yield 0·23 g (0·44 mmol; 60%), m.p. 178 - 180°C. Analysis calc. for $C_{29}H_{24}N_2O_3Ge$: C, 66·84; H, 4·64; N, 5·38%. Found: C, 66·43; H, 4·58; N, 5·61%. F.W.: calc., 521·11; found *(mass spectrum)*, 522.

6.19.3 Ph₂Ge(SalAp)

Using SalApH₂ (0·21 g; 0·98 mmol), Ph₂GeCl₂ (0·32 g; 1·1 mmol) and Na metal (46 mg; 2·0 mmol), and following the experimental procedure described in section 6.19.1, an orange solid was obtained. Crystals suitable for X-ray analysis were obtained after cooling the reaction mixture. Recrystallised from dichloromethane/hexane and dried under vacuum. Yield 0·19 g (0·43 mmol; 44%), m.p. 161 - 163°C. Analysis calc. for $C_{25}H_{19}NO_2Ge$: C, 68·55; H, 4·37; N, 3·20%. Found: C, 68·73; H, 4·44; N, 3·21%. F.W.: calc., 438·02; found *(mass spectrum)*, 439. Crystals suitable for structure determination were obtained from benzene/ hexane.

6.19.4 Ph₂Ge(SalBh)

Using SalBhH₂ (0·10 g; 0·42 mmol), Ph₂GeCl₂ (0·13 g; 0·44 mmol) and Na metal (19 mg; 0·83 mmol), and following the experimental procedure described in section 6.19.1, a yellow solid was obtained. Yield 80 mg (0·17 mmol; 41%), m.p. 156 - 160°C. Better analytical figures were obtained after the product was passed through a column (florisil/hexane) eluting with dichloromethane. A broad yellow band was collected and evaporated to dryness yielding a yellow solid which was washed with hexane and dried under vacuum. The thin faint yellow-brown band which remained stationary on the column was discarded. Analysis calc. for $C_{26}H_{20}N_2O_2Ge$: C, 67·15; H, 4·34; N, 6·02%. Found: C, 67·10; H, 4·46; N, 5·80%. F.W.: calc., 465·05; found *(mass spectrum)*, 466.

6.19.5 Ph$_2$Ge(Ap-β-Nap)

Using Ap-β-NapH$_2$ (94 mg; 0·36 mmol), Ph$_2$GeCl$_2$ (0·11 g; 0·37 mmol) and Na metal (16 mg; 0·70 mmol), and following the experimental procedure described in section 6.19.1, an orange-brown solid was obtained. Yield 75 mg (0·15 mmol; 43%), dec. ~110°C. Analysis calc. for C$_{28}$H$_{22}$N$_2$O$_2$Ge: C, 68·48; H, 4·52; N, 5·70%. Found: C, 67·89; H, 4·50; N, 6·90%. F.W.: calc., 491·09; found *(mass spectrum)*, 492.

6.19.6 Ph$_2$Ge(p^{Me}-Ap-β-Nap)

Using p^{Me}-Ap-β-NapH$_2$ (0·13 g; 0·47 mmol), Ph$_2$GeCl$_2$ (0·14 g; 0·47 mmol) and Na metal (22 mg; 0·96 mmol), and following the experimental procedure described in section 6.19.1, a burgundy solid was obtained. Yield 77 mg (0·15 mmol; 33%), dec. ~178°C. Analysis calc. for C$_{29}$H$_{22}$N$_2$OGe: C, 69·23; H, 4·41; N, 5·57%. Found: C, 69·50; H, 4·82; N, 6·88%. F.W.: calc., 503·10; found *(mass spectrum)*, 505.

6.20 Dimethyltin(IV) Complexes

6.20.1 Me$_2$Sn(BzacBh)

Using BzacBhH$_2$ (0·10 g; 0·36 mmol), Me$_2$SnCl$_2$ (78 mg; 0·36 mmol) and Na metal (18 mg; 0·78 mmol),.and following the experimental procedure described in 6.19.1, a bright yellow solid was obtained. Yield 0·13 g (0·30 mmol; 86%), m.p. 125 - 130°C. Analysis calc. for C$_{19}$H$_{20}$N$_2$O$_2$Sn: C, 53·44; H, 4·72; N, 6·56%. Found: C, 54·68; H, 4·78; N, 6·57%. F.W.: calc. 427·07; found *(mass spectrum)*, 428.

6.20.2 Me$_2$Sn(BzacSalh)

Using BzacSalhH$_2$ (0·14 g; 0·47 mmol), Me$_2$SnCl$_2$ (0·10 g; 0·46 mmol) and Na metal (24 mg; 1·0 mmol), and following the experimental procedure described in 6.19.1, a bright yellow solid was obtained. Yield 0·13 g (0·29 mmol; 64%), m.p. 166 - 167°C. Analysis calc. for C$_{19}$H$_{20}$N$_2$O$_3$Sn: C, 51·51; H, 4·55; N,6·32 %. Found: C, 51·54; H, 4·51; N, 6·32%. F.W.: calc. 443·07; found *(mass spectrum)*, 444.

6.20.3 Me₂Sn(SalAp)

Using SalApH₂ (0·10 g; 0·47 mmol), Me₂SnCl₂ (0·10 g; 0·46 mmol) and Na metal (25 mg; 1·1 mmol), and following the experimental procedure described in 6.19.1, a brown solid was obtained. Yield 0·12 g (0·33 mmol; 73%), m.p. 157 - 160°C (Lit.[143] 171 - 173°C). Analysis calc. for $C_{15}H_{15}NO_2Sn$: C, 50·05; H, 4·20; N, 3·89%. Found: C, 49·18; H, 4·39; N, 3·63%. F.W.: calc. 359·98; found *(mass spectrum)*, 360.

6.20.4 Me₂Sn(SalBh)

Using SalBhH₂ (0·10 g; 0·42 mmol), Me₂SnCl₂ (91 mg; 0·41 mmol) and Na metal (19 mg; 0·83 mmol), and following the experimental procedure described in 6.19.1, a fluorescent yellow solid was obtained. The product was purified by adding chloroform (LR; 10 ml), removing any insoluble material by filtering the solution through a cotton wool plug, and evaporating the solution to dryness. The solid was washed with hexane and dried under vacuum. Yield 96 mg (0·25 mmol; 60%), m.p. 140 - 142°C. Analysis calc. for $C_{16}H_{16}N_2O_2Sn$: C, 49·66; H, 4·17; N, 7·24%. Found: C, 51·10; H, 4·20; N, 7·43%. F.W.: calc. 387·01; found *(mass spectrum)*, 388.

6.20.5 Me₂Sn(Ap-β-Nap)

Using Ap-β-NapH₂ (0·15 g; 0·57 mmol), Me₂SnCl₂ (0·13 g; 0·59 mmol) and Na metal (26 mg; 1·1 mmol), and following the experimental procedure described in 6.19.1, a brown solid was obtained. Yield 0·12 g (0·29 mmol; 51%), m.p. 238 - 240°C. Analysis calc. for $C_{18}H_{18}N_2O_2Sn$: C, 52·34; H, 4·39; N, 6·78%. Found: C, 53·73; H, 4·16; N, 6·40%. F.W.: calc. 413·04; found *(mass spectrum)*, 329.

6.20.6 Me₂Sn(*p*^Me-Ap-β-Nap)

Using *p*^Me-Ap-β-NapH₂ (82 mg; 0·29 mmol), Me₂SnCl₂ (65 mg; 0·30 mmol) and Na metal (14 mg; 0·61 mmol), and following the experimental procedure described in 6.19.1, a brown solid was obtained. Yield 72 mg (0·17 mmol; 57%), m.p. 214 - 216°C. Analysis calc. for $C_{19}H_{18}N_2O_2Sn$: C, 53·69; H, 4·27; N, 6·59%. Found: C, 53·10; H, 4·45; N, 6·35%. F.W.: calc. 425·06; found *(mass spectrum)*, 426.

6.21 Dibutyltin(IV) Complexes

6.21.1 *n*-Bu$_2$Sn(BzacBh)

A similar experimental procedure to that described in section 6.19.1 was followed using BzacBhH$_2$ (0·15 g; 0·54 mmol), *n*-Bu$_2$SnCl$_2$ (0·16 g; 0·53 mmol) and Na metal (25 mg; 1·1 mmol). However after filtering the reaction mixture and evaporating the filtrate to dryness a cloudy orange oil was obtained. Hexane (AR; 10 ml) was added and any insoluble material removed by filtering through a cotton wool plug. This filtrate was evaporated to dryness affording an orange waxy solid which was dried under vacuum. Yield 0·15 g (29 mmol; 56%). Analysis calc. for C$_{25}$H$_{32}$N$_2$O$_2$Sn: C, 58·74; H, 6·31; N, 5·48%. Found: C, 56·12; H, 6·24; N, 5·31%. F.W.: calc., 511·23; found *(mass spectrum)*, 512.

6.21.2 *n*-Bu$_2$Sn(BzacSalh)

Using BzacSalhH$_2$ (0·10 g; 0·34 mmol), *n*-Bu$_2$SnCl$_2$ (0·10 g; 0·33 mmol) and Na metal (16 mg; 0·70 mmol), and following the experimental procedure described in section 6.21.1, a yellow-orange solid was obtained. Yield 0·17 g(0·32 mmol; 98%). Analysis calc. for C$_{25}$H$_{32}$N$_2$O$_3$Sn: C, 56·95; H, 6·12; N, 5·31%. Found: C, 55·21; H, 6·24; N, 5·13%. F.W.: calc., 527·23; found *(mass spectrum)*, 528.

6.21.3 *n*-Bu$_2$Sn(SalAp)

Using SalApH$_2$ (0·10 g; 0·47 mmol), *n*-Bu$_2$SnCl$_2$ (0·15 g; 0·49 mmol) and Na metal (27 mg; 1·8 mmol), and following the experimental procedure described in section 6.21.1, a brown oil was obtained. On standing for several weeks the oil solidified and the orange-brown solid was easily scraped off the sides of the flask. Yield 0·16 g (0·36 mmol; 77%), m.p. 58 - 60°C. Analysis calc. for C$_{21}$H$_{27}$NO$_2$Sn: C, 56·79; H, 6·13; N, 3·15%. Found: C, 55·00; H, 5·99; N, 2·97%. F.W.: calc., 444·12; found *(mass spectrum)*, 445.

6.21.4 *n*-Bu$_2$Sn(SalBh)

Using SalBhH$_2$ (0·10 g; 0·42 mmol), *n*-Bu$_2$SnCl$_2$ (0·13 g; 0·43 mmol) and Na metal (20 mg; 0·87 mmol), and following the experimental procedure described in section 6.21.1, a yellow oil was obtained. Yield 0·19 g (0·40 mmol; 97%). Analysis calc. for C$_{22}$H$_{28}$N$_2$O$_2$Sn: C, 56·08; H, 5·99; N, 5·95%.

Found: C, 53·38; H, 6·03; N, 5·32%. F.W.: calc., 471·17; found *(mass spectrum)*, 472.

6.21.5 *n*-Bu₂Sn(Ap-β-Nap)

Using Ap-β-NapH₂ (0·10 g; 0·38 mmol), *n*-Bu₂SnCl₂ (0·12 g; 0·39 mmol and Na metal (19 mg; 0·83 mmol)), and following the experimental procedure described in section 6·21.1, a brown solid was obtained. Yield 92 mg (0·19 mmol; 49%), m.p. 88 - 90°C. Analysis calc. for $C_{24}H_{28}N_2O_2Sn$: C, 58·21; H, 5·70; N, 5·66%. Found: C, 58·59; H, 5·96; N, 5·57%. F.W. calc.: 495·19; found *(mass spectrum)*, 496.

6.21.6 *n*-Bu₂Sn(*p*^{Me}Ap-β-Nap)

Using *p*^{Me}-Ap-β-NapH₂ (0·10 g; 0·36 mmol), *n*-Bu₂SnCl₂ (0·11 g; 0·36 mmol) and Na metal (20 mg; 0·87 mmol), and following the experimental procedure described in section 6.21.1, a purple-brown solid was obtained. Yield 0·15 g (0·29 mmol; 82%), m.p. 96 - 99°C. Analysis calc. for $C_{25}H_{30}N_2O_2Sn$: C, 58·97; H, 5·94; N, 5·50%. Found: C, 22·98; H, 2·66; N, 1·08%. F.W.: calc., 509·22; found *(mass spectrum)*, 510.

6.22 Diphenyltin(IV) Complexes

6.22.1 Ph₂Sn(BzacBh)

Using BzacBhH₂ (83 mg; 0·30 mmol), Ph₂SnCl₂ (0·10 g; 0·29 mmol) and Na metal (15 mg; 0·65 mmol), and following the same experimental procedure described in 6.19.1, a yellow solid was obtained. Yield 0·13 g (0·24 mmol; 81%), m.p. 159 - 162°C. Analysis calc. for $C_{29}H_{24}N_2O_2Sn$: C, 63·19; H, 4·43; N, 5·08%. Found: C, 63·86; H, 4·68; N, 5·73%. F.W.: calc., 551·21; found *(mass spectrum)*, 552.

6.22.2 Ph₂Sn(BzacSalh)

Using BzacSalhH₂ (0·10 g; 0·34 mmol), Ph₂SnCl₂ (0·12 g; 0·35 mmol) and Na metal (17 mg; 0·74 mmol), and following the experimental procedure described in 6.19.1, a dark yellow solid was obtained. Yield 0·15 g (0·26 mmol; 78%), m.p. 200 - 202°C. Analysis calc. for $C_{29}H_{24}N_2O_3Sn$: C, 61·41; H, 4·27; N, 4·94%. Found: C, 60·55; H, 4·26; N, 4·86%. F.W.: calc., 567·21; found *(mass spectrum)*, 568.

6.22.3 Ph₂Sn(SalAp)

Using SalApH₂ (0·12 g; 0·56 mmol), Ph₂SnCl₂ (0·20 g; 0·58 mmol) and Na metal (13 mg; 0·57 mmol), and following the experimental procedure described in 6.19.1, an orange solid was obtained. The crude material was recrystallised from dichloromethane/hexane and dried under vacuum. Yield 0·12 g (0·25 mmol; 44%), m.p. 208 - 210°C (Lit.[143] 215 - 216°C). Analysis calc. for $C_{25}H_{19}NO_2Sn$: C, 62·02; H, 3·96; N, 2·89%. Found: C, 61·36; H, 3·78; N, 2·91%. F.W.: calc., 484·12; found *(mass spectrum)*, 485.

6.22.4 Ph₂Sn(SalBh)

Using SalBhH₂ (0·15 g; 0·62 mmol), Ph₂SnCl₂ (0·22 g; 0·64 mmol) and Na metal (31 mg; 1·3 mmol), and following the experimental procedure described in 6.19.1, a fluorescent yellow solid was obtained. Yield 0·20 g (0·39 mmol; 63%), m.p. 153 - 155°C. Analysis calc. for $C_{26}H_{20}N_2O_2Sn$: C, 61·10; H,3·94; N, 5·48%. Found: C, 60·17; H, 3·96; N, 5·42%. F.W.: calc., 511·15; found *(mass spectrum)*, 512.

6.22.5 Ph₂Sn(Ap-β-Nap)

Using Ap-β-NapH₂ (0·20 g; 0·76 mmol), Ph₂SnCl₂ (0·25 g; 0·73 mmol) and Na metal (34 mg; 1·5 mmol), and following the experimental procedure described in 6.19.1, a dark brown solid was obtained. Yield 0·37 g (0·69 mmol; 95%), m.p. >300°C. Analysis calc. for $C_{28}H_{20}N_2O_2Sn$: C, 62·84; H, 3·77; N, 5·23%. Found: C, 61·58; H, 3·78; N, 5·23%. F.W.: calc., 535·17; found *(mass spectrum)*, 536.

6.22.6 Ph₂Sn(p^{Me}-Ap-β-Nap)

Using p^{Me}-Ap-β-NapH₂ (0·10 g; 0·36 mmol), Ph₂SnCl₂ (0·12 g; 0·35 mmol) and Na metal (19 mg; 0·83 mmol), and following the experimental procedure described in 6.19.1, a purple-brown solid was obtained. The product was purified by adding benzene (LR; 10 ml), removing any insoluble material by filtering the solution through a cotton wool plug, and evaporating the solution to dryness. After washing thoroughly with hexane, the solid was dried under vacuum. Yield 0·12 g (0·22 mmol; 63%), dec. ~150°C. Analysis calc. for $C_{29}H_{22}N_2O_2Sn$: C, 63·42; H, 4·04; N, 5·10%. Found: C, 59·95; H, 3·93; N, 4·87%. F.W.: calc., 549·20; found *(mass spectrum)*, 550.

6.23 Diphenyllead(IV) Complexes

6.23.1 Ph$_2$Pb(BzacBh)

Using BzacBhH$_2$ (65 mg; 0·23 mmol), Ph$_2$PbCl$_2$ (0·10 g; 0·23 mmol) and Na metal (12 mg; 0·52 mmol), and following the experimental procedure described in section 6.19.1, a yellow solid was obtained. The crude material was recrystallised from dichloromethane/hexane and dried under vacuum. Yield 0·10 g (0·16 mmol; 68%), m.p. 147 - 150°C. Analysis calc. for C$_{29}$H$_{24}$N$_2$O$_2$Pb: C, 54·45; H, 3·78; N, 4·38%. Found: C, 54·05; H, 3·60; N, 4·38%. F.W.: calc., 639·71; found *(mass spectrum)*, 640.

6.23.2 Ph$_2$Pb(BzacSalh)

Using BzacSalhH$_2$ (0·20 g; 0·67 mmol), Ph$_2$PbCl$_2$ (0·29 g; 0·67 mmol) and Na metal (30 mg; 1·3 mmol), and following the experimental procedure described in section 6.20.4, a bright yellow solid was obtained. Yield 0·39 g (0·59 mmol; 89%), m.p. 138 - 140°C. Analysis calc. for C$_{29}$H$_{24}$N$_2$O$_3$Pb: C, 53·12; H, 3·69; N, 4·27%. Found: C, 53·33; H, 3·86; N, 4·24%. F.W.: calc., 655·71; found *(mass spectrum)*, 657.

6.23.3 Ph$_2$Pb(SalAp)

Using SalApH$_2$ (50 mg; 0·23 mmol), Ph$_2$PbCl$_2$ (0·10 g; 0·23 mmol) and Na metal (11 mg; 0·48 mmol), and following the experimental procedure descibed in section 6.19.1, a yellow-orange solid was obtained. The crude material was recrystallised from dichloromethane/hexane) and dried under vacuum. Yield 0·12 g (0·21 mmol; 91%), m.p. 230 - 232°C (Lit.[105] 232 - 235°C). Analysis calc. for C$_{25}$H$_{19}$NO$_2$Pb: C, 52·44; H, 3·34; N, 2·44%. Found: C, 54·22; H, 3·42; N, 2·48%. F.W.: calc., 572·62; found *(mass spectrum)*, 573. Crystals suitable for X-ray analysis were obtained from dichloromethane/hexane.

6.23.4 Ph$_2$Pb(SalBh)

Using SalBhH$_2$ (0·10 g; 0·42 mmol), Ph$_2$PbCl$_2$ (0·18 g; 0·42 mmol) and Na metal (18 mg; 0·78 mmol), and following the experimental procedure described in section 6.19.1, a yellow solid was obtained. Yield 0·18 g (0·30 mmol; 72%), m.p. 178 - 180°C. Analysis calc. for C$_{26}$H$_{20}$N$_2$O$_2$Pb: C, 52·08; H, 3·36; N, 4·67%. Found: C, 52·05; H, 3·40; N, 4·67%. F.W.: calc., 599·65; found *(mass spectrum)*, 601.

6.23.5 Ph₂Pb(Ap-β-Nap)

Using Ap-β-NapH₂ (0·10 g; 0·38 mmol), Ph₂PbCl₂ (0·16 g; 0·37 mmol) and Na metal (17 mg; 0·74 mmol), and following the experimental procedure descibed in section 6.19.1, a purple-brown solid was obtained. The product was purified by column chromatography as in 6.19.4, this time eluting with chlorofom. Yield 0·17 g (0·27 mmol; 74%), m.p. >300°C. Analysis calc. for $C_{28}H_{20}N_2O_2Pb$: C, 53·92; H, 3·23; N, 4·49%. Found: C, 53·94; H, 3·54; N, 3·08%. F.W.: calc., 623·67; found *(mass spectrum)*, 617.

6.23.6 Ph₂Pb(p^{Me}-Ap-β-Nap)

Using p^{Me}-Ap-β-NapH₂ (99 mg; 0·36 mmol), Ph₂PbCl₂ (0·16 g; 0·37 mmol) and Na metal (19 mg; 0·83 mmol), and following the experimental procedure descibed in section 6.22.5, a purple-brown solid was obtained. Yield 0·18 g (0·28 mmol; 79%), m.p. >300°C. F.W.: calc., 637·70; found *(mass spectrum)*, 643, 638.

6.24 Triphenylantimony(V) Complexes

6.24.1 Ph₃Sb(BzacBh)

Using BzacBhH₂ (0·10 g; 0·36 mmol), Ph₃SbCl₂ (0·15 g; 0·35 mmol) and Na metal (16 mg; 0·70 mmol), the experimental procedure described in section 6.19.1 gave a yellow solid. Yield 0·18 g (0·29 mmol; 81%), m.p. 189 - 191°C. Analysis calc. for $C_{35}H_{29}N_2O_2Sb$: C, 66·58; H, 4·63; N, 4·44%. Found: C, 65·44; H, 4·56; N, 4·25%. F.W.: calc., 631·38; found *(mass spectrum)*, 631.

6.24.2 Ph₃Sb(BzacSalh)

Using BzacSalhH₂ (82 mg; 0·28 mmol), Ph₃SbCl₂ (0·12 g; 0·28 mmol) and Na metal (14 mg; 0·61 mmol), the experimental procedure described in section 6.19.1 gave a bright yellow solid. Yield 0·15 g (0·23 mmol; 84%), m.p. 187 - 189°C. Analysis calc. for $C_{35}H_{29}N_2O_3Sb$: C, 64·94; H, 4·52; N, 4·33%. Found: C, 63·95; H, 4·51; N, 3·92%. F.W.: calc., 647·38; found *(mass spectrum)*, 647.

6.24.3 Ph₃Sb(SalAp)

Using SalApH$_2$ (51 mg; 0·24 mmol), Ph$_3$SbCl$_2$ (98 mg; 0·23 mmol) and Na metal (15 mg; 0·65 mmol), the experimental procedure described in section 6.19.1 gave a mustard yellow solid. The crude material was recrystallised from dichloromethane/hexane and dried under vacuum. Yield 0·11 g (0·19 mmol; 84%), m.p. 252 - 253°C (Lit.[123] 249 - 250°C). Analysis calc. for C$_{31}$H$_{24}$NO$_2$Sb: C, 65·98; H, 4·29; N, 2·48%. Found: C, 65·47; H, 4·26; N, 2·46%. F.W.: calc., 564·29; found *(mass spectrum)*, 564. Crystals suitable for X-ray analysis were obtained from dichloromethane/hexane.

6.24.4 Ph₃Sb(SalBh)

Using SalBhH$_2$ (0·10 g; 0·42 mmol), Ph$_3$SbCl$_2$ (0·18 g; 0·42 mmol) and Na metal (19 mg; 0·83 mmol), the experimental procedure described in section 6.19.1 gave a pale yellow solid. Yield 0·22 g (0·37 mmol; 89%), m.p. 96 - 98°C. Analysis calc. for C$_{32}$H$_{25}$N$_2$O$_2$Sb: C, 65·00; H, 4·26; N, 4·39%. Found: C, 64·16; H, 4·29; N, 4·74%. F.W.: calc., 591·31; found *(mass spectrum)*, 593.

6.24.5 Ph₃Sb(Ap-β-Nap)

Using Ap-β-NapH$_2$ (0·10 g; 0·38 mmol), Ph$_3$SbCl$_2$ (0·16 g; 0·38 mmol) and Na metal (19 mg; 0·83 mmol), the experimental procedure described in section 6.22.6 gave a bugundy solid. Yield 0·20 g (0·33 mmol; 86%), dec. ~115°C. Analysis calc. for C$_{34}$H$_{25}$N$_2$O$_2$Sb: C,66·37; H, 4·10; N, 4·55%. Found: C, 66·36; H, 4·13; N, 4·28%. F.W.: calc., 615·34; found *(mass spectrum)*, 608.

6.24.6 Ph₃Sb(*p*^{Me}-Ap-β-Nap)

Using *p*^{Me}-Ap-β-NapH$_2$ (0·10 g; 0·36 mmol), Ph$_3$SbCl$_2$ (0·15 g; 0·35 mmol) and Na metal (18 mg; 0·78 mmol), the experimental procedure described in section 6.19.1 gave a dark burgundy crystalline solid. The product was purified by column chromatography as in Section 6.19.4. Yield 0·17 g (0·27 mmol; 76%), m.p. 214 - 215°C. Analysis calc. for C$_{35}$H$_{27}$N$_2$O$_2$Sb: C, 66·80; H, 4·32; N, 4·45%. Found: C, 66·91; H, 4·22; N, 4·39%. F.W.: calc., 629·36; found *(mass spectrum)*, 628.

6.25 Amide Complexes of Manganese

In all cases below, crude samples or the amide complexes were analysed by infrared and electronic spectroscopy, magnetic moment, electrochemistry, and conductivity measurement. Details of these are in the relevant sections in Chapter 3. Results from attempts made to purify the manganese compounds are discussed in Section 3.4. Unless otherwise stated, formula weights, yields and microanalytical calculations below are based on the anhydrous formula for the complexes.

6.25.1 $K_2[Mn(2\text{-}OC_6H_4CONC_6H_4O\text{-}2)_2].3.5H_2O$ -$K_2[MnL^1_2].xH_2O$

This complex was prepared by the literature method.[96]
To a solution of N-(2-hydroxyphenyl)salicylamide (0.10 g; 0.44 mmol) and powdered KOH (65 mg; 1.2 mmol) in dry methanol (5 ml) was added manganese(II) acetate tetrahydrate (54 mg; 0.22 mmol) forming a brown-black solution. While stirring at room temperature the solution turned green-black. Stirring was continued overnight and the solution was then cooled (8°C) for 3 days. The solution was then concentrated on a rotary evaporator to ~2.5 ml. The green-black solid which formed was collected and recrystallised from methanol. Yield 50 mg (0.077 mmol, 35% based on hydrated form), m.p. >300°C (not reported in Lit.[96]). F.W.: calc. (hydrated), 648.62; found *(mass spectrum)*, 585 (anhydrous formula).

6.25.2 $K_2[Mn(2\text{-}OC_6H_3(5\text{-}Cl)CONC_6H_4O\text{-}2)_2].xH_2O$ -$K_2[MnL^2_2].xH_2O$

Using N-(2-hydroxyphenyl)-5-chlorosalicylamide (0.51 g; 1.9 mmol), KOH (0.29 g; 5.2 mmol) and Mn(OAc)$_2$.4H$_2$O (0.24 g; 0.98 mmol), the experimental procedure described in 6.25.1 yielded a green-black crystalline solid. Yield 0.34 g (0.52 mmol, 53%), dec. ~150°C. F.W.: calc. for $C_{26}H_{14}N_2O_6Cl_2K_2Mn$, 654.45; found *(mass spectrum)*, 652. Analysis calc.: C, 47.72; H, 2.16; N, 4.28%. Found: C, 43.37; H, 2.33; N, 3.61%.

An attempt was made to purify the crude material obtained above by chromatography on an alumina/hexane column eluting with methanol.

6.25.3 $K_2[Mn(2-OC_6H_3(5-Cl)CONC_6H_3(5-Cl)O-2)_2].xH_2O$
$-K_2[MnL^4_2].xH_2O$

Using N-(5-chloro-2-hydroxyphenyl)-5-chlorosalicylamide (0·36 g; 1·2 mmol), KOH (0·18 g; 3·2 mmol) and $Mn(OAc)_2.4H_2O$ (0·15 g; 0·61 mmol), the experimental procedure described in 6.25.1 yielded a green-black solid. Yield 0·17 g (0·24 mmol, 38%), m.p. 258 - 260°C. F.W.: calc. for $C_{26}H_{12}N_2O_6Cl_4K_2Mn$, 723·34; found *(mass spectrum)*, 723. Analysis calc.: C, 43·17; H, 1·67; N, 3·87%. Found: C, 36·29, 36·70, 36·68, 35·97 and 39·63%; H, 2·29, 2·88, 2·97, 2·69 and 2·14%; N, 3·09, 2·62, 3·36, 2·70 and 3·27% for several samples, respectively.

6.25.4 $K_2[Mn(2-OC_6H_3(3-Me)CONC_6H_4O-2)_2].xH_2O$
$-K_2[MnL^5_2].xH_2O$

Using N-(2-hydroxyphenyl)-3-methylsalicylamide (0·30 g; 1·2 mmol), KOH (0·19 g; 3·4 mmol) and $Mn(OAc)_2.4H_2O$ (0·15 g; 0·61 mmol), the experimental procedure described in 6.25.1 yielded a green-black crystalline solid. Yield 0·23 g (0·37 mmol, 61%), dec 267°C. F.W.: calc. for $C_{28}H_{20}N_2O_6K_2Mn$, 613·62; found *(mass spectrum)*, 613. Analysis calc.: C, 54·81; H, 3·29; N, 4·57%. Found (duplicate analysis): C, 43·48 (43·51); H, 2·78 (2·73); N, 3·13 (3·24)%.

Analysis on a sample from a different preparation but following the same procedure described above gave: C, 46·20; H, 3·27; N, 3·27%.

6.25.5 $K_2[Mn(2-OC_6H_3(3-Me)CONC_6H_3(5-Cl)O-2)_2].xH_2O$
$-K_2[MnL^6_2].xH_2O$

Using N-(2-hydroxy-5-chlorophenyl)-3-methylsalicylamide (0·52 g; 1·9 mmol), KOH (0·28 g; 5·0 mmol) and $Mn(OAc)_2.4H_2O$ (0·23 g; 0·94 mmol), the experimental procedure described in 6.25.1 yielded a green-grey solid. Yield 0·27 g (0·40 mmol, 42%), dec. 250°C. F.W.: calc. for $C_{28}H_{18}N_2O_6Cl_2K_2Mn$, 682·51; found *(mass spectrum)*, 683. Analysis calc.: C, 49·28; H, 2·66; N, 4·10%. Found (duplicate analysis): C, 39·67 (37·95); H, 3·32 (2·93); N, 2·63 (2·24)%.

Analysis on a sample from a different preparation but following the same procedure described above gave: C, 41·56; H, 2·86; N, 2·74%.

6.25.6 $K_2[Mn(2-OC_6H_4CONC_{10}H_6O-2)_2].xH_2O$
$-K_2[MnL^7_2].xH_2O$

No solid was obtained when treating N-(2-naphthol)salicylamide (0·10 g; 0·36 mmol), KOH (40 mg; 0·71 mmol) and $Mn(OAc)_2.4H_2O$ (45 mg; 0·18 mmol) as in procedure 6.25.1, even after concentrating and cooling the solution repeatedly. The solution was evaporated to dryness giving a brown-black solid. Yield 0·17 g (0·25 mmol; 135%), dec. ~200°C. F.W.: calc. for $C_{34}H_{20}N_2O_6K_2Mn$, 685·68; found *(mass spectrum)*, 687.

An attempt was made to purify the crude material obtained above by recrystallisation from methanol/chloroform.

6.25.7 $K_2[Mn(2-OC_6H_3(5-Cl)CONC_{10}H_6O-2)_2].xH_2O$
$-K_2[MnL^8_2].xH_2O$

Using N-(2-naphthol)-5-chlorosalicylamide (80 mg; 0·25 mmol), KOH (29 mg; 0·52 mmol) and $Mn(OAc)_2.4H_2O$ (31 mg; 0·13 mmol), the procedure described in 6.25.6 yielded a brown-black solid. Yield 0·11 g (0·15 mmol; 115%), m.p. >300°C. A portion of this product was recrystallised from methanol/chloroform giving a brown-black solid. F.W.: calc. for $C_{34}H_{18}N_2O_6Cl_2K_2Mn$ (anhydrous), 754·57; found *(mass spectrum)*, 756 (crude) and 651 (recrystallised).

An attempt was made to purify the crude material obtained above by recrystallisation from methanol/chloroform.

6.25.8 $K_2[Mn(2-OC_6H_3(3-Me)CONC_{10}H_6O-2)_2].xH_2O$
$-K_2[MnL^9_2].xH_2O$

Using N-(2-naphthol)-3-methyl-salicylamide (0·10 g; 0·34 mmol), KOH (38 mg; 0·68 mmol) and $Mn(OAc)_2.4H_2O$ (43 mg; 0·18 mmol) in dry methanol (6 ml), the procedure described in 6.25.6 yielded a brown-black solid. Yield 0·19 g (0·27 mmol, 152%), dec. ~270 - 275°C. F.W.: calc. for $C_{36}H_{24}N_2O_6K_2Mn$, 713·74; found *(mass spectrum)*, 714.

An attempt was made to purify the crude material obtained above by recrystallisation from methanol/chloroform. F.W. found after recrystallisation *(mass spectrum)*, 714. Analysis calc.: C, 60·58; H, 3·39; N, 3·92%. Found (duplicate analysis): C, 44·48 (44·34); H, 3·32 (3·36); N, 2·15 (2·22)%.

6.26 Amide Complexes of Titanium

Glassware was flame-dried and cooled under N_2. All manipulations were carried out under an atmosphere of dinitrogen using Schlenk techniques. In all cases, the amide complexes were analysed by infrared and electronic spectroscopy, electrochemistry and conductivity measurement. Details of these are in the relevant sections in Chapter 3. Results from attempts made to purify the titanium compounds are discussed in Section 3.4. Unless otherwise stated, formula weights, yields and microanalytical calculations below are based on the anhydrous formula for the complexes.

6.26.1 $K_2[Ti(2-OC_6H_4CONC_6H_4O-2)_2].xH_2O$
$-K_2[TiL^1_2].xH_2O$

To a pale yellow solution of N-(2-hydroxyphenyl)salicylamide (0·13 g; 0·57 mmol) and powdered KOH (35 mg; 0·62 mmol) in dry methanol (6 ml) was added titanium tetrabutoxide (0·10 ml; 0·29 mmol) with stirring. The solution turned orange-red immediately. Stirring was continued overnight at room temperature during which time a yellow precipitate formed. After cooling the mixture for 6 days (8°C) the yellow precipitate (10 mg) was removed by filtration. The orange-red filtrate was concentrated and cooled, repeatedly, trying to obtain crystals. Eventually it was evaporated to dryness affording an orange transparent solid. Yield 0·14 g (0·24 mmol, 84%), dec. ~265°C. Analysis calc. for $C_{26}H_{16}N_2O_6K_2Ti$: C, 53·98; H, 2·79; N, 4·84%. Found: C, 51·90; H, 3·64; N, 4·35%. F.W.: calc., 578·53; found *(mass spectrum)*, 579.

An attempt was made to purify the crude material obtained above by chromatography on an alumina/hexane column eluting with methanol.

6.26.2 $K_2[Ti(2-OC_6H_3(5-Cl)CONC_6H_4O-2)_2].xH_2O$
$-K_2[TiL^2_2].xH_2O$

Using N-(2-hydroxyphenyl)-5-chlorosalicylamide (0·15 g; 0·57 mmol), powdered KOH (32 mg; 0·57 mmol) and $Ti(OBu)_4$ (0·10 ml; 0·29 mmol), the experimental procedure described in 6.26.1 yielded an orange-brown solid. Yield 0·17 g (0·26 mmol, 91%), dec. ~250°C. Purification by column chromatography was attempted. Analysis calc. for $C_{26}H_{14}N_2O_6Cl_2K_2Ti$: C, 48·24; H, 2·18; N, 4·33%. Found: C, 42·71; H, 3·01; N, 3·71%. F.W.: calc., 647·42; found *(mass spectrum)*, 647.

An attempt was made to purify the crude material obtained above by chromatography on a florisil/(95% chloroform:5% methanol) column eluting with methanol. F.W. found after chromatography *(mass spectrum)*, m/e >647.

6.26.3 $K_2[Ti(2\text{-}OC_6H_4CONC_6H_3(5\text{-}Cl)O\text{-}2)_2].xH_2O$ $\text{-}K_2[TiL^3{}_2].xH_2O$

Using N-(5-chloro-2-hydroxyphenyl)salicylamide (0·15 g; 0·57 mmol), powdered KOH (32 mg; 0·57 mmol) and Ti(OBu)₄ (0·10 ml; 0·29 mmol), the experimental procedure described in 6.26.1 yielded an orange-red solid. Yield 0·21 g (0·32 mmol, 112%), dec. ~250°C. F.W. calc. for $C_{26}H_{14}N_2O_6Cl_2K_2Ti$: 647·42; found *(mass spectrum)*, 646.

An attempt was made to purify the crude material obtained above by recrystallisation from methanol and chromatography on an alumina/hexane column eluting with methanol. Analysis calc. for $C_{26}H_{14}N_2O_6Cl_2Ti$: C, 48·24; H, 2·18; N, 4·33%. Found (after column chromatography): C, 36·92; H, 2·89; N, 3·09%.

6.26.4 $K_2[Ti(2\text{-}OC_6H_3(5\text{-}Cl)CONC_6H_3(5\text{-}Cl)O\text{-}2)_2].xH_2O$ $\text{-}K_2[TiL^4{}_2].xH_2O$

Using N-(5-chloro-2-hydroxyphenyl)-5-chlorosalicylamide (0·17 g; 0·57 mmol), powdered KOH (32 mg; 0·57 mmol) and Ti(OBu)₄ (0·10 ml; 0·29 mmol), the experimental procedure described in 6.26.1 yielded an orange-red solid. Yield 0·22 g (0·31 mmol, 106%), dec. ~200°C. Analysis calc. for $C_{26}H_{12}N_2O_6Cl_4K_2Ti$: C, 43·60; H, 1·69; N, 3·91%. Found (duplicate analysis): C, 38·82 (38·89); H, 2·56 (2·61); N, 3·29 (3·29)%. F.W.: calc., 716·31; found *(mass spectrum)*, 717.

Attempts were made to purify the crude material obtained above by chromatography on a florisil/(95% chloroform:5% methanol) column eluting with methanol, and on an alumina/hexane column eluting with methanol.

6.26.5 $K_2[Ti(2\text{-}OC_6H_3(3\text{-}Me)CONC_6H_4O\text{-}2)_2].xH_2O$ $\text{-}K_2[TiL^5{}_2].xH_2O$

Using N-(2-hydroxyphenyl)-3-methylsalicylamide (0·14 g; 0·58 mmol), powdered KOH (32 mg; 0·57 mmol) and Ti(OBu)₄ (0·10 ml; 0·29 mmol), the experimental procedure described in 6.26.1 yielded an orange-red crystalline

solid. Yield 0·10 g (0·16 mmol, 57%), m.p. >300°C. F.W.: calc. for $C_{28}H_{20}N_2O_6K_2Ti$, 606·58; found *(mass spectrum)*, 607.

An attempt was made to purify the crude material obtained above by chromatography on a florisil/(95% chloroform:5% methanol) column eluting with methanol.

6.26.6 $K_2[Ti(2-OC_6H_3(3-Me)CONC_6H_3(5-Cl)O-2)_2].xH_2O$ $-K_2[TiL^6{}_2].xH_2O$

Using N-(5-chloro-2-hydroxyphenyl)-3-methyl-salicylamide (0·16 g; 0·58 mmol), powdered KOH (32 mg; 0·57 mmol) and $Ti(OBu)_4$ (0·10 ml; 0·29 mmol), the experimental procedure described in 6.26.1 yielded an orange-red crystalline solid. Yield 0·17 g (0·25 mmol, 87%), m.p. >300°C. F.W.: calc. for $C_{28}H_{18}N_2O_6Cl_2K_2Ti$:, 675·47; found *(mass spectrum)*, 677.

6.26.7 $K_2[Ti(2-OC_6H_4CONC_{10}H_6O-2)_2].xH_2O$ $-K_2[TiL^7{}_2].xH_2O$

Using N-(2-naphthol)salicylamide (0·16 g; 0·57 mmol), powdered KOH (32 mg; 0·57 mmol) and $Ti(OBu)_4$ (0·10 ml; 0·29 mmol), the experimental procedure described in 6.26.1 yielded an orange-brown solid. Yield 0·21 g (0·31 mmol, 107%), dec. ~250°C. Analysis calc. for $C_{34}H_{20}N_2O_6K_2Ti$: C, 60·17; H, 2·97; N, 4·13%. Found (duplicate analysis): C, 56·98 (56·51); H, 3·86 (3·65); N, 3·36 (3·22)%. F.W.: calc., 678·65; found *(mass spectrum)*, 677.

Attempts were made to purify the crude material obtained above by chromatography on a florisil/(95% chloroform:5% methanol) column eluting with methanol, and on an alumina/hexane column eluting with methanol. Analysis found after chromatography (alumina): C, 51·01; H, 3·80; N, 3·03%

6.26.8 $K_2[Ti(2-OC_6H_3(5-Cl)CONC_{10}H_6O-2)_2].xH_2O$ $-K_2[TiL^8{}_2].xH_2O$

Using N-(2-naphthol)-5-chlorosalicylamide (0·18 g; 0·57 mmol), powdered KOH (32 mg; 0·57 mmol) and $Ti(OBu)_4$ (0·10 ml; 0·29 mmol), the experimental procedure described in 6.26.1 yielded a brown crystalline material. Yield 0·24 g (0·32 mmol, 111%), m.p. >300°C. F.W.: calc. for $C_{34}H_{18}N_2O_6Cl_2K_2Ti$, 747·54; found *(mass spectrum)*, 748.

6.26.9 $K_2[Ti(2-OC_6H_3(3-Me)CONC_{10}H_6O-2)_2].xH_2O$
      $-K_2[TiL^9_2].xH_2O$

Using N-(2-naphthol)-3-methylsalicylamide (0·11 g; 0·38 mmol), powdered KOH (32 mg; 0·57 mmol) and Ti(OBu)4 (~0·065 ml; 0·19 mmol), the experimental procedure described in 6.26.1 yielded a brown solid. Yield 0·18 g (0·25 mmol, 135%), m.p. >300°C. F.W.: calc. for $C_{36}H_{24}N_2O_6K_2Ti$, 706·70; found *(mass spectrum)*, 707.

6.27   Amide Complex of Vanadium

6.27.1   **Attempted preparation of** $K_2[V(2-OC_6H_4CONC_6H_4O-2)_2].xH_2O$
      $-K_2[VL^1_2].xH_2O$

Method (i)

VO(acac)2 (58 mg; 0·22 mmol) was added to a pale yellow solution of N-(2-hydroxyphenyl)salicylamide (0·10 g; 0·44 mmol) and KOH (75 mg; 1·3 mmol) in dry methanol (5 ml). The resultant dark brown solution was stirred overnight at room temperature before cooling (8°C) for 2 days. Most of the solvent was removed, under vacuum, affording a brown sticky solid. Attempts to recrystallise with dropwise addition of ether were unsuccessful. The solvents were removed and a small amount of methanol added. The red-brown solution was filtered removing a small amount of white solid (infrared showed this to be inorganic material). The brown filtrate was evaporated to dryness on a steam bath (70°C) yielding a brown solid. Yield 81 mg. F.W.: calc. for $C_{26}H_{16}N_2O_6K_2V$, 581·57; found *(mass spectrum)*, 537.

Method (ii)

The reaction above was repeated in refluxing methanol affording a light brown solid. F.W.: found *(mass spectrum)*, 343.

Method (iii)

The experimental procedure described in method *(i)* using VOCl2.2H2O (39 mg; 0·22 mmol), amide(0·10 g; 0·44 mmol) and KOH (74 mg; 1·3 mmol), yielded.a grey-brown solid. Yield 0·17 g. F.W.: found *(mass spectrum)*, 344.

Method (iv)

The same product was obtained by repeating the above preparation in refluxing methanol.

Method (v)

Following the same experimental procedure in method *(i)* using distilled and deoxygenated methanol, and stirring the solution for 2 days afforded a brown solid. Yield 0·13 g, dec. ~200°C. F.W.: found *(mass spectrum)*, 583.

6.28   Amide Complexes of Iron

In all cases below, crude samples or the amide compounds were investigated by infrared spectroscopy, magnetic moment and conductivity measurement. Details of these are in the relevant sections in Chapter 3. Unless otherwise stated, formula weight and microanalytical calculations below are based on the anhydrous formula for the complex.

Attempted preparations of:

6.28.1 $K_2[Fe(2\text{-}OC_6H_4CONC_6H_4O\text{-}2)_2].xH_2O$ $\text{-}K_2[FeL^1_2].xH_2O$

Using $Fe(acac)_3$ (77 mg; 0·22 mmol), N-(2-hydroxyphenyl)salicylamide (0·10 g; 0·45 mmol) and KOH (38 mg; 0·68 mmol) in dry methanol (6 ml), the same experimental procedure described in 6.25.1 was followed. No solid precipitated by repeatedly concentrating and cooling the solution. The solution was then evaporated to dryness yielding a dark brown solid. Yield 0·15 g, dec. ~120°C. Analysis calc. for $C_{26}H_{16}N_2O_6K_2Fe$: C, 53·24; H, 2·75; N, 4·78%. Found (duplicate analysis): C, 49·08 (48·91); H, 2·52 (2·42); N, 2·73 (2·70)%. F.W.: calc., 586·47; found *(mass spectrum)*, 587.

6.28.2 $K_2[Fe(2\text{-}OC_6H_4CONC_6H_3(5\text{-}Cl)O\text{-}2)_2].xH_2O$ $\text{-}K_2[FeL^3_2].xH_2O$

Using $Fe(acac)_3$ (67 mg; 0·19 mmol) N-(5-chloro-2-hydroxyphenyl)salicyl-amide (0·10 g; 0·38 mmol) and KOH (34 mg; 0·61 mmol) in dry methanol (6 ml), the experimental procedure described in 6.25.1 yielded a brown-black

solid. Yield 0·17 g. F.W.: calc. for $C_{26}H_{14}N_2O_6Cl_2K_2Fe$, 655·36; found *(mass spectrum)*, 656.

6.28.3 $K_2[Fe(2\text{-}OC_6H_3(5\text{-}Cl)CONC_6H_3(5\text{-}Cl)O\text{-}2)_2].xH_2O$
$-K_2[FeL^4{}_2].xH_2O$

Using Fe(acac)$_3$ (59 mg; 0·17 mmol), N-(5-chloro-2-hydroxyphenyl)-5-chlorosalicylamide (0·10 g; 0·34 mmol) and KOH (38 mg; 0·68 mmol) in dry methanol (9 ml), the experimental procedure described in 6.25.1 yielded a dark brown solid. Yield 0·18 g. F.W.: calc. for $C_{26}H_{12}N_2O_6Cl_4K_2Fe$, 724·25; found *(mass spectrum)*, 726.

6.29   Attempted Preparation of $Ti(OC_6H_4CH_2OC_6H_4O)_2$

Assuming the orange oil, yielded in Section 6.6.2, to contain some 2,2'-dihydroxybenzylphenyl ether, a portion (0·41 g) was dissolved in dry ethanol (25 ml). LiOAc.2H$_2$O (0·40 g; 3·9 mmol) was added forming a red-brown solution. After stirring for 5 minutes at room temperature, Ti(OBu)$_4$ (0·32 ml; 0·93 mmol) was added. The slightly darker solution was heated under reflux for 1·5 hours and allowed to cool overnight. No precipitate was obtained after cooling (8°C) the solution for several days. Removal of most of the solvent afforded a red-brown solid which was collected. After washing with hexane the solid appeared a clay-brown colour. The filtrate was evaporated to dryness affording a red-brown residue which was recrystallised from chloroform/hexane.

<u>First crop</u>: yield 0·16 g. *Infrared spectrum:* very broad absorptions at 3700 - 3000 s, 2380 m, 1730 m, 1610 s, 1257 m, 1100 m, 1060 s and 875 s cm^{-1}.

<u>Second crop</u>: yield 0·36 g, m.p. 94°C. *Infrared spectrum:* broad absorptions at 3700 -3100 m, 1710 w, 1610 s, 1255 s, 1105 m, 1025 m, 873 m, 810 m and 745 m cm^{-1}. F.W. calc. for $C_{26}H_{20}O_6Ti$, 476·34; found *(EI mass spectrum)* 371, 329, 265, 213, 191, and found *(FAB mass spectrum)*, 258.

6.30 Attempted Preparation of Ti(OC$_6$H$_4$CH=CHC$_6$H$_4$O)$_2$

The following experiments were carried out under an atmosphere of dinitrogen:

Method (i)

Ti(OBu)$_4$ (0·10 ml; 0·29 mmol) was added to a solution of 2,2'-dihydroxy-stilbene (92 mg; 0·43 mmol) and LiOAc.2H$_2$O (0·11 g; 1·1 mmol) in dry ethanol (20 ml). A yellow solution was produced which soon became cloudy. The mixture was heated under reflux for 30 minutes and allowed to cool to room temperature. A yellow solid was collected. The filtrate was concentrated yielding a second crop of white solid.
Yellow ppt.: yield 44 mg. *Infrared spectrum:* showed it to be inorganic material.
White ppt.: yield not recorded. *Infrared spectrum:* showed it to be a mixture of unreacted 2,2'-dihydroxystilbene and lithium acetate.

Method (ii)

The procedure above was repeated using TiCl$_4$ (0·01 ml; 9·1 × 10^{-5} mol), 2,2'-dihydroxystilbene (27 mg; 0·13 mmol) and lithium acetate (34 mg; 0·33 mmol). No precipitate formed. The yellow solution was evaporated to dryness under vacuum affording a red oil. Attempts to crystallise with ethanol/hexane failed. Removal of these solvents however gave a brown solid. Yield 65 mg.
Infrared spectrum: showed to be unreacted 2,2'-dihydroxystilbene with some lithium acetate.

Method (iii)

2,2'-Dihydroxystilbene (0·10 g; 0·47 mmol) was added to a solution of sodium metal (27 mg; 1·2 mmol) in dry ethanol (10 ml) forming a cloudy yellow solution. After stirring for 5 minutes at room temperature the solution was evaporated to dryness yielding a yellow powder. Dry THF (5 ml) was added and the solution transferred to a dry box, flushed with dinitrogen, where TiCl$_4$ (0·026 ml; 0·24 mmol) was added. On addition of the tetrachloride, a cloudy orange-brown solution formed which faded to orange-yellow after sirring overnight. Removal of solvent gave an orange solid.
Infrared spectrum: 3600 - 3200 w, 1590 s, 1500 w cm^{-1}.

Dry THF (7 ml) was added to the orange solid from above. Some yellow undissolved material was filtered off under dinitrogen (Schlenk filtration). The orange filtrate was evaporated to dryness, under vacuum, giving an orange solid.

Yellow ppt.: yield 44 mg. *Infrared spectrum:* 3350 m, 1610 w, 1593 w, 1505 w cm^{-1} (a very weak spectrum of unreacted 2,2'-dihydroxystilbene).

Orange ppt.: yield 0·18 g. F.W.: calc. for $C_{28}H_{20}O_2Ti$, 468·36; found *(mass spectrum)* 504, 210 (most intense). *Infrared spectrum:* 3340 w, 1610 sh, 1593 s, 1505 w cm^{-1}. *UV-VIS* (MeOH) for a concentration of $3·57 \times 10^{-3}$ g in 250 ml: bands were observed at $\lambda = 230$ sh, 277 and 326 nm.

6.31 Microanalysis

Microanalyses were performed by the Canadian Microanalytical Service Ltd., Delta, B.C., or the Chemical and Micro Analytical Microanalytical Services Pty. Ltd., Belmont, Australia.

Titanium, manganese and potassium contents were performed on the amide complexes $K_2[TiL^1_2]$ and $K_2[MnL^4_2]$ by Mr. Nick Robinson *et al.* at the Waite Institute, Adelaide, South Australia. The complexes were analysed by atomic emission methods based on inductively coupled plasma (ICP) sources to determine the potassium, titanium and manganese contents. The accurately weighed samples were dissolved in aqueous 5% nitric acid. Solutions were prepared such that the concentration of potassium was near 50 ppm

6.32 Physical Measurements

6.32.1 Spectral measurements

6.32.1.1 Infrared spectra

All infrared spectra were recorded on a Perkin-Elmer 1700 X Series Fourier Transform Infrared Spectrometer. Samples were prepared as nujol mulls using sodium chloride plates.

6.32.1.2 Electronic spectra

All spectra in the ultraviolet-visible region were recorded on a Hewlett-Packard 8452A Diode Array Spectrometer. Spectra for the compounds were determined at a concentration near 10^{-5} mol dm^{-3}.

6.32.1.3 Mass spectra

Mass spectra were recorded by Mr. Tom Blumenthal in the Department of Chemistry, University of Adelaide, South Australia. Standard electron impact (EI) and, for high melting compounds, fast atom bombardment (FAB) techniques were used.

Contradictory mass spectral evidence as to the presence of the desired material may have been due to the unreliability of the mass spectral service available.

6.32.1.4 Nuclear magnetic resonance spectra

Spectra for all Schiff bases and azo dyes, as well as their complexes, were recorded on a Bruker AC-P 300 spectrometer by the service available in the Department of Chemistry. All other spectra were recorded on a Jeol JNM-PMX 60 NMR spectrometer, including spectra for determination of effective magnetic moments using the Evans method.[197]

6.32.2 Conductance measurements

Conductivity experiments were carried out in methanol at 298·2 K using a Philips PW 9527 Digital Conductivity Meter. This technique involves measuring the electrical resistance of a solution at a particular constant temperature. Using a conductivity cell consisting of two parallel platinum electrodes of area A (cm^2) and distance d (cm) apart. The resistance, R (ohm), of a solution is then given by:

$$R = \rho \frac{d}{A} \qquad\qquad (6.1)$$

where ρ (ohm cm) is the specific resistance.

The reciprocal of ρ is known as the specific conductance, κ (ohm^{-1} cm^{-1}), so that the conductance of a one centimetre cube of solution is defined as:

$$\kappa = \frac{1}{R} \times \frac{d}{A} \qquad (6.2)$$

Quantities d and A are not readily measured. Instead, the resistance of a solution of KCl with accurately known specific conductance is measured, and the cell constant d/A (cm^{-1}) for a particular conductivity cell, calculated. Knowing the cell constant, κ for any other electrolyte solution may be determined. κ is dependant on the molar concentration and on the ionic composition or charge type of the electrolyte.

To compare the conductances of the different compounds and hence to ascertain charge types, the molar conductance (ohm^{-1} cm^2 mol^{-1}) is determined, defined by:

$$\Lambda_m = \frac{1000\kappa}{C} \qquad (6.3)$$

where C is the molar concentration (mol dm^{-3}) and κ is the specific conductance (ohm^{-1} cm^{-1}).

The conductivity cell was calibrated using a solution of KCl (0·0100 mol dm^{-3}; $\kappa = 1·413 \times 10^{-3}$ ohm^{-1} cm^{-1})[237] and molar conductivities for the complexes were determined at a concentration near 10^{-3} mol dm^{-3} in methanol, assuming the general formula $K_2[ML^n_2].3·5H_2O$ for complexes.

6.32.3 Magnetic moment measurements

The molar diamagnetic susceptibilities (X_M) of the amide ligands in the deprotonated form were calculated using Pascal's constants for the diamagnetism of the constituent atoms, taking into account the deviation from Pascals additivity rules for the ligands containing naphthyl rings.[198a,b] The values for the molar diamagnetic susceptibilities of all the ligands prepared are listed below in Table 6.1.

Table 6.1: Molar Diamagnetic Susceptibilities of the Deprotonated Amide Ligands by Pascal's constants.

Ligand	$X_M \times 10^6$
L^1	-113
L^2	-127
L^3	-127
L^4	-141
L^5	-125
L^6	-139
L^7	-221
L^8	-235
L^9	-233

The mass susceptibility of the amide ligands were also determined on a Johnson Matthey magnetic susceptibility balance, using the equation:

$$X = \frac{Cl(R-R_0)}{10^9 m} \qquad (6.4)$$

where C = calibration constant for the balance (1·024), l = length of sample in tube (cm), R_0 = reading for empty tube, R = reading for tube with sample, and m = mass of sample in tube (g).

Using Evans method, magnetic moment measurements on the amide complexes of manganese and iron were carried out using a Jeol JNM-PMX 60 NMR spectrometer. Methanol was sealed in a fine capillary tube, approximately 4 cm in length, which was then placed in the NMR tube (507 PP). A solution of the complex under investigation, at a concentration near 10^{-3} M in methanol, was added to the NMR tube to a level approximately 3 mm from the top of the capillary tube. The solution was allowed to equilibrate to 308·2 K, in the spectrometer, before recording its

spectrum. The mass susceptibility, X, of the metal ions was calculated using Equation 6.5

$$X = \frac{3\delta\nu}{2\pi\nu_0 m} + X_0 \qquad (6.5)$$

where $\delta\nu$ is the frequency shift (Hz), ν_0 is the frequency at which the proton resonance is being studied (60 MHz for the JNM-PMX 60), m is the mass (g) of sample contained in 1 ml of solution and X_0 is the mass susceptibility of the solvent (0.668×10^{-6} cm^3 g^{-1} for methanol[13]).

The effective magnetic moments (B.M.) were calculated using Equation 6.6

$$\mu_{eff} = 2.84\sqrt{X_{M(corr)} \times T} \qquad (6.6)$$

where $X_{M(corr)}$ = molar susceptibility (c.g.s. units) corrected for any diamagnetic effects and T = temperature (K).

6.32.4 Electrochemistry

A Bioanalytical Systems (BAS) 100 electrochemical analyser was used for all cyclic voltammetry, normal pulse voltammetry and Osteryoung square wave voltammetry measurements. The BAS 100 was connected to an Impact EN-P1091 dot matrix printer, a HIPLOT DMP-40 Drum plotter and an IBM personal computer XT.

6.33 Electrochemical Equipment

6.33.1 Cell

Voltammetry experiments were carried out in a single cell equipped with a teflon cap containing holes of appropriate size to accomodate the three electrodes and tubing for purging the system.

6.33.2 Solvents

HPLC grade dimethylsulphoxide and dry dichloromethane (Section 6.1.3) were used to study the bis(binegative tridentate) and the bis(trinegative tridentate) complexes, respectively.

6.33.3 Reagents

Et_4NClO_4 was prepared and supplied by T. Rodopoulos, Dept. of Chemistry, University of Adelaide, South Australia. Bu_4NBF_4, 15-Crown-5 and silver nitrate were obtained from Aldrich Chemical Co. Inc.

6.33.4 Electrodes

Glassy-carbon and platinum electrodes were commercially prepared (Bioanalytical Systems) and consisted of a glassy-carbon/platinum disc mounted on a Kel-F sheath. Both electrodes were polished with 0·05 µm alumina on a high speed polishing wheel and washed with high purity water in an ultrasonic bath.

The Ag/Ag^+ reference electrode was prepared by enclosing a silver wire in a slender glass tube, containing a solution of 0·10 mol dm^{-3} electrolyte and 0·01 mol dm^{-3} silver nitrate, which was connected to a porous vycor plug with heat-shrink tubing.

6.33.5 Electrochemical Experiments

Dimethylsulphoxide containing 0·10 mol dm^{-3} tetraethylammonium perchlorate, or in some cases 0·10 mol dm^{-3} Bu_4NBF_4, was the medium used to study Schiff base and azo dye complexes. Dichloromethane containing 0·05 mol dm^{-3} tetraethylammonium perchlorate was used to study the amide complexes. Approximately 6 ml of the background solution was deoxygenated by bubbling high purity argon gas through the solution for 10 minutes. A cyclic voltammogram on the background medium was recorded before adding 10 - 20 mg of the compound under investigation. The solution was further degassed (3 minutes) before the voltammogram experiment was performed on the solution, which was protected by an argon "blanket".

In all the electrochemical experiments carried out, except for those on the amide complexes, a small amount of ferrocene was added to the solutions.

The essentially reversible oxidation/reduction process of ferrocene was used as a reference. This was not possible in the cases with the amide complexes of manganese due to interference of the redox couple of ferrocene with the Mn(V)/M(IV) couple in the complexes.

6.34 Computing

A Lasaer Turbo XT personal computer connected to the Hewlett-Packard 8452A Diode Array Spectrophotometer was used to save the ultraviolet-visible spectral data. The spectral data was then converted from MS-DOS format to Macintosh format and transferred to a Macintosh Classic microcomputer using the data transfer and conversion program APPLE FILE EXCHANGE.[238] The spectra were printed using the graphing and data analysis program IGOR.[239]

Electrochemical data was transferred between the Bioanalytical Systems 100 electrochemical analyser and an IBM compatible personal computer using BASIC programmes. The program BASIBM[240] was used to convert the BAS 100 files in to hexadecimal files on the computer. Then the program HEXCON[240] was employed to convert the hexadecimal files into text files. Finally, the file for each voltammogram was converted from MS-DOS format to Macintosh format and transferred to a Macintosh Classic microcomputer using the data transfer and conversion program APPLE FILE EXCHANGE.[238] Printouts of all the voltammograms were obtained using the graphing and data analysis program IGOR.[239]

References

1   J. Costamaga, J. Vargas, R. Latorre, A. Alvarado and G. Mena, *Coord. Chem. Rev.*, 1992, **119**, 67.

2   G.D. Lawrence and D.T. Sawyer, *Coord. Chem. Rev.*, 1978, **27**, 173.

3   T.J. Collins, R.D. Powell, C. Slebodnick and E.S. Uffelman, *J. Am. Chem. Soc.*, 1990, **112**, 899.

4   T.J. Collins, K.L. Kostka, E. Münck and E.S. Uffelman, *J. Am. Chem. Soc.*, 1990, **112**, 5637.

5   E.A. Pasek and D.K. Straub, *Inorg. Chem.*, 1972, **11**(2), 259.

6   F.A. Cotton and G.Wilkinson, "Advanced Inorganic Chemistry, a comprehensive text", Fourth Edition, John Wiley and Sons. Inc., New York, 1980. (a) p693, (b) p709, (c) p720, (d) p737, (e) p751, (f) p381, (g) p634, (h) p1311, (i) p471, (j) p470, (k) p185 - 187, (l) p440, (m) p667 and (n) p208.

7   S.E. Jones, D-H. Chin and D.T. Sawyer, *Inorg. Chem.*, 1981, **20**, 4257.

8   T.J. Collins and S.W. Gordon-Wylie, *J. Am. Chem. Soc.*, 1989, **111**, 4511.

9   M.F. Iskander, L. Labib, M.M.Z. Nour El-Din and M. Tawfik, *Polyhedron*, 1989, **8**(23), 2755.

10   M. Nath, C.L. Sharma and N. Sharma, *Synth. React. Inorg. Met.-Org. Chem.*, 1991, **21**(5), 807

11   A. Butler and C.J. Carrano, *Coord. Chem. Rev.*, 1991, **109**, 61 and references cited therein.

12   W. Levason and C.A. McAuliffe, *Coord. Chem. Rev.*, 1972, **7**, 353.

13   "The Chemical Rubber Co. Handbook of Chemistry and Physics", Sixty-fourth Edition, CRC Press, Inc., USA, 1983-1984.

14 H. Ōkawa, M. Nakamura and S. Kida, *Bull. Chem. Soc. Jpn.*, 1982, **55**, 466.

15 S. Pal, P. Ghosh and A. Chakravorty, *Inorg. Chem.*, 1985, **24**, 3704.

16 D-H. Chin, D.T. Sawyer, W.P. Schaefer and C.J. Simmons, *Inorg. Chem.*, 1983, **22**, 752.

17 D.Rehder, Angew. *Chem. Int. Ed. Engl.*, 1991, **30**, 148.

18 C. Woitha and D. Rehder, *Angew. Chem. Int. Ed. Engl.*, 1990, **29**(12), 1438.

19 B. Galeffi, M. Postel, A. Grand and P. Rey, *Inorg. Chim. Acta*, 1989, **160**, 87.

20 C.R. Cornman, J. Kampf, M.S. Lah and V.L. Pecoraro, *Inorg. Chem.*, 1992, **31**, 2035.

21 C.L. Simpson and C.G. Pierpont, *Inorg. Chem.*, 1992, **31**, 4308.

22 W. Bansse, E. Ludwig, E. Uhlemann, F. Weller, K. Dehnicke and W. Herrmann, *Z. Anorg. Allg. Chem.*, 1992, **613**, 36.

23 B. Singh and K. Srivastav, *Proc. Ind. Acad. Sci. (Chim. Sci.)*, 1992, **104**(4), 457.

24 K. Ramesh, T.K. Lal and R.N. Mukherjee, *Polyhedron*, 1992, **11**(23), 3083.

25 J.C. Dutton, G.D. Fallon and K.S. Murray, *Inorg. Chem.*, 1988, **27**, 34.

26 X. Li, M.S. Lah and V.L. Pecoraro, *Inorg. Chem.*, 1988, **27**, 4657.

27 A. Hills, D.L. Hughes, G.J. Leigh and J.R. Sanders, *J. Chem. Soc., Dalton Trans.*, 1991, 325.

28 A. Neves, A.S. Ceccato, I. Vencato, Y.P. Mascarenhas and C. Erasmus-Buhr, *J. Chem. Soc., Chem. Commun.*, 1992, 652.

29 N.V. Gerbeleu, Y.A. Simonov, V.B. Arion, V.M. Leovac, K.I. Turta, K.M. Indrichan, D.I. Gradinaru, V.E. Zavodnik and T.I. Malinovskii, *Inorg. Chem.*, 1992, **31**, 3264.

30 E.A. Páez, W.T. Oosterhuis and D.L. Weaver, *Chem. Commun.*, 1970, 506.

31 D.J. Gulliver and W. Levason, *Coord. Chem. Rev.*, 1982, **46**, 1 and references cited therein.

32 A.R. Hendrickson, R.L. Martin and N.M. Rohde, Inorg. Chem., 1974, **13**(8), 1933.

33 E.A. Paez, D.L. Weaver and W.T. Oosterhuis, *J. Chem. Phys.*, 1972, **57**(9), 3709 and references cited therein.

34 A. Stassinopoulos, G. Schulte, G.C. Papaefthymiou and J.P. Caradonna, *J.Am. Chem. Soc.*, 1991, **113**, 8686.

35 M. Koikawa, H. Ōkawa, Y. Maeda and S. Kida, *Inorg. Chim. Acta*, 1992, **194**, 75.

36 W. Shaozu, C. Yin and Z. Yulan, *Synth. React. Met.-Org. Chem.*, 1991, **21**(4), 599.

37 S.R. Cooper, Y.B. Koh and K.N. Raymond, *J. Am. Chem. Soc.*, 1982, **104**(19), 5092.

38 P.J. Bosserman and D.T. Sawyer, *Inorg. Chem.*, 1982, **21**, 1545 and references cited therein.

39 B.A. Borgias, S.R. Cooper, Y.B. Koh and K.N. Raymond, *Inorg. Chem.*, 1984, **23**, 1009.

40 R.P. Henry, P.C.H. Mitchell and J.E. Prue, *J. Chem. Soc. (A)*, 1971, 3392.

41 C.J. Hawkins and T.A. Kabanos, *Inorg. Chem.*, 1989, **28**, 1084.

42 T.A. Kabanos, A.M.Z. Slawin, D.J. Williams and J.D. Woolins, *J. Chem. Soc. Dalton Trans.*, 1992, 1423.

43 D. Zirong, S. Bhattacharya, J.K. McCusker, P.M. Hagen, D.N. Hendrickson and C.G. Pierpont, *Inorg. Chem.*, 1992, **31**, 870.

44 P.J. Antikainen and P.J. Mälkönen, *Z. Anorg. Allg. Chem.*, 1959, **299**, 292.

45   O. Lindqvist, *Acta Chem. Scand.*, 1967, **21**(6), 1473.

46   D.F. Evans, A.M.Z. Slawin, D.J. Williams, C.Y. Wong and J.D. Woolins, 1992, *J. Chem. Soc. Dalton Trans.*, 1992, 2383.

47   M.A.V. Ribeiro da Silva and M.L.C.C.H. Ferrão, *Pure and Appl. Chem.*, 1988, **60**(8), 1225.

48   T.W. Hambley, C.J. Hawkins and T.A. Kabanos, *Inorg. Chem.*, 1987, **26**, 3740.

49   Y. Hoshino, A. Endo, K. Shimizu and G.P. Satô, *J. Electroanal. Chem.*, 1988, **246**, 225.

50   E.M. Rubtsov, *Koord. Khim.*, 1989, **15**(5), 579.

51   T.N. Srivastava and J.D. Singh, *Ind. J. Chem.*, 1990, **29A**, 703.

52   N.S. Bhandari, K.Uppal, A.K. Singh and B.L. Khandelwal, *Ind. J. Chem.*, 1991, **30A**, 95.

53   J.A.S. Smith and E.J. Wilkins, *J. Chem. Soc. (A)*, 1966, 1749.

54   R.C. Mehrotra, R. Bohra and D.P. Gaur, "Metal β-Diketonates and Allied Derivatives", Academic Press, 1978, pg. 17.

55   T. Shimizutani and Y. Yoshikawa, *Inorg. Chem.*, 1991, **30**, 3236.

56   D.W. Thompson, *Inorg. Chem.*, 1969, **8**(9), 2015.

57   G.K. Sandhu, R. Hundal and E.R.T. Tiekink, *J. Organomet. Chem.*, 1991, **412**, 31.

58   B.K. Tejankar, R.J. Rao and H.P.S. Chauhan, *Synth. React. Inorg. Met.-Org. Chem.*, 1991, **21**(8), 1179.

59   G.K. Sandhu, R. Hundal and E.R.T. Teikink, *J. Organomet. Chem.*, 1992, **430**, 15.

60   C. Vasta, V.K. Jain, T.K. Das and E.R.T. Tiekink, *J. Organomet. Chem.*,1991, **421**, 21.

61   J.H. Wengrovius and M.F. Garbauskas, *Organometallics*, 1992, **11**, 1334.

62   C. Vatsa, V.K. Jain and T. Kesavadas, *Ind. J. Chem.*, 1991, **30A**, 451.

63   J. Holeček, A. Lyčka, M. Nádvorník and K. Handlíř, *Collect. Czech. Chem. Commun.*, 1991, **56**, 1908.

64   G.K. Sanhu and N.S. Boparoy, *J. Organomet. Chem.*,1991, **420**, 23.

65   G.K. Sandhu and N.S. Boparoy, *J. Organomet. Chem.*, 1991, **411**, 89.

66   M. Gielen, A. El Kloufi, M. Biesemans, R. Willem and J. Meunier-Piret, *Polyhedron*, 1992, **11**(15), 1861.

67   P.C. Srivastava and A. Trivedi, *Ind. J. Chem.*, 1990, **29A**, 489.

68   N.W. Alcock, J. Culver and S.M. Roe, *J. Chem. Soc. Dalton Trans.*, 1992, 1477.

69   D.W. Margerum, *Pure and Appl. Chem.*, 1983, **55**(1), 23.

70   M.M. Shoukry and V.M. Hosny, *Trans. Met. Chem.*, 1989, **14**, 69.

71   R. Eisenberg, *Progr. Inorg. Chem.*, 1970, **12**, 295.

72   D.E. Hamilton, *Inorg. Chem.*, 1991, **30**, 1671.

73   K.B. Pandeya and D. Khare, *Synth. React. Inorg. Met.-Org. Chem.*, 1992, **22**(5), 521.

74   A. Syamal and M.R. Maurya, *Coord. Chem. Rev.*, 1989, **95**, 183.

75   K. Yamanouchi and S. Yamada, *Inorg. Chim. Acta*, 1975, **12**, 9.

76   B.S. Saraswat, G. Srivastava and R.C. Mehrotra, *J. Organomet. Chem.*,1977, **129**, 155.

77   N.S. Biradar and V.H. Kulkarni, *J. Inorg. Nucl. Chem.*, 1971, **33**, 2451.

78   M. Nath, N. Sharma and C.L. Sharma, *Synth. React. Inorg. Met.-Org. Chem.*, 1989, **19**(4), 339.

79   L.E. Khoo and F.E. Smith, *Polyhedron*, 1982, **1**(2), 213.

80   C. Saxena and R.V. Singh, *Synth. React. Inorg. Met.-Org. Chem.*, 1992, **22**(8), 1061.

81   M. Nath, N. Sharma and C.L. Sharma, *Synth. React. Inorg. Met.-Org. Chem.*, 1990, **20**(5), 623.

82   M.P. Degaonkar, S. Gopinathan and C. Gopinathan, *Synth. React. Inorg. Met.-Org. Chem.*, 1989, **19**(6), 613.

83   T.N. Srivastava, A.K.S. Chauhan and M. Agarwal, *Synth. React. Inorg. Met.-Org. Chem.*, 1980, **10**(1), 29.

84   M. Das and S.E. Livingstone, *Inorg. Chim. Acta*, 1976, **19**, 5.

85   A. Saxena and J.P. Tandon, *Polyhedron*, 1983, **2**(6), 443.

86   M. Nath, N. Sharma and C.L. Sharma, *Synth. React. Inorg. Met.-Org. Chem.*, 1991, **21**(1), 51.

87   M. Nath, N. Sharma and C.L. Sharma, *Synth. React. Inorg. Met.-Org. Chem.*, 1990, **20**(10), 1355.

88   S.K. Pandit, S. Gopinathan and C. Gopinathan, *Ind. J. Chem.*, 1982, **21A**, 1004.

89   A.A. Diamantis, M.R. Snow and J.A. Vanzo, *J.Chem. Soc. Chem. Comm.*, 1976, 264.

90   D. Fairlie, Honours Dissertation, The University of Adelaide, Australia, 1977.

91   I.W. Roberts, Honours Dissertation, The University of Adelaide, Australia, 1978.

92   Md.A. Salam, Ph.D. Dissertation, University of Adelaide, Australia, 1986.

93   P.S. Moritz, Ph.D. Dissertation, University of Adelaide, Australia, 1987.

94   R.T. Jones, University of Adelaide, South Australia, Private Communications.

95   M.S. Raizada and M.N. Srivastava, *Synth. React. Inorg. Met.-Org. Chem.*, 1992, **22**(4), 393.

96   M. Koikawa, H. Ōkawa and S. Kida, *J. Chem. Soc. Dalton Trans.*, 1988, 641.

97   M. Manikas, Honours Dissertation, The University of Adelaide, Australia, 1987.

98   J.E. Huheey, "Inorganic Chemistry: Principles of Structure and Reactivity", Third Edition, Harper and Row, New York, 1983. (a) p578, (b) p230, (c) p313.

99   J.E. Huheey, E.A. Keiter and R.L. Keiter, "Inorganic Chemistry: Principles of Structure and Reactivity", Fourth Edition, Harper and Row, New York, 1993, p879.

100   G. Cerveau, C. Chult, RJ.P. Corriu and C. Reyé, *Organometallics*, 1991, **10**(5), 1511.

101   G. Wilkinson, R.D. Gillard and J.A. McCleverty, "Comprehensive Coordination Chemistry: The Synthesis, Reactions, Properties and Applications of Coordination Compounds", Vol. 3, Pergamon Books Ltd., UK, 1987, Chapter 26.

102   I.R. Beattie and G.P. McQuillan, *J. Chem. Soc.*, 1963, 1519.

103   M. Kaupp and P.v.R. Schleyer, *J. Amer. Chem. Soc.*, 1993, **115**, 1061.

104   Q.Y. Xu, J.-M. Barbe and K.M. Kadish, *Inorg. Chem.*, 1988, **27**, 2373.

105   R. Bosco and R. Cefalù, *J. Organomet. Chem..*, 1971, **26**, 225.

106   H.B. Stegmann, M. Schenkl and K. Scheffler, *J. Organomet. Chem.*, 1991, **414**, 145.

107   J.T. Pinhey, *Aust. J. Chem.*, 1991, **44**, 1353.

108   M.P. Degaonkar, S. Gopinathan and C. Gopinathan, *Ind. J. Chem.* 1989, **28A**, 678.

109   P. Dixit, K. Singh and J.P. Tandon, *Ind. J. Chem.*, 1989, **28A**, 909.

110   A.K. Varshney and J.P. Tandon, *Synth. React. Inorg. Met.-Org. Chem.*, 1987, **17**(6), 651.

111 N.S. Biradar, V.H. Kulkarni and N.N. Sirmokadam, *J. Inorg. Nucl. Chem.*, 1972, **34**, 3651.

112 S.N. Poddar and N.S. Das, *J. Ind. Chem. Soc.*, 1973, **L**, 431.

113 H.A. Meinema, E. Rivarola and J.G. Noltes, *J. Organomet. Chem.*, 1969, **17**, 71

114 Y. Matsumura, M. Shindo and R. Okawara, *J. Organomet. Chem.*, 1971, **27**, 357.

115 R.G. Geol and H.S. Prasad, *Inorg. Chem.*, 1972, **11**(9), 2141.

116 H.A. Meinema, A. Mackor and J.G. Noltes, *J. Organomet. Chem.*, 1972, **37**, 285.

117 J.N.R. Ruddick and J.R. Sams, *J. Organomet. Chem.*, 1977, **128**, C41.

118 N. Kanehisa, K. Onuma, S. Uda, K. Hirabayashi, Y. Kai, N. Yasuoka and N. Kasai, *Bull. Chem. Soc. Jpn.*, 1978, **51**(8), 2222.

119 V.K. Jain, R. Bohra and R.C. Mehrotra, *J. Organomet. Chem.*, 1980, **184**, 57.

120 M. Domagala, F. Huber and H. Preut, *Z. Anorg. Allg. Chem.*, 1990, **582**, 37.

121 H.A. Hodali and A.Q. Hussein, *Synth. React. Inorg. Met.-Org. Chem.*, 1990, **20**(10), 1413.

122 V.K. Jain, R. Bohra and R.C. Mehrotra, "Structure and Bonding", Vol. **52**, Springer-Verlag, Berlin, 1982, p147.

123 F. Di Bianca, E. Rivarola, A.L. Spek, H.A. Meinema and J.G. Noltes, *J. Organomet. Chem.*, 1973, **63**, 293.

124 H.A. Meinema, J.G. Noltes, F.Di Bianca, N. Bertazzi, E. Rivarola and R.Barbieri, *J. Organomet. Chem.*, 1976, **107**, 249.

125 V.K. Jain, R. Bohra and R.C. Mehrotra, *Aust. J. Chem.*, 1980, **33**, 2749.

126 N.K. Jha and D.M. Joshi, *Synth. React. Inorg. Met.-Org. Chem.*, 1984, **14**(4), 455.

127 P. Raj and A.K. Aggarwal, *Synth. React. Inorg. Met.-Org. Chem.*, 1992, **22**(5), 543.

128 R. Barbieri, *Inorg. Chim. Acta*, 1992, **191**, 253.

129 A.K. Saxena and F. Huber, *Coord. Chem. Rev.*, 1989, **95**, 109.

130 T.A. Kabanos, A.D. Keramidas, D. Mentzafos, U. Russo, A. Terzis and J.M. Tsangaris, *J. Chem. Soc. Dalton Trans.*, 1992, 2729.

131 J.W. Nicholson, *J. Chem. Ed.*, 1989, **66**(8), 621.

132 N.N. Greenwood and A. Earnshaw, "Chemistry of the Elements", Pergamon Press Ltd., New York, 1984, p460.

133 A.A. Diamantis, M. Manikas, Md. A. Salam, M.R. Snow and E.R.T. Tiekink, *Aust. J. Chem.*,1988, **41**, 453.

134 A.A. Diamantis, M. Manikas, Md. A. Salam and E.R.T. Tiekink, *Zeit. Krist.*, 1992, **202**, 154.

135 R. Salmén, K.E. Malterud and B.F. Pedersen, *Acta Chem. Scand.*, 1988, **A42**, 493.

136 A.C. Olivieri, R.B. Wilson, I.C. Paul and D.Y. Curtin, *J. Am. Chem. Soc.*, 1989, **111**, 5525.

137 A.A. Diamantis, University of Adelaide, South Australia, Private Communications.

138 T.N. Srivastava, J.D. Singh and S,K, Srivastava, *Synth. React. Inorg. Met.-Org. Chem.*,1990, **20**(5), 503.

139 W.E. Rudzinski, T.M. Aminabhavi, N.S. Biradar and C.S. Patil, *Inorg. Chim. Acta*, 1983, **69**, 83.

140 T.N. Srivastava, A.K.S. Chauhan and G.K. Mehrotra, *Synth. React. Inorg. Met.-Org. Chem.*, 1982, **12**, 705.

141 Y.D. Kulkarni, N. Saxena and O.P. Srivastava, *Ind. J. Chem.*, 1990, **29A**, 77.

142 J.N.R. Ruddick and J.R. Sams, *J. Organomet. Chem.*, 1973, **60**, 233.

143　F. Maggio, R. Bosco, R. Cefalù and R. Barbieri, *Inorg. Nucl. Chem. Lett.*, 1968, **4**, 389.

144　K. Kawakami and T. Tanaka, *J. Organomet. Chem.*, 1973, **49**, 409.

145　A. van den Bergen, R.J. Cozens and K.S. Murray, *J. Chem. Soc. (A)*, 1970, 3060.

146　L.J. Bellamy, "The Infrared Spectra of Complex Molecules", John Wiley and Sons, Inc., New York, 1958, Chapter 14.

147　D.H. Williams and I. Fleming, "Spectroscopic Methods in Organic Chemistry", Third Edition, McGraw-Hill Book Co. Ltd., London, 1980. (a) p49, (b) p8, (c) p51 and 58, (d) p143.

148　P.L. Pickard and G.W. Polly, *J. Am. Chem. Soc.*, 1976, **76**, 5169.

149　A. Saxena, J.P. Tandon, K.C. Molloy and J.J. Zuckerman, *Inorg. Chim. Acta*, 1982, **63**, 71.

150　S. Sharma, R. Bohra and R.C. Mehrotra, *Synth. React. Inorg. Met.-Org. Chem.*, 1992, **22**(1), 43.

151　R.C. Poller, *J. Inorg. Nucl. Chem.*, 1962, **24**, 593.

152　S.-G. Teoh, S.-B. Teo and G.-Y. Yeap, *Polyhedron*, 1991, **10**(23/24), 2683.

153　M.S. Raizada, *Synth. React. Inorg. Met.-Org. Chem.*, 1987, **17**(6), 625.

154　M. Bouâlam, J. Meunier-Piret, M. Biesemans, R. Willem and M. Gielen, *Inorg. Chim. Acta*, 1992, **198-200**, 249.

155　S.-G. Teoh, S.-B. Teo, G.-Y. Yeap and J.-P. Declercq, *J. Coord. Chem.*, 1992, **25**, 327.

156　A.B.P. Lever, "Inorganic Electronic Spectroscopy", Second Edition, Elsevier Science Publishing Co. Inc., New York, 1984. (a) Chapter 5 and (b) Chapter 2.

157　C. Kutal, *Coord. Chem. Rev.*, 1990, **99**, 213.

158 J.N. Murrel, "The Theory of the Electronic Spectra of Organic Molecules", Meuthuen and Co. Ltd. London, 1963, p183.

159 D. Sutton, "Electronic Spectra of Transition Metal Complexes", McGraw-Hill, London, 1968, p12.

160 P. Dixit and J.P. Tandon, *J. Prakt. Chem.*, 1989, **331**(4), 659.

161 R. Cefalù, R. Bosco, F. Bonati, F. Maggio and R. Barbieri, *Z. Anorg. Allg. Chem.*, 1970, **376**, 180.

162 A. Kumari, R.V. Singh and J.P. Tandon, *Ind. J. Chem.*, 1991, **30A**, 468.

163 P.R. Shukla, M.C. Sharma, M. Bhatt, N. Ahmad and S.K. Srivastava, *Ind. J. Chem.*, 1990, **29A**, 186.

164 B.P. Singh, G. Srivastava and R.C. Mehrotra, *J. Organomet. Chem.*, 1979, **171**, 35.

165 K. Kawakami, M. Miya-Uchi and T. Tanaka, *J. Inorg. Nucl. Chem.*, 1971, **33**, 3773.

166 K.Kawakami and R.Okawara, *J. Organomet. Chem.*, 1966, **6**, 249.

167 M.G. Muralidhara and V. Chandrasekhar, *Ind. J. Chem.*, 1991, **30A**, 487.

168 C.D. Chandler, G.D. Fallon, A.J. Koplick and B.O. West, *Aust. J. Chem.*, 1987, **40**, 1427.

169 R. Gupta, Y.P. Singh and A.K. Rai, *Ind. J. Chem.*, 1991, **30A**, 541.

170 V.H. Preut, F, Huber, R. Barbieri and N. Bertazzi, *Z. Anorg. Allg. Chem.*, 1976, **423**, 75.

171 V.H. Preut, F. Huber, H.-J. Haupt, R. Cefalù and R. Barbieri, *Z. Anorg. Allg. Chem.*, 1974, **410**, 88.

172 R. Okawara and M. Wada, *Adv. Organomet. Chem.*, 1967, **5**, 137.

173 Y. Kawasaki, T. Tanaka and R Okawara, *J. Organomet. Chem.*, 1966, **6**, 97.

174 E.L. Muetterties and C.M. Wright, *J. Am. Chem. Soc.*, 1964, **86**, 5132.

175 B.Y.K. Ho and J.J. Zuckerman, *J. Organomet. Chem.*, 1973, **49**, 1.

176 V.H. Preut, H.-J. Haupt, F. Huber, R. Cefalù and R. Barbieri, *Z. Anorg. Allg. Chem.*, 1974, **407**(3), 257.

177 S.W. Ng, V.G.K. Das and E.R.T. Tiekink, *J. Organomet. Chem.*,1991, **411**, 121

178 H.-K. Fun, S.-B. Teo, S.-G. Teoh and G.-Y. Yeap, *Acta Cryst.*, 1991, **C47**, 1845.

179 B. Salgado, E. Freijanes, A.S. González, J.S. Casas, J. Sordo, U. Casellato and R. Graziani, *Inorg. Chim. Acta*, 1991, **185**,137.

180 R. Willem, M. Biesemans, F. Kayser, M. Bouâlam and M. Gielen, *Inorg. Chim. Acta*, 1992, **197**, 25.

181 K.M. Lo, S. Selvaratnam, S.W. Ng, C. Wei and V.G.K. Das, *J. Organomet. Chem.*, 1992, **430**, 149.

182 K.-M. Lo, V.G.K. Das, W.-H. Yip and T.C.W. Mak, *J. Organomet. Chem.*,1991, **412**, 21.

183 G.M. Bancroft, B.W. Davies, N.C. Payne and T.K. Sham, *J.Chem. Soc. Dalton Trans.*, 1975, 973.

184 P.G. Harrison and T.J. King, *J.Chem. Soc. Dalton Trans.*, 1974, 2298.

185 S.M.S.V. Doidge-Harrison, R.A. Howie, J.T.S. Irvine, G. Spencer and J.L. Wardell, *J. Organomet. Chem.*,1991, **414**, C5.

186 G. Goel, E. Maslowsky,Jr. and C.V. Senoff, *Inorg Chem.*, 1971, **10**(11), 2572.

187 M. Domagala, F. Huber and H. Preut, *Z. Anorg. Allg. Chem.*, 1989, **574**, 130.

188 N. Bertazzi, F. Di Bianca, T.C. Gibb, N.N. Greenwood, H.A. Meinema and J.G. Noltes, *J. Chem. Soc. Dalton Trans.*, 1977, 957.

189 R.T. Morrison and R.N. Boyd, "Organic Chemistry", Fourth Edition, Allyn and Bacon, Inc., Boston, 1983. (a) p235, (b) p537.

190   M. Koikawa, M. Gotoh, H. Okawa, S. Kida and T. Kohzuma, *J. Chem. Soc. Dalton Trans.*, 1989, 1613.

191   L.L. Diaddario, W.R. Robinson and D.W. Margerum, *Inorg. Chem.*, 1983, **22**, 1021.

192   E. Kimura, A. Sakonaka and R. Machida, *J. Am. Chem. Soc.*, 1982, **104**, 4255.

193   J.A. Christie, T.J. Collins, T.E. Krafft, B.D. Santarsiero and G.H. Spies, *J. Chem. Soc., Chem. Commun.*, 1984, 198.

194   C. Rüchardt and S. Rochlitz, *Liebigs Ann. Chem.*, 1974, 15.

195   W.J. Geary, *Coord. Chem. Rev.*, 1971, 81.

196   S.F.A. Kettle, "Coordination Compounds. Studies in Modern Chemistry", Nelson Ltd., Great Britain, 1977, Appendix 5.

197   D.F. Evans, *J. Chem Soc.*, 1959, 2003.

198   P.W. Selwood, "Magnetochemistry", First Edition, Interscience publishers, Inc., New York, 1943. (a) p52 and (b) p135.

199   P.W. Selwood, "Magnetochemistry", Second Edition, Interscience publishers, Inc., New York, 1956, p78.

200   J. Lewis and R.G. Wilkins, "Modern Coordination Chemistry: Principles and methods", Interscience Publishers Ltd., New York, 1960, p407.

201   K.M. Mackay and R.A. Mackay, "Introduction to Modern Inorganic Chemistry", Second Edition, Intertext Books, London, 1973, p170.

202   C. Weygand and G. Hilgetag, "Preparative Organic Chemistry", John Wiley and Sons, New York, 1972. (a) p361 and (b) p369.

203   J March, "Advanced Organic Chemistry: Reactions, Mechanisms and Structure", Fourth Edition, John Wiley and Sons, Inc., New York, 1992. (a) p386 and (b) p407.

204   T.W. Greene, "Protective Groups in Organic Synthesis", John Wiley and Sons, Inc., Canada, 1981, p295.

205 R.A.W. Johnstone and M. E. Rose, *Tetrahedron*, 1979, **35**, 2169.

206 E. Langhals and H. Langhals, *Tet. Lett.*, 1990, **31**(6), 859.

207 D.R. Benedict, T.A. Bianchi and L.A. Cate, *Synthesis*, 1979, 428.

208 R.A. Massey-Westrop, University of Adelaide, South Australia, Private Communications.

209 R.E. Ireland and S.C Welch, *J. Am. Chem. Soc.*, 1970, **92**(24), 7232.

210 R.H. Prager and Y.T. Tan, *Tet. Lett.*, 1967, No.38, 3661.

211 R.E. Ireland, M.I. Dawson, S.C. Welch, A. Hagenbach, J. Bordner and B. Trus, *J. Am. Chem. Soc.*, 1973, **95**(23), 7829.

212 R.E. Ireland and D.M. Walba, "Organic Syntheses", 1977, **56**, 44.

213 F.G. Mann and M.J. Pragnell, *J. Chem. Soc.*, 1965, 4120.

214 A.F. Kluge, K.G. Untch and J.H. Fried, *J. Am. Chem. Soc.*, 1972, **94**, 7827.

215 T. Aoyama and T. Shioiri, *Tet. Lett.*, 1990, **31**(38), 5507.

216 Y. Kanaoka, K. Tanizawa, E. Sato, O. Yonemitsu and Y. Ban, *Chem. Pharm. Bull.*, 1967, **15**(5), 593.

217 Y. Kanaoka, M. Machida, O. Yonemitsu and Y. Ban, *Chem. Pharm. Bull.* 1965, **13**(9), 1065.

218 R.J. Patolia and K.N. Trivedi, *Ind. J. Chem.*, 1983, **22B**, 444.

219 J. Tirado-Rives, M.A. Oliver, F.R. Fronczek and R.D. Gandour, *J. Org. Chem.*, 1984, **49**, 1627.

220 J.T. Maloy, *J. Chem. Ed.*, 1983, **60**(4), 285.

221 D.H. Evans, K.M. O'Connell, R.A. Petersen and M.J. Kelly, *J. Chem. Ed.*, 1983, **60**(4), 290.

222 User's Manual for BAS-100 Electrochemical Analyser.

223 J. Osteryoung, *J. Chem. Ed.*, 1983, **60**(4), 296.

224 M. Lovrić, Š. Komorsky-Lovrić and R.W. Murray, *Electrochim. Acta*, 1988, **33**(6), 739.

225 A.M. Bond, T.L.E. Henderson, D.R. Mann, T.F. Mann, W. Thormann and C.G. Zoski, *Anal. Chem.*, 1988, **60**, 1878.

226 B.H. Mahan, "University Chemistry", Third Edition, Addison-Wesley Publishing Co., Canada, 1975, p646.

227 A.I. Vogel, "A Textbook of Practical Organic Chemistry including Qualitative Organic Analysis" Third Edition, Longmans, London, 1956. (a) p167, (b) p169, (c) p132, (d) p669 and (e) p71, Figure II, 8, 1*(c)*.

228 D.D. Perrin, W.L.F. Armarego and D.R. Perrin, "Purification of Laboratory Chemicals", First Edition, Pergamon Press Ltd., London, 1966. (a) p262 and (b) p110.

229 B.E. Bryant and W.C. Fernelius, *Inorg. Synth.*, 1957, **5**, 115.

230 R. Ramage, *Tetrahedron*, 1971, **27**, 1499.

231 C. Kashima, A. Tomotake and Y. Omote, *J. Org. Chem.*, 1987, **52**, 5616.

232 G. Brauer, "Handbüch der Preparativen Anorganischen Chemie", Ferdinand Enke Verlag Stuttgart, Erster Band, Germany, 1962, p646.

233 W. Foerst, "Newer Methods of Preparative Chemistry", Vol. 2, Academic press, New York, 1967, p151.

234 D.L. Fields, J.B. Miller and D.D. Reynolds, J. Org. Chem., 1964, **29**, 2640.

235 G.S. Misra and J.S. Shukla, *J. Ind. Chem. Soc.*, 1951, **28**(5), 277.

236 C.J. Easton, University of Adelaide, South Australia, Private communications.

237 J.O'M. Bockris and A.K.N. Reddy, "Modern Electrochemistry", Vol. 1, Plenum Press,New York, 1970, p446.

238 Apple Computer, Inc., Apple File Exchange v6.0.7, 1990.

239 WaveMetrics, Igor v1.25, 1991.

240 G.S. Laurence, University of Adelaide, South Australia.

Appendix

Table A.1: Bond Distances (Å) in $Ph_2Ge(SalAp)$. Primed atoms refer to disorder in the atomic positions.

O(1)	--- Ge	1·921(4)	O(2)	--- Ge	1·918(4)
N(1)	--- Ge	2·04(2)	N(1')	--- Ge	2·01(2)
C(111)	--- Ge	1·945(4)	C(121)	--- Ge	1·946(5)
C(1)	--- O(1)	1·333(5)	C(9)	--- O(2)	1·310(5)
C(6)	--- N(1)	1·49(2)	C(7)	--- N(1)	1·31(4)
C(7')	--- N(1')	1·27(5)	C(8)	--- C(7)	1·46(3)
C(8)	--- N(1')	1·54(3)	C(2)	--- C(1)	1·371(7)
C(6)	--- C(1)	1·404(7)	C(3)	--- C(2)	1·389(8)
C(4)	--- C(3)	1·374(9)	C(5)	--- C(4)	1·334(9)
C(6)	--- C(5)	1·374(8)	C(7')	--- C(6)	1·45(3)
C(9)	--- C(8)	1·386(7)	C(13)	--- C(8)	1·395(8)
C(10)	--- C(9)	1·403(6)	C(11)	--- C(10)	1·377(7)
C(12)	--- C(11)	1·349(8)	C(13)	--- C(12)	1·353(8)
C(112)	--- C(111)	1·380(6)	C(116)	--- C(111)	1·375(6)
C(113)	--- C(112)	1·383(7)	C(114)	--- C(113)	1·350(8)
C(115)	--- C(114)	1·364(7)	C(116)	--- C(115)	1·380(8)
C(122)	--- C(121)	1·386(7)	C(126)	--- C(121)	1·389(6)
C(123)	--- C(122)	1·389(8)	C(124)	--- C(123)	1·366(8)
C(125)	--- C(124)	1·357(7)	C(126)	--- C(125)	1·382(6)

Table A.2: Bond Angles (degrees) in Ph₂Ge(SalAp). Primed atoms refer to disorder in the atomic positions.

O(2)	- Ge	- O(1)	167·6(2)
N(1)	- Ge	- O(2)	95·0(7)
N(1')	- Ge	- O(2)	71·5(8)
C(111) - Ge		- O(1)	93·5(2)
C(111) - Ge		- N(1)	116·9(4)
C(121) - Ge		- O(1)	92·3(2)
C(121) - Ge		- N(1)	120·6(3)
C(121) - Ge		- C(111)	121·2(2)
C(9)	- O(2)	- Ge	123·2(3)
C(7)	- N(1)	- Ge	124(2)
C(7')	- N(1')	- Ge	124(3)
C(8)	- N(1')	- C(7')	113(2)
C(6)	- C(1)	- O(1)	118·4(4)
C(3)	- C(2)	- C(1)	119·0(6)
C(5)	- C(4)	- C(3)	119·4(6)
C(1)	- C(6)	- N(1)	101·1(8)
C(5)	- C(6)	- C(1)	119·9(5)
C(7')	- C(6)	- C(1)	136(1)
C(6)	- C(7')	- N(1')	118(2)
C(9)	- C(8)	- C(7)	134·6(8)
C(13)	- C(8)	- C(7)	104·7(8)
C(8)	- C(9)	- O(2)	121·3(5)
C(10)	- C(9)	- C(8)	117·9(4)
C(12)	- C(11)	- C(10)	121·0(5)
C(12)	- C(13)	- C(8)	119·8(6)
C(116) - C(111) - Ge			120·6(4)
C(113) - C(112) - C(111)			120·9(5)
C(115) - C(114) - C(113)			118·8(5)
C(115) - C(116) - C(111)			120·8(5)
C(126) - C(121) - Ge			120·5(4)
C(123) - C(122) - C(121)			121·1(5)
C(125) - C(124) - C(123)			120·8(5)
C(125) - C(126) - C(121)			121·1(5)

Table A.2: continued...

N(1)	- Ge	- O(1)	72·6(7)
N(1')	- Ge	- O(1)	96·3(8)
C(111)	- Ge	- O(2)	91·7(2)
C(111)	- Ge	- N(1')	122·9(3)
C(121)	- Ge	- O(2)	94·6(2)
C(121)	- Ge	- N(1')	114·4(4)
C(1)	- O(1)	- Ge	122·0(3)
C(6)	- N(1)	- Ge	121(1)
C(7)	- N(1)	- C(6)	115(2)
C(8)	- N(1')	- Ge	123(1)
C(2)	- C(1)	- O(1)	122·6(5)
C(6)	- C(1)	- C(2)	119·0(5)
C(4)	- C(3)	- C(2)	121·3(5)
C(6)	- C(5)	- C(4)	121·4(6)
C(5)	- C(6)	- N(1)	139·0(9)
C(8)	- C(7)	- N(1)	117(2)
C(7')	- C(6)	- C(5)	104(1)
C(9)	- C(8)	- N(1')	97·1(8)
C(13)	- C(8)	- N(1')	142·3(9)
C(13)	- C(8)	- C(9)	120·5(5)
C(10)	- C(9)	- O(2)	120·8(5)
C(11)	- C(10)	- C(9)	119·9(5)
C(13)	- C(12)	- C(11)	120·8(6)
C(112)	- C(111)	- Ge	121·9(3)
C(116)	- C(111)	- C(112)	117·5(4)
C(114)	- C(113)	- C(112)	121·0(6)
C(116)	- C(115)	- C(114)	121·0(5)
C(122)	- C(121)	- Ge	121·9(4)
C(126)	- C(121)	- C(122)	117·5(5)
C(124)	- C(123)	- C(122)	119·5(6)
C(126)	- C(125)	- C(124)	120·0(5)

Table A.3: Bond Distances (Å) in Ph$_2$Sn(SalAp). Primed atoms refer to disorder in the atomic positions.

O(1)	---	Sn(1)	2·081(3)	O(2) --- Sn(1)	2·067(4)
N(1)	---	Sn(1)	2·220(6)	N(1') --- Sn(1)	2·12(2)
C(111)	---	Sn(1)	2·118(5)	C(121) --- Sn(1)	2·111(5)
C(1)	---	O(1)	1·341(6)	C(9) --- O(2)	1·331(6)
C(7)	---	N(1)	1·23(1)	C(6) --- N(1)	1·482(8)
C(7')	---	N(1')	1·52(5)	C(8) --- C(7)	1·478(9)
C(8)	---	N(1')	1·53(2)	C(2) --- C(1)	1·387(7)
C(6)	---	C(1)	1·392(7)	C(3) --- C(2)	1·361(7)
C(4)	---	C(3)	1·373(7)	C(5) --- C(4)	1·372(7)
C(6)	---	C(5)	1·366(7)	C(7') --- C(6)	1·51(3)
C(9)	---	C(8)	1·393(8)	C(13) --- C(8)	1·390(8)
C(10)	---	C(9)	1·402(7)	C(11) --- C(10)	1·362(8)
C(12)	---	C(11)	1·365(8)	C(13) --- C(12)	1·353(9)
C(112)	---	C(111)	1·380(6)	C(116) --- C(111)	1·376(7)
C(113)	---	C(112)	1·386(8)	C(114) --- C(113)	1·376(8)
C(115)	---	C(114)	1·373(8)	C(116) --- C(115)	1·382(8)
C(122)	---	C(121)	1·392(7)	C(126) --- C(121)	1·374(7)
C(123)	---	C(122)	1·380(8)	C(124) --- C(123)	1·362(8)
C(125)	---	C(124)	1·392(7)	C(126) --- C(125)	1·394(7)

Table A.4: Bond Angles (degrees) in Ph$_2$Sn(SalAp). Primed atoms refer to disorder in the atomic positions.

O(2)	- Sn(1)	- O(1)	159·8(2)
N(1)	- Sn(1)	- O(2)	86·1(2)
N(1')	- Sn(1)	- O(2)	60·1(7)
C(111)	- Sn(1)	- O(1)	95·4(2)
C(111)	- Sn(1)	- N(1)	113·2(2)
C(121)	- Sn(1)	- O(1)	93·0(2)
C(121)	- Sn(1)	- N(1)	125·3(2)
C(121)	- Sn(1)	- C(111)	120·9(2)
C(9)	- O(2)	- Sn(1)	127·2(4)
C(7)	- N(1)	- Sn(1)	126·6(6)
C(7')	- N(1')	- Sn(1)	119(2)
C(8)	- N(1')	- C(7')	103(2)
C(6)	- C(1)	- O(1)	121·1(5)
C(3)	- C(2)	- C(1)	120·2(5)
C(5)	- C(4)	- C(3)	119·1(5)
C(1)	- C(6)	- N(1)	109·5(5)
C(5)	- C(6)	- C(1)	121·6(4)
C(7')	- C(6)	- C(1)	147(1)
C(6)	- C(7')	- N(1')	110(2)
C(9)	- C(8)	- C(7)	128·9(6)
C(13)	- C(8)	- O(7)	111·5(6)
C(8)	- C(9)	- O(2)	122·6(5)
C(10)	- C(9)	- C(8)	118·3(5)
C(12)	- C(11)	- C(10)	121·7(5)
C(12)	- C(13)	- C(8)	121·1(6)
C(116)	- C(111)	- Sn(1)	120·8(4)
C(113)	- C(112)	- C(111)	120·3(5)
C(113)	- C(114)	- C(113)	120·1(5)
C(115)	- C(116)	- C(111)	121·1(5)
C(126)	- C(121)	- Sn(1)	119·5(3)
C(123)	- C(122)	- C(121)	120·6(6)
C(125)	- C(124)	- C(123)	120·9(5)
C(125)	- C(126)	- C(121)	121·6(5)

Table A.4: continued...

N(1)	- Sn(1)	- O(1)	74·1(2)
N(1')	- Sn(1)	- O(1)	99·8(7)
C(111)	- Sn(1)	- O(2)	96·0(2)
C(111)	- Sn(1)	- N(1')	117·5(5)
C(121)	- Sn(1)	- O(2)	95·4(2)
C(121)	- Sn(1)	- N(1')	118·3(5)
C(1)	- O(1)	- Sn(1)	118·1(3)
C(6)	- N(1)	- Sn(1)	113·8(4)
C(7)	- N(1)	- C(6)	119·4(7)
C(8)	- N(1')	- Sn(1)	137(2)
C(2)	- C(1)	- O(1)	121·2(5)
C(6)	- C(1)	- C(2)	117·7(5)
C(4)	- C(3)	- C(2)	121·6(5)
C(6)	- C(5)	- C(4)	119·8(5)
C(5)	- C(6)	- N(1)	128·9(5)
C(7')	- C(6)	- C(5)	92(1)
C(8)	- C(7)	- N(1)	123·4(8)
C(9)	- C(8)	- N(1')	88(1)
C(13)	- C(8)	- N(1')	152(1)
C(13)	- C(8)	- C(9)	119·6(5)
C(10)	- C(9)	- O(2)	119·1(6)
C(11)	- C(10)	- C(9)	119·8(6)
C(13)	- C(12)	- C(11)	119·4(6)
C(112)	- C(111)	- Sn(1)	120·2(4)
C(116)	- C(111)	- C(112)	119·0(5)
C(114)	- C(113)	- C(112)	120·0(5)
C(116)	- C(115)	- C(114)	119·6(6)
C(122)	- C(121)	- Sn(1)	121·9(4)
C(126)	- C(121)	- C(122)	118·5(5)
C(124)	- C(123)	- C(122)	120·1(6)
C(126)	- C(125)	- C(124)	118·2(5)

Table A.5: Bond Distances in Ph₂Pb(SalAp). Primed atoms refer to the atoms in the other half of the molecule in the dimer.

O(1)	--- Pb	2·246(4)	N(1)	--- Pb	2·337(5)
O(1')	--- Pb	2·766(4)	O(2)	--- Pb	2·327(4)
C(111)	--- Pb	2·151(6)	C(121)	--- Pb	2·166(6)
C(1)	--- O(1)	1·327(7)	C(9)	--- O(2)	1·285(7)
C(6)	--- N(1)	1·439(8)	C(7)	--- N(1)	1·300(8)
C(2)	--- C(1)	1·399(9)	C(6)	--- C(1)	1·400(9)
C(3)	--- C(2)	1·38(1)	C(4)	--- C(3)	1·38(1)
C(5)	--- C(4)	1·36(1)	C(6)	--- C(5)	1·40(1)
C(8)	--- C(7)	1·425(9)	C(9)	--- C(8)	1·427(9)
C(13)	--- C(8)	1·422(9)	C(10)	--- C(9)	1·407(9)
C(11)	--- C(10)	1·380(9)	C(12)	--- C(11)	1·37(1)
C(13)	--- C(12)	1·36(1)	C(112)	--- C(111)	1·373(9)
C(116)	--- C(111)	1·39(1)	C(113)	--- C(112)	1·38(1)
C(114)	--- C(113)	1·38(1)	C(115)	--- C(114)	1·38(1)
C(116)	--- C(115)	1·40(1)	C(122)	--- C(121)	1·403(9)
C(126)	--- C(121)	1·385(9)	C(123)	--- C(122)	1·40(1)
C(124)	--- C(123)	1·36(1)	C(125)	--- C(124)	1·39(1)
C(126)	--- C(125)	1·38(1)			

Table A.6: Bond Angles (Degrees) in Ph$_2$Pb(SalAp). Primed atoms refer to the atoms in the other half of the molecule in the dimer.

N(1)	- Pb	- O(1')	138·1(2)
C(111)	- Pb	- N(1)	103·6(2)
C(121)	- Pb	- N(1)	100·0(2)
O(1)	- Pb	- O(2)	150·5(2)
O(1)	- Pb	- C(111)	95·7(2)
O(1)	- Pb	- O(1')	65·3(2)
O(2)	- Pb	- C(111)	82·2(2)
O(2)	- Pb	- O(1')	142·7(2)
Pb	- O(1)	- C(1)	116·8(4)
Pb'	- O(1)	- C(1)	128·5(4)
C(6)	- N(1)	- Pb	112·9(4)
C(7)	- N(1)	- C(6)	120·5(5)
C(3)	- C(2)	- C(1)	121·4(7)
C(5)	- C(4)	- C(3)	121·4(7)
C(1)	- C(6)	- N(1)	115·3(6)
C(5)	- C(6)	- C(1)	120·6(6)
C(9)	- C(8)	- C(7)	126·5(6)
C(13)	- C(8)	- C(9)	118·5(6)
C(11)	- C(10)	- C(9)	122·6(6)
C(13)	- C(12)	- C(11)	119·8(6)
C(112)	- C(111)	- Pb	121·6(5)
C(116)	- C(111)	- C(112)	120·7(6)
C(114)	- C(113)	- C(112)	120·6(8)
C(116)	- C(115)	- C(114)	118·9(9)
C(122)	- C(121)	- Pb	118·8(5)
C(126)	- C(121)	- C(122)	121·1(6)
C(124)	- C(123)	- C(122)	121·5(7)
C(126)	- C(125)	- C(124)	121·4(7)

Table A.6: continued...

C(111) - Pb	- O(1')		84·1(2)
C(121) - Pb	- O(1')		86·4(2)
C(121) - Pb	- C(111)		153·5(2)
O(1) - Pb	- N(1)		72·9(2)
O(1) - Pb	- C(121)		102·4(2)
O(2) - Pb	- N(1)		79·0(2)
O(2) - Pb	- C(121)		90·7(2)
Pb - O(1)	- Pb'		114·7(2)
Pb - O(2)	- C(9)		132·7(4)
C(7) - N(1)	- Pb		126·4(4)
C(6) - C(1)	- C(2)		117·7(6)
C(4) - C(3)	- C(2)		119·3(7)
C(6) - C(5)	- C(4)		119·5(7)
C(5) - C(6)	- N(1)		124·0(6)
C(8) - C(7)	- N(1)		129·7(6)
C(13) - C(8)	- C(7)		115·0(6)
C(10) - C(9)	- C(8)		116·8(6)
C(12) - C(11)	- C(10)		120·1(6)
C(12) - C(13)	- C(8)		122·1(6)
C(116) - C(111)	- Pb		117·7(5)
C(113) - C(112)	- C(111)		119·3(8)
C(115) - C(114)	- C(113)		120·7(8)
C(115) - C(116)	- C(111)		119·9(7)
C(126) - C(121)	- Pb		120·1(5)
C(123) - C(122)	- C(121)		117·9(7)
C(125) - C(124)	- C(123)		119·4(7)
C(125) - C(126)	- C(121)		118·8(7)

Table A.7: Bond Distances (Å) in Ph₃Sb(SalAp). Primed atoms refer to disorder in the atomic positions and atoms followed by an "a" refer to molecule 2.

O(1)	--- Sb	2·065(8)	O(2)	--- Sb	2·033(9)
N(1)	--- Sb	2·26(2)	N(1')	--- Sb	2·29(2)
C(14)	--- Sb	2·11(1)	C(20)	--- Sb	2·153(8)
C(26)	--- Sb	2·15(1)	C(1)	--- O(1)	1·35(1)
C(13)	--- O(2)	1·34(1)	N(1')	--- N(1)	0·84(2)
C(6)	--- N(1)	1·55(3)	C(7)	--- N(1)	1·31(7)
C(7')	--- N(1)	0·87(3)	C(7)	--- N(1')	0·91(2)
C(7')	--- N(1')	1·23(9)	C(8)	--- N(1')	1·52(3)
C(2)	--- C(1)	1·44(2)	C(6)	--- C(1)	1·41(2)
C(3)	--- C(2)	1·38(2)	C(4)	--- C(3)	1·38(2)
C(5)	--- C(4)	1·34(2)	C(6)	--- C(5)	1·37(2)
C(7')	--- C(6)	1·48(5)	C(7')	--- C(7)	0·98(4)
C(8)	--- C(7)	1·42(3)	C(9)	--- C(8)	1·39(2)
C(13)	--- C(8)	1·41(2)	C(10)	--- C(9)	1·35(2)
C(11)	--- C(10)	1·39(2)	C(12)	--- C(11)	1·38(1)
C(13)	--- C(12)	1·40(2)	C(15)	--- C(14)	1·46(2)
C(19)	--- C(14)	1·37(2)	C(16)	--- C(15)	1·38(2)
C(17)	--- C(16)	1·37(2)	C(18)	--- C(17)	1·37(2)
C(19)	--- C(18)	1·41(2)	C(21)	--- C(20)	1·40(2)
C(25)	--- C(20)	1·38(2)	C(22)	--- C(21)	1·37(1)
C(23)	--- C(22)	1·31(2)	C(24)	--- C(23)	1·43(2)
C(25)	--- C(24)	1·40(1)	C(27)	--- C(26)	1·39(2)
C(31)	--- C(26)	1·39(2)	C(28)	--- C(27)	1·39(2)
C(29)	--- C(28)	1·41(2)	C(30)	--- C(29)	1·36(1)

Table A.7: continued...

C(31)	---	C(30)	1·38(2)	O(1a) --- Sb(a)	2·047(8)
O(2a)	---	Sb(a)	2·080(8)	N(1a') --- Sb(a)	2·28(2)
N(1a)	---	Sb(a)	2·31(2)	C(14a) --- Sb(a)	2·12(1)
C(26a)	---	Sb(a)	2·16(1)	C(20a) --- Sb(a)	2·155(8)
C(1a)	---	O(1a)	1·36(1)	C(13a) --- O(2a)	1·32(1)
N(1a)	---	N(1a')	0·87(2)	C(7a') --- N(1a')	1·31(7)
C(7a)	---	N(1a')	0·99(3)	C(8a) --- N(1a')	1·49(3)
C(6a)	---	N(1a)	1·50(3)	C(7a') --- N(1a)	0·90(2)
C(7a)	---	N(1a)	1·27(8)	C(2a) --- C(1a)	1·40(2)
C(6a)	---	C(1a)	1·41(2)	C(3a) --- C(2a)	1·39(2)
C(4a)	---	C(3a)	1·35(1)	C(5a) --- C(4a)	1·35(2)
C(6a)	---	C(5a)	1·41(2)	C(7a') --- C(6a)	1·47(3)
C(7a)	---	C(7a')	0·89(4)	C(8a) --- C(7a)	1·52(4)
C(9a)	---	C(8a)	1·38(1)	C(13a) --- C(8a)	1·40(2)
C(10a)	---	C(9a)	1·37(2)	C(11a) --- C(10a)	1·40(2)
C(12a)	---	C(11a)	1·38(1)	C(13a) --- C(12a)	1·41(1)
C(15a)	---	C(14a)	1·39(2)	C(19a) --- C(14a)	1·42(2)
C(16a)	---	C(15a)	1·38(2)	C(17a) --- C(16a)	1·36(2)
C(18a)	---	C(17a)	1·40(2)	C(19a) --- C(18a)	1·40(2)
C(27a)	---	C(26a)	1·39(1)	C(31a) --- C(26a)	1·38(2)
C(30a)	---	C(29a)	1·32(2)	C(31a) --- C(30a)	1·40(2)
C(21a)	---	C(20a)	1·40(2)	C(25a) --- C(20a)	1·40(2)
C(22a)	---	C(21a)	1·39(1)	C(23a) --- C(22a)	1·43(2)
C(24a)	---	C(23a)	1·32(2)	C(25a) --- C(24a)	1·40(2)

Table A.8: Bond Angles (Degrees) in Ph₃Sb(SalAp). Primed atoms refer to disorder in the atomic positions and atoms followed by an "a" refer to molecule 2.

O(2)	- Sb	- O(1)	161·6(3)
N(1)	- Sb	- O(2)	89·1(9)
N(1')	- Sb	- O(2)	68·6(9)
C(14)	- Sb	- O(1)	89·4(4)
C(14)	- Sb	- N(1)	83·0(6)
C(20)	- Sb	- O(1)	98·1(5)
C(20)	- Sb	- N(1)	170·6(9)
C(20)	- Sb	- C(14)	95·5(5)
C(26)	- Sb	- O(2)	88·9(4)
C(26)	- Sb	- N(1')	80·1(7)
C(26)	- Sb	- C(20)	95·8(5)
C(13)	- O(2)	- Sb	122·8(8)
C(6)	- N(1)	- Sb	117(2)
C(7)	- N(1)	- Sb	125(2)
C(7)	- N(1)	- C(6)	118(2)
C(7')	- N(1)	- N(1')	92(8)
C(7')	- N(1)	- C(7)	49(5)
C(7)	- N(1')	- Sb	174(4)
C(7')	- N(1')	- Sb	122(3)
C(7')	- N(1')	- C(7)	52(3)
C(8)	- N(1')	- N(1)	163(4)
C(8)	- N(1')	- C(7')	118(3)
C(6)	- C(1)	- O(1)	124(1)
C(3)	- C(2)	- C(1)	118(1)
C(5)	- C(4)	- C(3)	122(1)
C(1)	- C(6)	- N(1)	103(2)
C(5)	- C(6)	- C(1)	121(1)

Table A.8: continued...

N(1)	- Sb	- O(1)	72·6(9)
N(1')	- Sb	- O(1)	93·0(9)
N(1')	- Sb	- N(1)	21·2(6)
C(14)	- Sb	- O(2)	89·7(4)
C(14)	- Sb	- N(1')	88·9(7)
C(20)	- Sb	- O(2)	100·3(4)
C(20)	- Sb	- N(1')	168·1(9)
C(26)	- Sb	- O(1)	88·4(4)
C(26)	- Sb	- N(1)	85·7(6)
C(26)	- Sb	- C(14)	168·6(5)
C(1)	- O(1)	- Sb	119·4(8)
N(1')	- N(1)	- Sb	82(3)
C(6)	- N(1)	- N(1')	161(4)
C(7)	- N(1)	- N(1')	44(3)
C(7')	- N(1)	- Sb	174(6)
C(7')	- N(1)	- C(6)	69(5)
N(1)	- N(1')	- Sb	77(3)
C(7)	- N(1')	- N(1)	97(6)
C(7')	- N(1')	- N(1)	45(4)
C(8)	- N(1')	- Sb	120(2)
C(8)	- N(1')	- C(7)	66(3)
C(2)	- C(1)	- O(1)	118(1)
C(6)	- C(1)	- C(2)	118(1)
C(4)	- C(3)	- C(2)	121(1)
C(6)	- C(5)	- C(4)	120(1)
C(5)	- C(6)	- N(1)	136(2)
C(7')	- C(6)	- N(1)	33(1)

Table A.8: continued...

C(7')	- C(6)	- C(1)	136(2)
N(1')	- C(7)	- N(1)	40(3)
C(7')	- C(7)	- N(1')	81(7)
C(8)	- C(7)	- N(1')	78(3)
N(1')	- C(7')	- N(1)	43(5)
C(6)	- C(7')	- N(1')	121(3)
C(7)	- C(7')	- N(1')	47(4)
C(7)	- C(8)	- N(1')	35·8(9)
C(9)	- C(8)	- C(7)	106(2)
C(13)	- C(8)	- C(7)	134(2)
C(10)	- C(9)	- C(8)	122(1)
C(12)	- C(11)	- C(10)	122(1)
C(8)	- C(13)	- O(2)	124(1)
C(12)	- C(13)	- C(8)	118(1)
C(19)	- C(14)	- Sb	124·1(9)
C(16)	- C(15)	- C(14)	119(1)
C(18)	- C(17)	- C(16)	120(1)
C(18)	- C(19)	- C(14)	122(1)
C(25)	- C(20)	- Sb	120·2(9)
C(22)	- C(21)	- C(20)	121(1)
C(24)	- C(23)	- C(22)	121(1)
C(24)	- C(25)	- C(20)	121(1)
C(31)	- C(26)	- Sb	123·2(9)
C(28)	- C(27)	- C(26)	122(1)
C(30)	- C(29)	- C(28)	121(1)
C(30)	- C(31)	- C(26)	121(1)
N(1a')	- Sb(a)	- O(1a)	92(1)

Table A.8: continued...

C(7')	- C(6)	- C(5)	103(2)
C(7')	- C(7)	- N(1)	42(4)
C(8)	- C(7)	- N(1)	118(2)
C(8)	- C(7)	- C(7')	159(5)
C(6)	- C(7')	- N(1)	78(4)
C(7)	- C(7')	- N(1)	90(9)
C(7)	- C(7')	- C(6)	167(6)
C(9)	- C(8)	- N(1')	141(2)
C(13)	- C(8)	- N(1')	99(1)
C(13)	- C(8)	- C(9)	120(1)
C(11)	- C(10)	- C(9)	118(1)
C(13)	- C(12)	- C(11)	120(1)
C(12)	- C(13)	- O(2)	118(1)
C(15)	- C(14)	- Sb	118·2(9)
C(19)	- C(14)	- C(15)	118(1)
C(17)	- C(16)	- C(15)	121(1)
C(19)	- C(18)	- C(17)	120(1)
C(21)	- C(20)	- Sb	121·8(9)
C(25)	- C(20)	- C(21)	117·9(8)
C(23)	- C(22)	- C(21)	121(1)
C(25)	- C(24)	- C(23)	118(1)
C(27)	- C(26)	- Sb	119·1(9)
C(31)	- C(26)	- C(27)	118(1)
C(29)	- C(28)	- C(27)	118(1)
C(31)	- C(30)	- C(29)	120(1)
O(2a)	- Sb(a)	- O(1a)	161·8(3)
N(1a')	- Sb(a)	- O(2a)	70(1)

Table A.8: continued...

N(1a)	- Sb(a)	- O(1a)	70·9(9)
N(1a)	- Sb(a)	- N(1a')	21·7(6)
C(14a)	- Sb(a)	- O(2a)	88·0(4)
C(14a)	- Sb(a)	- N(1a)	87·7(7)
C(26a)	- Sb(a)	- O(2a)	89·6(4)
C(26a)	- Sb(a)	- N(1a)	80·6(6)
C(20a)	- Sb(a)	- O(1a)	100·3(4)
C(20a)	- Sb(a)	- N(1a')	168(1)
C(20a)	- Sb(a)	- C(14a)	96·7(5)
C(1a)	- O(1a)	- Sb(a)	120·5(8)
N(1a)	- N(1a')	- Sb(a)	82(2)
C(7a')	- N(1a')	- N(1a)	43(3)
C(7a)	- N(1a')	- N(1a)	86(6)
C(8a)	- N(1a')	- Sb(a)	120(2)
C(8a)	- N(1a')	- C(7a')	115(2)
N(1a')	- N(1a)	- Sb(a)	77(2)
C(6a)	- N(1a)	- N(1a')	166(4)
C(7a')	- N(1a)	- N(1a')	95(6)
C(7a)	- N(1a)	- Sb(a)	128(3)
C(7a)	- N(1a)	- C(6a)	116(2)
C(2a)	- C(1a)	- O(1a)	118(1)
C(6a)	- C(1a)	- C(2a)	119(1)
C(4a)	- C(3a)	- C(2a)	121(1)
C(6a)	- C(5a)	- C(4a)	122(1)
C(5a)	- C(6a)	- N(1a)	138(1)
C(7a')	- C(6a)	- N(1a)	35·4(9)

Table A.8: continued...

N(1a)	- Sb(a)	- O(2a)	90·9(9)
C(14a)	- Sb(a)	- O(1a)	89·6(4)
C(14a)	- Sb(a)	- N(1a')	82·0(6)
C(26a)	- Sb(a)	- O(1a)	89·0(4)
C(26a)	- Sb(a)	- N(1a')	86·1(6)
C(26a)	- Sb(a)	- C(14a)	168·0(5)
C(20a)	- Sb(a)	- O(2a)	97·9(4)
C(20a)	- Sb(a)	- N(1a)	170·3(9)
C(20a)	- Sb(a)	- C(26a)	95·3(4)
C(13a)	- O(2a)	- Sb(a)	120·9(8)
C(7a')	- N(1a')	- Sb(a)	125(2)
C(7a)	- N(1a')	- Sb(a)	168(5)
C(7a)	- N(1a')	- C(7a')	43(4)
C(8a)	- N(1a')	- N(1a)	159(4)
C(8a)	- N(1a')	- C(7a)	73(4)
C(6a)	- N(1a)	- Sb(a)	117(2)
C(7a')	- N(1a)	- Sb(a)	172(5)
C(7a')	- N(1a)	- C(6a)	71(3)
C(7a)	- N(1a)	- N(1a')	51(3)
C(7a)	- N(1a)	- C(7a')	45(3)
C(6a)	- C(1a)	- O(1a)	123(1)
C(3a)	- C(2a)	- C(1a)	120(1)
C(5a)	- C(4a)	- C(3a)	120(1)
C(1a)	- C(6a)	- N(1a)	104(1)
C(5a)	- C(6a)	- C(1a)	118(1)
C(7a')	- C(6a)	- C(1a)	139(2)

Table A.8: continued...

C(7a')	- C(6a)	- C(5a)	103(2)
C(6a)	- C(7a')	- N(1a')	115(2)
C(7a)	- C(7a')	- N(1a')	49(4)
C(7a)	- C(7a')	- C(6a)	164(5)
C(7a')	- C(7a)	- N(1a')	88(7)
C(8a)	- C(7a)	- N(1a')	69(3)
C(8a)	- C(7a)	- C(7a')	156(5)
C(9a)	- C(8a)	- N(1a')	139(2)
C(13a)	- C(8a)	- N(1a')	103(1)
C(13a)	- C(8a)	- C(9a)	118(1)
C(11a)	- C(10a)	- C(9a)	118(1)
C(13a)	- C(12a)	- C(11a)	119(1)
C(12a)	- C(13a)	- O(2a)	116(1)
C(15a)	- C(14a)	- Sb(a)	119(1)
C(19a)	- C(14a)	- C(15a)	118(1)
C(17a)	- C(16a)	- C(15a)	121(2)
C(19a)	- C(18a)	- C(17a)	118(1)
C(27a)	- C(26a)	- Sb(a)	118·5(9)
C(31a)	- C(26a)	- C(27a)	119(1)
C(29a)	- C(28a)	- C(27a)	119(1)
C(31a)	- C(30a)	- C(29a)	121(1)
C(21a)	- C(20a)	- Sb(a)	119·1(9)
C(25a)	- C(20a)	- C(21a)	120·6(9)
C(23a)	- C(22a)	- C(21a)	118(1)
C(25a)	- C(24a)	- C(23a)	121(1)

Table A.8: continued...

N(1a)	- C)7a')	- N(1a')	41(3)
C(6a)	- C(7a')	- N(1a)	74(3)
C(7a)	- C(7a')	- N(1a)	90(7)
N(1a)	- C(7a)	- N(1a')	43(3)
C(7a')	- C(7a)	- N(1a)	45(4)
C(8a)	- C(7a)	- N(1a)	112(3)
C(7a)	- C(8a)	- N(1a')	38(1)
C(9a)	- C(8a)	- C(7a)	101(2)
C(13a)	- C(8a)	- C(7a)	141(2)
C(10a)	- C(9a)	- C(8a)	123(1)
C(12a)	- C(11a)	- C(10a)	121(1)
C(8a)	- C(13a)	- O(2a)	124(1)
C(12a)	- C(13a)	- C(8a)	120(1)
C(19a)	- C(14a)	- Sb(a)	122(1)
C(16a)	- C(15a)	- C(14a)	120(1)
C(18a)	- C(17a)	- C(16a)	121(1)
C(18a)	- C(19a)	- C(14a)	121(1)
C(31a)	- C(26a)	- Sb(a)	122·9(9)
C(28a)	- C(27a)	- C(26a)	121(1)
C(30a)	- C(29a)	- C(28a)	121(1)
C(30a)	- C(31a)	- C(26a)	120(1)
C(25a)	- C(20a)	- Sb(a)	120·1(8)
C(22a)	- C(21a)	- C(20a)	120(1)
C(24a)	- C(23a)	- C(22a)	122(1)
C(24a)	- C(25a)	- C(20a)	119(1)